The Gaia's "living and breathing" Milky Way

Alejandra Recio-Blanco
Observatoire de la Côte d'Azur (Lab. Lagrange)

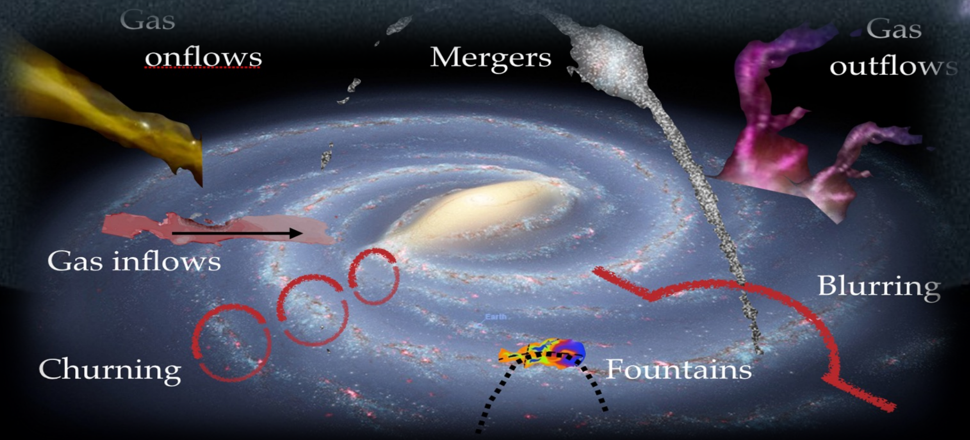

OBSERVATOIRE DE LA CÔTE D'AZUR
UNIVERSITÉ CÔTE D'AZUR

esa
gaia

Gaia stellar populations

1. The Gaia revolution on Galactic stellar populations and its keys

2. The chemical cartography of the Milky Way

3. - Gaia: "*Mesdames et messieurs, the stellar populations*"
    - Disc structure and chemical gradients
    - Disc kinematic disturbances
    - Halo populations

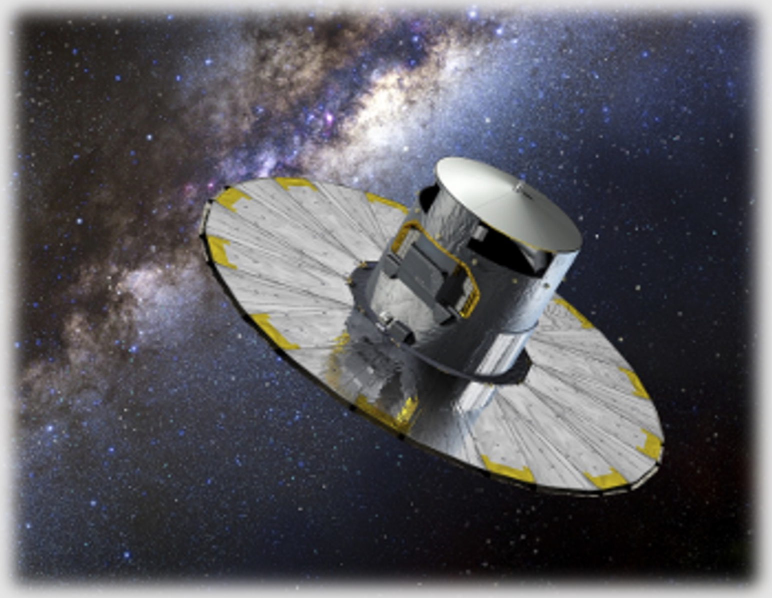

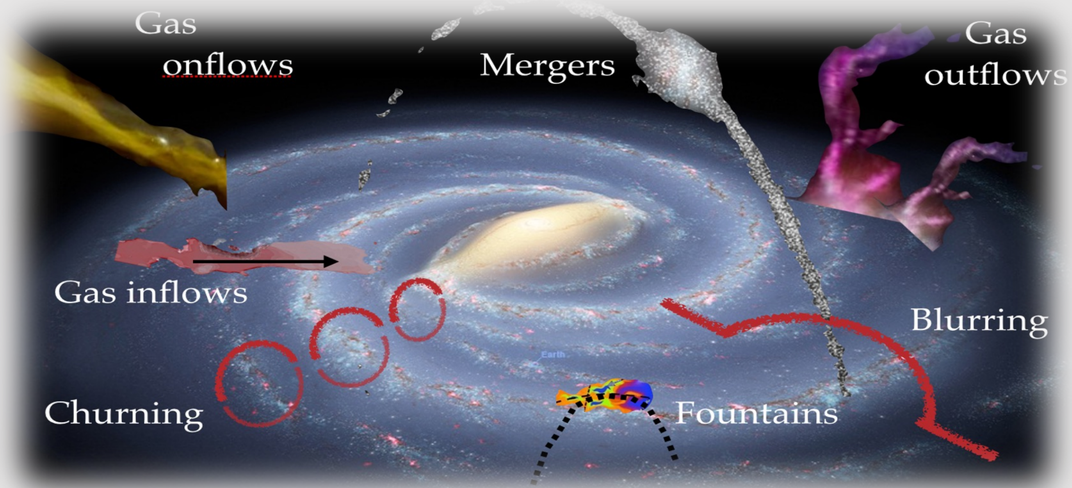

Gaia stellar populations

1. The Gaia revolution on Galactic stellar populations and its keys

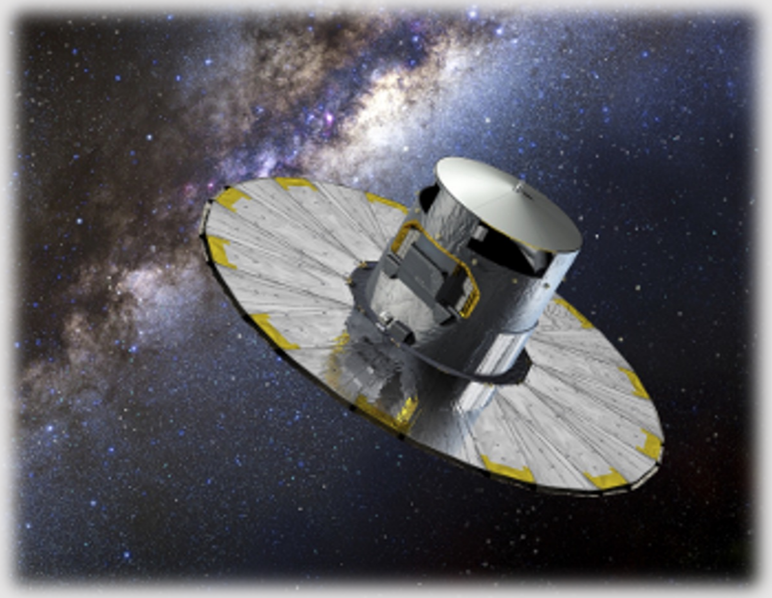

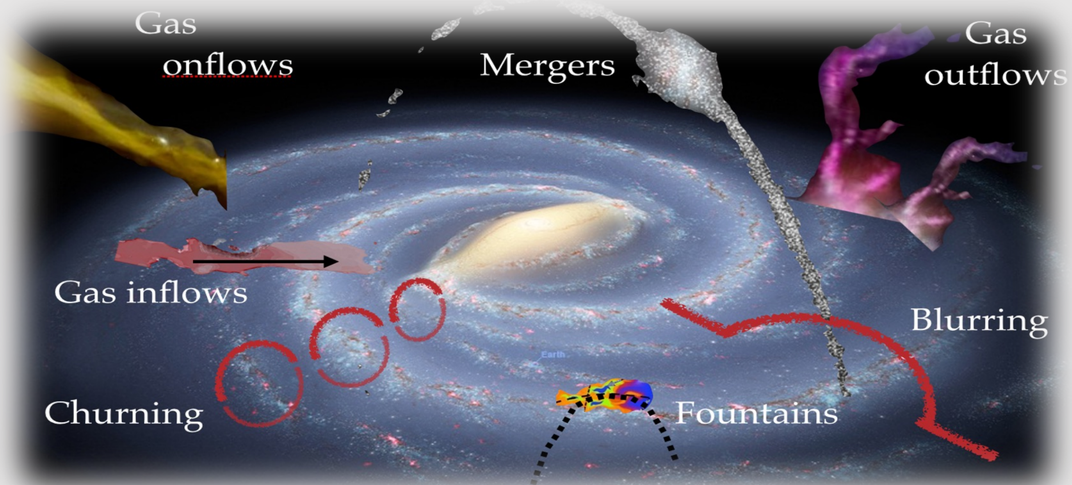

Ptolemy (150)

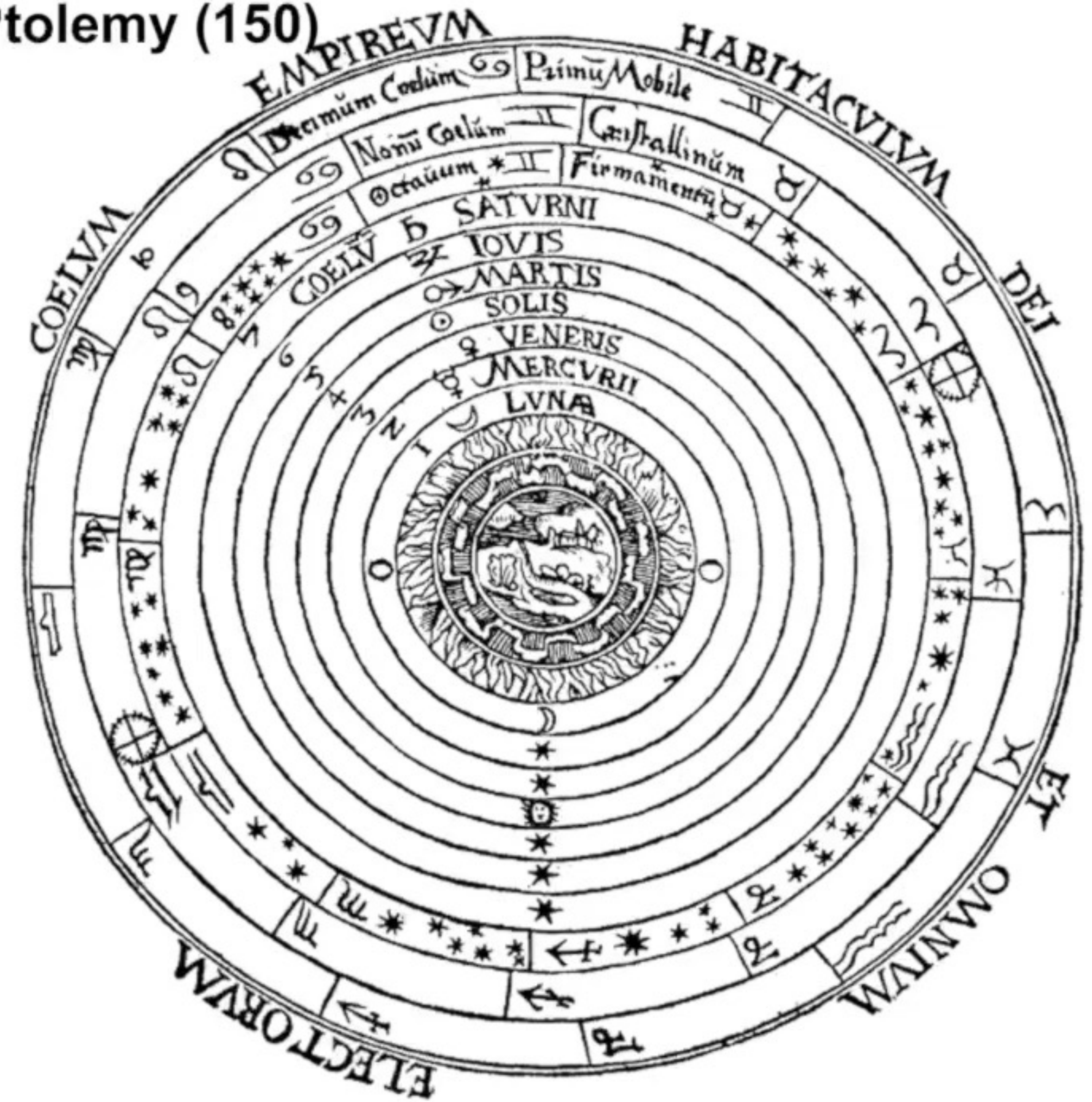
COELVM EMPIREVM HABITACVLVM DEI ET OMNIVM ELECTORVM
Primu Mobile
Decimum Coelum
Cristallinum
Nonu Coelum
Firmamentu
Octauum
SATVRNI
IOVIS
COELV
MARTIS
SOLIS
VENERIS
MERCVRII
LVNÆ

The keys of the Gaia revolution

- Parallaxes: the depth of the sky...

Stellar parallaxes

Number of the published stellar parallaxes (number of stars with at least one parallax) before *Hipparcos*.

Year	number	notes
1840	3	61 Cygni, Vega, α Cent
1850	20	
1890	40	
1910	300	with 52 photographic parallaxes
1925	2000	photographic plates
1965	6000	Yale catalogue
1980	8000	just before *Hipparcos*

Stars lay at large, but finite distances!

Stellar positions

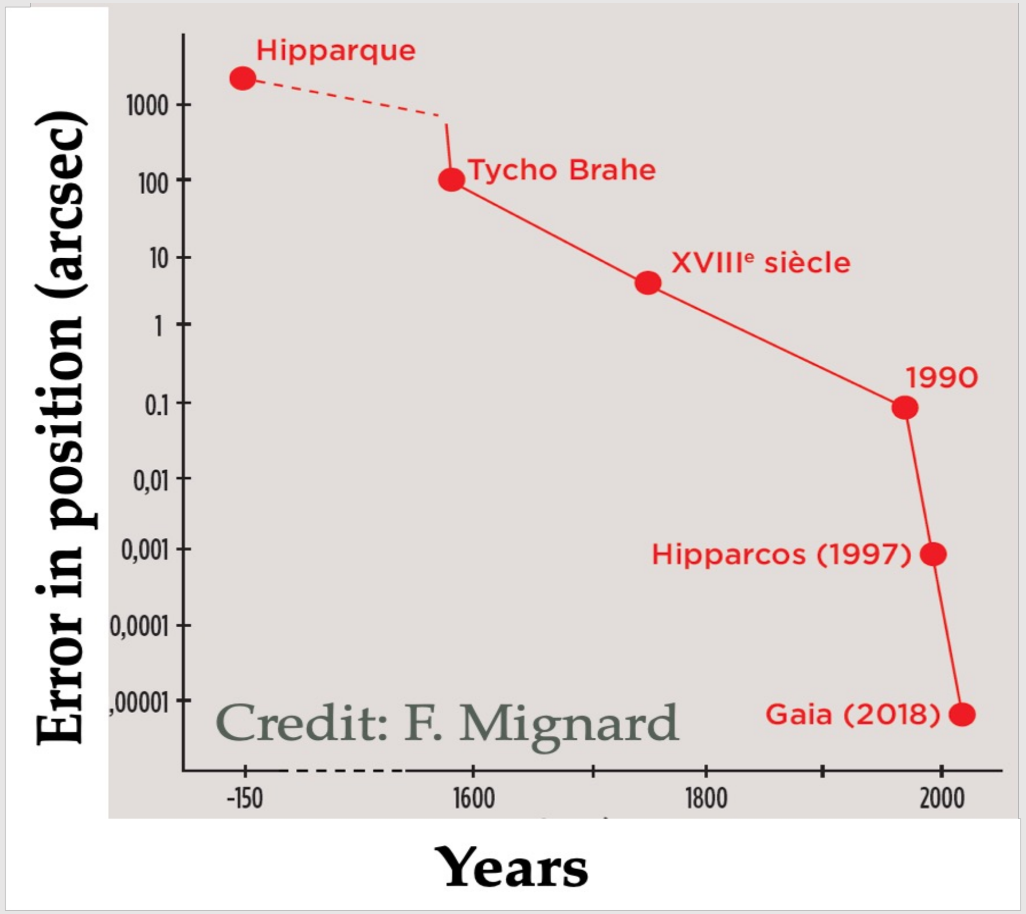

« (We have) lived to see the day when the sounding line in the Universe of stars had at last touched bottom »

J. Herschel (President of the British Royal Astronomical Society, ~1840)

The keys of the Gaia revolution

- Parallaxes: the depth of the sky…

- **Number statistics:** 1.8 billion stars (astrometry+photometry)
  33 million stars (spectroscopy) Nb increasing!

Photometry

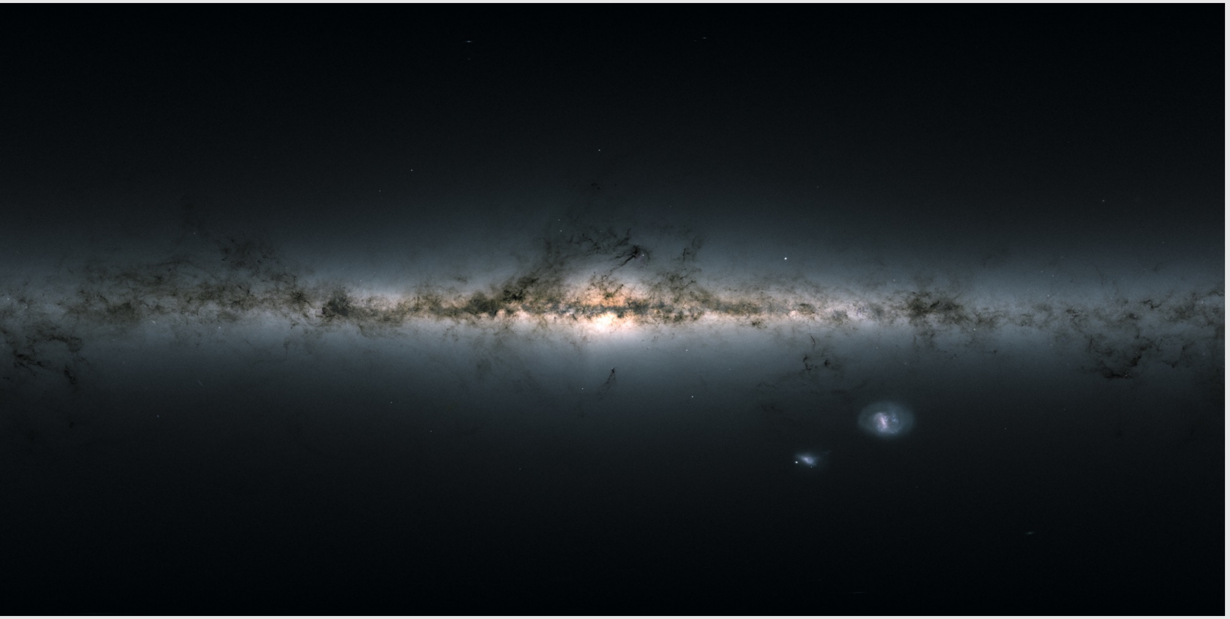

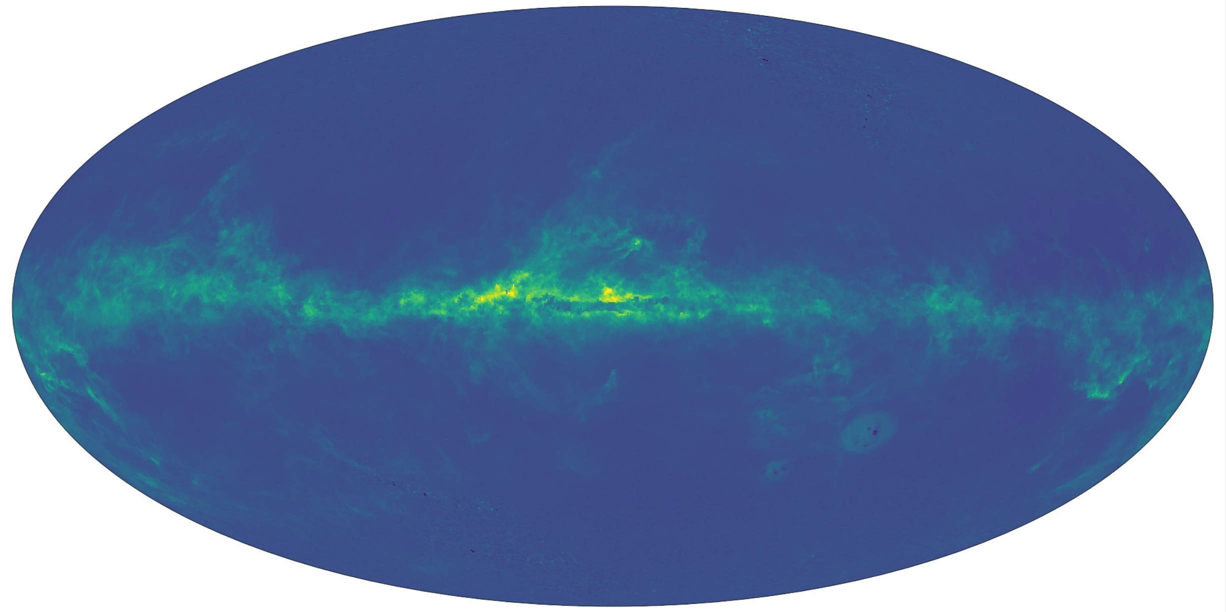

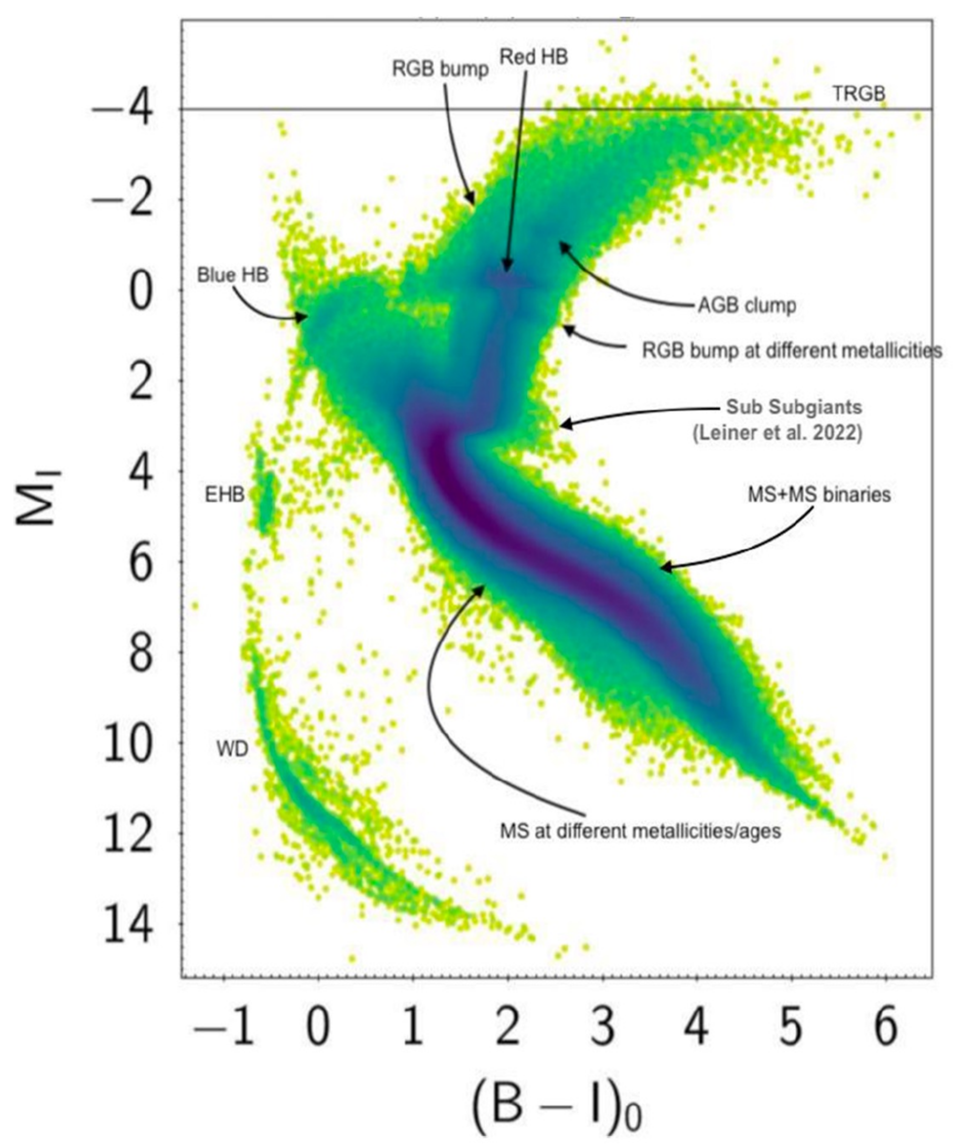

Gaia Collaboration, Montegriffo et al. 2022

Spectroscopy

Gaia DR3: 33.6 milion stars with radial velocity determinations

Katz et al. 2022

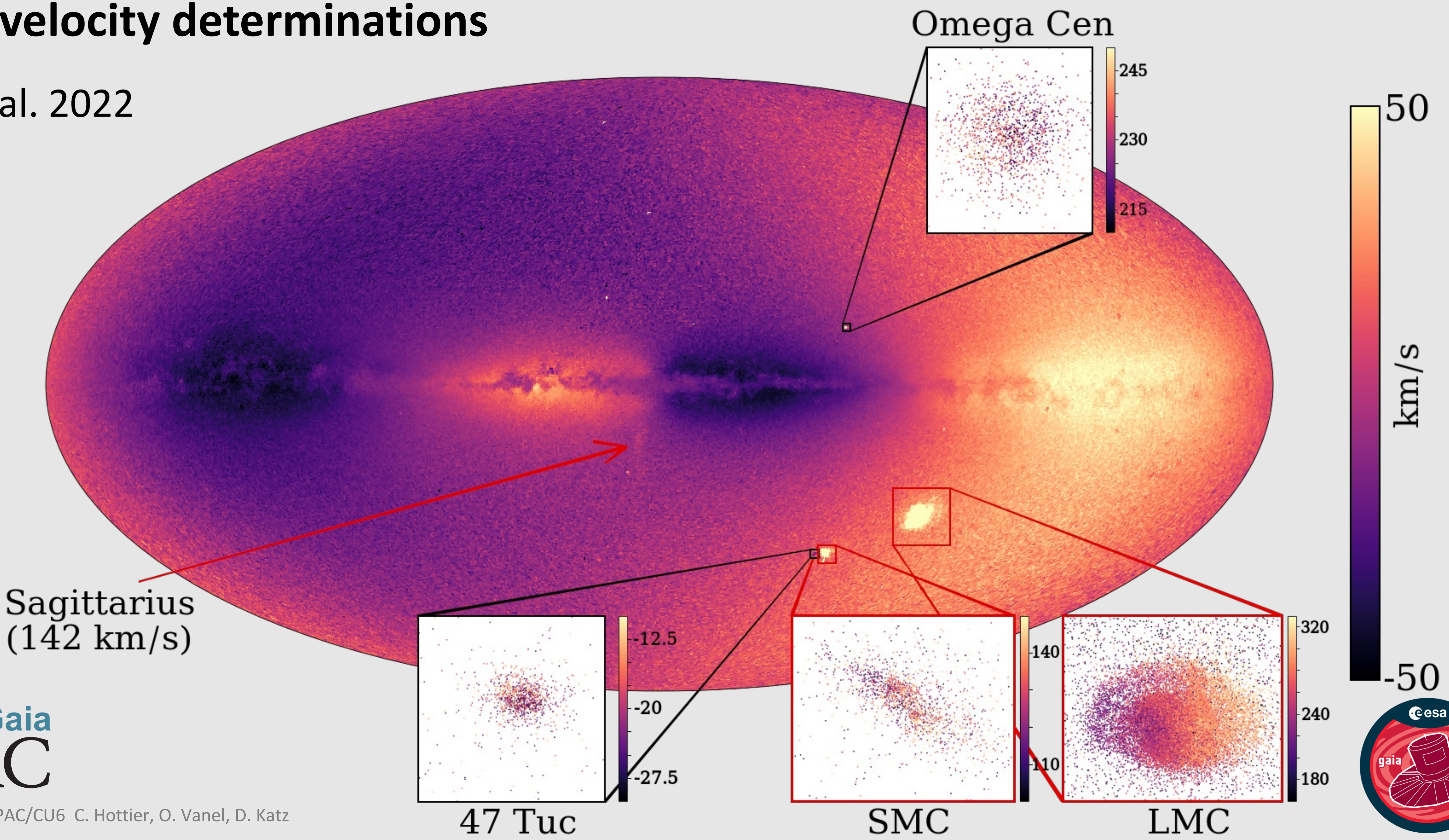

Gaia DPAC

Credits: ESA/GAIA/DPAC/CU6 C. Hottier, O. Vanel, D. Katz

Gaia DR3: 5.6 milion stars with chemo-physical parameters

Spectroscopy

Recio-Blanco et al. 2022

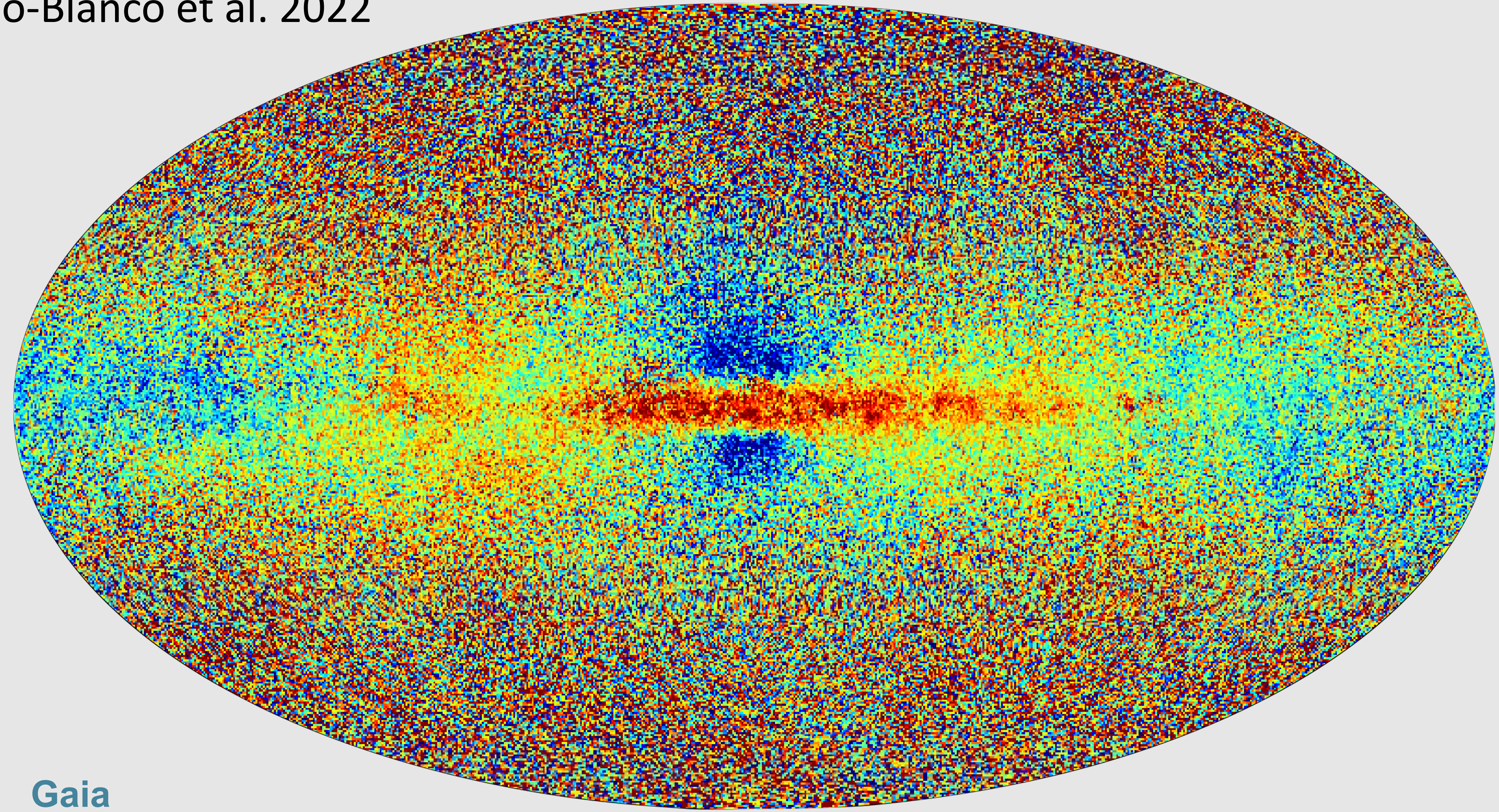

Gaia Collaboration, Recio-Blanco et al. 2022

The keys of the Gaia revolution

- Parallaxes: the depth of the sky...
- **Number statistics:** 1.8 billion stars (astrometry+photometry)
  33 million stars (spectroscopy) Nb increasing!
- **Precise stellar parameters:** space observations (no Earth's atmosphere)
  extremely good control of systematics

The keys of the Gaia revolution

Gaia/RVS is **SPACE spectroscopy** ≠ ground based spectroscopy

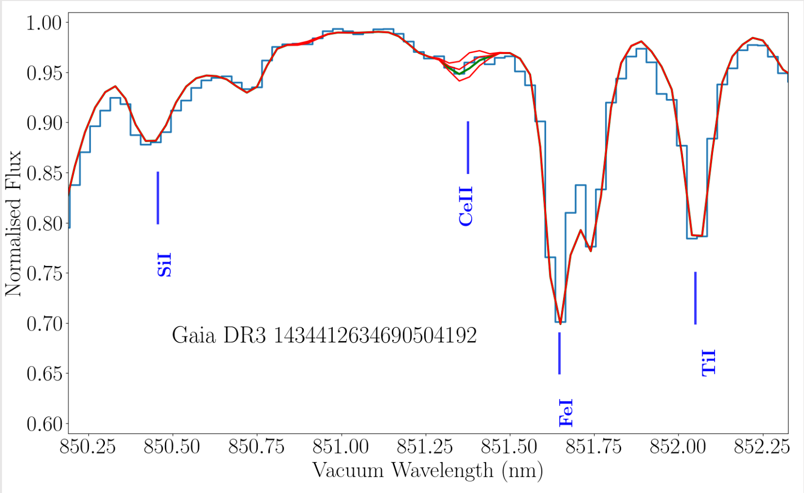

Parametrization quality comparable to ground-based surveys of higher spectral resolution and wavelength coverage.

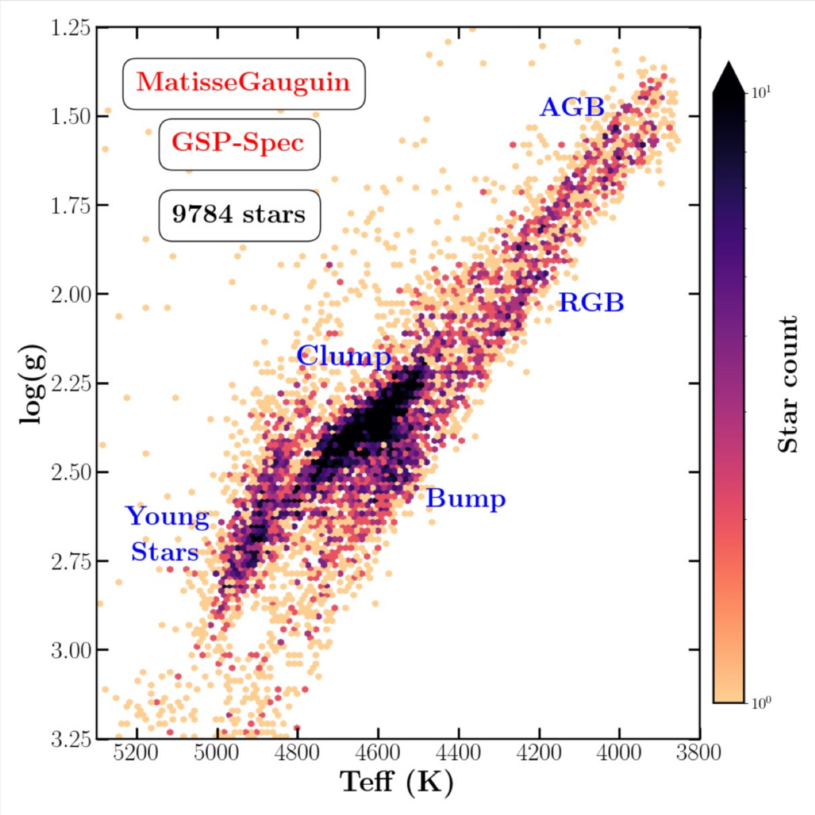

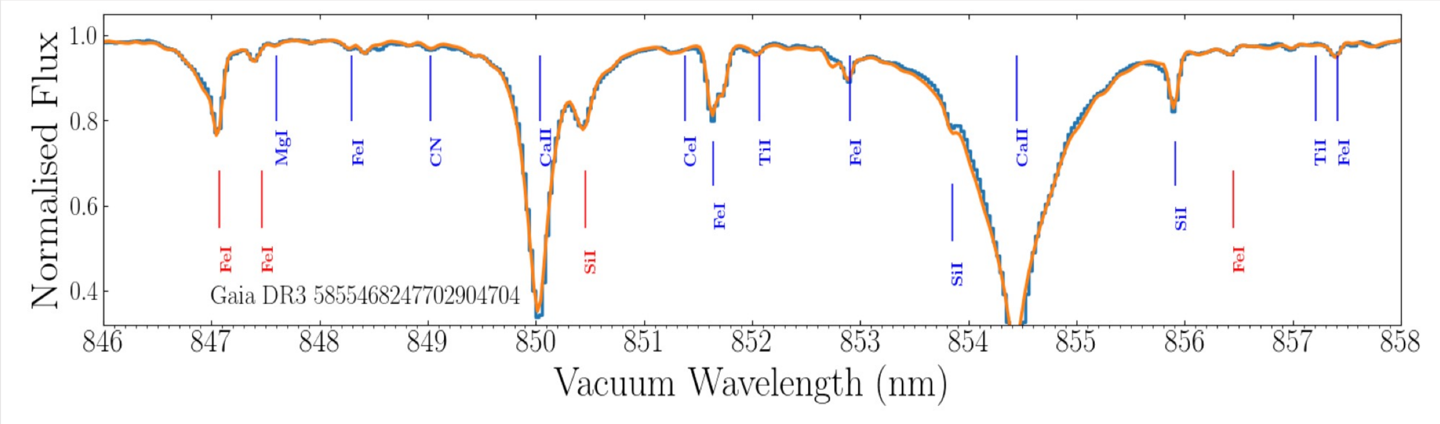

Recio-Blanco et al. 2022

The keys of the Gaia revolution

- Parallaxes: the depth of the sky...
- **Number statistics:** 1.8 billion stars (astrometry+photometry)
  33 million stars (spectroscopy) Nb increasing!
- **Precise stellar parameters:** space observations (no Earth's atmosphere)
  extremely good control of systematics
- Time-series (continuous observations for years): **evolution!**
  - Proper motions

Astrometry

Gaia DPAC

Gaia EDR3: 1.8 milion stars with astrometric solutions

The keys of the Gaia revolution

- Parallaxes: the depth of the sky...
- **Number statistics:** 1.8 billion stars (astrometry+photometry)
  33 million stars (spectroscopy) Nb increasing!
- **Precise stellar parameters:** space observations (no Earth's atmosphere)
  extremely good control of systematics
- **Time-series** (continuous observations for years): **evolution!**
  - Proper motions
  - Solar System acceleration

Gaia Collaboration, Klioner et al. 2020

Astrometry

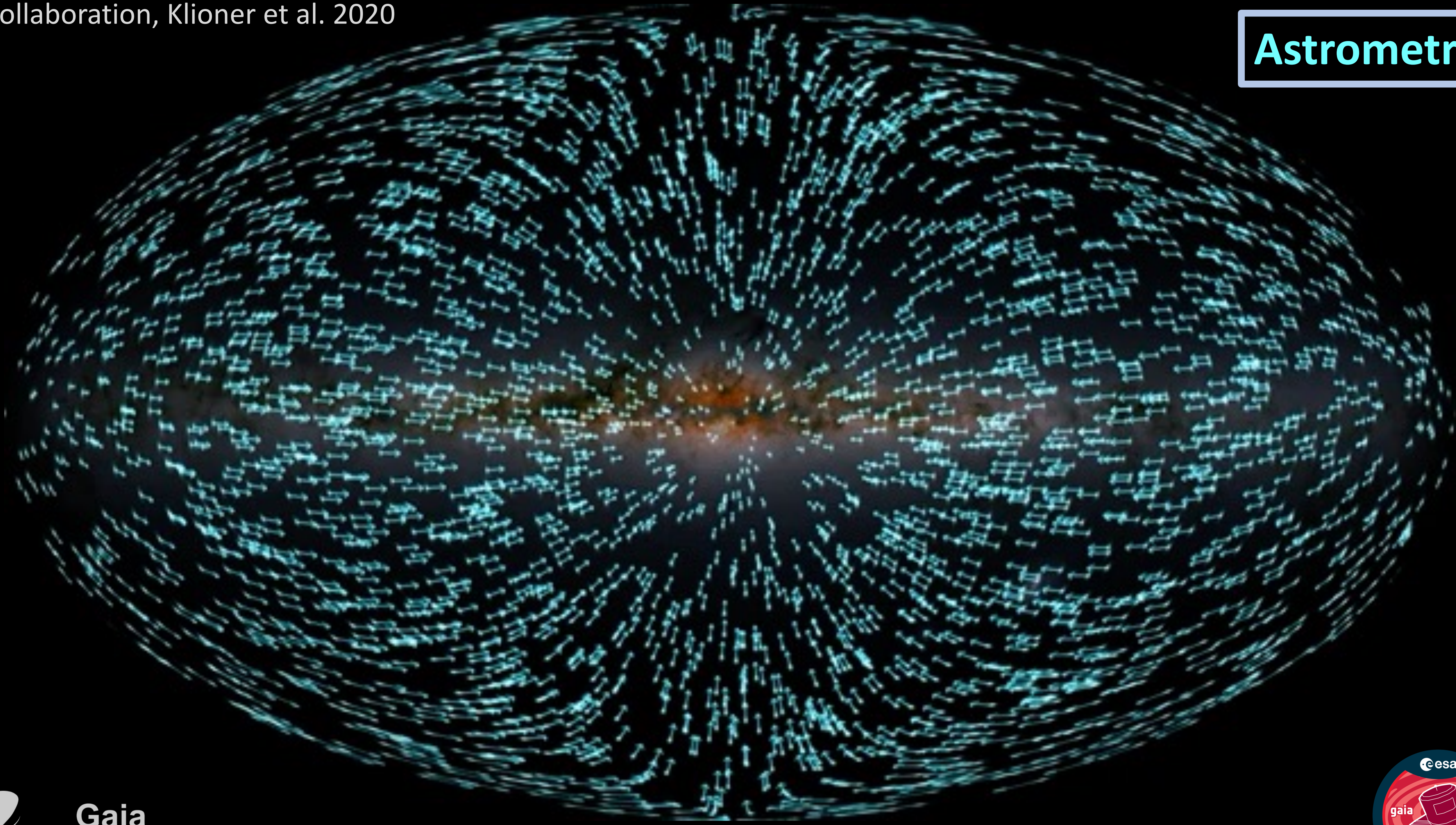

Gaia EDR3: acceleration of the Solar System

The keys of the Gaia revolution

- Parallaxes: the depth of the sky...
- **Number statistics:** 1.8 billion stars (astrometry+photometry)
  33 million stars (spectroscopy) Nb increasing!
- **Precise stellar parameters:** space observations (no Earth's atmosphere)
  extremely good control of systematics
- Time-series (continuous observations for years): **evolution!**
  - Proper motions
  - Solar System acceleration
  - Stellar variability

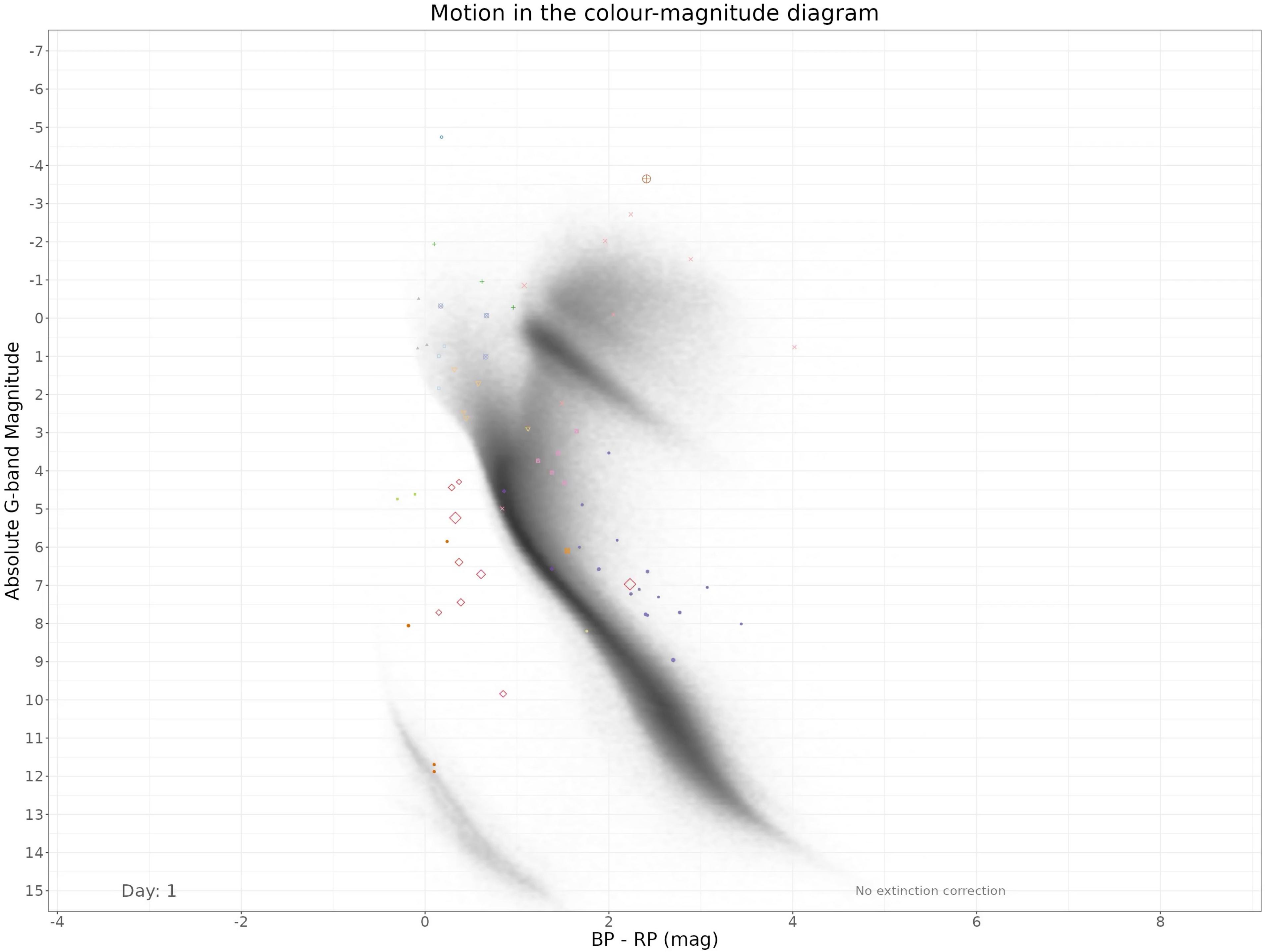

Photometry

Time-series over 34 months
Continuous observations!

Eyer et al. et al. 2022

The keys of the Gaia revolution

- Parallaxes: the depth of the sky...
- **Number statistics:** 1.8 billion stars (astrometry+photometry)
  33 million stars (spectroscopy) Nb increasing!
- **Precise stellar parameters:** space observations (no Earth's atmosphere)
  extremely good control of systematics
- Time-series (continuous observations for years): **evolution!**
  - Proper motions
  - Solar System acceleration
  - Stellar variability
  - Binaries and their orbital solutions

ASTROMETRIC BINARIES WITHIN 50PC

Gaia Collaboration, Arénou et al. 2022

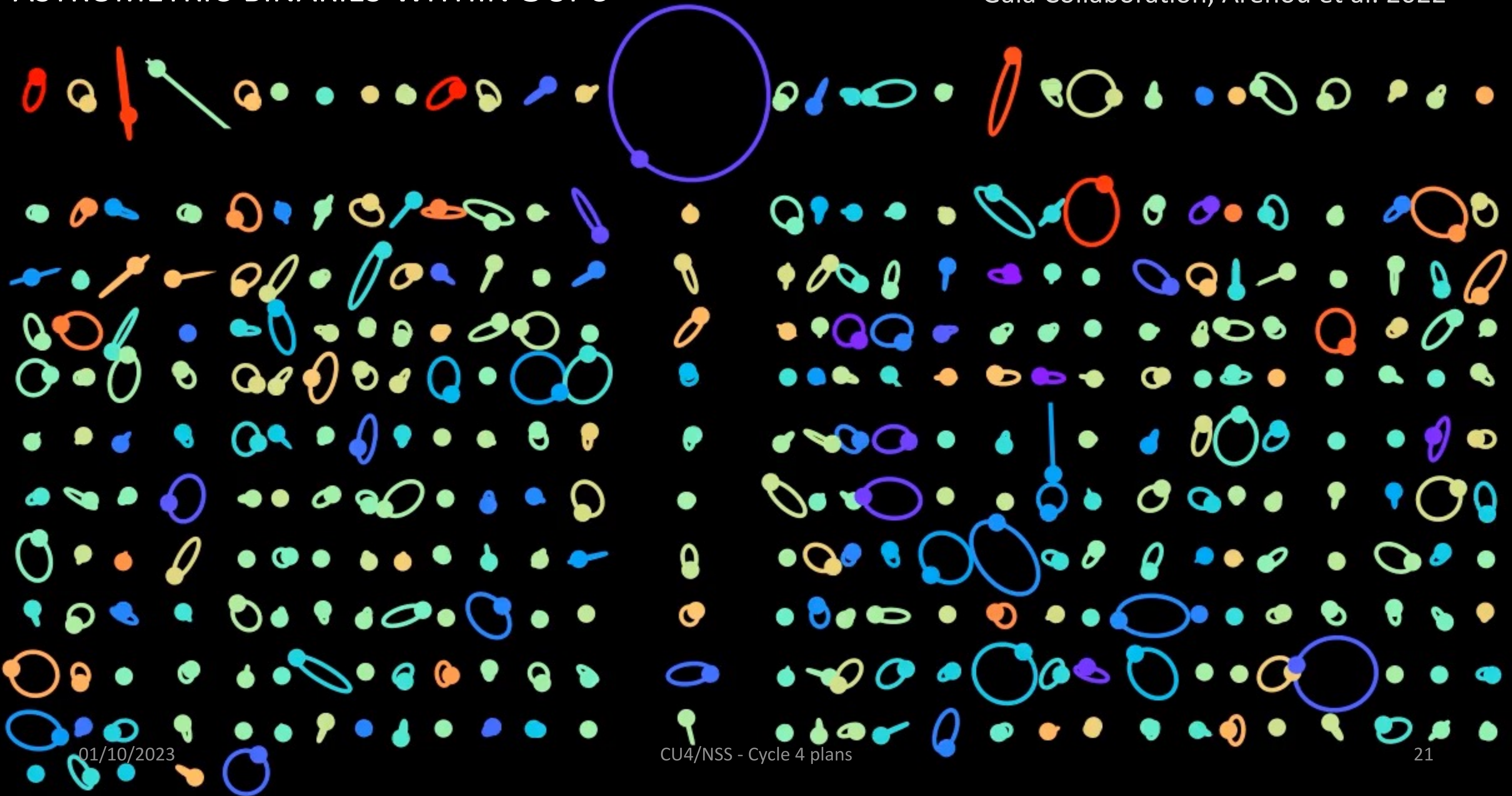

The keys of the Gaia revolution

- **Parallaxes: the depth of the sky...**
- **Number statistics:** 1.8 billion stars (astrometry+photometry)
  33 million stars (spectroscopy) Nb increasing!
- **Precise stellar parameters:** space observations (no Earth's atmosphere)
  extremely good control of systematics
- **Time-series** (continuous observations for years): **evolution!**
  - **Proper motions**
  - **Solar System acceleration**
  - **Stellar variability**
  - **Binaries and their orbital solutions**
- **Chemical composition of matter**

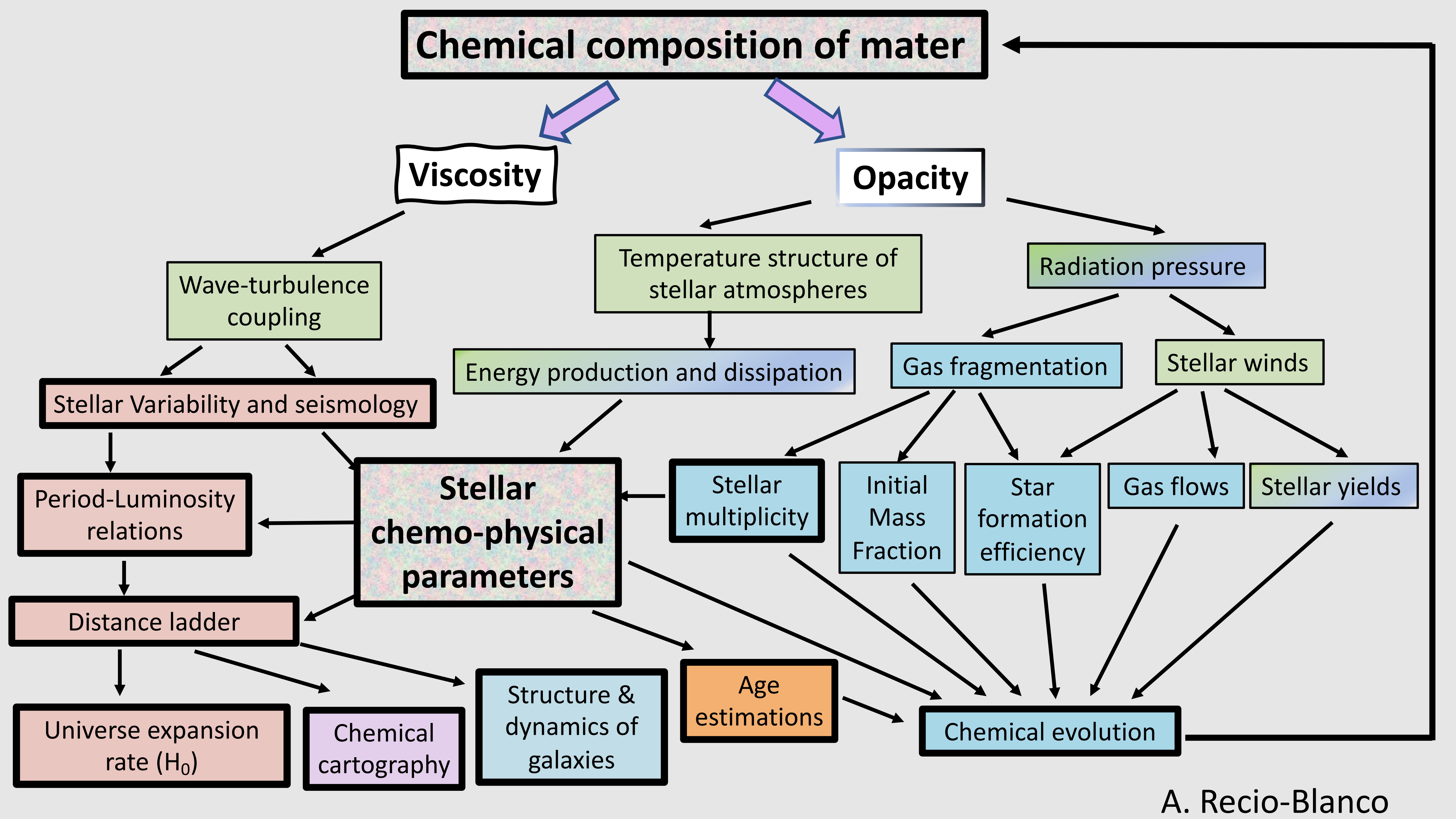
Chemical composition of mater
Viscosity
Opacity
Wave-turbulence coupling
Temperature structure of stellar atmospheres
Radiation pressure
Stellar Variability and seismology
Energy production and dissipation
Gas fragmentation
Stellar winds
Period-Luminosity relations
Stellar chemo-physical parameters
Stellar multiplicity
Initial Mass Fraction
Star formation efficiency
Gas flows
Stellar yields
Distance ladder
Age estimations
Universe expansion rate (H_0)
Chemical cartography
Structure & dynamics of galaxies
Chemical evolution
A. Recio-Blanco

Gaia stellar populations

1. The Gaia revolution on Galactic stellar populations and its keys

2. The chemical cartography of the Milky Way

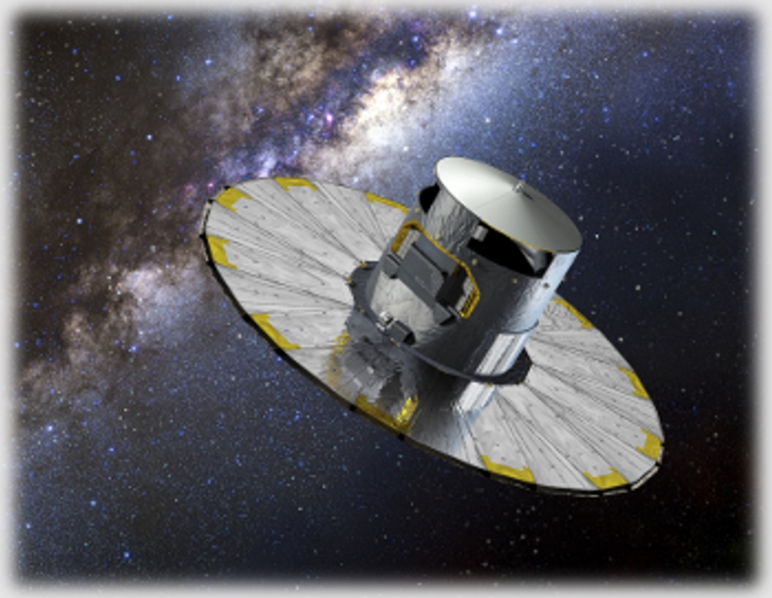

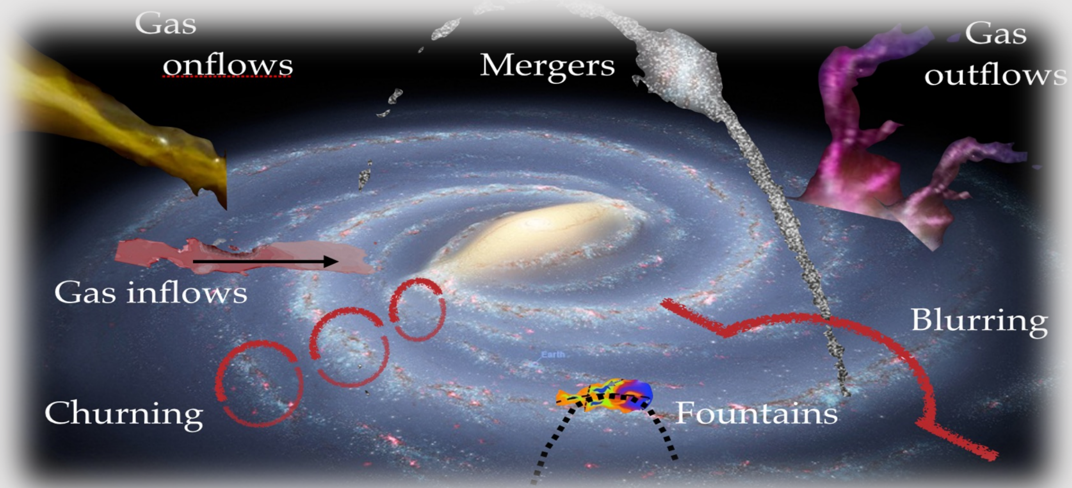

Vincent Van Gogh
(1888)

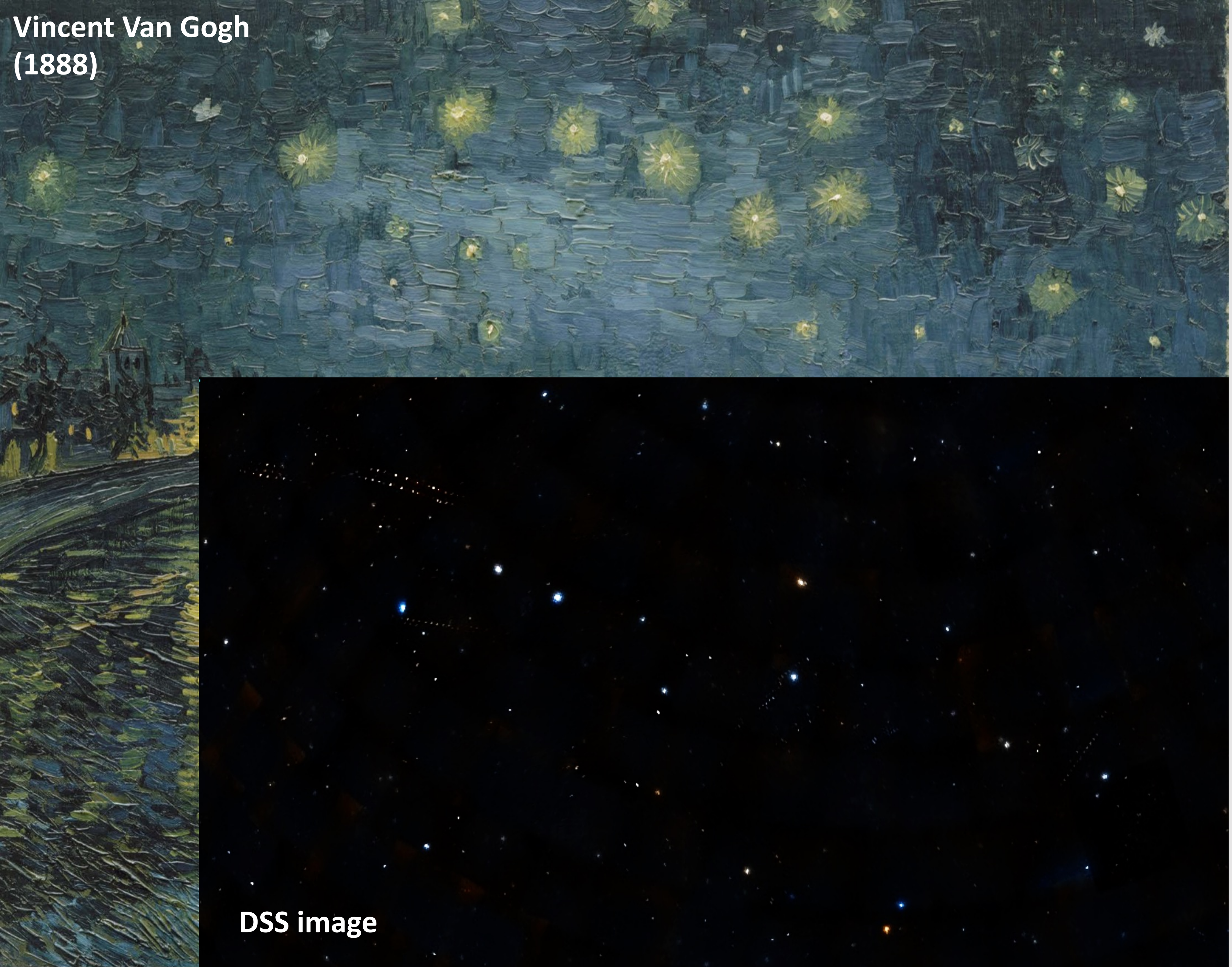
Vincent Van Gogh
(1888)
DSS image

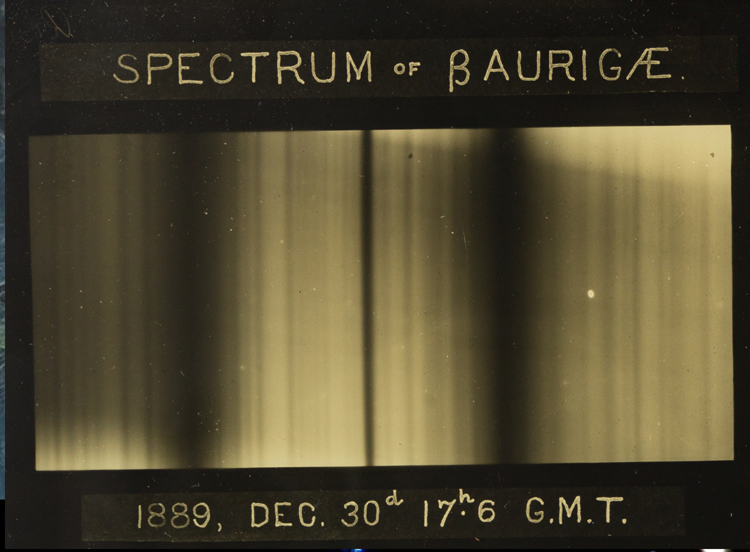

Henry Drapper Memorial work at the Harvard of Observatory (1889)

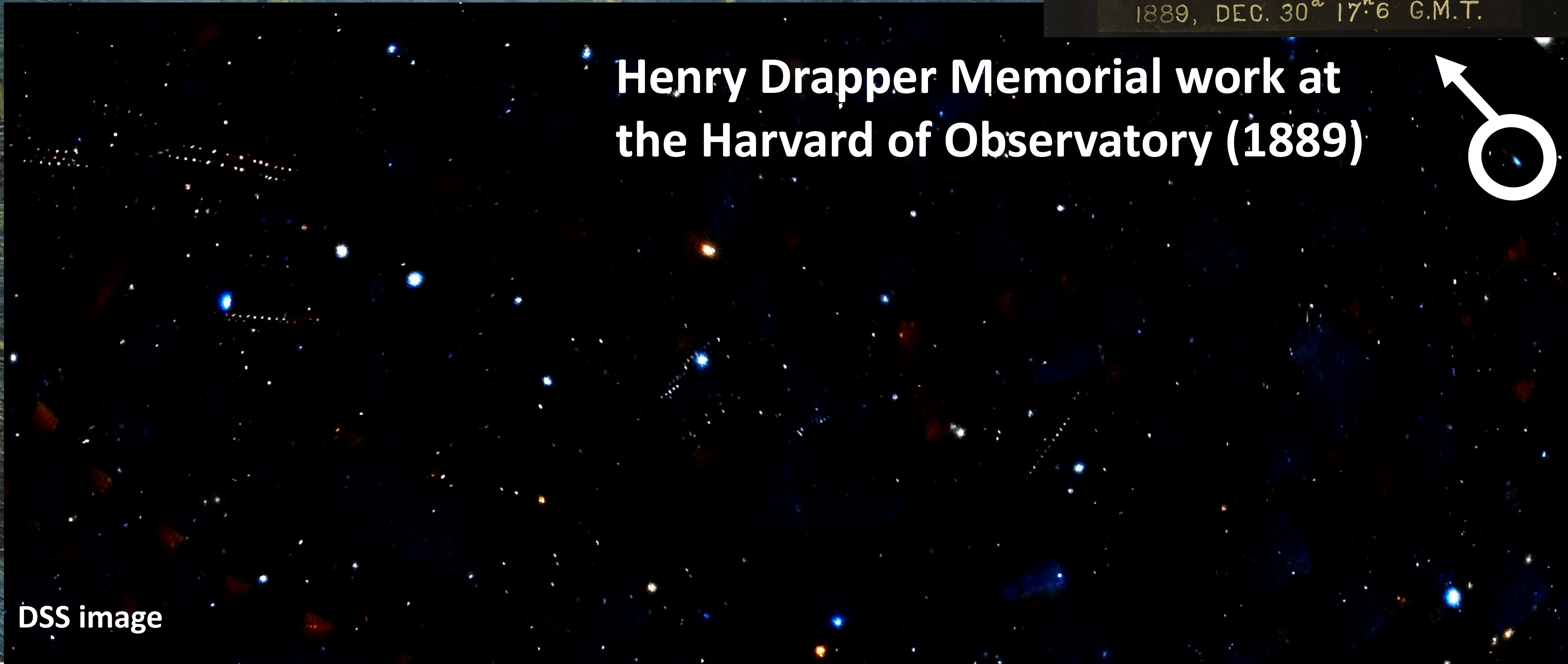

Spectroscopy

Angelo Secchi

William Huggins

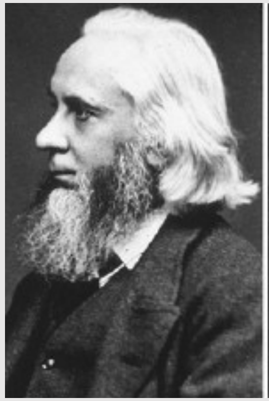

Margaret Lindsay Huggins

The Harvard computers

Charles Pickering

Antonia Maury

Annie Jump Cannon

Spectroscopy

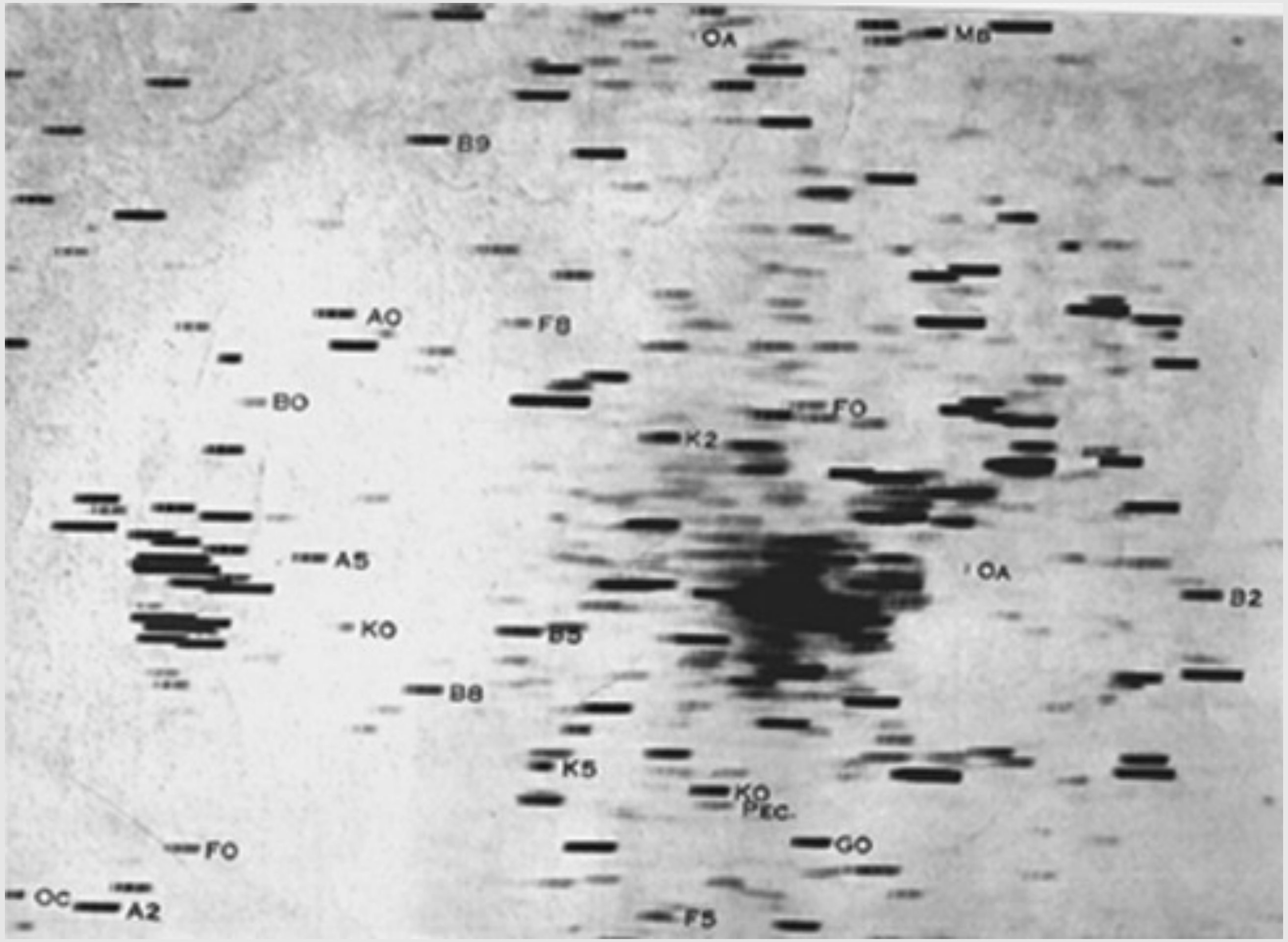

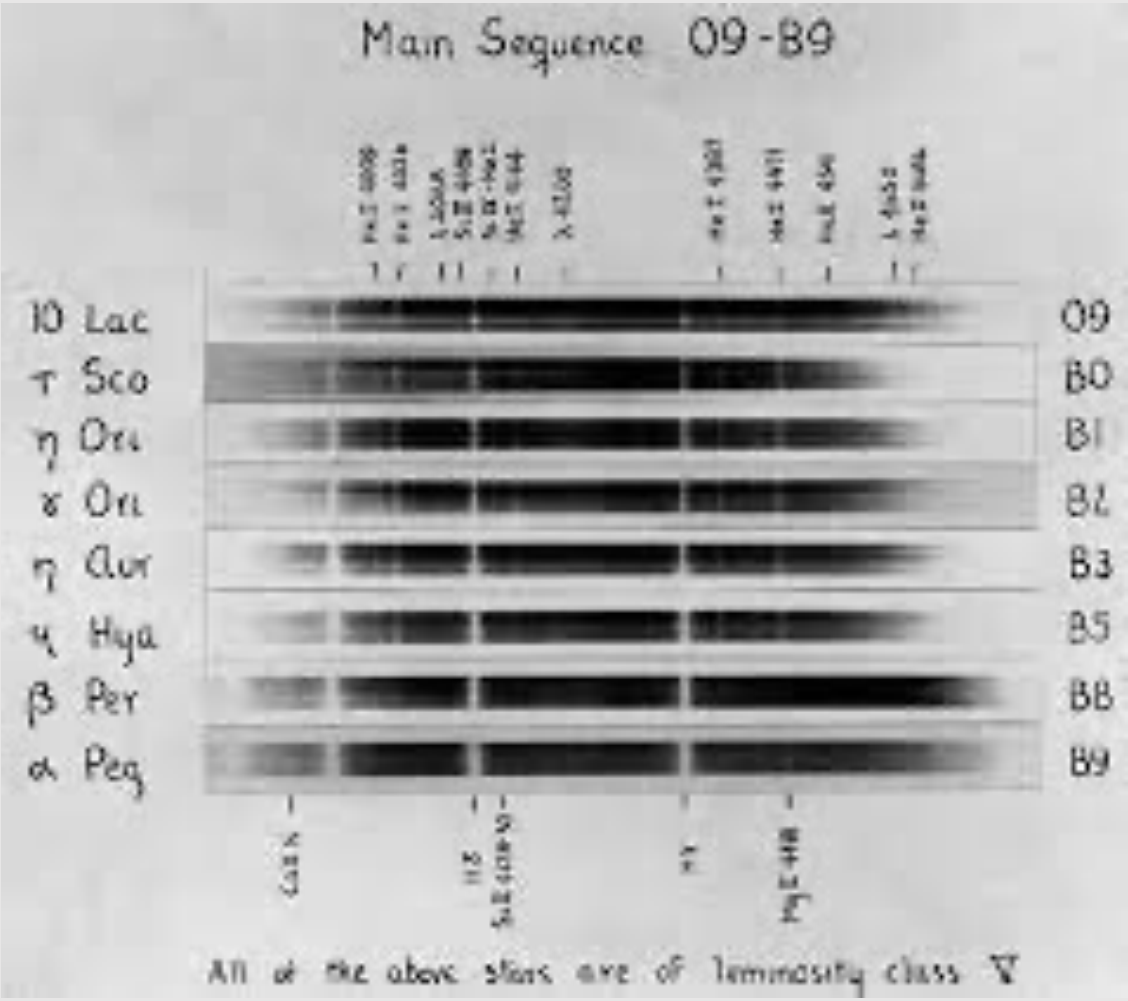

CARTE PHOTOGRAPHIQUE DU CIEL

Position du centre pour 1900 { Æ = 12h 48m ; D = + 20°

Zone +20° N° 97

Observatoire de Paris

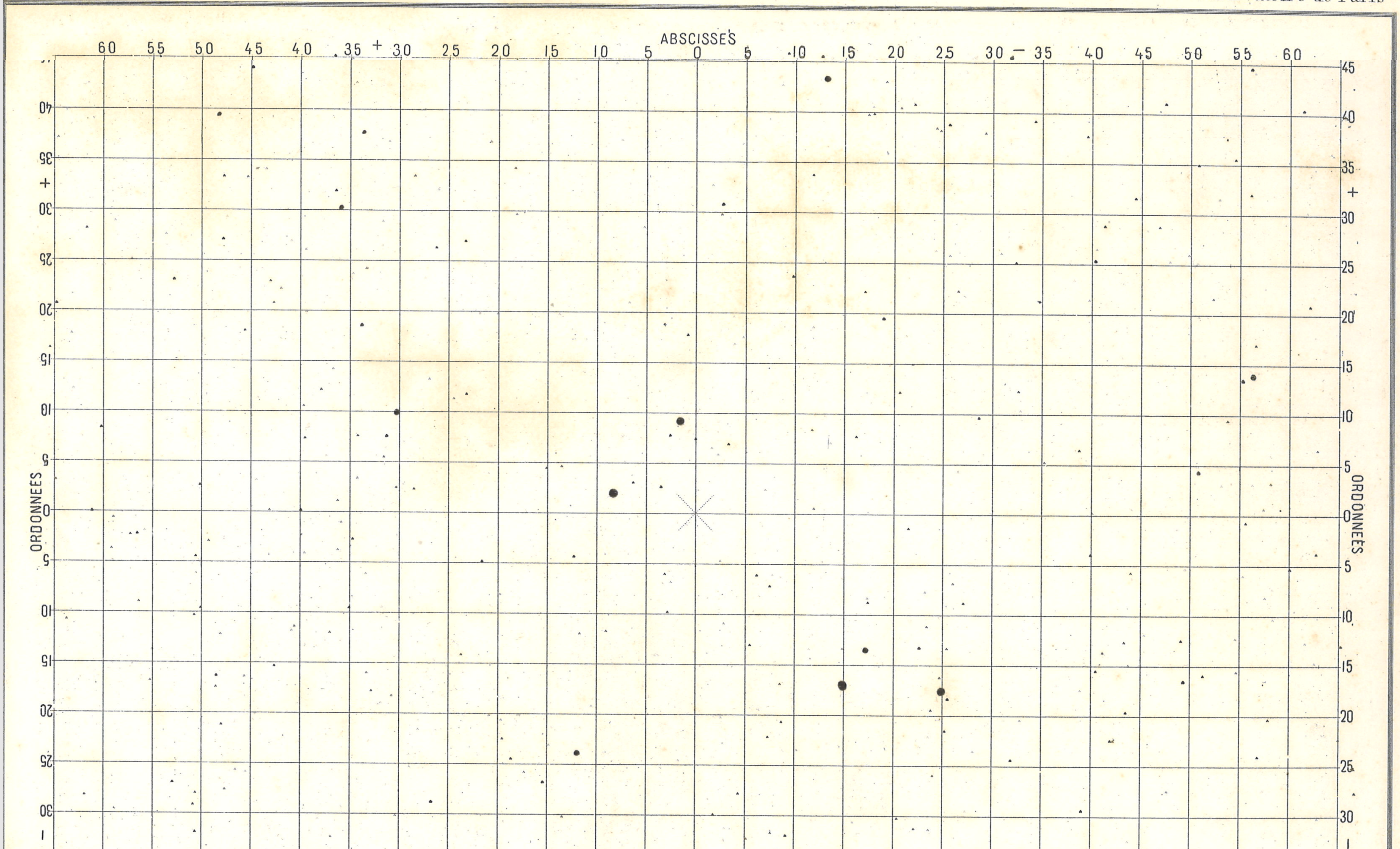

Atomic Physics Spectroscopy

- **Stellar physical parameters**
- **Chemical composition**
- **Line-of-sight velocity -> 3D motions**

Cecilia Payne

George Gamow

Hans Bethe

Margaret Burbidge

Atomic Physics

Spectroscopy

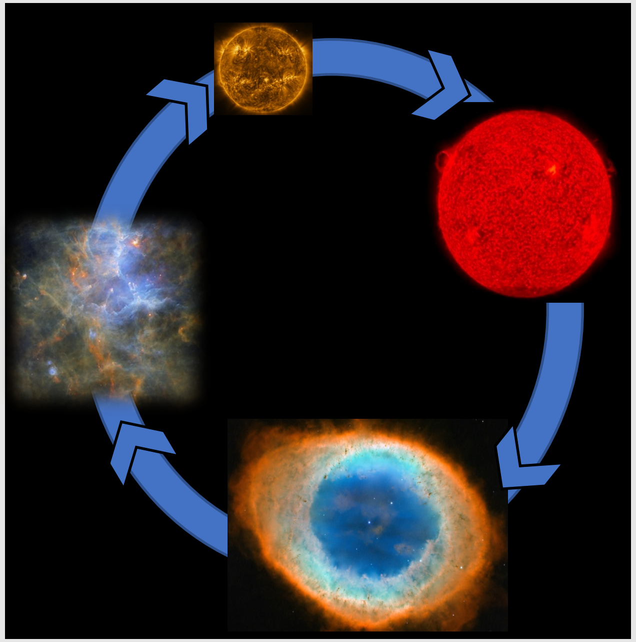

- Stellar physical parameters
- Chemical composition
- Line-of-sight velocity -> 3D motions

Evolution

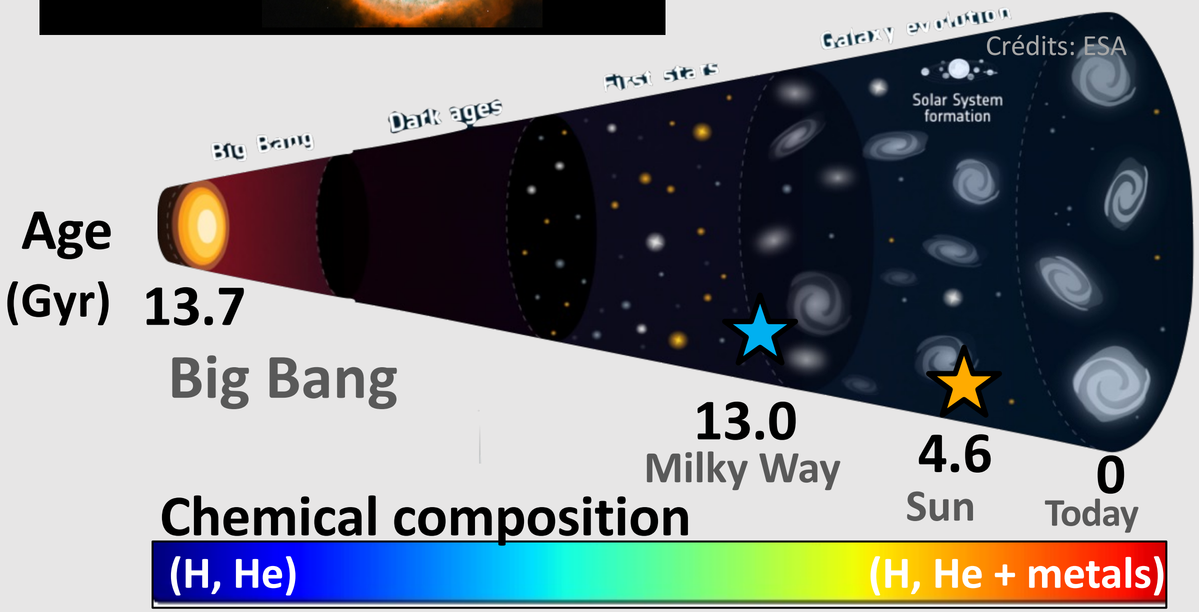

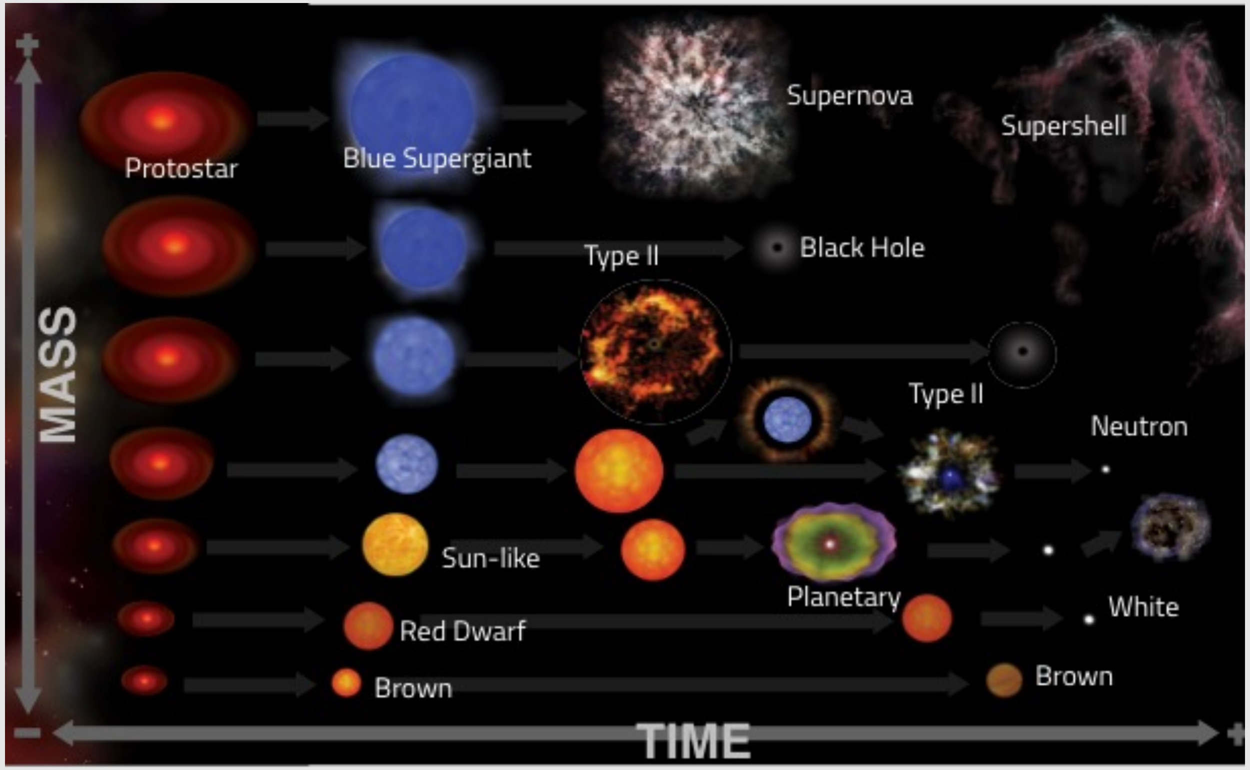

Gaia revolutions: roots and keys

Gaia combines the **astrometric** approach of **classical astronomy** with the **physical** approach of **modern astrophysics.**

This is enhanced by:

- High number statistics
- High precision
- Time series observations

Detailed evolution of the Galaxy in its environment

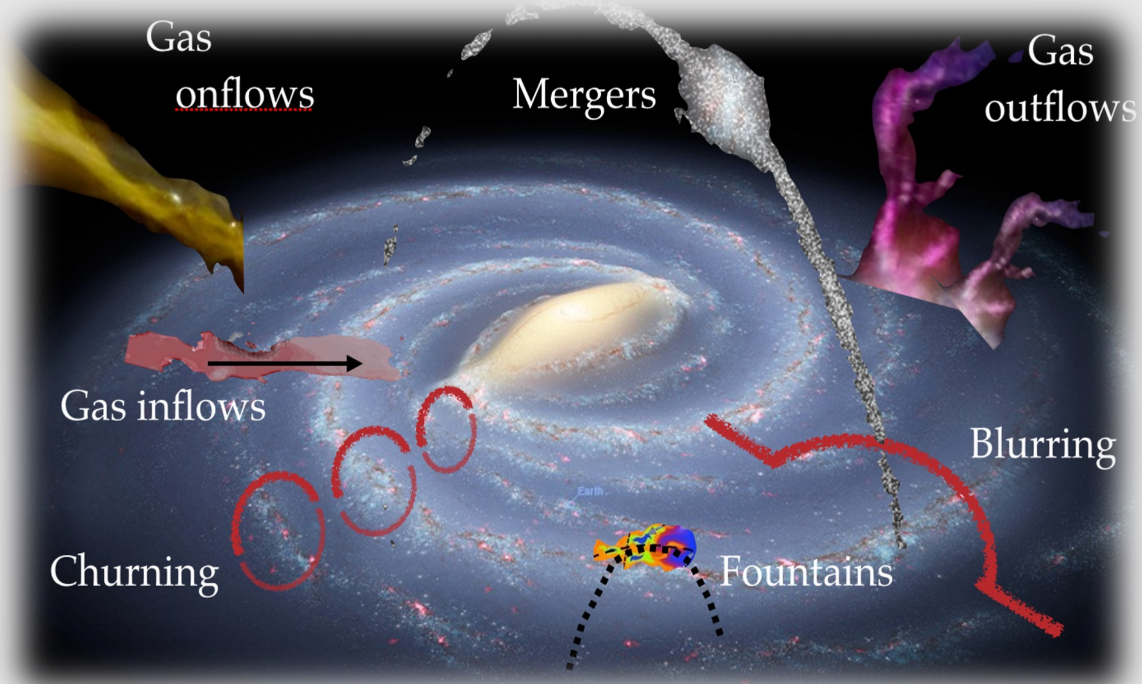

Gaia/RVS: a space spectroscopic survey

RVS

Resolving power:
11 500

Wavelength domain:
846 - 870 nm

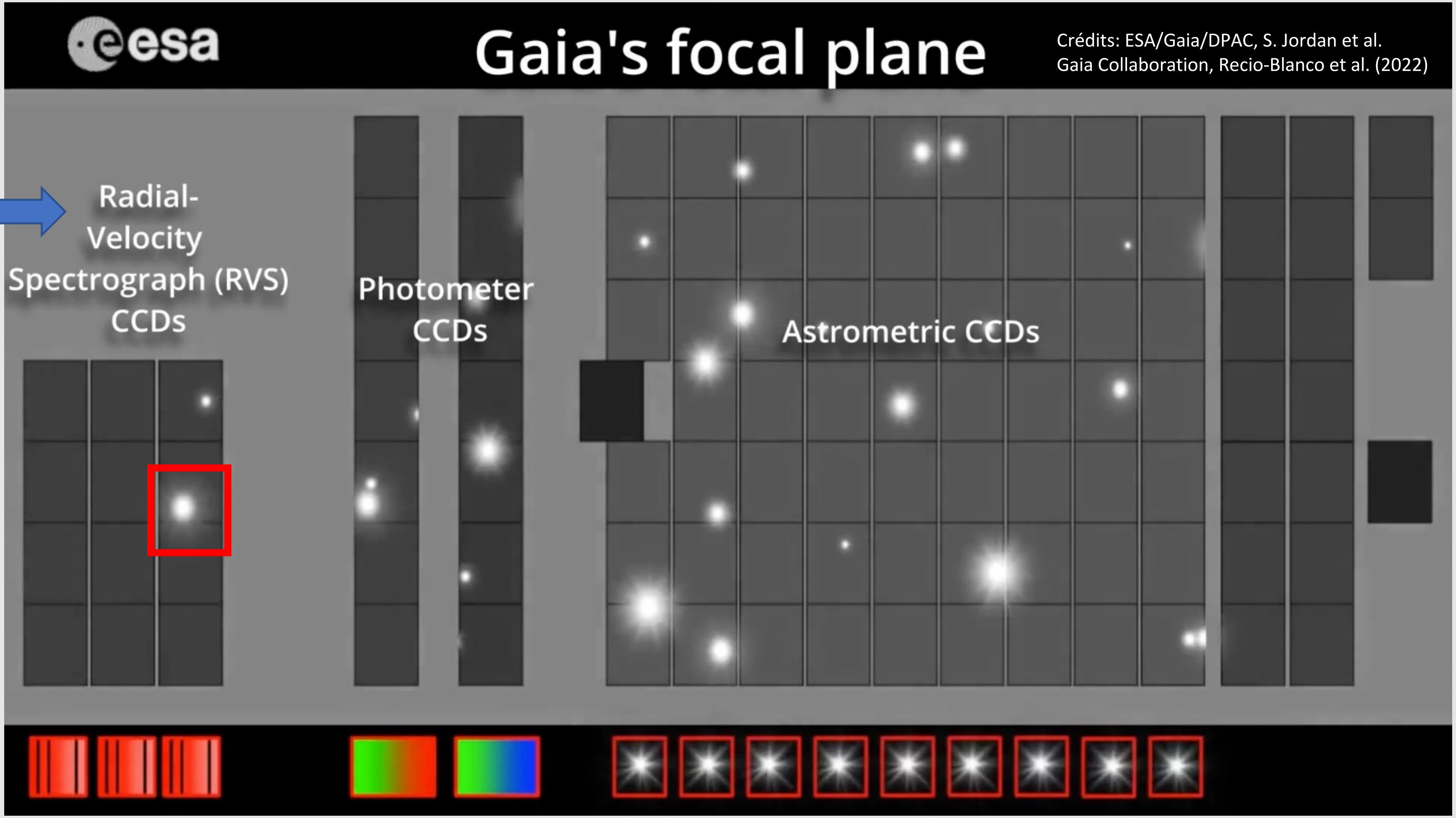

Gaia/RVS: a space spectroscopic survey

CU8/GSPspec: The chemical composition of 5.6 million stars

Apsis DPAC/CU8 pipeline

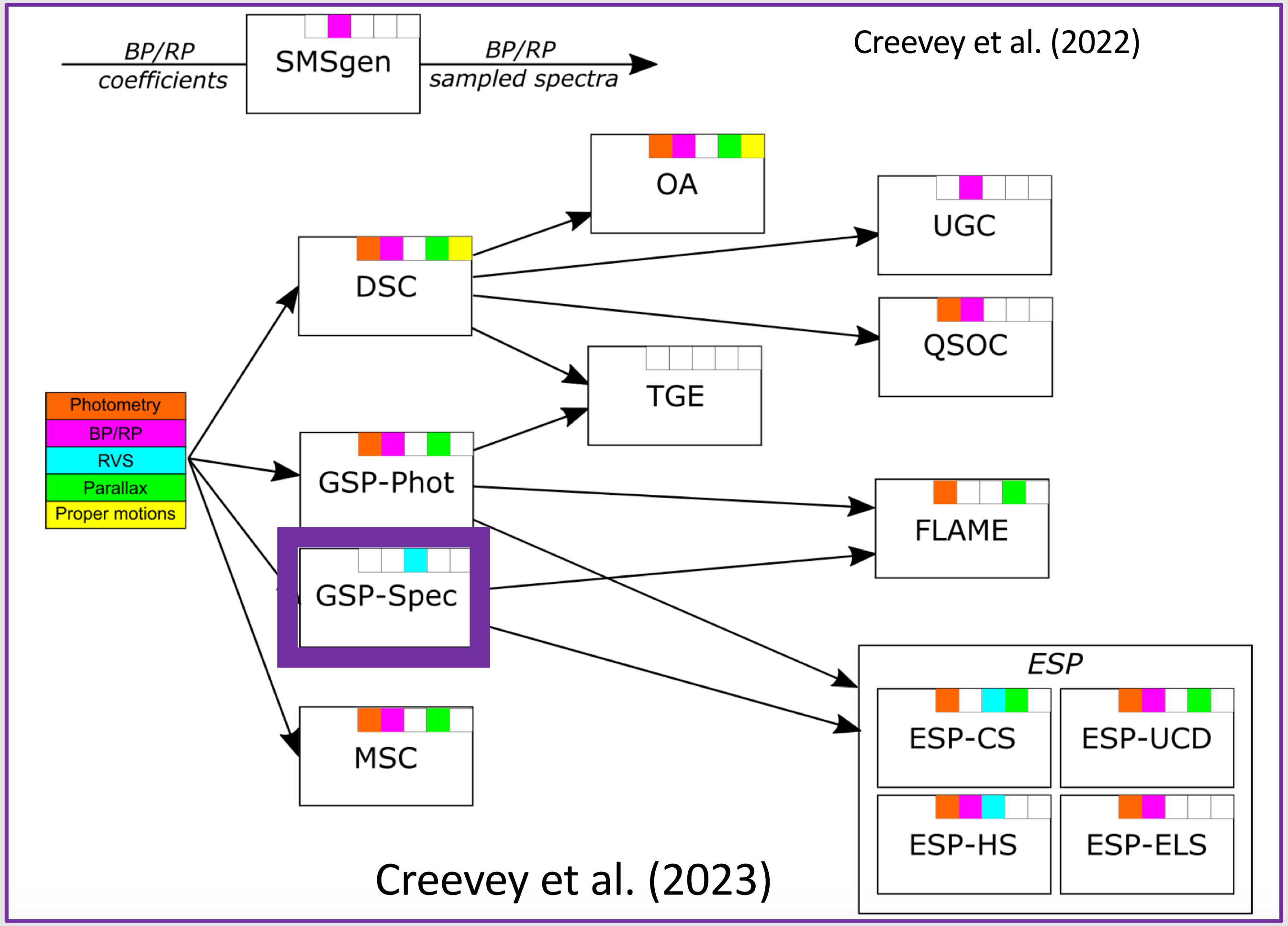

GSPspec (Recio-Blanco et al. 2023) is an up-stream module of the Astrophysical parameters inference system (Creevey et al. 2023)

Treats RVS stacked spectra produced by DPAC/CU6 (Katz et al. 2023)

Gaia/RVS/GSPspec   GSPspec (Recio-Blanco et al. 2023)

Gaia DPAC

MatisseGauguin

AstrophysicalParameters table in the Gaia Archive

Atmospheric Parameters
Individual chemical abundances
Differential CN EW
Diffuse Interstellar Band parameters

DR3 operations at DPCC (CNES-Toulouse)
6.9 million spectra treated
50 MC realisations of each RVS spectrum -> APs uncertainties
110 000 h spread on 2100 cores
Execution time= 150h
One second per spectrum

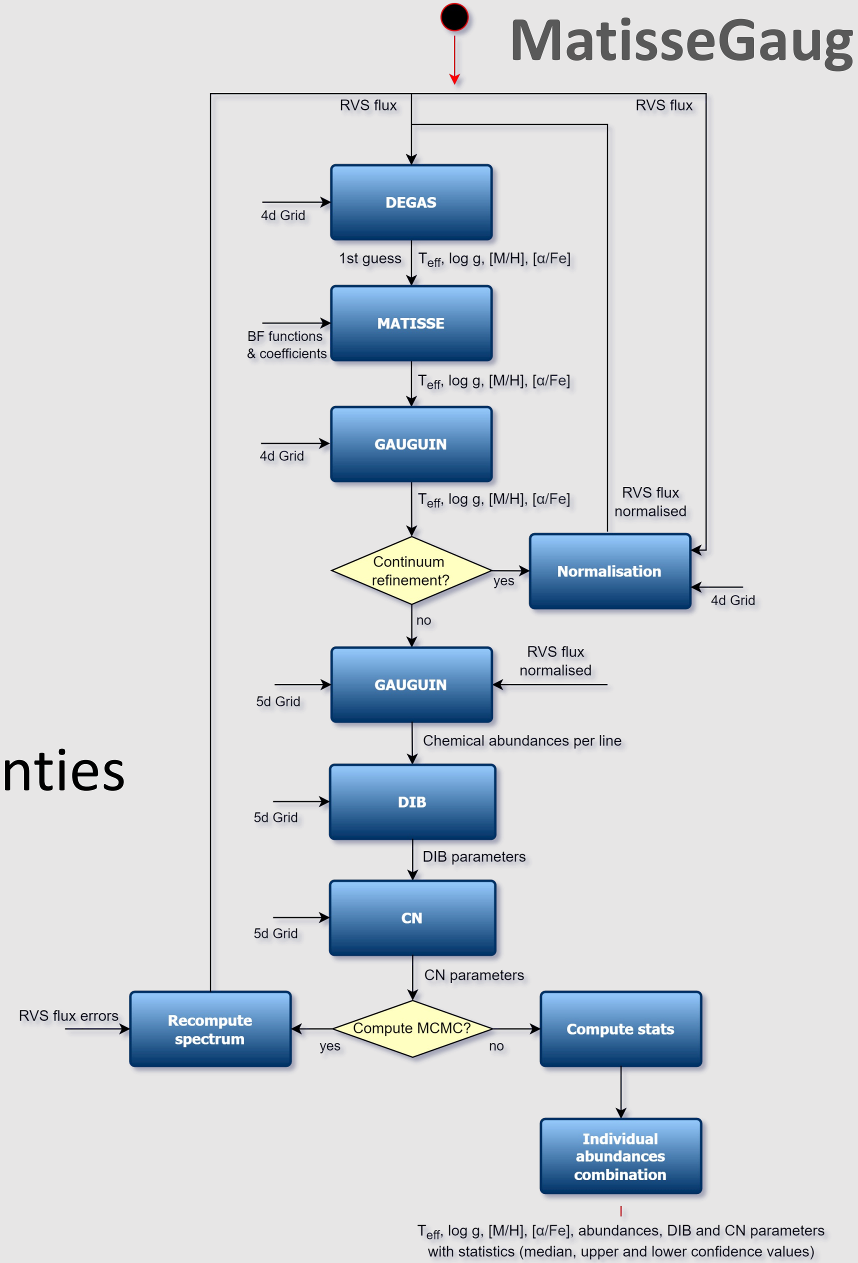

Inside the GSPSpec module:
MatisseGauguin workflow (parameters)

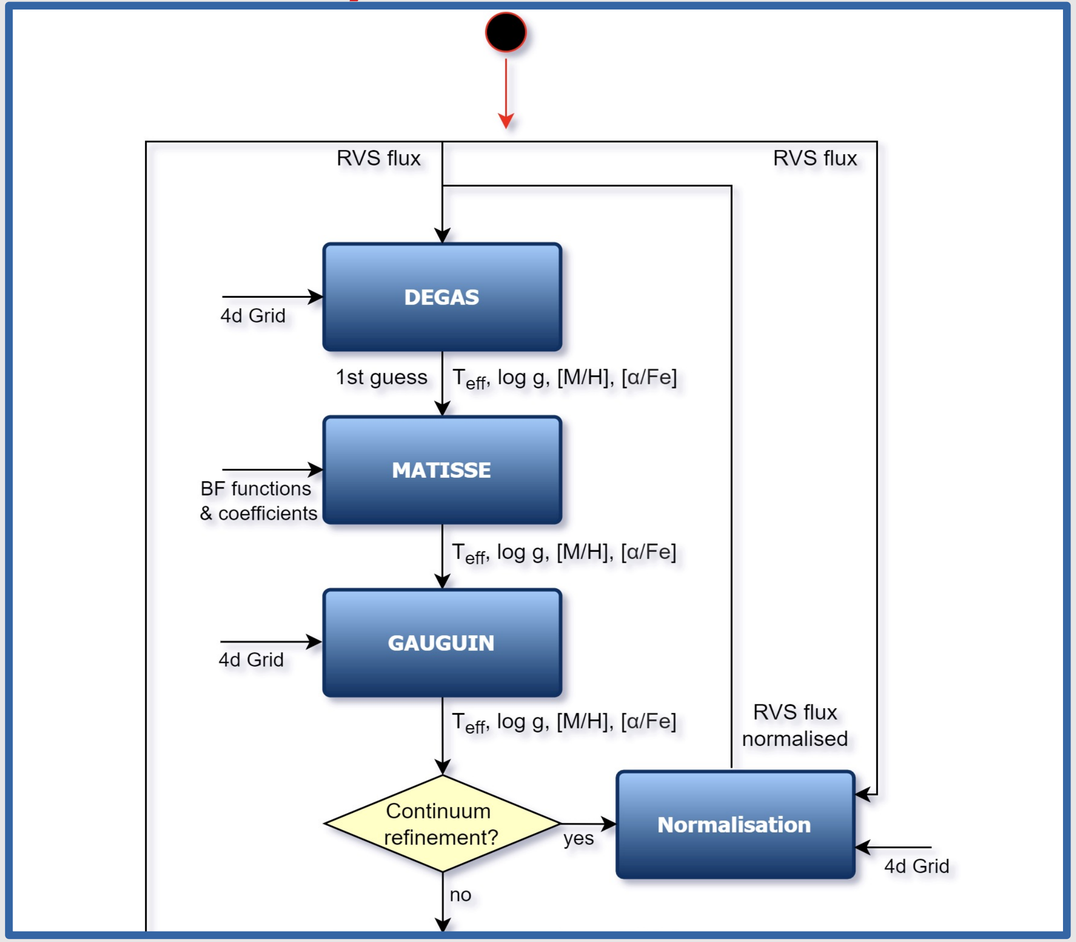

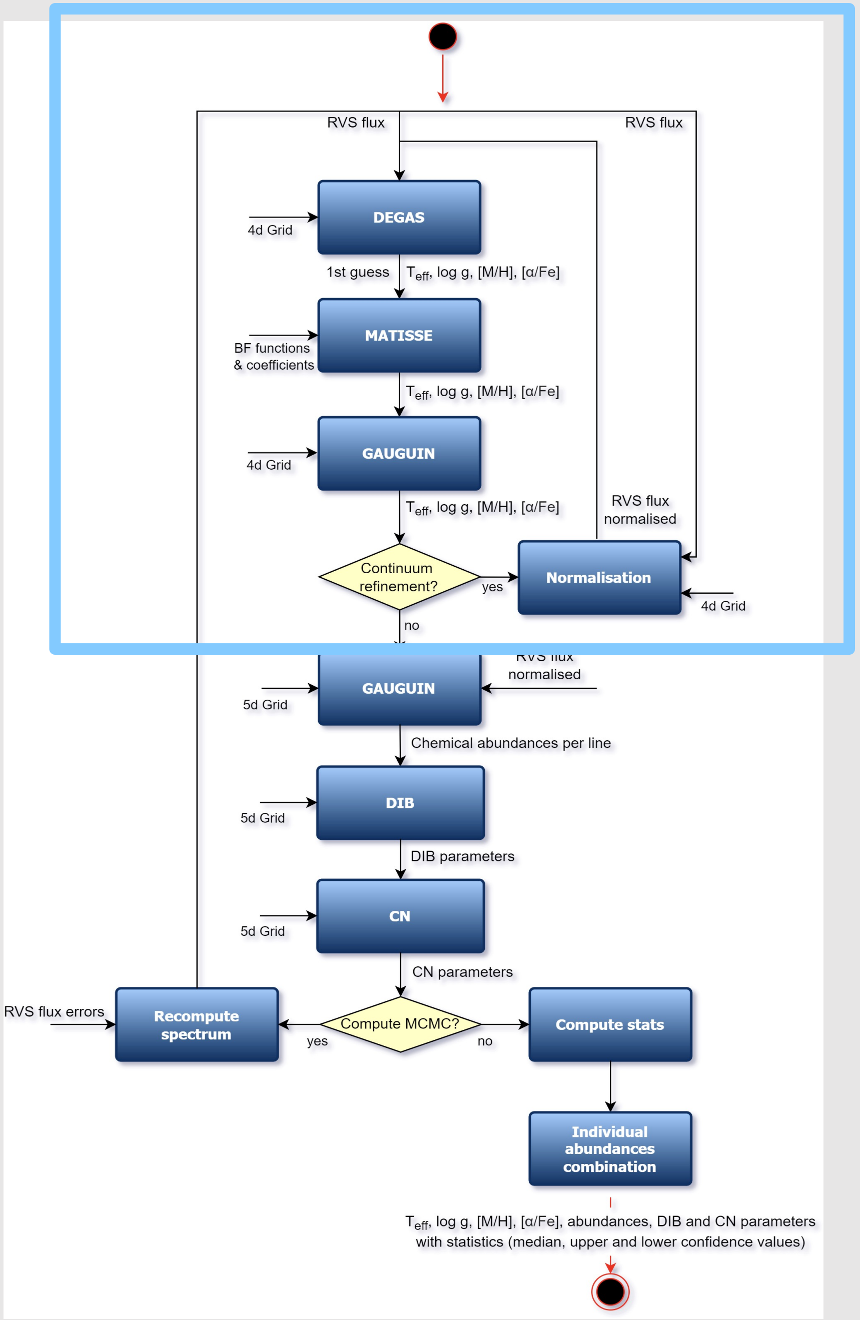

Gaia/RVS: a model driven success

- **MATISSE** : Recio-Blanco et al. 2006

Projection method. Local multilinear regression

Synthetic grid spectra

Correlation matrix

$c_{ij} = S_i S_j$

$$B_{\theta_i}(\lambda) = \sum_j \alpha_{ij} S_j(\lambda)$$

$$\Theta_i = C\alpha_i.$$

Training phase

Stellar parameters
Teff, logg, [M/H], [alpha/Fe]

Observed spectrum

$$\hat{\theta}_i = \sum_\lambda B_{\theta_i}(\lambda) O(\lambda).$$

Application phase

Inside the GSPSpec module: MatisseGauguin workflow (abundances)

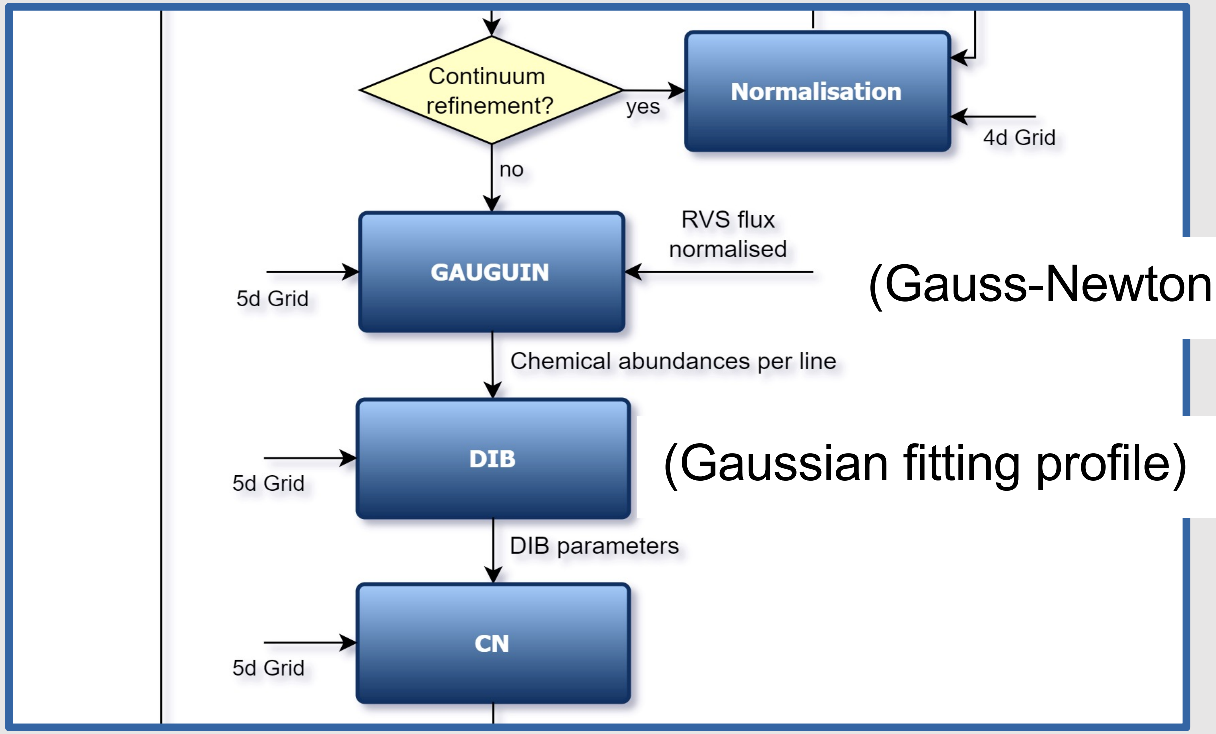

(Gauss-Newton)

(Gaussian fitting profile)

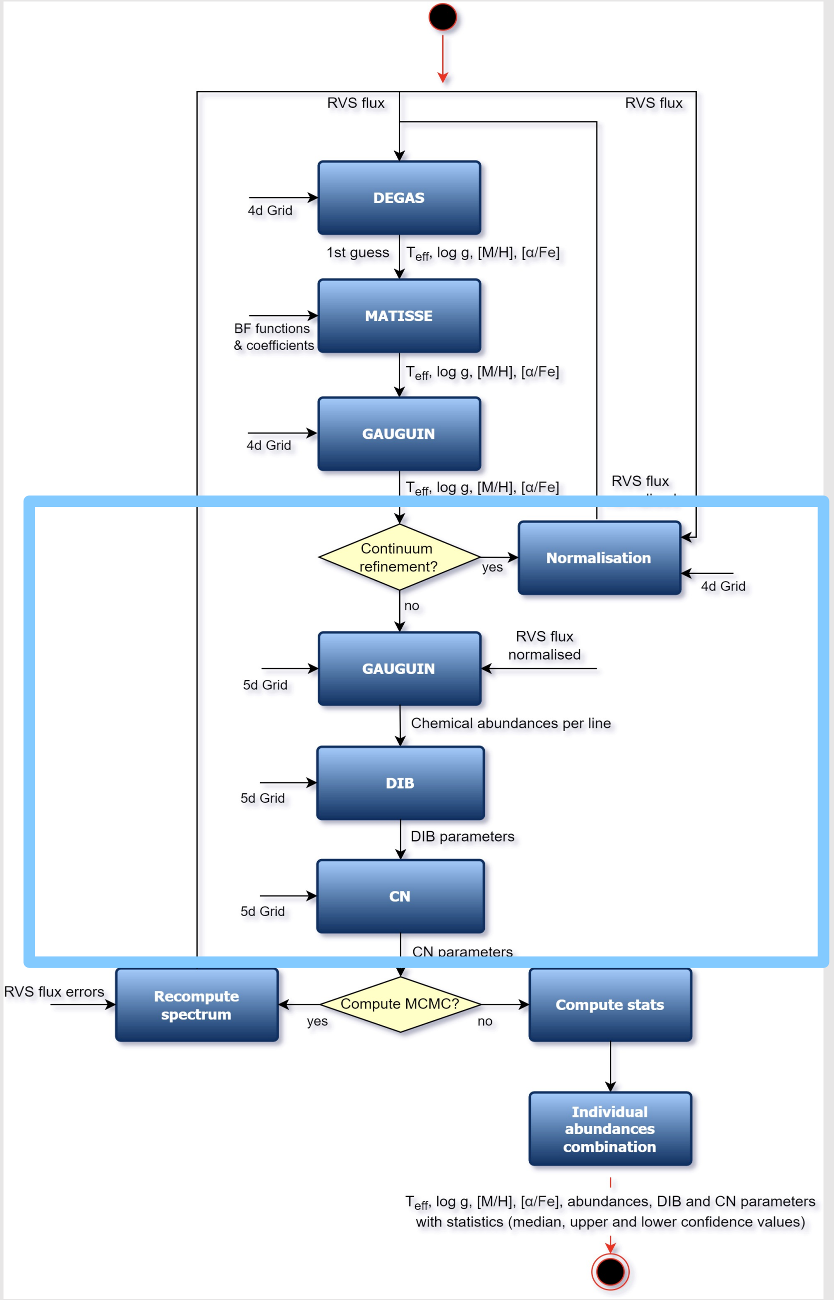

Gaia/RVS: a model driven success

- **GAUGUIN :** Bijaoui, Recio-Blanco et al. 2012

Optimization method. Gauss-Newton algorithm

Linearization around a parameter set Θ associated to a theoretical spectrum $\mathbf{S}_0$. Corrections obtained with:

Observed spectrum

Synthetic spectrum

$$\delta\Theta = (\mathbf{J}^T\mathbf{J})^{-1}\mathbf{J}^T(\mathbf{O} - \mathbf{S}_0)$$

Jacobian matrix $[\partial S(l, \Theta(0))/\partial\theta i]$

Used after MATISSE -> atmospheric parameters

Used alone -> individual chemical abundances

GAUGUIN is used **both** for the **atmospheric parameters** and the **chemical abundances**

Inside the GSPSpec module: MatisseGauguin workflow (errors)

Error propagation through **50 random realisations** of the input spectra using its error→ Loop over MatisseGauguin

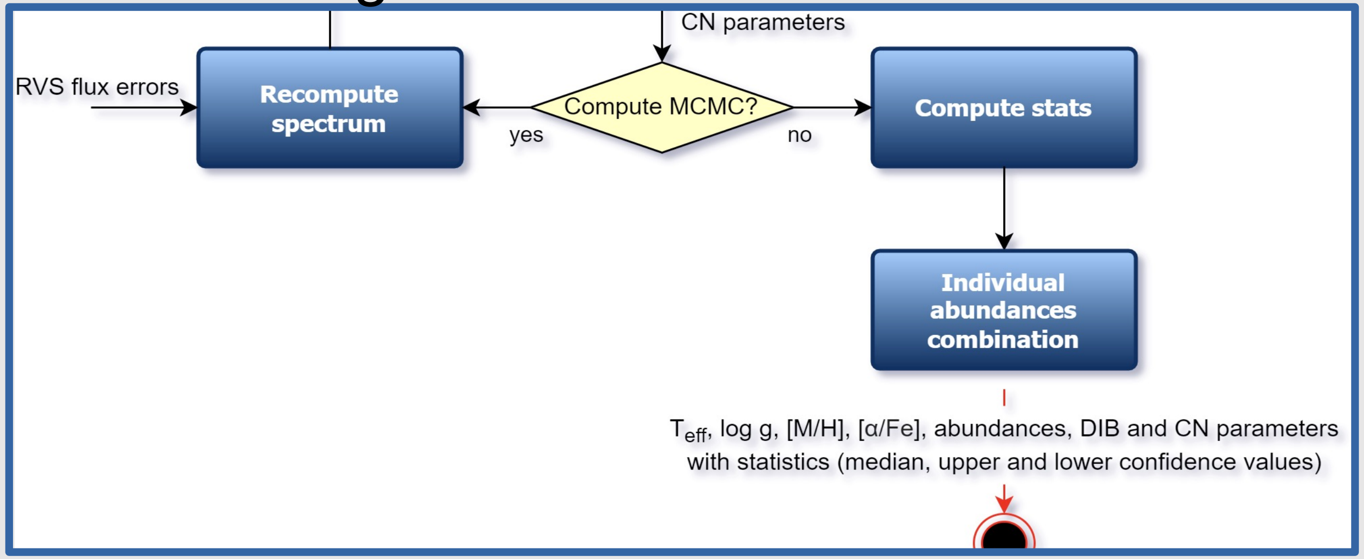

When finished, perform statistics, line combination, flags...

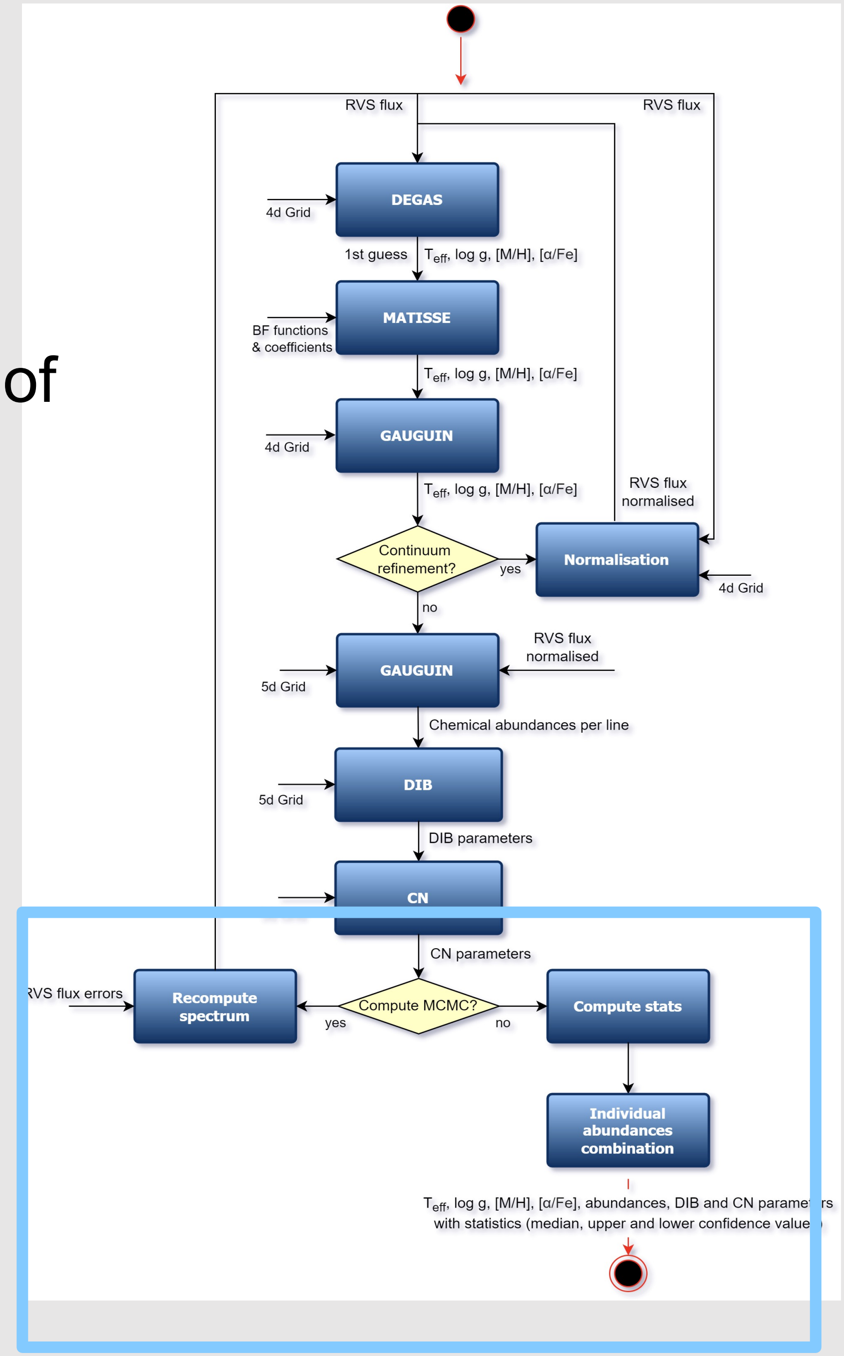

Synthetic spectra GRIDS:

MARCS atm. models
+
Turbospectrum

Added more nodes in the metal poor regime for Fe, Ca and Si

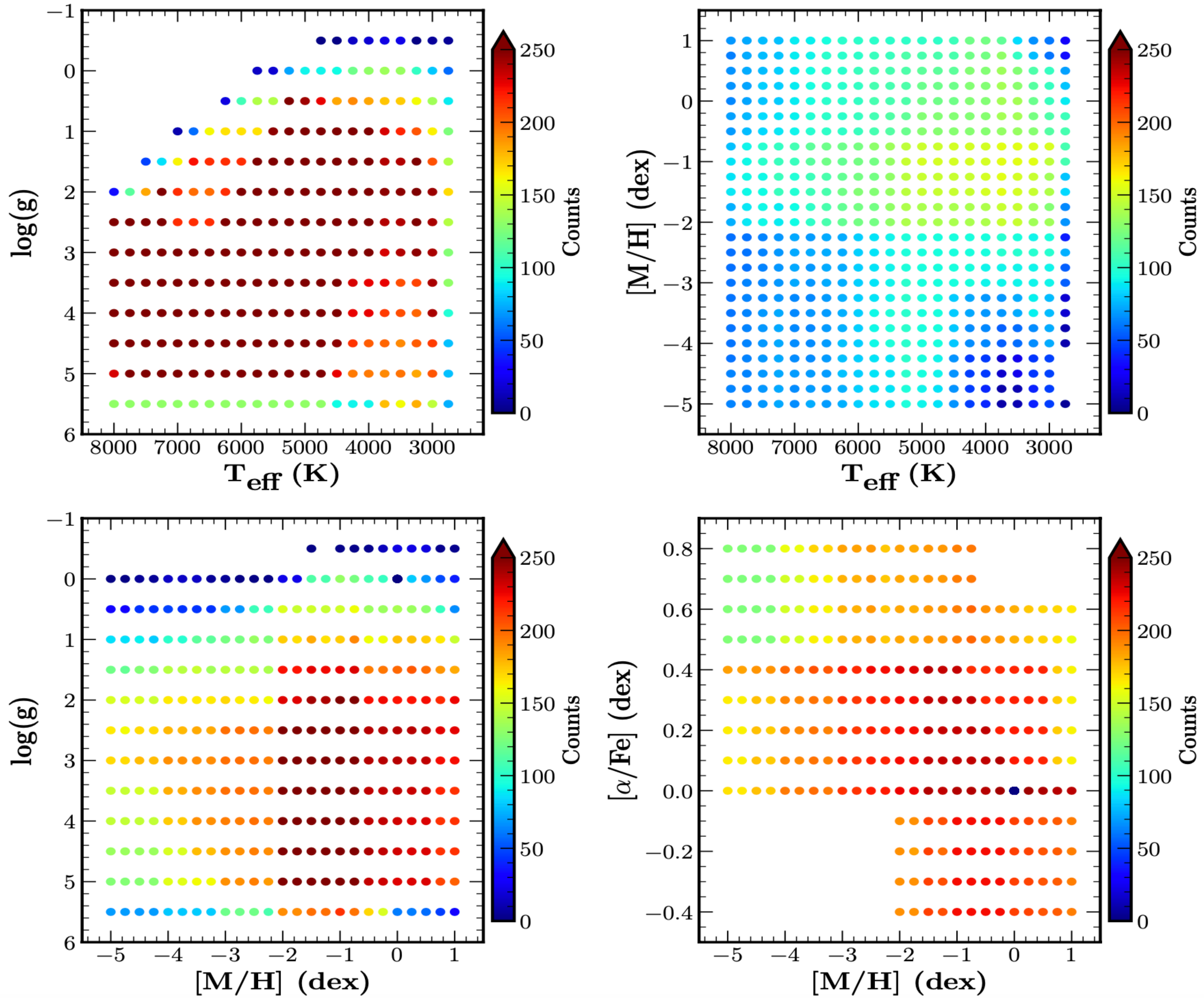

Synthetic spectra GRIDS:

MARCS atm. Models + Turbospectrum

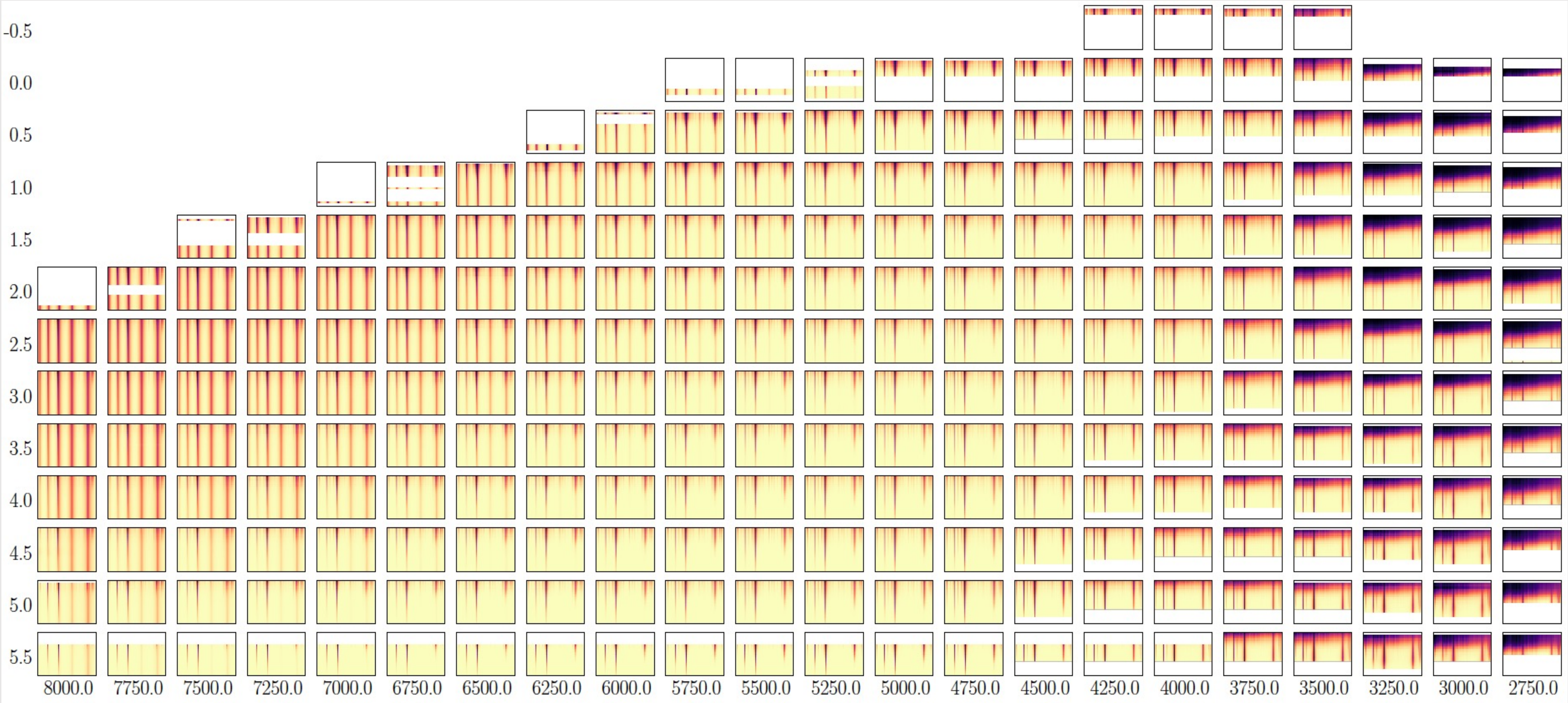

Atomic lines:

33 lines selected after several quality evaluation test and inspection
See Recio-Blanco et al. 2023 and Contursi et al. 2021

Elt	λ	λ_{ab}^{-}	λ_{ab}^{+}	λ_{norm}^{-}	λ_{norm}^{+}
N I	863.161	863.071	863.281	862.891	863.371
N I	868.579	868.489	868.699	868.309	868.939
Mg I	847.602	847.512	847.692	847.212	847.812
Si I	853.851	853.731	853.941	853.371	854.961
*Si I	855.916	855.856	856.036	855.376	856.156
Si I	868.872	868.782	868.992	868.602	869.232
*S I	867.258	866.988	867.378	866.898	867.998
*S I	869.701	869.551	869.821	869.281	869.971
Ca I	863.631	863.511	863.691	863.361	863.931
Ca II	849.856	849.706	849.976	849.586	850.276
Ca II	850.216	850.156	850.276	849.886	850.306
Ca II	854.264	854.114	854.384	853.544	854.864
Ca II	854.624	854.564	854.744	854.294	854.804
Ca II	866.272	866.152	866.332	866.002	866.572
Ca II	866.632	866.512	866.692	866.302	866.782
*Ti I	852.069	851.979	852.129	851.799	852.249
Ti I	857.209	857.119	857.269	856.999	857.359
Ti I	869.472	869.382	869.562	869.292	869.832
Cr I	855.118	855.058	855.208	854.878	855.478
Cr I	864.567	864.447	864.627	864.207	864.867
*Fe I	848.296	848.206	848.446	847.666	848.896
*Fe I	851.641	851.551	851.851	851.281	852.001
*Fe I	852.901	852.691	853.081	852.481	853.321
Fe I	857.416	857.296	857.506	856.876	858.166
Fe I	858.462	858.312	858.612	858.132	858.762
Fe I	862.397	862.277	862.517	862.127	862.697
Fe I	867.713	867.593	867.863	867.443	868.013
*Fe I	869.101	868.891	869.191	868.441	869.821
Fe II	858.794	858.764	858.824	858.254	859.274
Ni I	863.937	863.847	864.027	863.697	864.147
Zr II	852.748	852.658	852.838	852.388	853.018
*Ce II	851.375	851.285	851.465	851.015	851.555
Nd II	859.389	859.299	859.479	859.209	859.689

Atomic lines:

Each line has its own window for **an additional normalisation** (see Santos-Peral et al. 2020)

Elt	λ	λ^{-}_{ab}	λ^{+}_{ab}	λ^{-}_{norm}	λ^{+}_{norm}
N I	863.161	863.071	863.281	862.891	863.371
N I	868.579	868.489	868.699	868.309	868.939
Mg I	847.602	847.512	847.692	847.212	847.812
Si I	853.851	853.731	853.941	853.371	854.961
*Si I	855.916	855.856	856.036	855.376	856.156
Si I	868.872	868.782	868.992	868.602	869.232
*S I	867.258	866.988	867.378	866.898	867.998
*S I	869.701	869.551	869.821	869.281	869.971
Ca I	863.631	863.511	863.691	863.361	863.931
Ca II	849.856	849.706	849.976	849.586	850.276
Ca II	850.216	850.156	850.276	849.886	850.306
Ca II	854.264	854.114	854.384	853.544	854.864
Ca II	854.624	854.564	854.744	854.294	854.804
Ca II	866.272	866.152	866.332	866.002	866.572
Ca II	866.632	866.512	866.692	866.302	866.782
*Ti I	852.069	851.979	852.129	851.799	852.249
Ti I	857.209	857.119	857.269	856.999	857.359
Ti I	869.472	869.382	869.562	869.292	869.832
Cr I	855.118	855.058	855.208	854.878	855.478
Cr I	864.567	864.447	864.627	864.207	864.867
*Fe I	848.296	848.206	848.446	847.666	848.896
*Fe I	851.641	851.551	851.851	851.281	852.001
*Fe I	852.901	852.691	853.081	852.481	853.321
Fe I	857.416	857.296	857.506	856.876	858.166
Fe I	858.462	858.312	858.612	858.132	858.762
Fe I	862.397	862.277	862.517	862.127	862.697
Fe I	867.713	867.593	867.863	867.443	868.013
*Fe I	869.101	868.891	869.191	868.441	869.821
Fe II	858.794	858.764	858.824	858.254	859.274
Ni I	863.937	863.847	864.027	863.697	864.147
Zr II	852.748	852.658	852.838	852.388	853.018
*Ce II	851.375	851.285	851.465	851.015	851.555
Nd II	859.389	859.299	859.479	859.209	859.689

Atomic lines:

Also, each line has a different abundance determination window depending on the blends, presence of other lines...

Elt	λ	λ^-_{ab}	λ^+_{ab}	λ^-_{norm}	λ^+_{norm}
N I	863.161	863.071	863.281	862.891	863.371
N I	868.579	868.489	868.699	868.309	868.939
Mg I	847.602	847.512	847.692	847.212	847.812
Si I	853.851	853.731	853.941	853.371	854.961
*Si I	855.916	855.856	856.036	855.376	856.156
Si I	868.872	868.782	868.992	868.602	869.232
*S I	867.258	866.988	867.378	866.898	867.998
*S I	869.701	869.551	869.821	869.281	869.971
Ca I	863.631	863.511	863.691	863.361	863.931
Ca II	849.856	849.706	849.976	849.586	850.276
Ca II	850.216	850.156	850.276	849.886	850.306
Ca II	854.264	854.114	854.384	853.544	854.864
Ca II	854.624	854.564	854.744	854.294	854.804
Ca II	866.272	866.152	866.332	866.002	866.572
Ca II	866.632	866.512	866.692	866.302	866.782
*Ti I	852.069	851.979	852.129	851.799	852.249
Ti I	857.209	857.119	857.269	856.999	857.359
Ti I	869.472	869.382	869.562	869.292	869.832
Cr I	855.118	855.058	855.208	854.878	855.478
Cr I	864.567	864.447	864.627	864.207	864.867
*Fe I	848.296	848.206	848.446	847.666	848.896
*Fe I	851.641	851.551	851.851	851.281	852.001
*Fe I	852.901	852.691	853.081	852.481	853.321
Fe I	857.416	857.296	857.506	856.876	858.166
Fe I	858.462	858.312	858.612	858.132	858.762
Fe I	862.397	862.277	862.517	862.127	862.697
Fe I	867.713	867.593	867.863	867.443	868.013
*Fe I	869.101	868.891	869.191	868.441	869.821
Fe II	858.794	858.764	858.824	858.254	859.274
Ni I	863.937	863.847	864.027	863.697	864.147
Zr II	852.748	852.658	852.838	852.388	853.018
*Ce II	851.375	851.285	851.465	851.015	851.555
Nd II	859.389	859.299	859.479	859.209	859.689

Atomic lines:

Calcium triplet is special: abundance measurement looking at the "wings"

Elt	λ	λ^-_{ab}	λ^+_{ab}	λ^-_{norm}	λ^+_{norm}
N I	863.161	863.071	863.281	862.891	863.371
N I	868.579	868.489	868.699	868.309	868.939
Mg I	847.602	847.512	847.692	847.212	847.812
Si I	853.851	853.731	853.941	853.371	854.961
*Si I	855.916	855.856	856.036	855.376	856.156
Si I	868.872	868.782	868.992	868.602	869.232
*S I	867.258	866.988	867.378	866.898	867.998
*S I	869.701	869.551	869.821	869.281	869.971
Ca I	863.631	863.511	863.691	863.361	863.931
Ca II	849.856	849.706	849.976	849.586	850.276
Ca II	850.216	850.156	850.276	849.886	850.306
Ca II	854.264	854.114	854.384	853.544	854.864
Ca II	854.624	854.564	854.744	854.294	854.804
Ca II	866.272	866.152	866.332	866.002	866.572
Ca II	866.632	866.512	866.692	866.302	866.782
*Ti I	852.069	851.979	852.129	851.799	852.249
Ti I	857.209	857.119	857.269	856.999	857.359
Ti I	869.472	869.382	869.562	869.292	869.832
Cr I	855.118	855.058	855.208	854.878	855.478
Cr I	864.567	864.447	864.627	864.207	864.867
*Fe I	848.296	848.206	848.446	847.666	848.896
*Fe I	851.641	851.551	851.851	851.281	852.001
*Fe I	852.901	852.691	853.081	852.481	853.321
Fe I	857.416	857.296	857.506	856.876	858.166
Fe I	858.462	858.312	858.612	858.132	858.762
Fe I	862.397	862.277	862.517	862.127	862.697
Fe I	867.713	867.593	867.863	867.443	868.013
*Fe I	869.101	868.891	869.191	868.441	869.821
Fe II	858.794	858.764	858.824	858.254	859.274
Ni I	863.937	863.847	864.027	863.697	864.147
Zr II	852.748	852.658	852.838	852.388	853.018
*Ce II	851.375	851.285	851.465	851.015	851.555
Nd II	859.389	859.299	859.479	859.209	859.689

Atomic lines:

Some doublets/triplets or consecutive lines of the same element are treated as a unique line.
(but the individual line cases have also been tested)

Elt	λ	λ^{-}_{ab}	λ^{+}_{ab}	λ^{-}_{norm}	λ^{+}_{norm}
N I	863.161	863.071	863.281	862.891	863.371
N I	868.579	868.489	868.699	868.309	868.939
Mg I	847.602	847.512	847.692	847.212	847.812
Si I	853.851	853.731	853.941	853.371	854.961
*Si I	855.916	855.856	856.036	855.376	856.156
Si I	868.872	868.782	868.992	868.602	869.232
*S I	867.258	866.988	867.378	866.898	867.998
*S I	869.701	869.551	869.821	869.281	869.971
Ca I	863.631	863.511	863.691	863.361	863.931
Ca II	849.856	849.706	849.976	849.586	850.276
Ca II	850.216	850.156	850.276	849.886	850.306
Ca II	854.264	854.114	854.384	853.544	854.864
Ca II	854.624	854.564	854.744	854.294	854.804
Ca II	866.272	866.152	866.332	866.002	866.572
Ca II	866.632	866.512	866.692	866.302	866.782
*Ti I	852.069	851.979	852.129	851.799	852.249
Ti I	857.209	857.119	857.269	856.999	857.359
Ti I	869.472	869.382	869.562	869.292	869.832
Cr I	855.118	855.058	855.208	854.878	855.478
Cr I	864.567	864.447	864.627	864.207	864.867
*Fe I	848.296	848.206	848.446	847.666	848.896
*Fe I	851.641	851.551	851.851	851.281	852.001
*Fe I	852.901	852.691	853.081	852.481	853.321
Fe I	857.416	857.296	857.506	856.876	858.166
Fe I	858.462	858.312	858.612	858.132	858.762
Fe I	862.397	862.277	862.517	862.127	862.697
Fe I	867.713	867.593	867.863	867.443	868.013
*Fe I	869.101	868.891	869.191	868.441	869.821
Fe II	858.794	858.764	858.824	858.254	859.274
Ni I	863.937	863.847	864.027	863.697	864.147
Zr II	852.748	852.658	852.838	852.388	853.018
*Ce II	851.375	851.285	851.465	851.015	851.555
Nd II	859.389	859.299	859.479	859.209	859.689

Gaia/RVS: a space spectroscopic survey

CU8/GSPspec: The chemical composition of 5.6 million stars

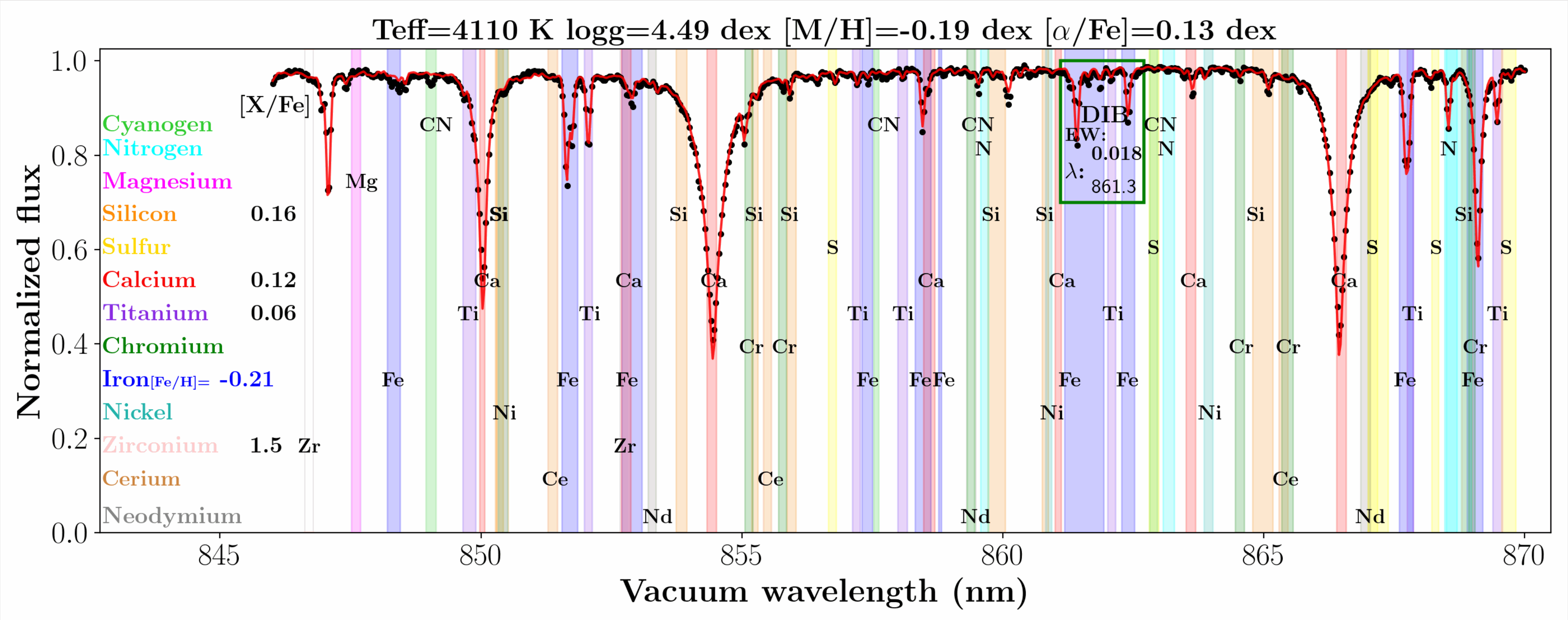

Credits:ESA/GAIA/DPAC-CU8-CU6 Recio-Blanco and the GSPspec team

Galactic alchemists

Different nucleosynthetic channels

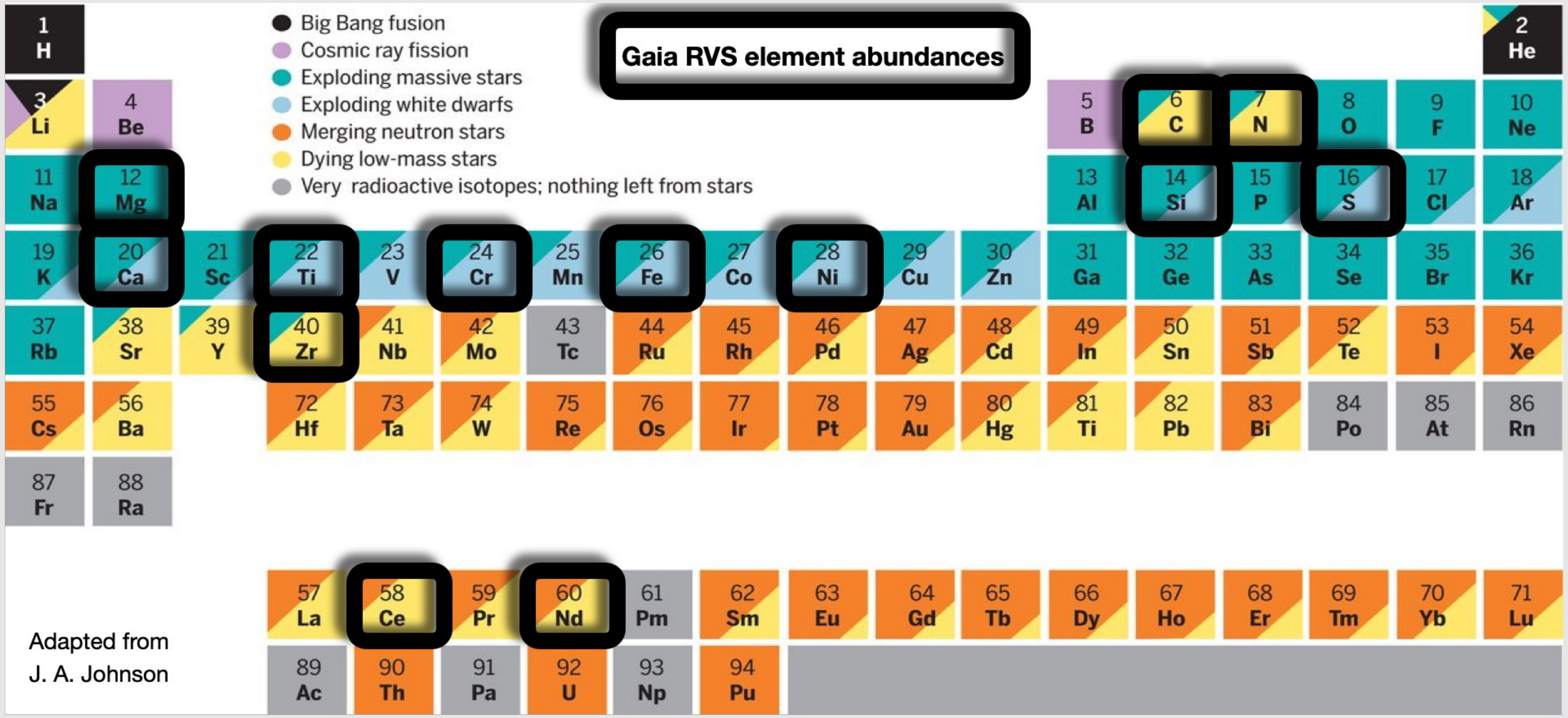

credits C. Chiappini

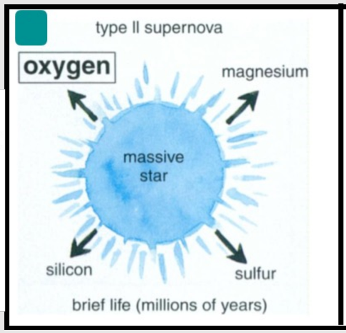

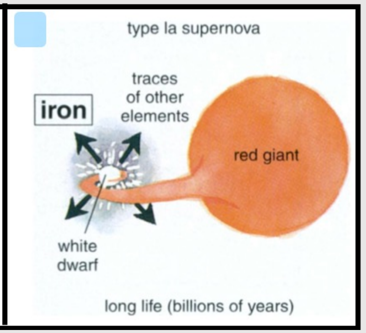

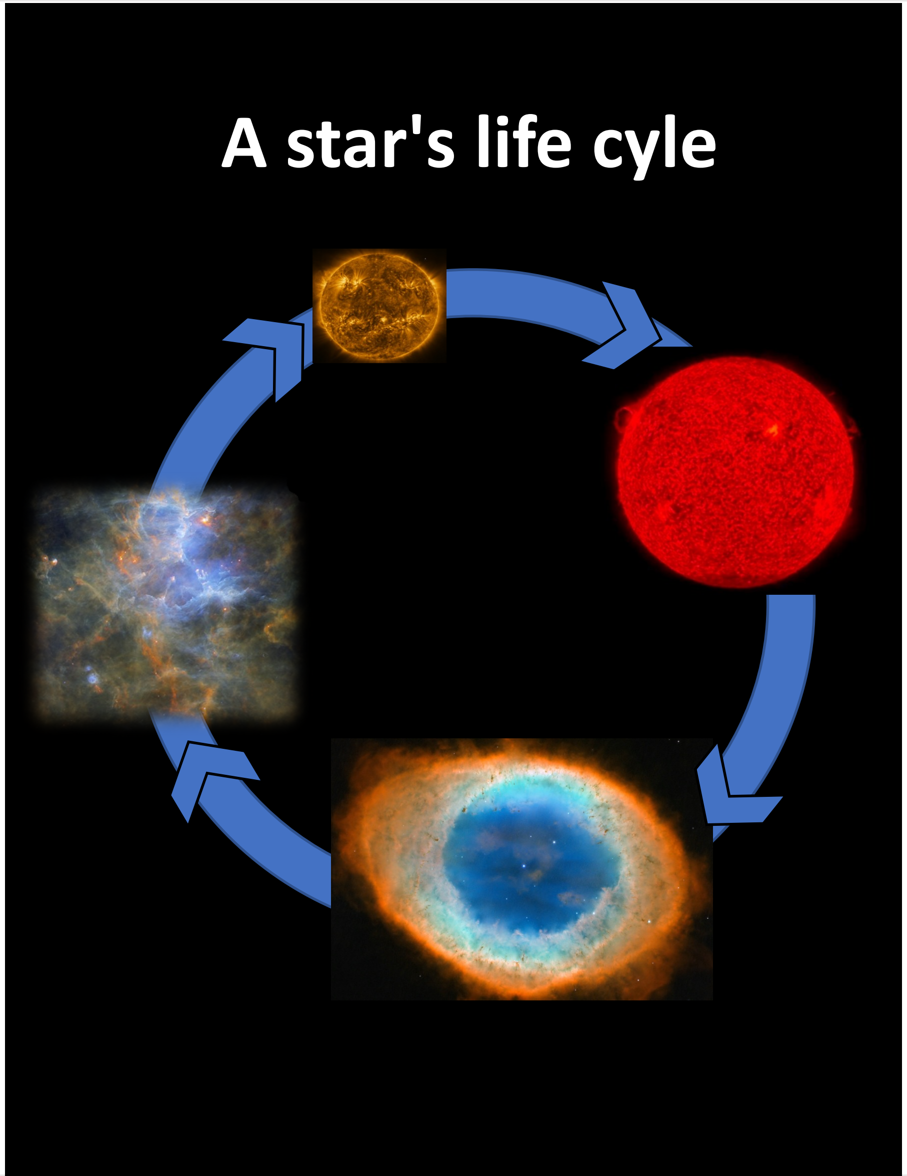

Gaia/RVS: a space spectroscopic survey

CU8/GSPspec: The chemical composition of 5.6 million stars

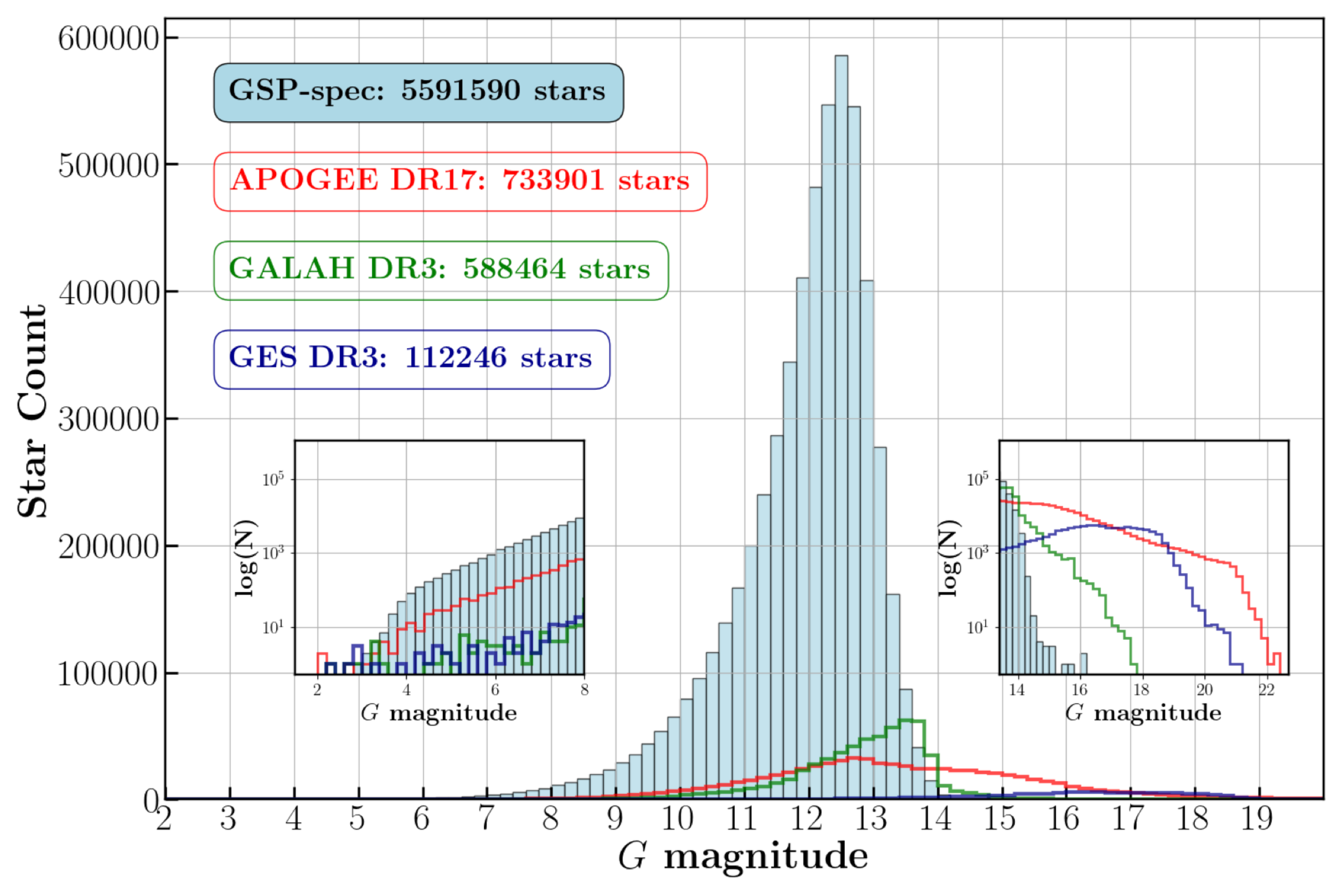

Gaia/RVS: a space spectroscopic survey

CU8/GSPspec: The chemical composition of 5.6 million stars

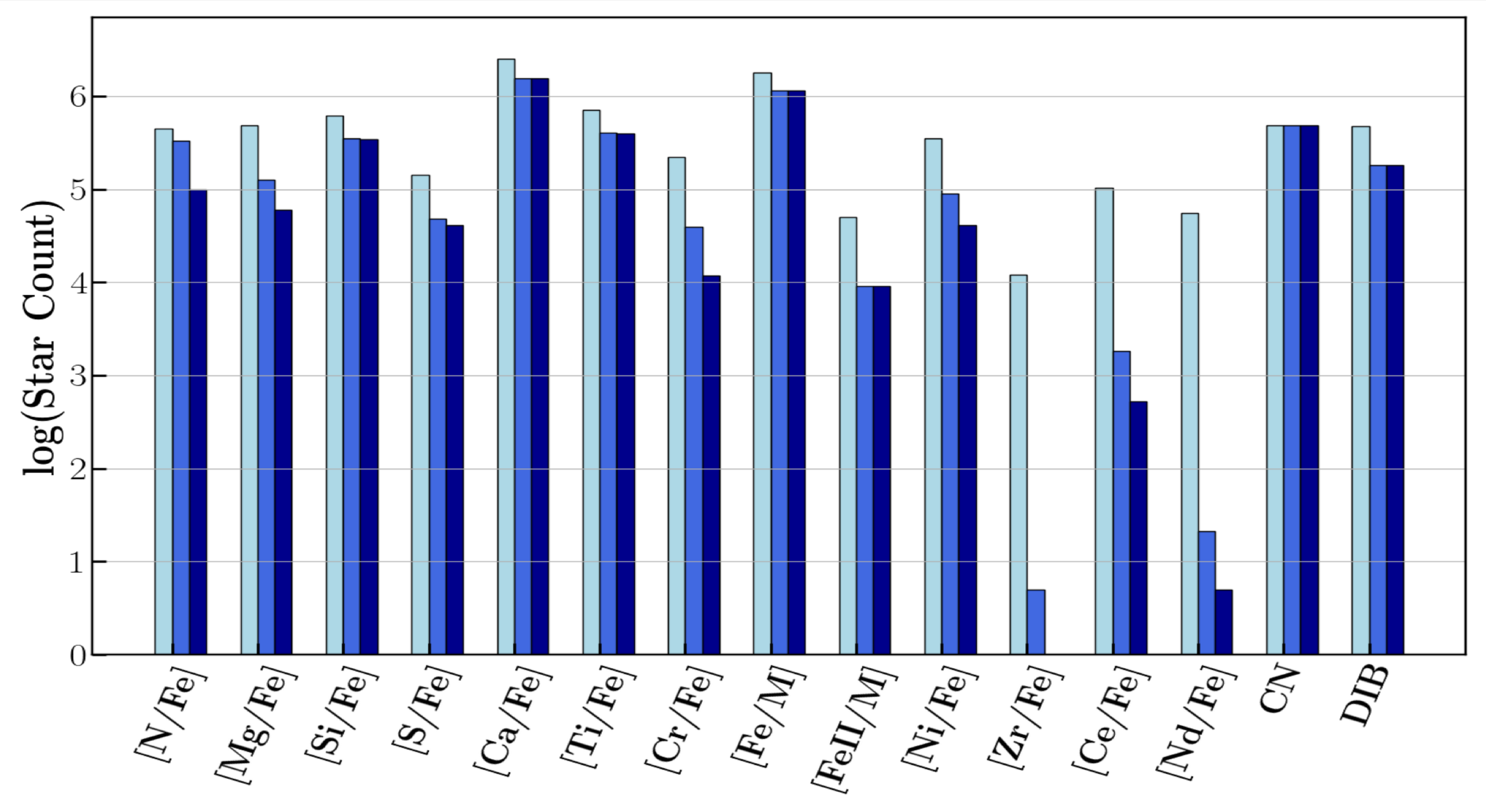

Gaia/RVS: a model driven success

MARCS atmosphere models + turbospectrum

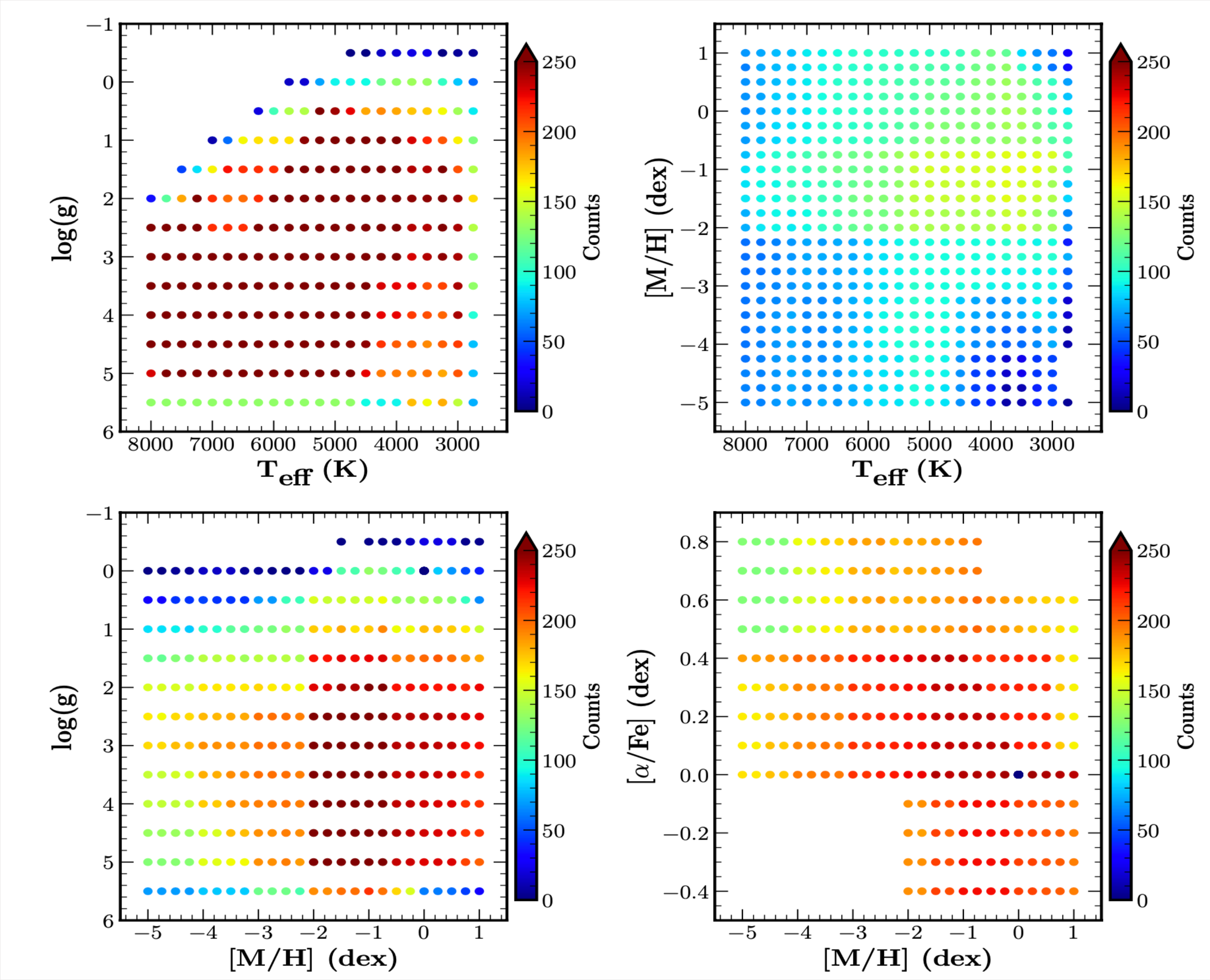

Elt	λ	λ^-_{ab}	λ^+_{ab}	λ^-_{norm}	λ^+_{norm}
N I	863.161	863.071	863.281	862.891	863.371
N I	868.579	868.489	868.699	868.309	868.939
Mg I	847.602	847.512	847.692	847.212	847.812
Si I	853.851	853.731	853.941	853.371	854.961
*Si I	855.916	855.856	856.036	855.376	856.156
Si I	868.872	868.782	868.992	868.602	869.232
*S I	867.258	866.988	867.378	866.898	867.998
*S I	869.701	869.551	869.821	869.281	869.971
Ca I	863.631	863.511	863.691	863.361	863.931
Ca II	849.856	849.706	849.976	849.586	850.276
Ca II	850.216	850.156	850.276	849.886	850.306
Ca II	854.264	854.114	854.384	853.544	854.864
Ca II	854.624	854.564	854.744	854.294	854.804
Ca II	866.272	866.152	866.332	866.002	866.572
Ca II	866.632	866.512	866.692	866.302	866.782
*Ti I	852.069	851.979	852.129	851.799	852.249
Ti I	857.209	857.119	857.269	856.999	857.359
Ti I	869.472	869.382	869.562	869.292	869.832
Cr I	855.118	855.058	855.208	854.878	855.478
Cr I	864.567	864.447	864.627	864.207	864.867
*Fe I	848.296	848.206	848.446	847.666	848.896
*Fe I	851.641	851.551	851.851	851.281	852.001
*Fe I	852.901	852.691	853.081	852.481	853.321
Fe I	857.416	857.296	857.506	856.876	858.166
Fe I	858.462	858.312	858.612	858.132	858.762
Fe I	862.397	862.277	862.517	862.127	862.697
Fe I	867.713	867.593	867.863	867.443	868.013
*Fe I	869.101	868.891	869.191	868.441	869.821
Fe II	858.794	858.764	858.824	858.254	859.274
Ni I	863.937	863.847	864.027	863.697	864.147
Zr II	852.748	852.658	852.838	852.388	853.018
*Ce II	851.375	851.285	851.465	851.015	851.555
Nd II	859.389	859.299	859.479	859.209	859.689

Comparison with Literature: Teff

Literature: APOGEE DR17, GALAH-DR3, RAVE-DR6

In grey: Medium quality sample
In Green: Best quality sample
(Will be explained later)

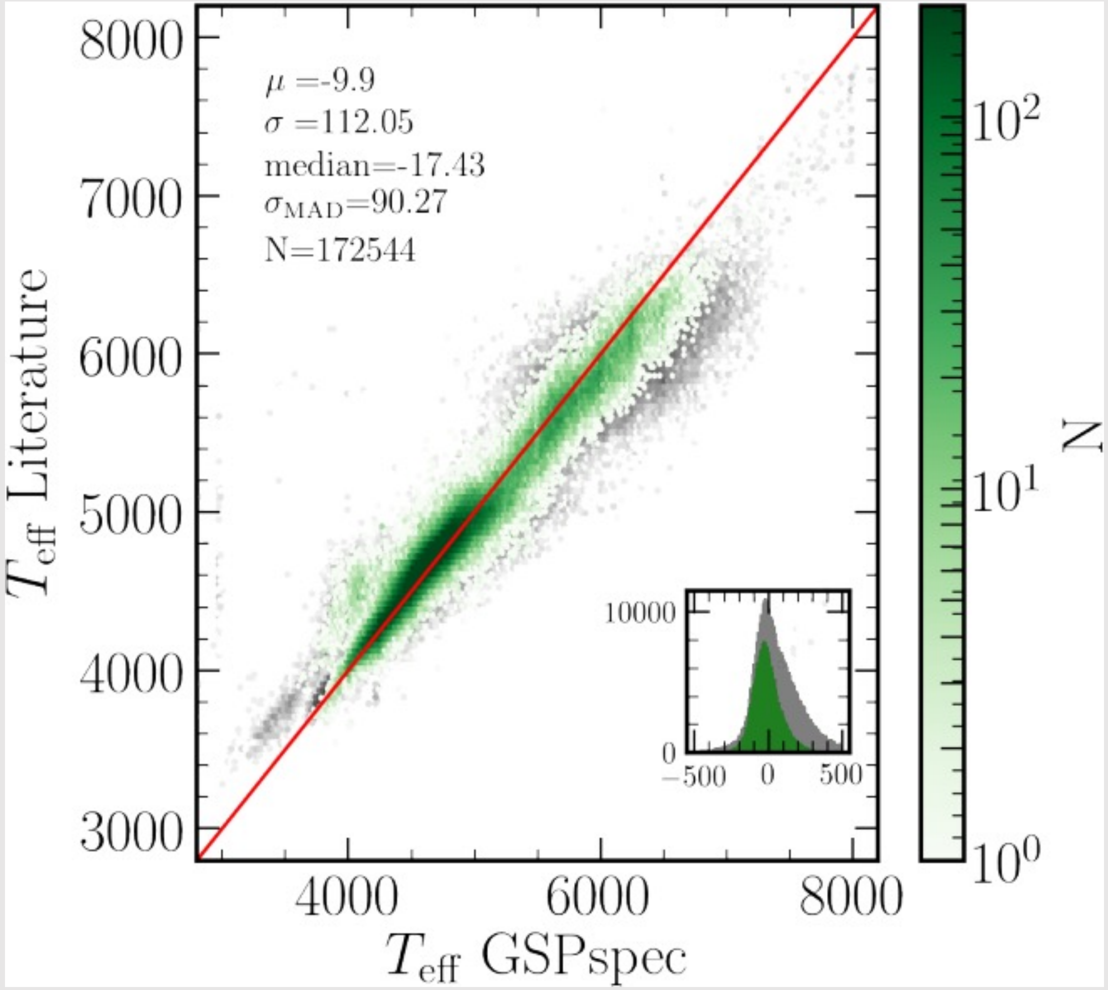

Gaia/RVS: a space spectroscopic survey

Comparison with Literature: logg !

Literature: APOGEE DR17, GALAH-DR3, RAVE-DR6

In grey: Medium quality sample
In Green: Best quality sample
(Will be explained later)

Bias detected. Solution: calibration

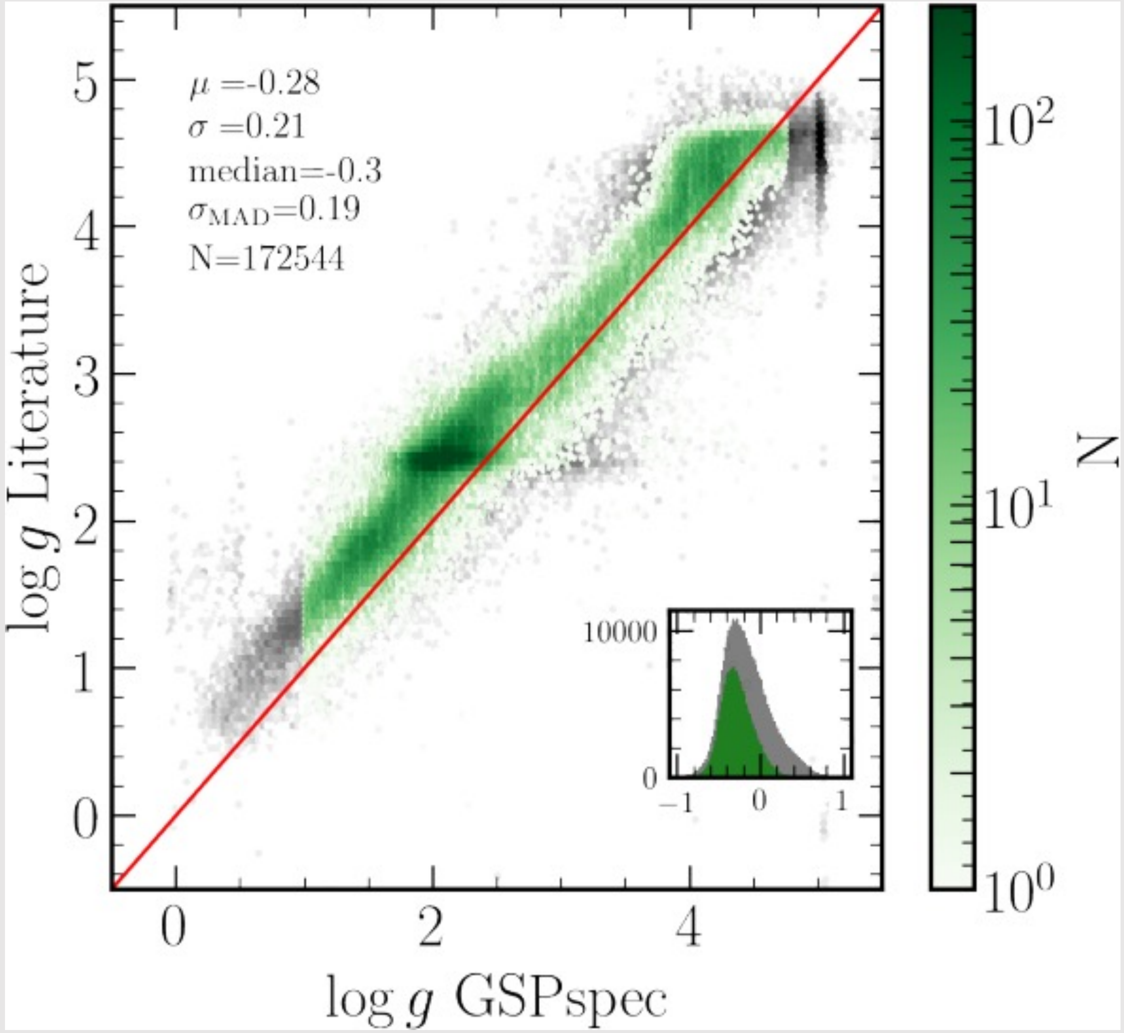

Comparison with Literature: [M/H]

Literature: APOGEE DR17, GALAH-DR3, RAVE-DR6

In grey: Medium quality sample
In Green: Best quality sample
(Will be explained later)

Apparently no bias on average, but **slightly subestimated** (**overestimated**) metallicities are found for **giants** (**dwarfs**)

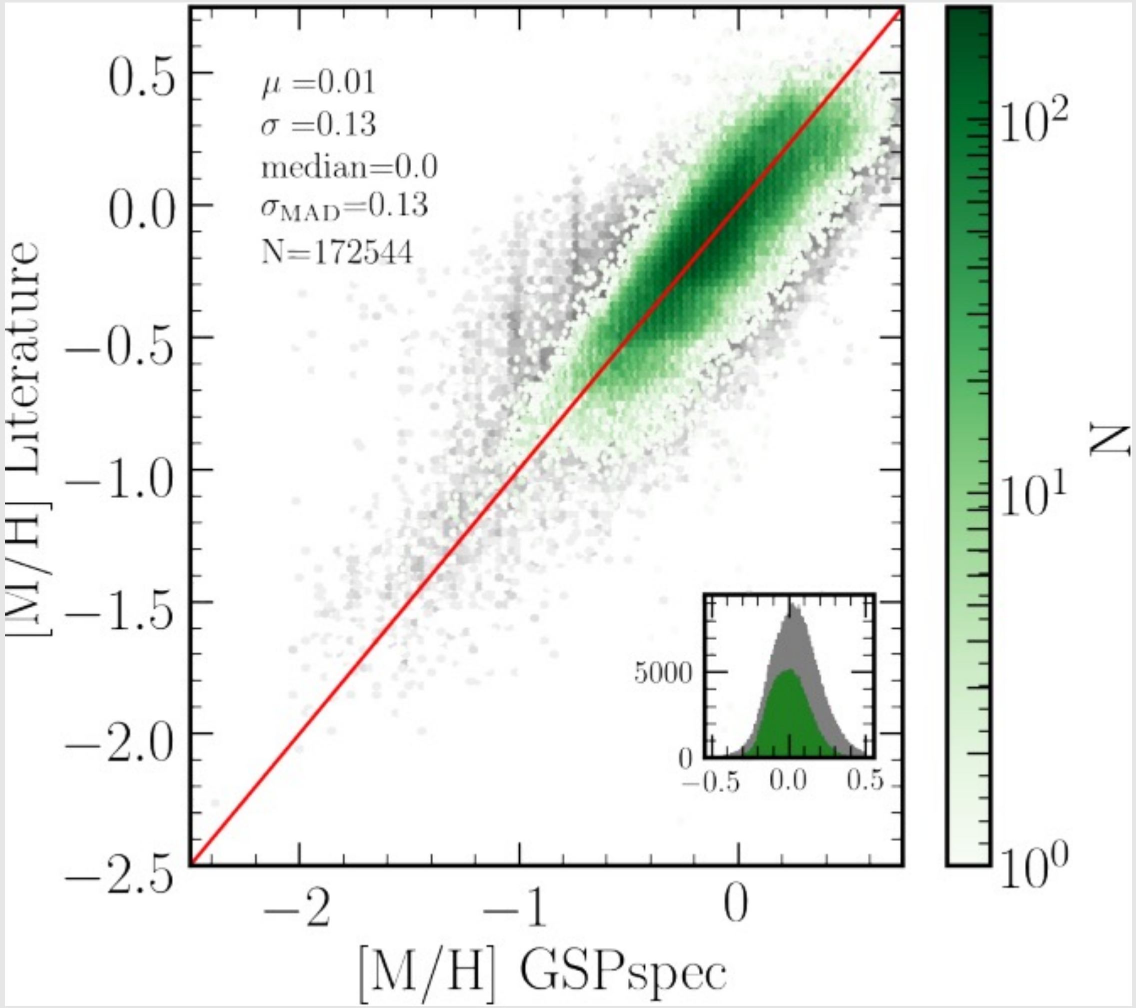

CU8/GSPspec: Offset corrections (parameters)

$$X_{Calibr.} = X_{Uncalibr.} + p_0 + p_1 \log(g) + p_2 \log(g)^2 + p_3 \log(g)^3 + p_4 \log(g)^4$$

Parameter	p_0	p_1	p_2	p_3	p_4
log(g)	0.4496	-0.0036	-0.0224		
[M/H]	0.274	-0.1373	-0.0050	0.0048	
$[M/H]_{OC}$	-0.7541	1.8108	-1.1779	0.2809	-0.0222

Full table in **Recio-Blanco et al. (2022)**

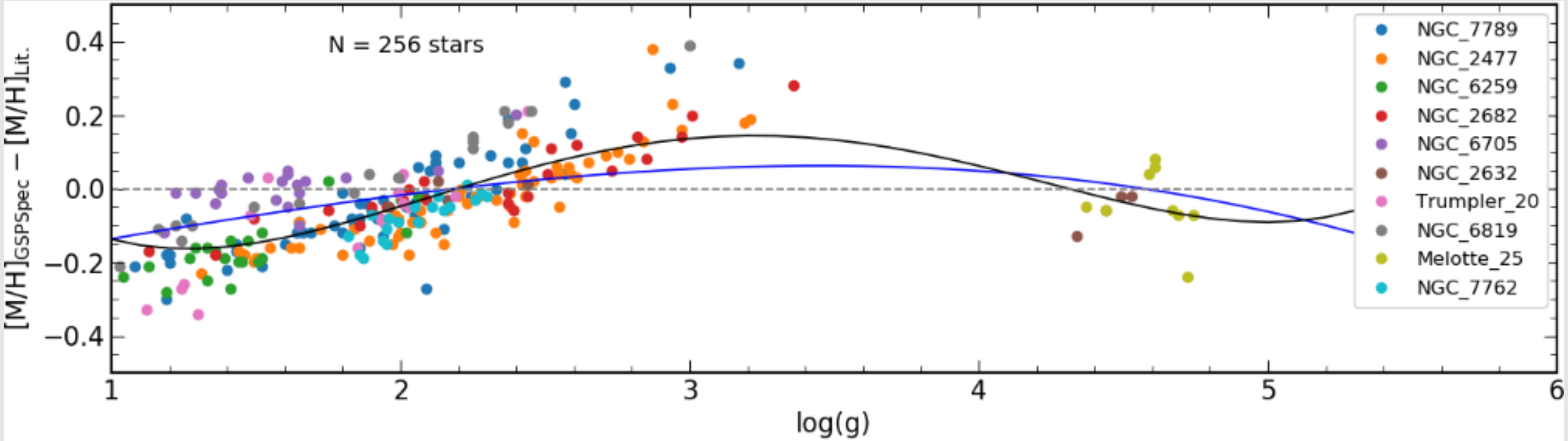

Fig. 13. Metallicity bias with respect to the literature as a function of log(g) for the open cluster stars, excluding dwarfs with S/N lower than 50. The colour code used for each cluster is indicated in the legend. Solid blue line corresponds to the general metallicity correction while the black line refers to that specifically obtained from the open clusters.

Gaia/RVS: a space spectroscopic survey

CU8/GSPspec: Comparison with ground-based surveys

[Ca/Fe]

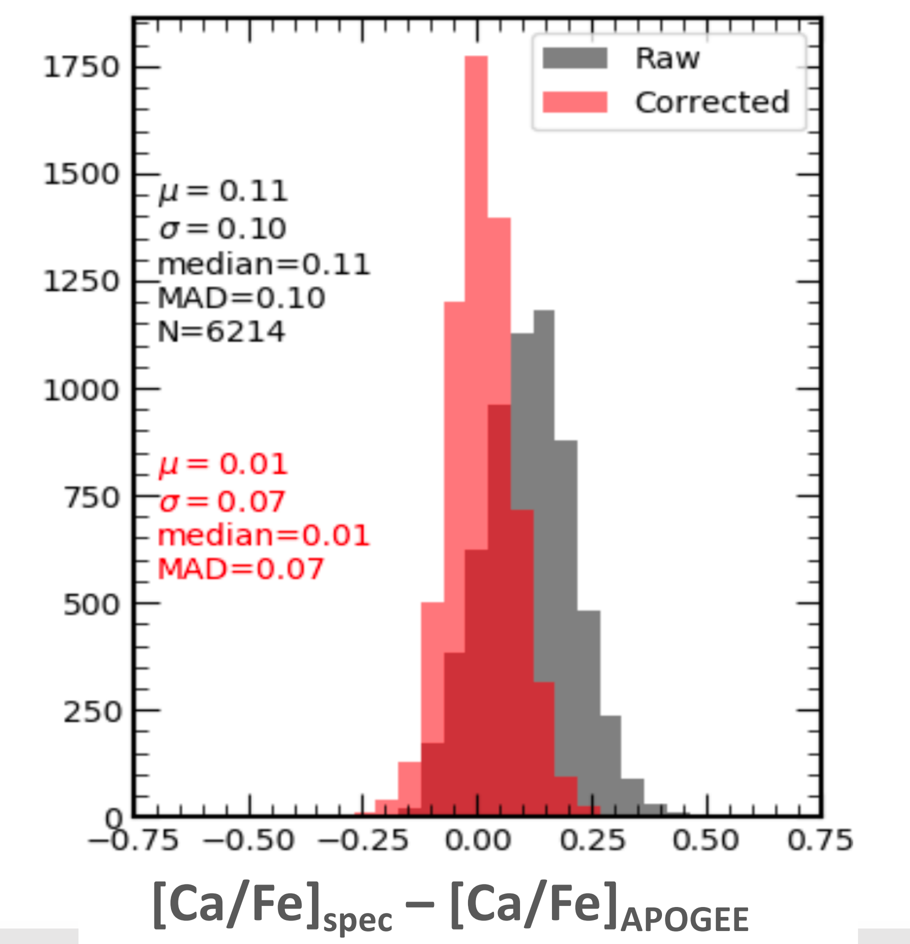

Recio-Blanco et al. (2023)

[Ce/Fe]

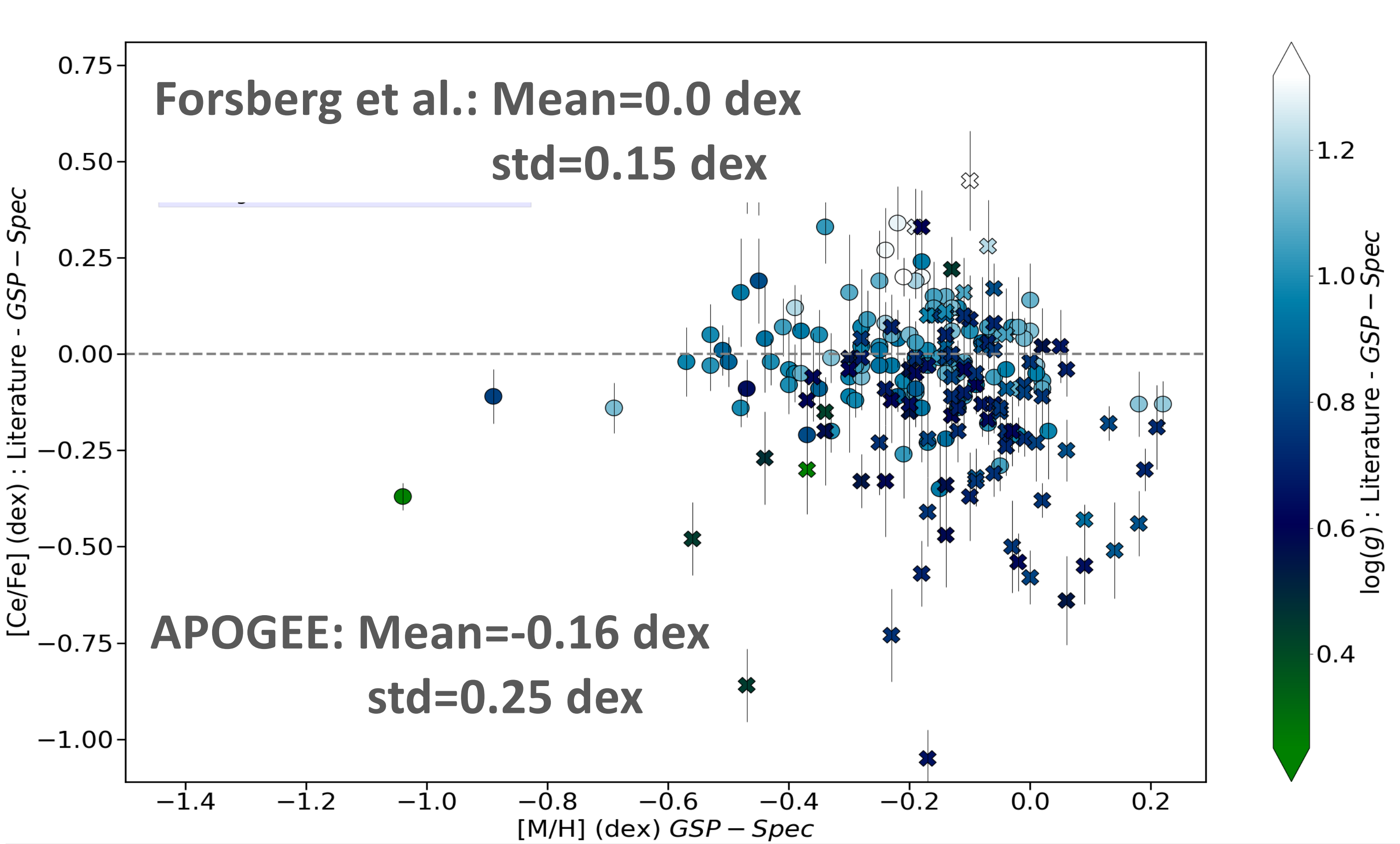

Contursi et al. (2022)

CU8/GSPspec: Offset corrections (abundances)

$$X_{Calibr.} = X_{Uncalibr.} + p_0 + p_1 \log(g) + p_2 \log(g)^2 + p_3 \log(g)^3 + p_4 \log(g)^4$$

Full table in **Recio-Blanco et al. (2023)**

Element	p_0	p_1	p_2	p_3	p_4	Recommended interval		*extrapol* flag
	As a function of log(g)					Min log(g)	Max log(g)	
[α/Fe]	-0.5809	0.7018	-0.2402	0.0239	0.0000	1.01	4.85	0
[Ca/Fe]	-0.6250	0.7558	-0.2581	0.0256	0.0000	1.01	4.85	0
[Mg/Fe]	-0.7244	0.3779	-0.0421	-0.0038	0.0000	1.30	4.38	0
[S/Fe]	-17.6080	12.3239	-2.8595	0.2192	0.0000	3.38	4.81	0
[Si/Fe]	-0.3491	0.3757	-0.1051	0.0092	0.0000	1.28	4.85	0
[Ti/Fe]	-0.2656	0.4551	-0.1901	0.0209	0.0000	1.01	4.39	0
[Cr/Fe]	-0.0769	-0.1299	0.1009	-0.0200	0.0000	1.01	4.45	0
[Fe I/H]	0.3699	-0.0680	0.0028	-0.0004	0.0000	1.01	4.85	0
[Fe II/H]	35.5994	-27.9179	7.1822	-0.6086	0.0000	3.53	4.82	0
[Ni/Fe]	-0.2902	0.4066	-0.1313	0.0105	0.0000	1.41	4.81	0
[N/Fe]	0.0975	-0.0293	0.0238	-0.0071	0.0000	1.21	4.79	0
[α/Fe]	-0.2838	0.3713	-0.1236	0.0106	0.0002	0.84	4.44	≤ 1
[Ca/Fe]	-0.3128	0.3587	-0.0816	-0.0066	0.0020	0.84	4.98	≤ 1
	As a function of $t = T_{eff}/5750$					Min T_{eff}	Max T_{eff}	
[α/Fe]	-6.6960	20.8770	-21.0976	6.8313	0.0000	4000	6830	≤ 1
[Ca/Fe]	-7.4577	23.2759	-23.6621	7.7657	0.0000	4000	6830	≤ 1
[S/Fe]	0.1930	-0.2234	0.0000	0.0000	0.0000	5700	6800	≤ 1

CU8/GSPspec: Offset corrections (abundances)

$$X_{Calibr.} = X_{Uncalibr.} + p_0 + p_1 \log(g) + p_2 \log(g)^2 + p_3 \log(g)^3 + p_4 \log(g)^4$$

Full table in **Recio-Blanco et al. (2023)**

Element	p_0	p_1	p_2	p_3	p_4	Recommended interval		*extrapol* flag
	As a function of log(g)					Min log(g)	Max log(g)	
[α/Fe]	-0.5809	0.7018	-0.2402	0.0239	0.0000	1.01	4.85	0
[Ca/Fe]	-0.6250	0.7558	-0.2581	0.0256	0.0000	1.01	4.85	0
[Mg/Fe]	-0.7244	0.3779	-0.0421	-0.0038	0.0000	1.30	4.38	0
[S/Fe]	-17.6080	12.3239	-2.8595	0.2192	0.0000	3.38	4.81	0
[Si/Fe]	-0.3491	0.3757	-0.1051	0.0092	0.0000	1.28	4.85	0
[Ti/Fe]	-0.2656	0.4551	-0.1901	0.0209	0.0000	1.01	4.39	0
[Cr/Fe]	-0.0769	-0.1299	0.1009	-0.0200	0.0000	1.01	4.45	0
[Fe I/H]	0.3699	-0.0680	0.0028	-0.0004	0.0000	1.01	4.85	0
[Fe II/H]	35.5994	-27.9179	7.1822	-0.6086	0.0000	3.53	4.82	0
[Ni/Fe]	-0.2902	0.4066	-0.1313	0.0105	0.0000	1.41	4.81	0
[N/Fe]	0.0975	-0.0293	0.0238	-0.0071	0.0000	1.21	4.79	0
[α/Fe]	-0.2838	0.3713	-0.1236	0.0106	0.0002	0.84	4.44	≤ 1
[Ca/Fe]	-0.3128	0.3587	-0.0816	[illegible]	0.0020	0.84	4.98	≤ 1
	As a function of $t = T_{eff}/5750$					Min T_{eff}	Max T_{eff}	
[α/Fe]	-6.6960	20.8770	-21.0976	6.8313	0.0000	4000	6830	≤ 1
[Ca/Fe]	-7.4577	23.2759	-23.6621	7.7657	0.0000	4000	6830	≤ 1
[S/Fe]	0.1930	-0.2234	0.0000	0.0000	0.0000	5700	6800	≤ 1

Out of this range, keep the edge values (suggestion)

CU8/GSPspec: Offset corrections (abundances)

$$X_{Calibr.} = X_{Uncalibr.} + p_0 + p_1 \log(g) + p_2 \log(g)^2 + p_3 \log(g)^3 + p_4 \log(g)^4$$

Full table in **Recio-Blanco et al. (2023)**

Element	p_0	p_1	p_2	p_3	p_4	Recommended interval		*extrapol* flag
	As a function of log(g)					Min log(g)	Max log(g)	
[α/Fe]	-0.5809	0.7018	-0.2402	0.0239	0.0000	1.01	4.85	0
[Ca/Fe]	-0.6250	0.7558	-0.2581	0.0256	0.0000	1.01	4.85	0
[Mg/Fe]	-0.7244	0.3779	-0.0421	-0.0038	0.0000	1.30	4.38	0
[S/Fe]	-17.6080	12.3239	-2.8595	0.2192	0.0000	3.38	4.81	0
[Si/Fe]	-0.3491	0.3757	-0.1051	0.0092	0.0000	1.28	4.85	0
[Ti/Fe]	-0.2656	0.4551	-0.1901	0.0209	0.0000	1.01	4.39	0
[Cr/Fe]	-0.0769	-0.1299	0.1009	-0.0200	0.0000	1.01	4.45	0
[Fe I/H]	0.3699	-0.0680	0.0028	-0.0004	0.0000	1.01	4.85	0
[Fe II/H]	35.5994	-27.9179	7.1822	-0.6086	0.0000	3.53	4.82	0
[Ni/Fe]	-0.2902	0.4066	-0.1313	0.0105	0.0000	1.41	4.81	0
[N/Fe]	0.0975	0.0293	0.0238	0.0071	0.0000	1.21	4.79	0
[α/Fe]	-0.2838	0.3713	-0.1236	0.0106	0.0002	0.84	4.44	≤ 1
[Ca/Fe]	-0.3128	0.3587	-0.0816	-0.0066	0.0020	0.84	4.98	≤ 1
	As a function of $t = T_{\rm eff}/5750$					Min $T_{\rm eff}$	Max $T_{\rm eff}$	
[α/Fe]	-6.6960	20.8770	-21.0976	6.8313	0.0000	4000	6830	≤ 1
[Ca/Fe]	-7.4577	23.2759	-23.6621	7.7657	0.0000	4000	6830	≤ 1
[S/Fe]	0.1930	-0.2234	0.0000	0.0000	0.0000	5700	6800	≤ 1

CU8/GSPspec: Offset corrections (abundances)

$$X_{Calibr.} = X_{Uncalibr.} + p_0 + p_1 \log(g) + p_2 \log(g)^2 + p_3 \log(g)^3 + p_4 \log(g)^4$$

Full table in **Recio-Blanco et al. (2023)**

Element	p_0	p_1	p_2	p_3	p_4	Recommended interval		*extrapol* flag
	As a function of log(g)					Min log(g)	Max log(g)	
[α/Fe]	-0.5809	0.7018	-0.2402	0.0239	0.0000	1.01	4.85	0
[Ca/Fe]	-0.6250	0.7558	-0.2581	0.0256	0.0000	1.01	4.85	0
[Mg/Fe]	-0.7244	0.3779	-0.0421	-0.0038	0.0000	1.30	4.38	0
[S/Fe]	-17.6080	12.3239	-2.8595	0.2192	0.0000	3.38	4.81	0
[Si/Fe]	-0.3491	0.3757	-0.1051	0.0092	0.0000	1.28	4.85	0
[Ti/Fe]	-0.2656	0.4551	-0.1901	0.0209	0.0000	1.01	4.39	0
[Cr/Fe]	-0.0769	-0.1299	0.1009	-0.0200	0.0000	1.01	4.45	0
[Fe I/H]	0.3699	-0.0680	0.0028	-0.0004	0.0000	1.01	4.85	0
[Fe II/H]	35.5994	-27.9179	7.1822	-0.6086	0.0000	3.53	4.82	0
[Ni/Fe]	-0.2902	0.4066	-0.1313	0.0105	0.0000	1.41	4.81	0
[N/Fe]	0.0975	-0.0293	0.0238	-0.0071	0.0000	1.21	4.79	0
[α/Fe]	-0.2838	0.3713	-0.1236	0.0106	0.0002	0.84	4.44	≤ 1
[Ca/Fe]	-0.3128	0.3587	-0.0816	-0.0066	0.0020	0.84	4.98	≤ 1
	As a function of $t = T_{\rm eff}/5750$					Min $T_{\rm eff}$	Max $T_{\rm eff}$	
[α/Fe]	-6.6960	20.8770	-21.0976	6.8313	0.0000	4000	6830	≤ 1
[Ca/Fe]	-7.4577	23.2759	-23.6621	7.7657	0.0000	4000	6830	≤ 1
[S/Fe]	0.1930	-0.2234	0.0000	0.0000	0.0000	5700	6800	≤ 1

Family of GSP-Spec Flags

To be used and adapted to your scientific goal

Parameters flags (rows 1–13)

Abundance flags (rows 14–39)

CN/DIB flags (rows 40–41)

Chain character number - name	Considered quality aspect	Possible adopted values	Related subsection and table
1 **vbroadT**	vbroad induced bias in $T_{\rm eff}$	0,1,2,9	8.1 & C.1
2 **vbroadG**	vbroad induced bias in $\log(g)$	0,1,2,9	8.1 & C.1
3 **vbroadM**	vbroad induced bias in [M/H]	0,1,2,9	8.1 & C.1
4 **vradT**	vrad induced bias in $T_{\rm eff}$	0,1,2,9	8.2 & C.2
5 **vradG**	vrad induced bias in $\log(g)$	0,1,2,9	8.2 & C.2
6 **vradM**	vrad induced bias in [M/H]	0,1,2,9	8.2 & C.2
7 **fluxNoise**	flux noise uncertainties	0,1,2,3,4,5,9	8.3 & C.3, C.4
8 **extrapol**	extrapolation	0,1,2,3,4,9	8.4 & C.5, C.6
9 **negFlux**	negative flux pixels	0,9	8.5 & C.7
10 **nanFlux**	NaN flux pixels	0,1,9	8.5 & C.7
11 **emission**	emission line	0,1,9	8.5 & C.7
12 **nullFluxErr**	null uncertainties	0,1,9	8.5 & C.7
13 **KMgiantPar**	KM-type giant stars	0,1,2,9	8.6 & C.8
14 **NUpLim**	Nitrogen abundance upper limit	0,1,2,9	8.7 & C.9
15 **NUncer**	Nitrogen abundance uncertainty quality	0,1,2,9	8.7 & C.10
16 **MgUpLim**	Magnesium abundance upper limit	0,1,2,9	8.7 & C.9
17 **MgUncer**	Magnesium abundance uncertainty quality	0,1,2,9	8.7 & C.10
18 **SiUpLim**	Silicon abundance upper limit	0,1,2,9	8.7 & C.9
19 **SiUncer**	Silicon abundance uncertainty quality	0,1,2,9	8.7 & C.10
20 **SUpLim**	Sulphur abundance upper limit	0,1,2,9	8.7 & C.9
21 **SUncer**	Sulphur abundance uncertainty quality	0,1,2,9	8.7 & C.10
22 **CaUpLim**	Calcium abundance upper limit	0,1,2,9	8.7 & C.9
23 **CaUncer**	Calcium abundance uncertainty quality	0,1,2,9	8.7 & C.10
24 **TiUpLim**	Titanium abundance upper limit	0,1,2,9	8.7 & C.9
25 **TiUncer**	Titanium abundance uncertainty quality	0,1,2,9	8.7 & C.10
26 **CrUpLim**	Chromium abundance upper limit	0,1,2,9	8.7 & C.9
27 **CrUncer**	Chromium abundance uncertainty quality	0,1,2,9	8.7 & C.10
28 **FeUpLim**	Neutral iron abundance upper limit	0,1,2,9	8.7 & C.9
29 **FeUncer**	Neutral iron abundance uncertainty quality	0,1,2,9	8.7 & C.10
30 **FeIIUpLim**	Ionised iron abundance upper limit	0,1,2,9	8.7 & C.9
31 **FeIIUncer**	Ionised iron abundance uncertainty quality	0,1,2,9	8.7 & C.10
32 **NiUpLim**	Nickel abundance upper limit	0,1,2,9	8.7 & C.9
33 **NiUncer**	Nickel abundance uncertainty quality	0,1,2,9	8.7 & C.10
34 **ZrUpLim**	Zirconium abundance upper limit	0,1,2,9	8.7 & C.9
35 **ZrUncer**	Zirconium abundance uncertainty quality	0,1,2,9	8.7 & C.10
36 **CeUpLim**	Cerium abundance upper limit	0,1,2,9	8.7 & C.9
37 **CeUncer**	Cerium abundance uncertainty quality	0,1,2,9	8.7 & C.10
38 **NdUpLim**	Neodymium abundance upper limit	0,1,2,9	8.7 & C.9
39 **NdUncer**	Neodymium abundance uncertainty quality	0,1,2,9	8.7 & C.10
40 **DeltaCNq**	Cyanogen differential equivalent width quality	0,1,2,9	8.9 & C.12
41 **DIBq**	DIB quality flag	0,1,2,3,4,5,9	8.8 & C.13

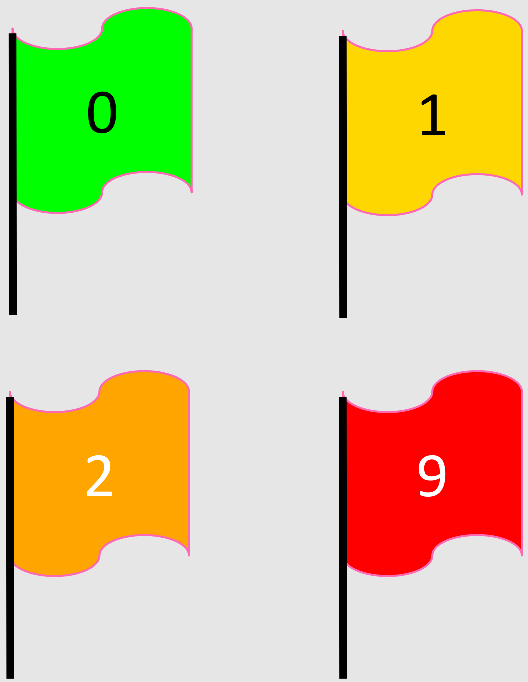

Full table in **Recio-Blanco et al. (2023)**

Family of GSP-Spec Flags

KM flag

Problems with the molecular lines in the cool regime. Dependence of F_{min}

Image: Kiel diagram colorcoded with density

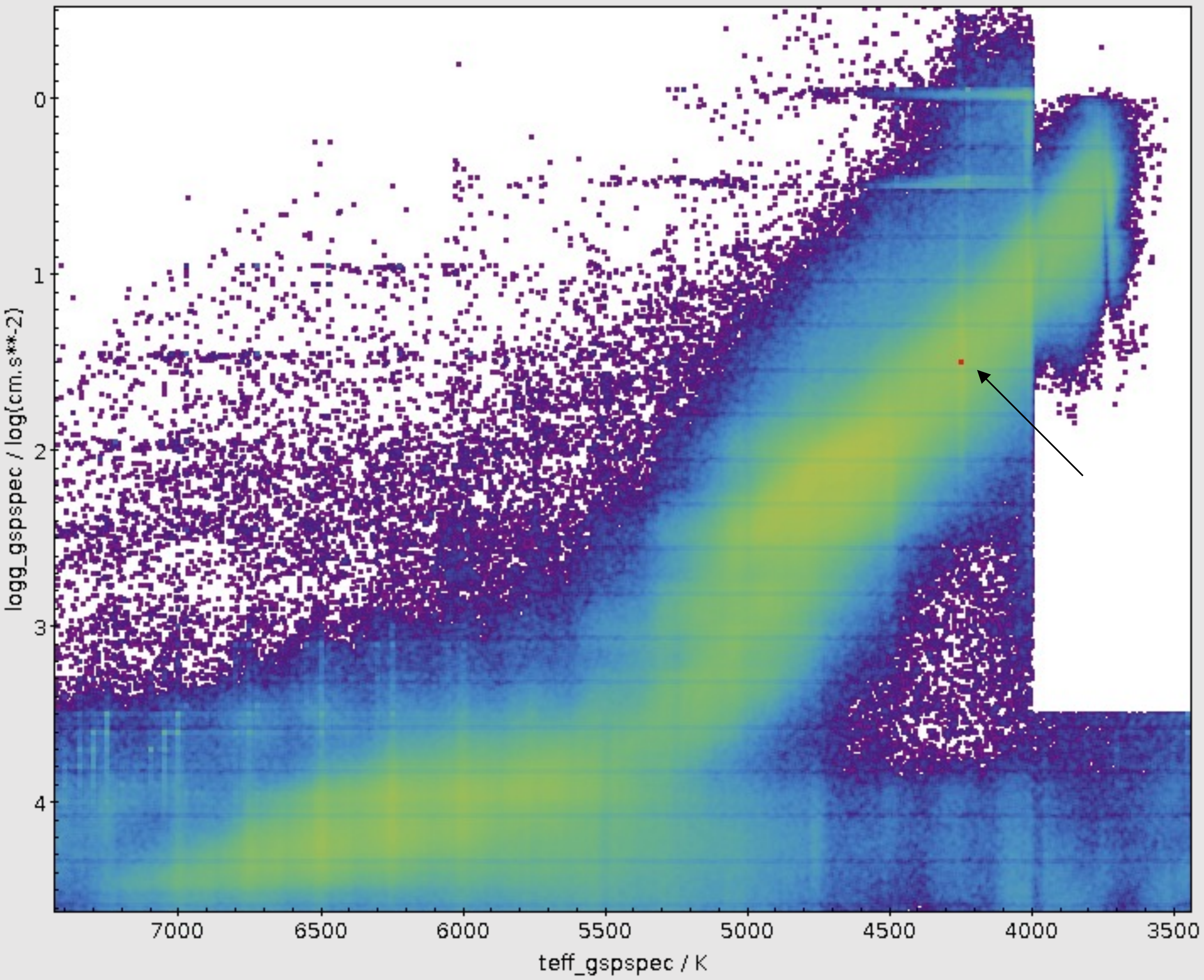

Gaia DR3: 5.6 milion stars with chemo-physical parameters

Spectroscopy

Recio-Blanco et al. 2022

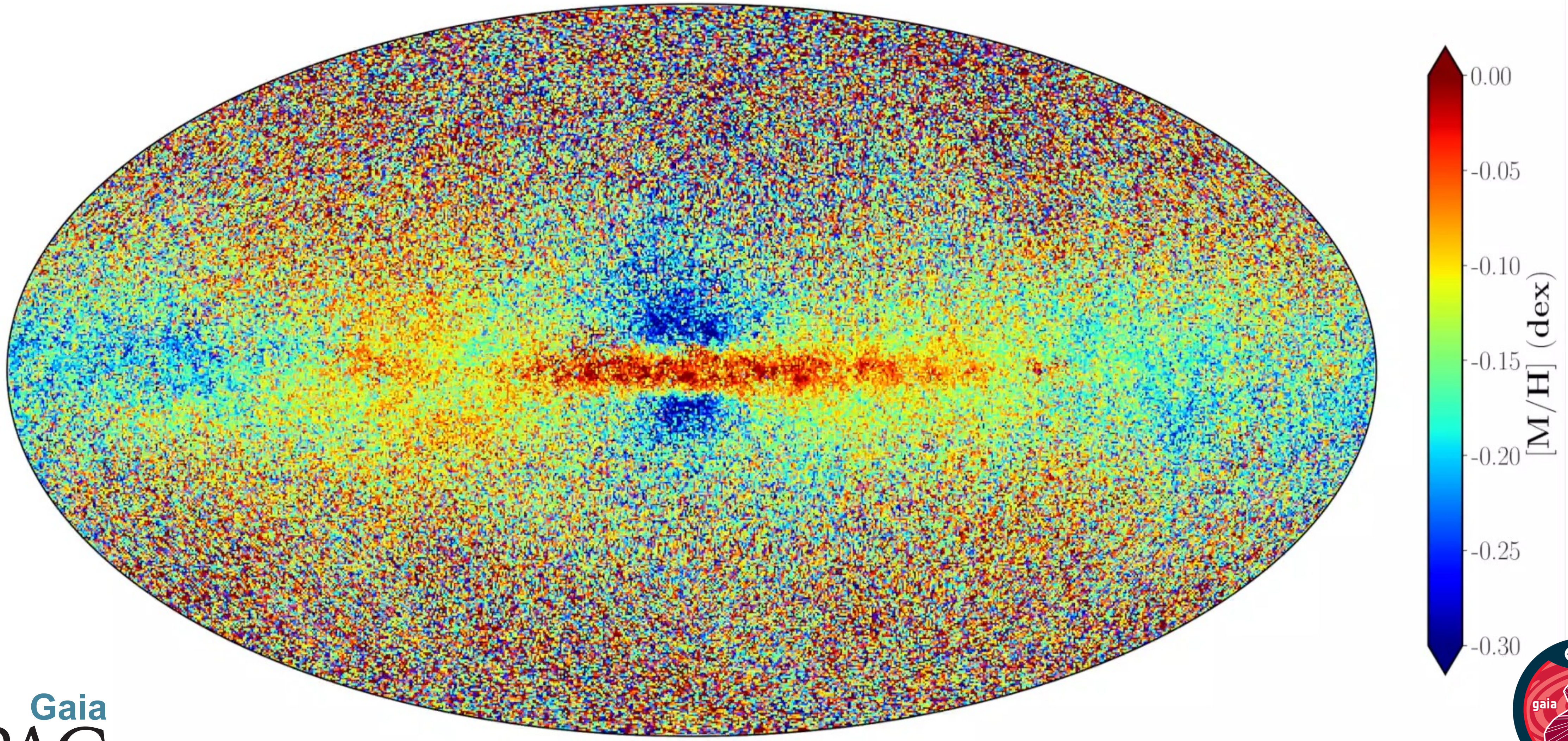

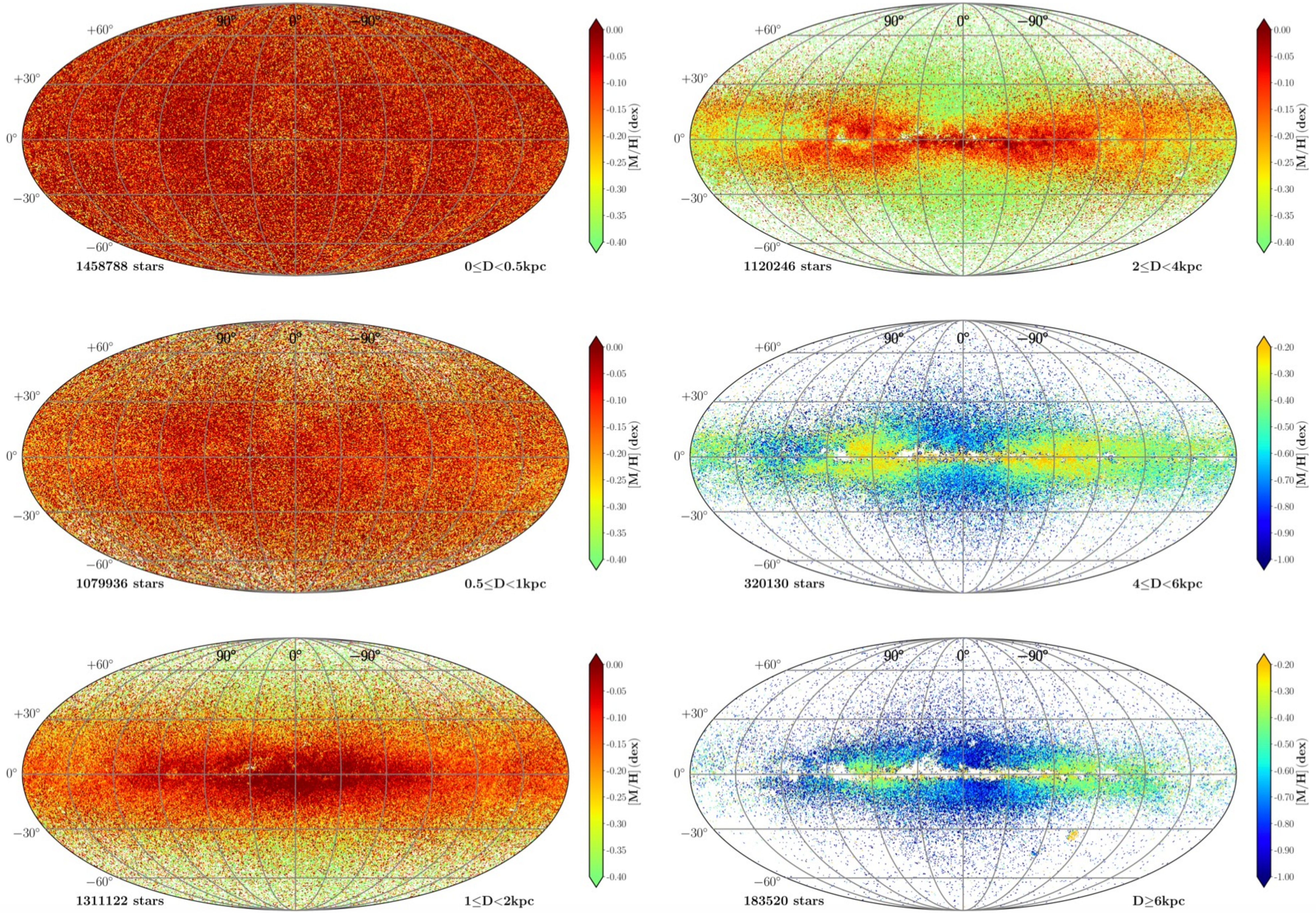

Gaia Collaboration, Recio-Blanco et al. (2022)

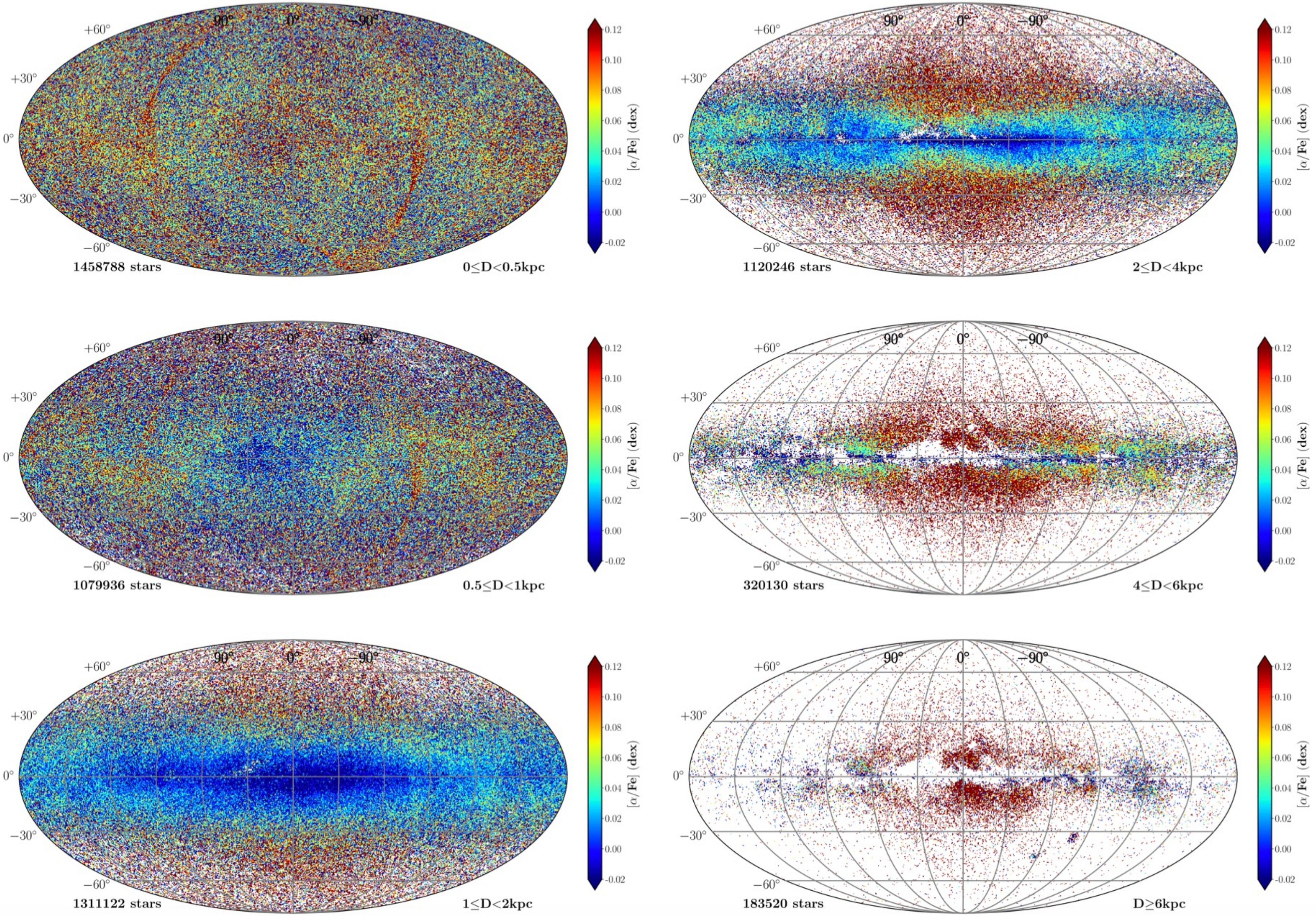

Gaia Collaboration, Recio-Blanco et al. (2022)

Gaia stellar populations

1. The Gaia revolution on Galactic stellar populations and its keys
2. The chemical cartography of the Milky Way
3. - Gaia: "*Mesdames et messieurs, the stellar populations*"
    - Disc structure and chemical gradients
    - Disc kinematic disturbances
    - Halo populations

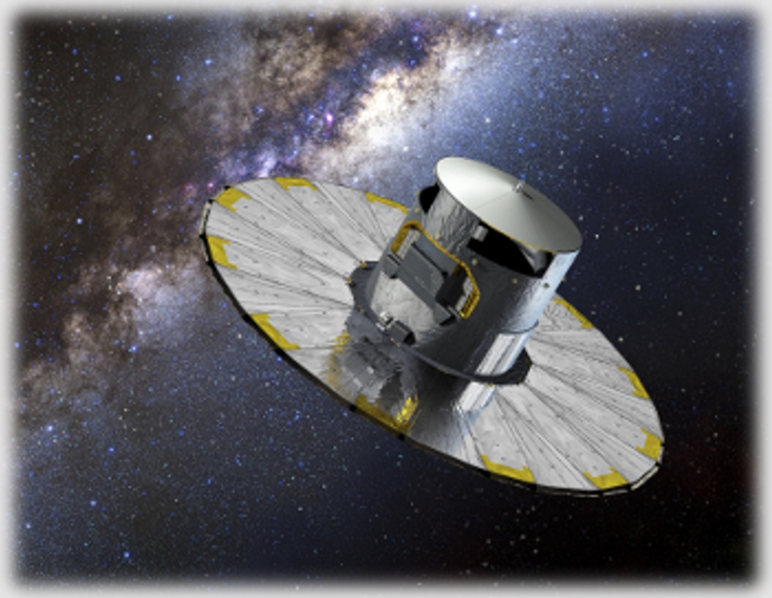

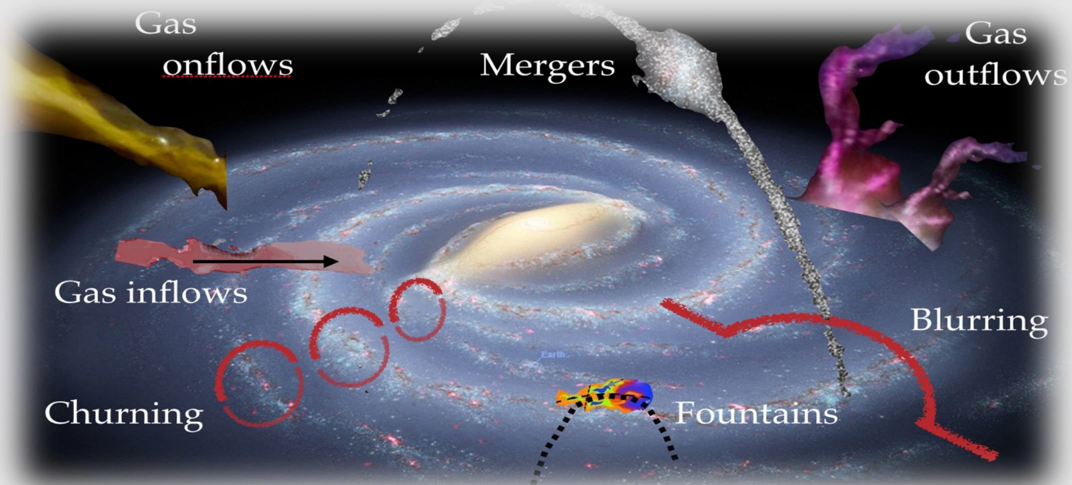

THE H-R DIAGRAMME to dig into Milky Way stellar populations

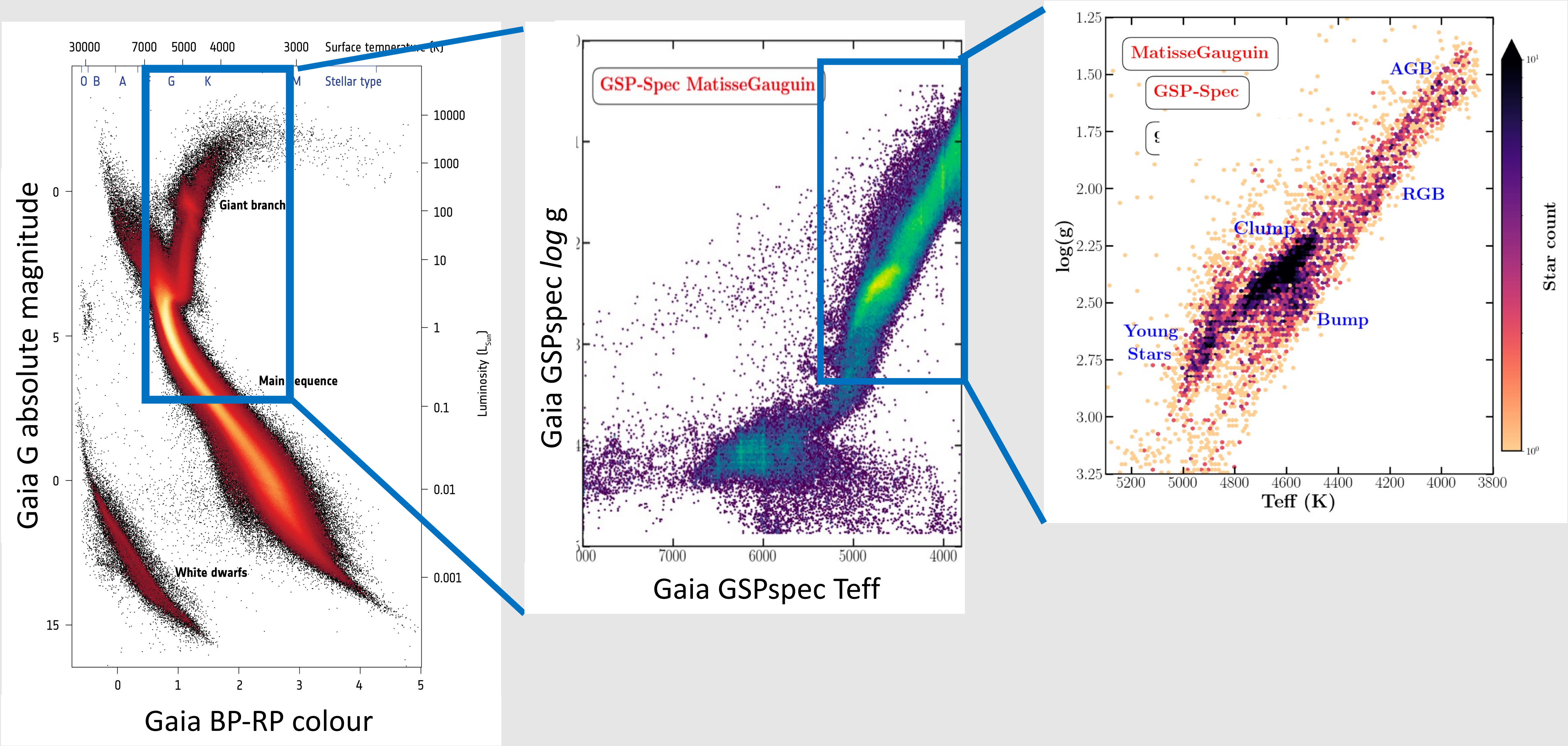

Galactic disc: landscapes

Selection function

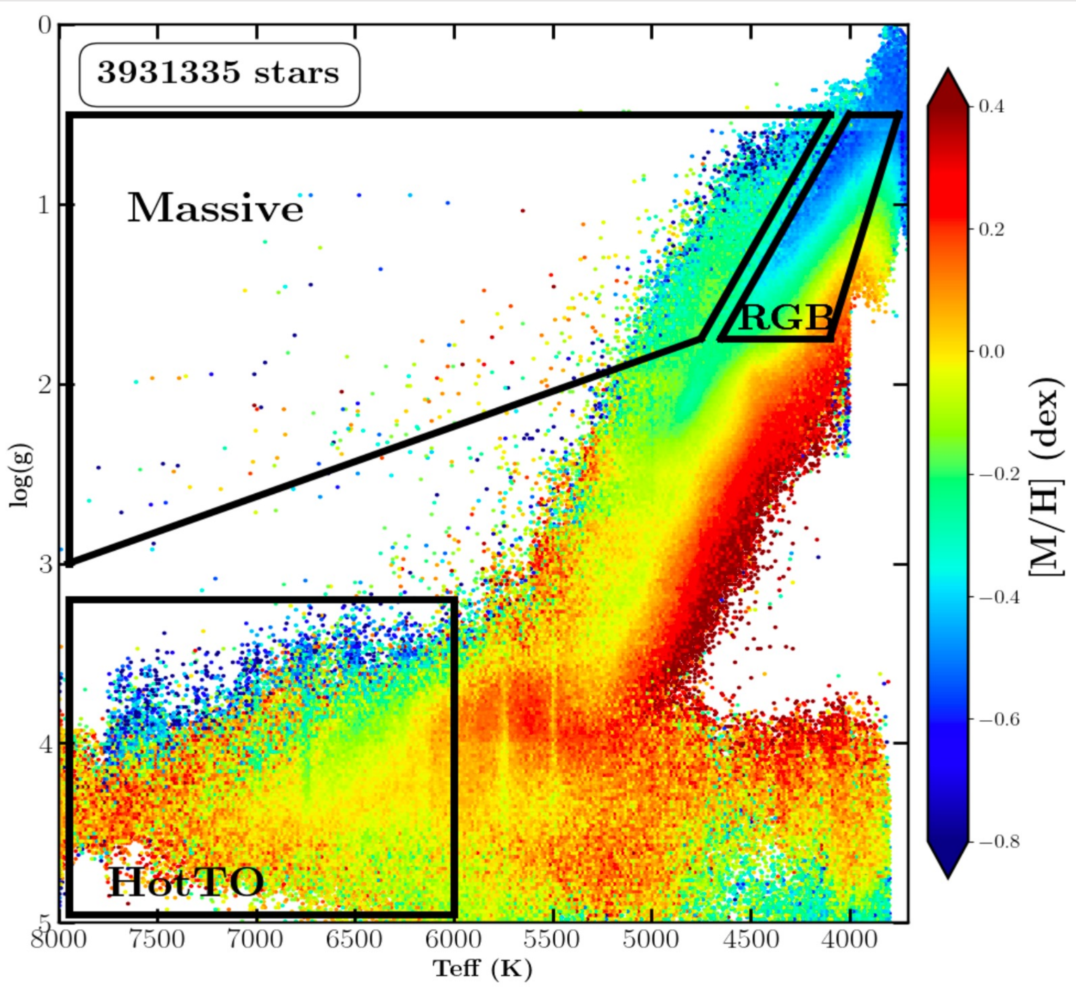

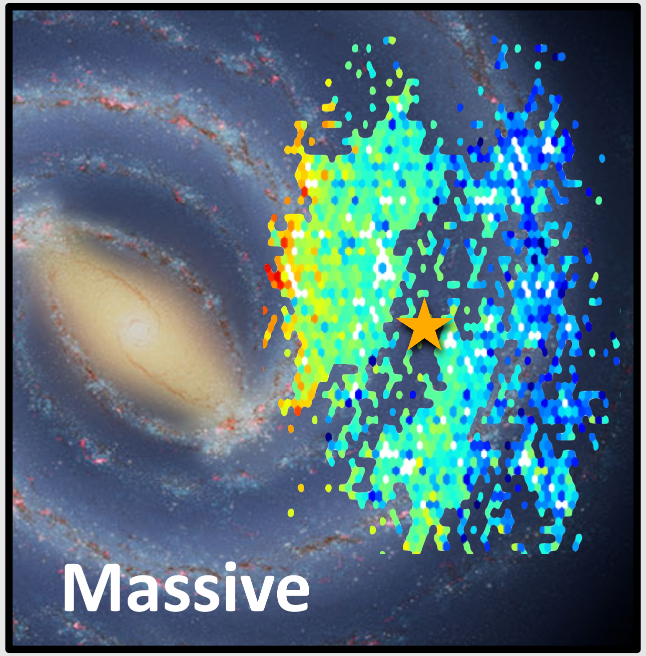

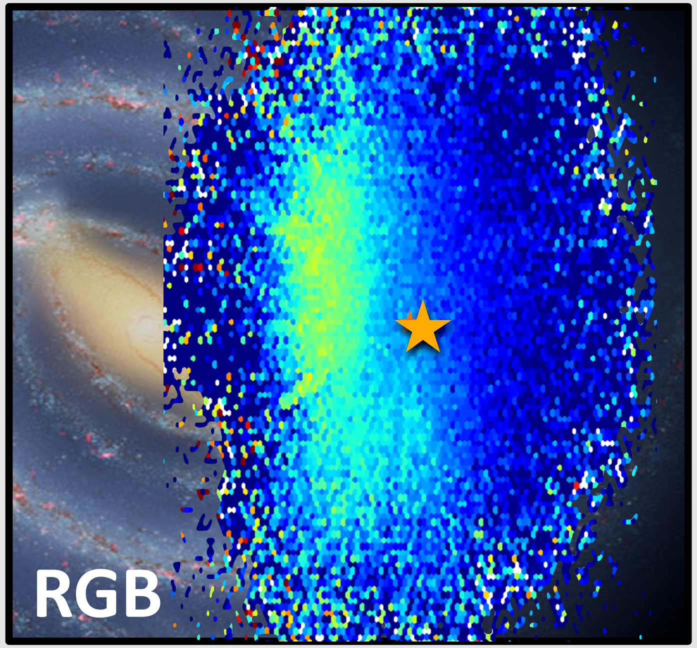

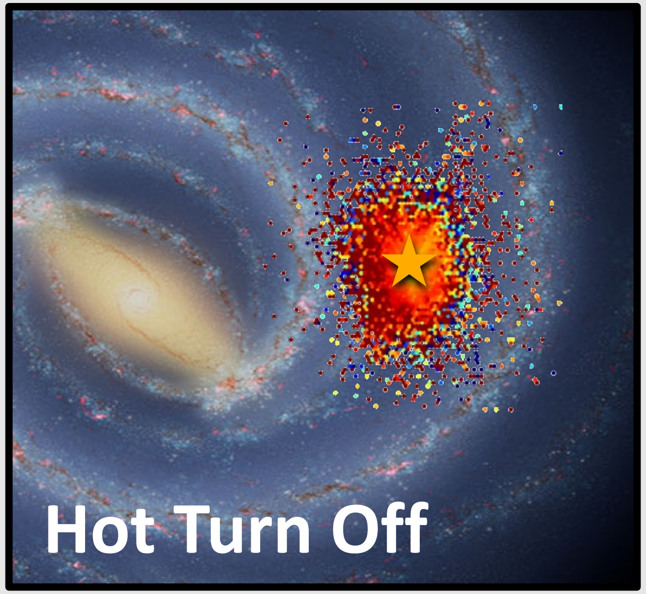

Gaia Collaboration, ARB et al. (2023)

Galactic disc: structure and chemical gradients

Global view of the disc : luminous RGB stars

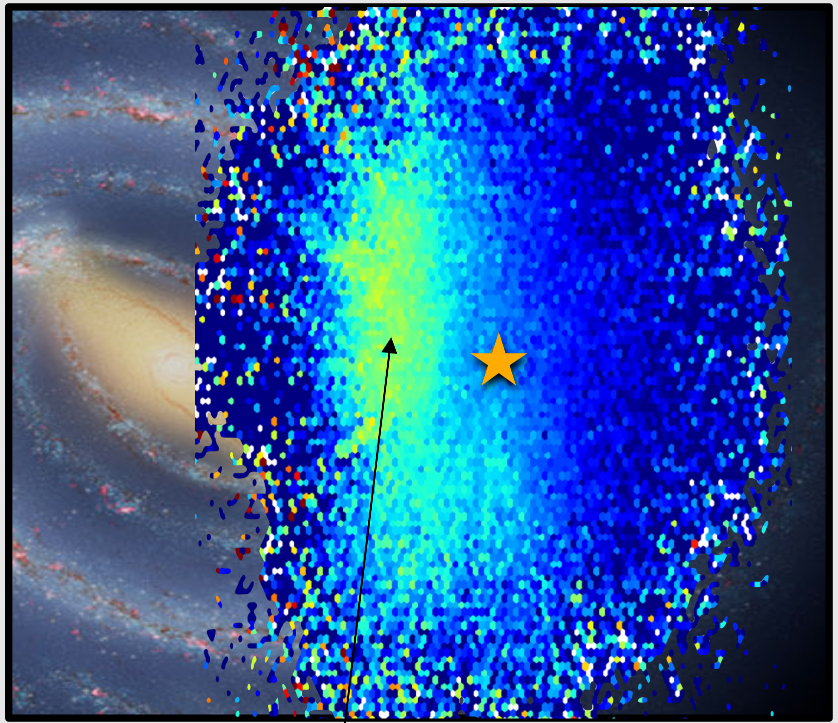

Innermost spiral arm and bar

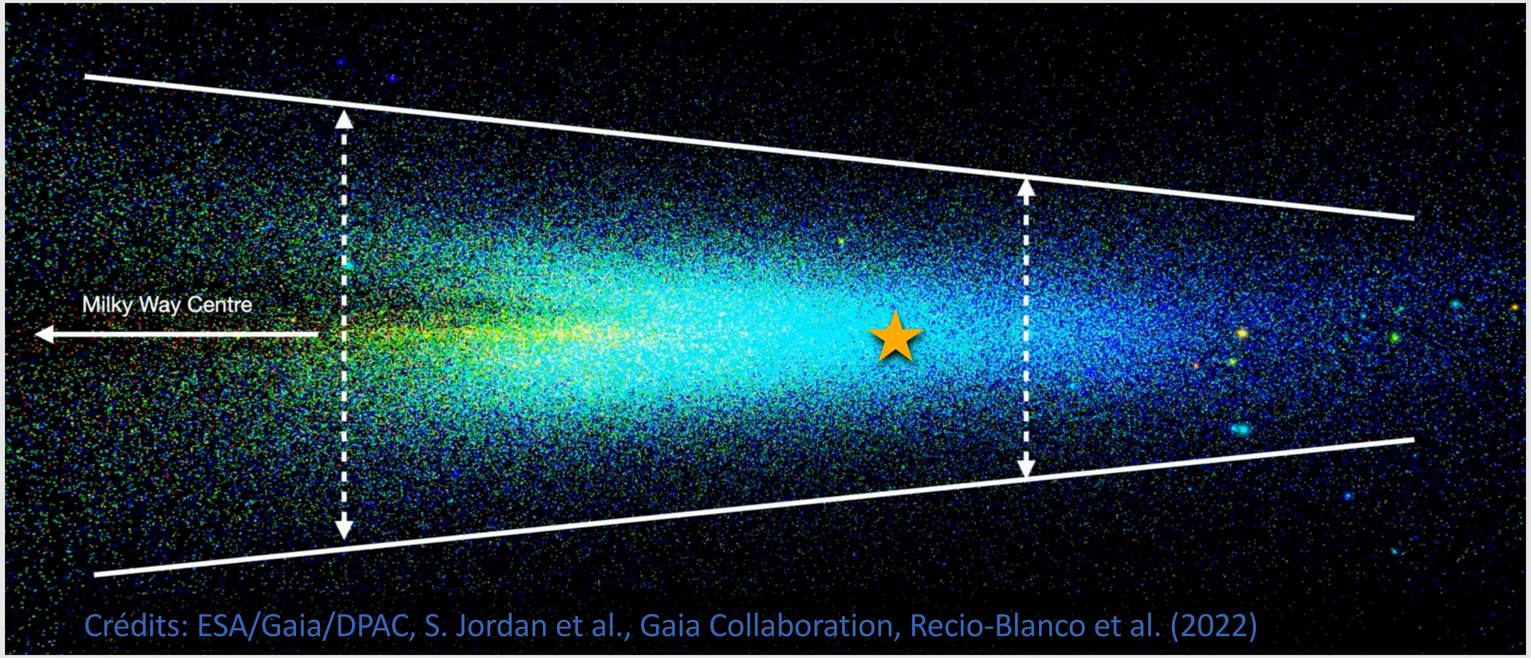

Crédits: ESA/Gaia/DPAC, S. Jordan et al., Gaia Collaboration, Recio-Blanco et al. (2022)

We observe the disc vertical chemical gradient.

Strong symmetry above/below the Galactic plane

Galactic disc: structure and chemical gradients

Young stellar populations in the spiral arms

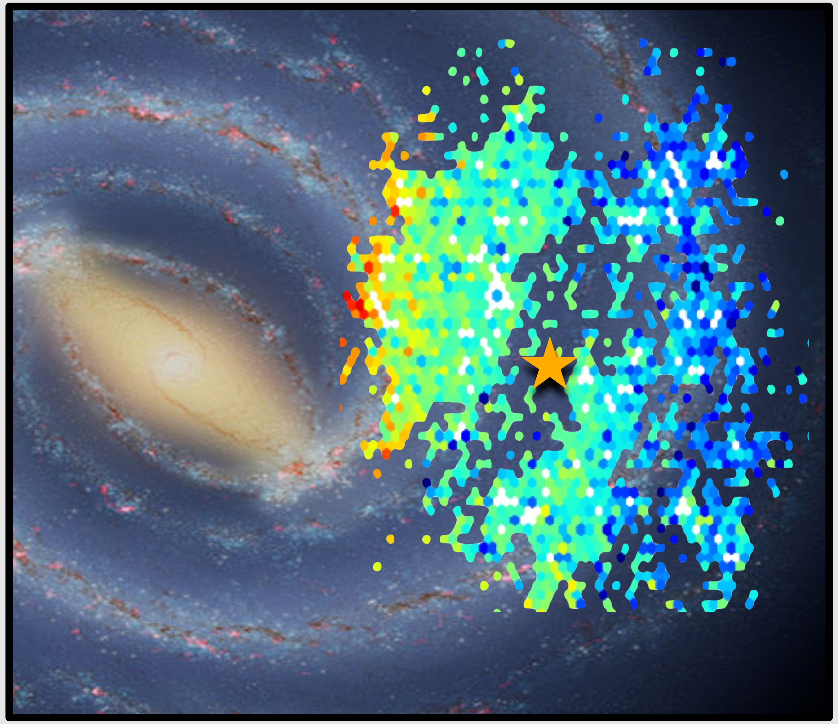

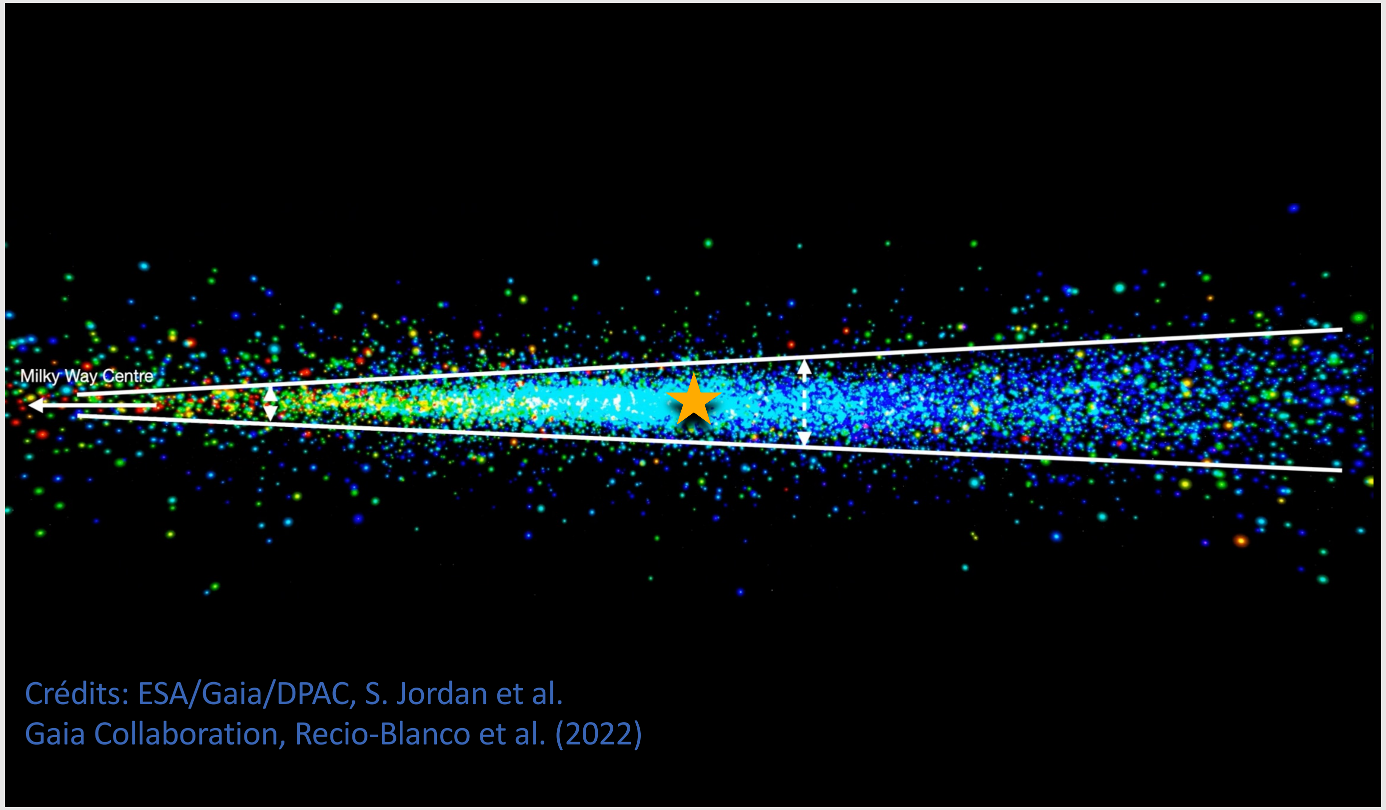

The thin disc

- Radial chemical gradient -> precise quantification with different tracers
- The flare: the thin disc gets thicker as we move outwards

Galactic disc: structure and chemical gradients

Young stellar populations in the spiral arms

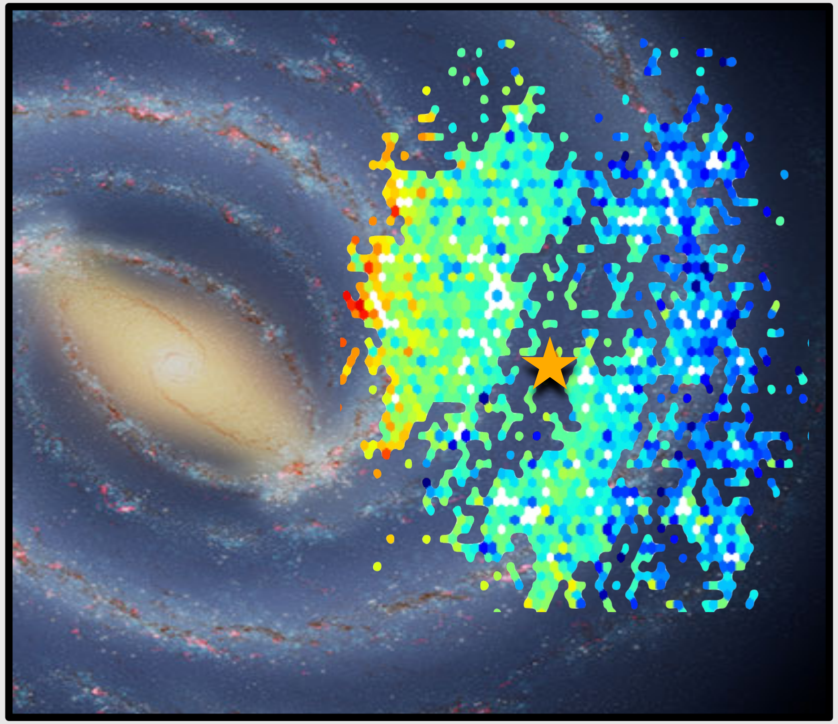

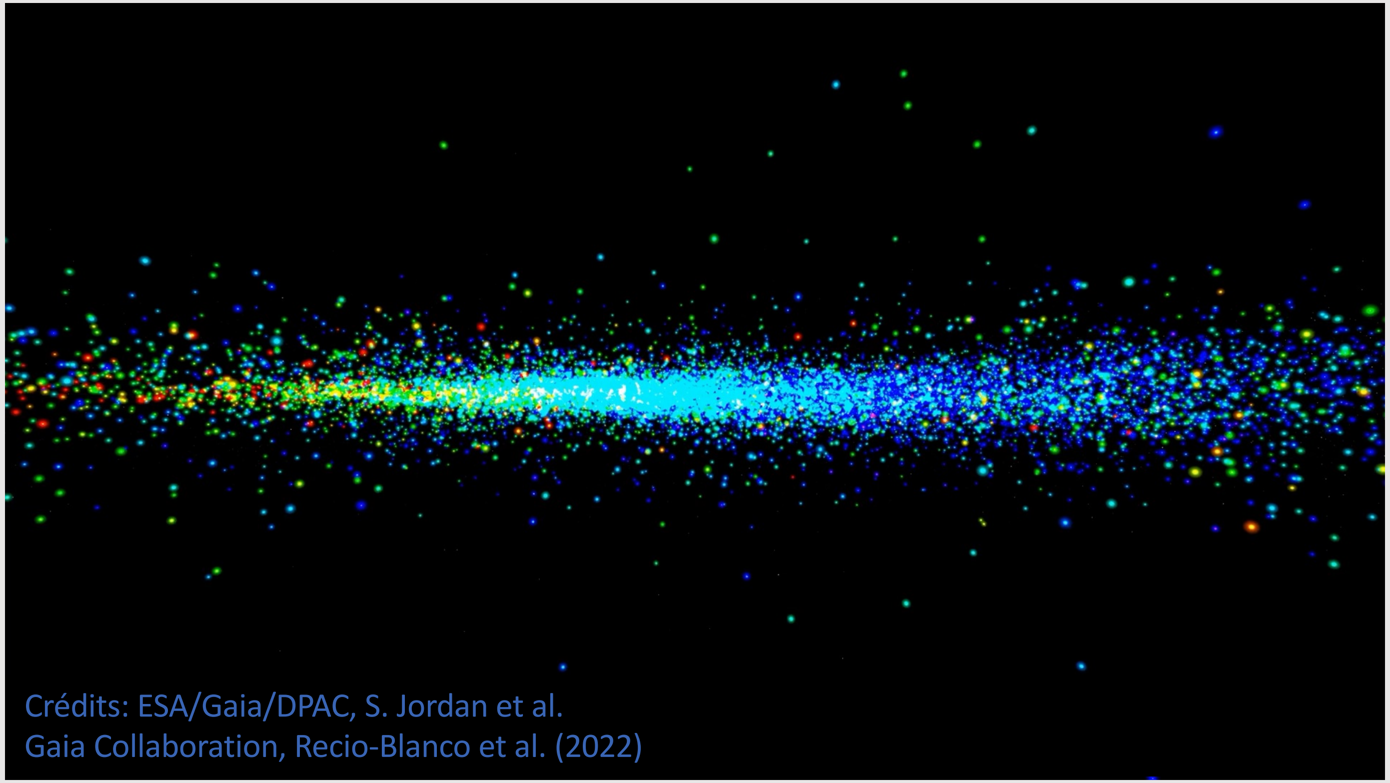

We couple chemistry and orbits thanks to DR3 radial velocities

Katz et al. (2023)

Spiral arms : signatures in density and chemical abundances

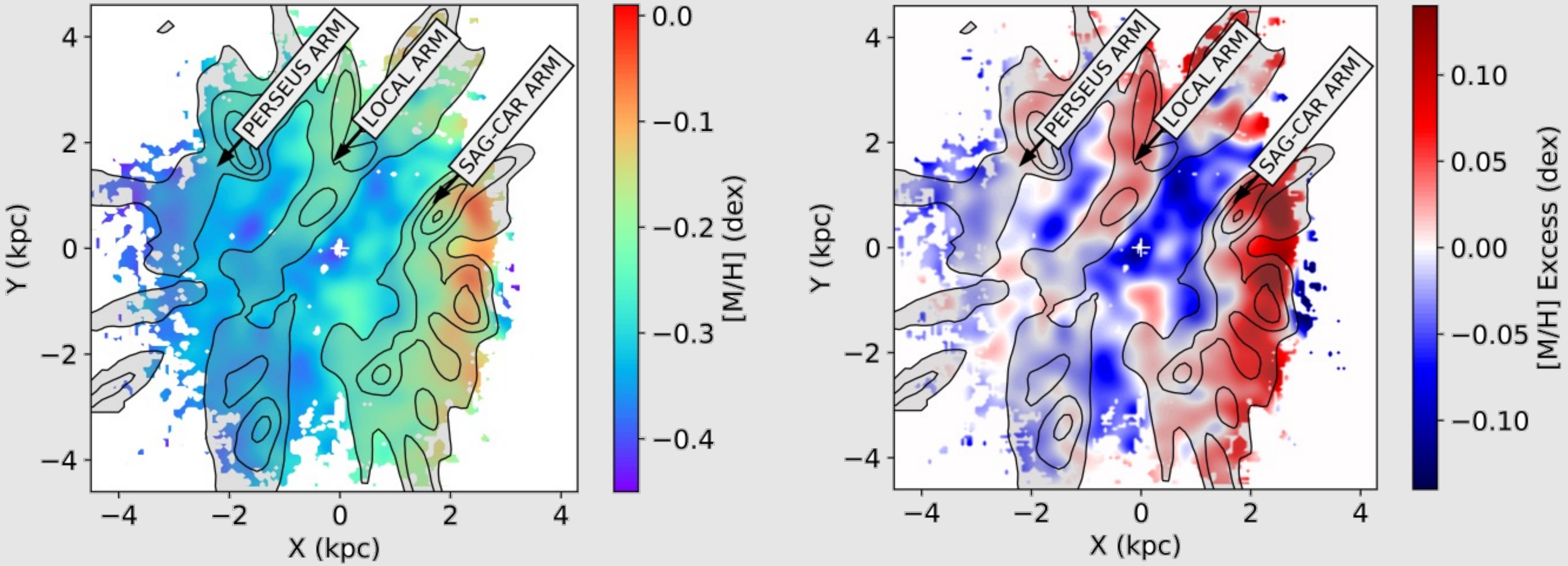

Poggio et al. 2022

From Arms

Spiral arms : signatures in density and chemical abundances

High enough precision and nb statistics to select stars in different age bins.

Chemical signature of the Spiral Arms

Poggio, ARB et al. (2022)

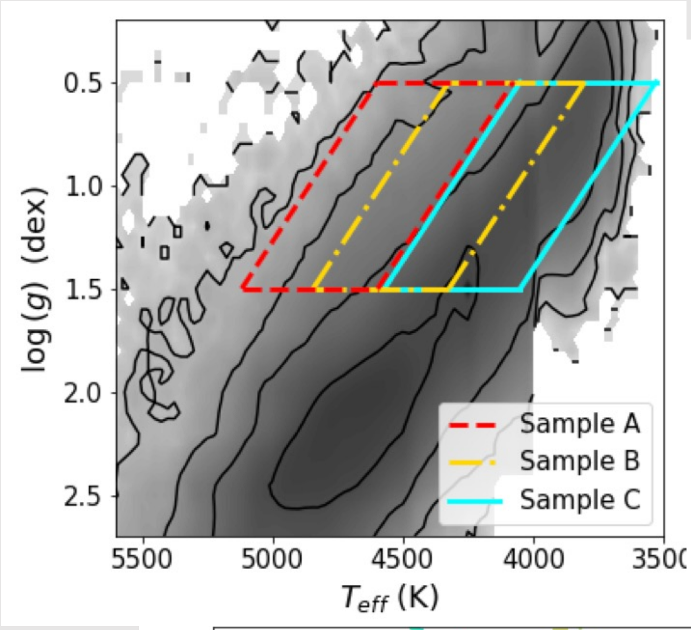

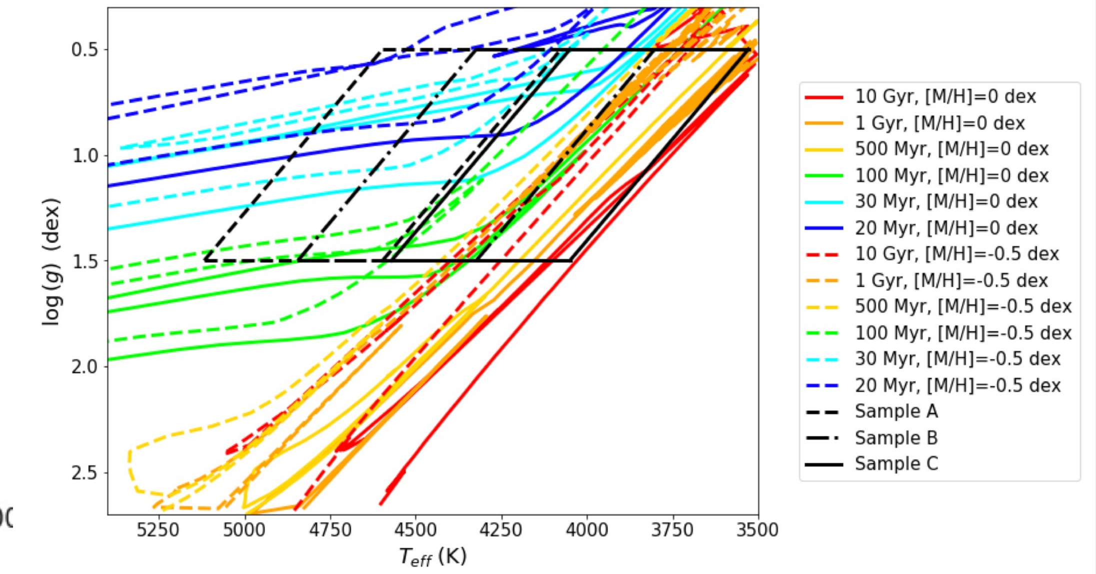

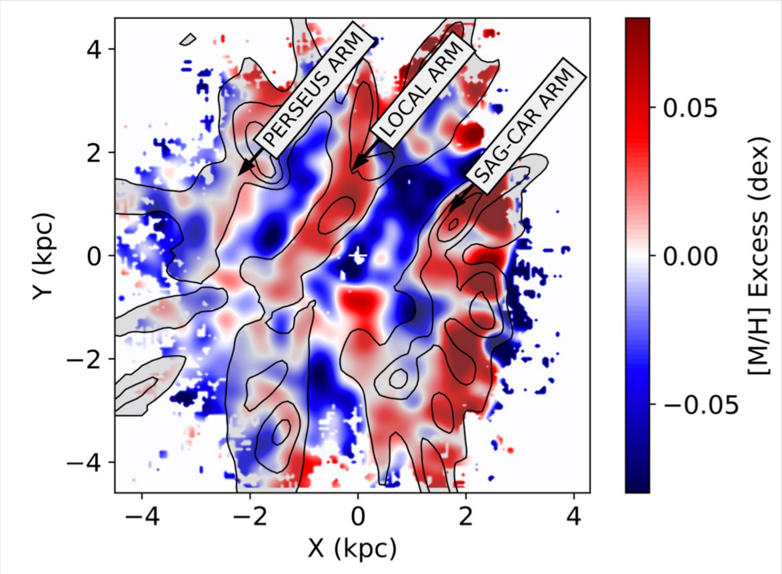

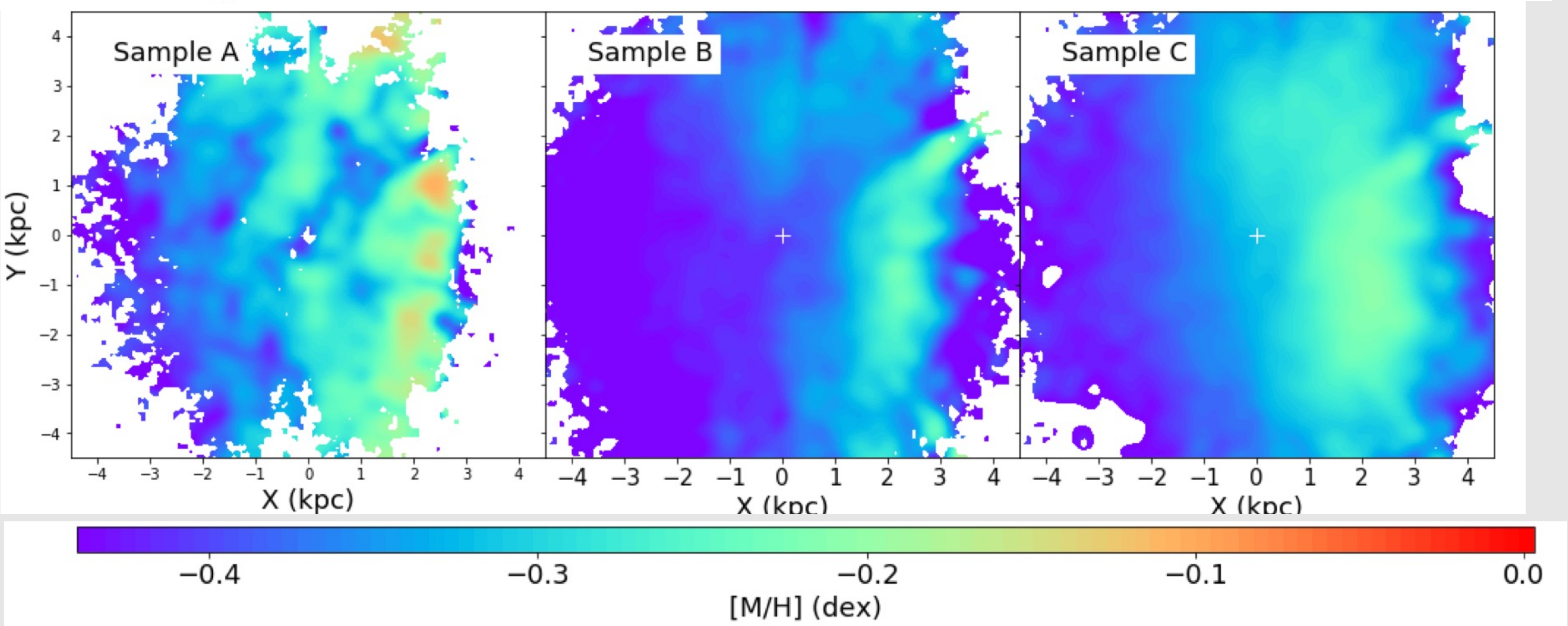

Spiral arms : signatures in density and chemical abundances

Poggio et al. (2022)

From a 1D radial gradient to ...

a 2D radial gradient

+

Chemical signature of the Spiral Arms

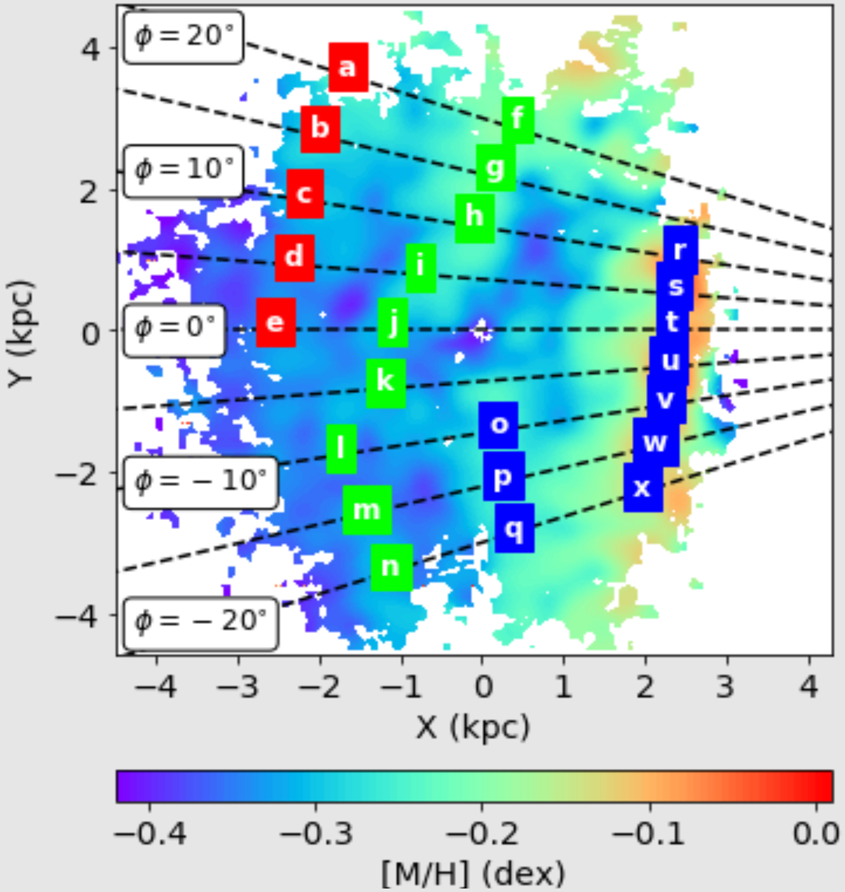

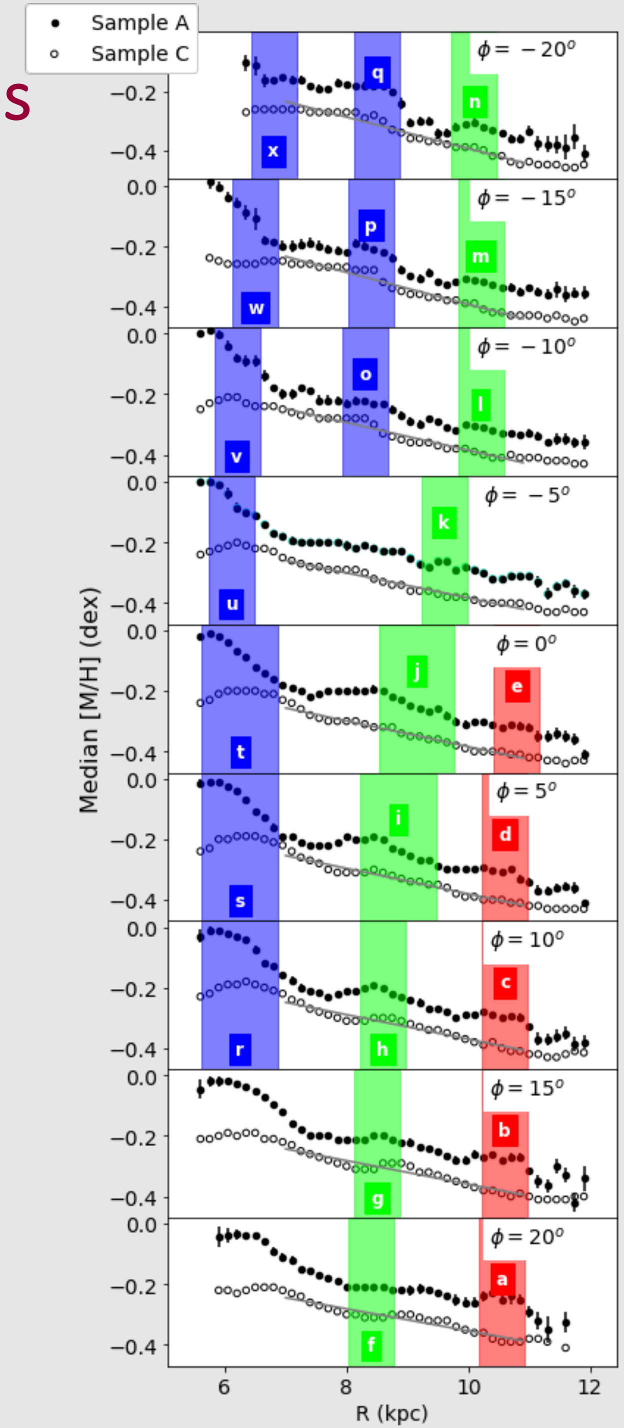

Spiral arms : signatures in density and chemical abundances

Age<1Gyr **Age>1Gyr**

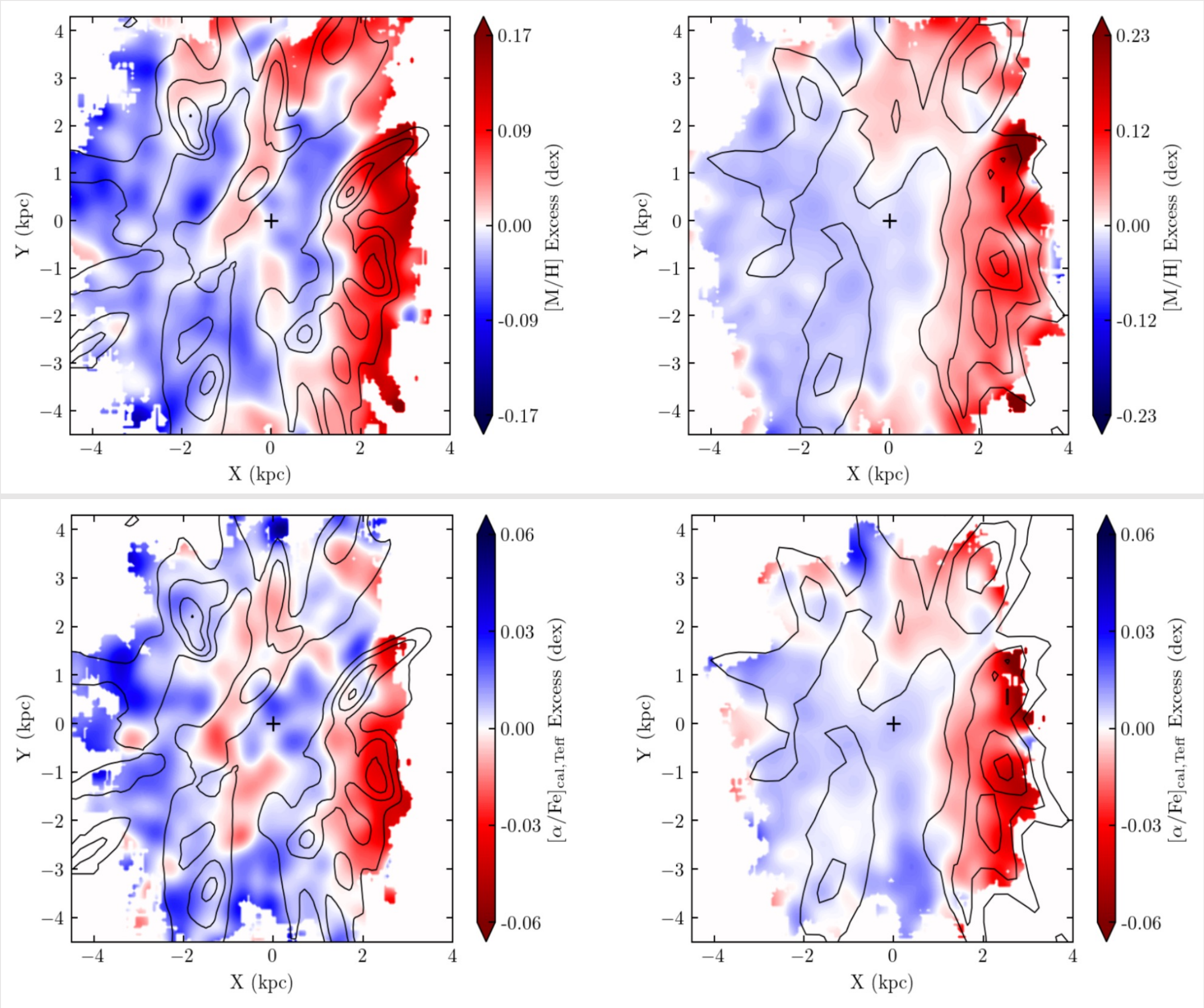

Barbillon et al., in prep.

Marie Barbillon
(attending the EES!!)

Metallicity signatures of the spiral arms both **in the young** (Poggio et al. 2022) **and the old population** (Barbillon et al., in prep.)

The spiral arms signature is **visible in the relative abundance of α-elements with respect to iron.**

The fluctuation in α-elements is higher than in iron.

Spiral arms : signatures in density and chemical abundances

2D chemical evolution model

Elements synthesised on short time scales (i.e., oxygen and europium) exhibit larger abundance fluctuations.

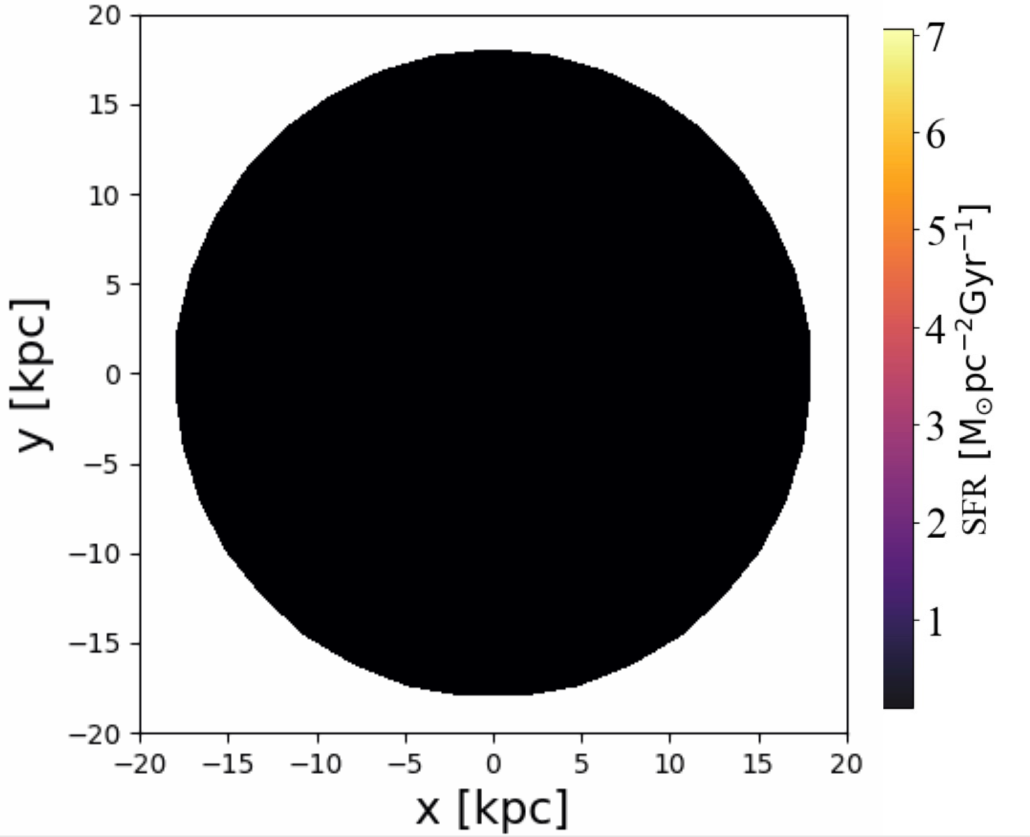

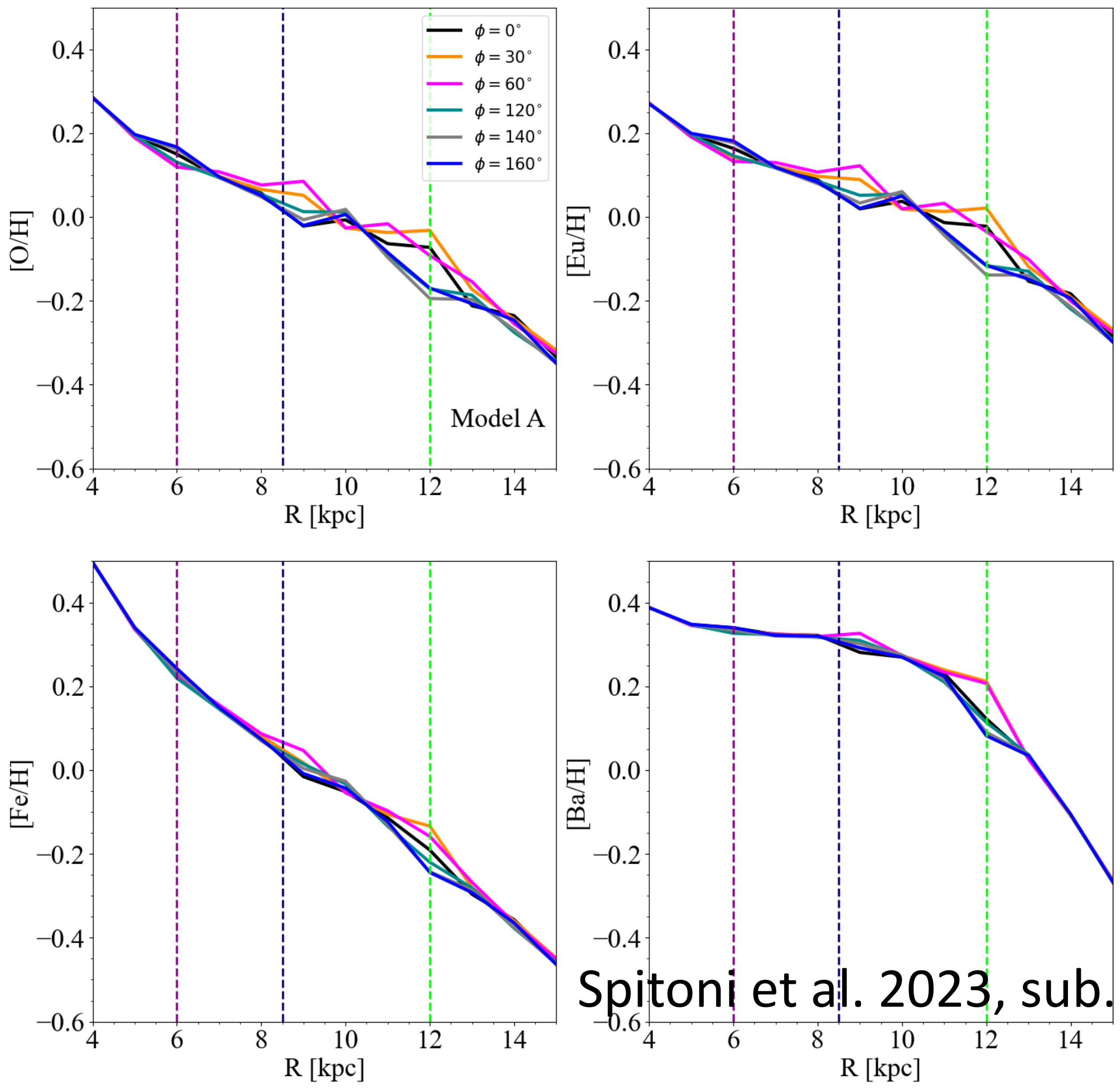

Spitoni et al. 2023, sub.

Spiral arms : signatures in density and chemical abundances

Agreement with Gaia observations if at most recent times the spiral arm structure is transient (co-rotating with the disc).

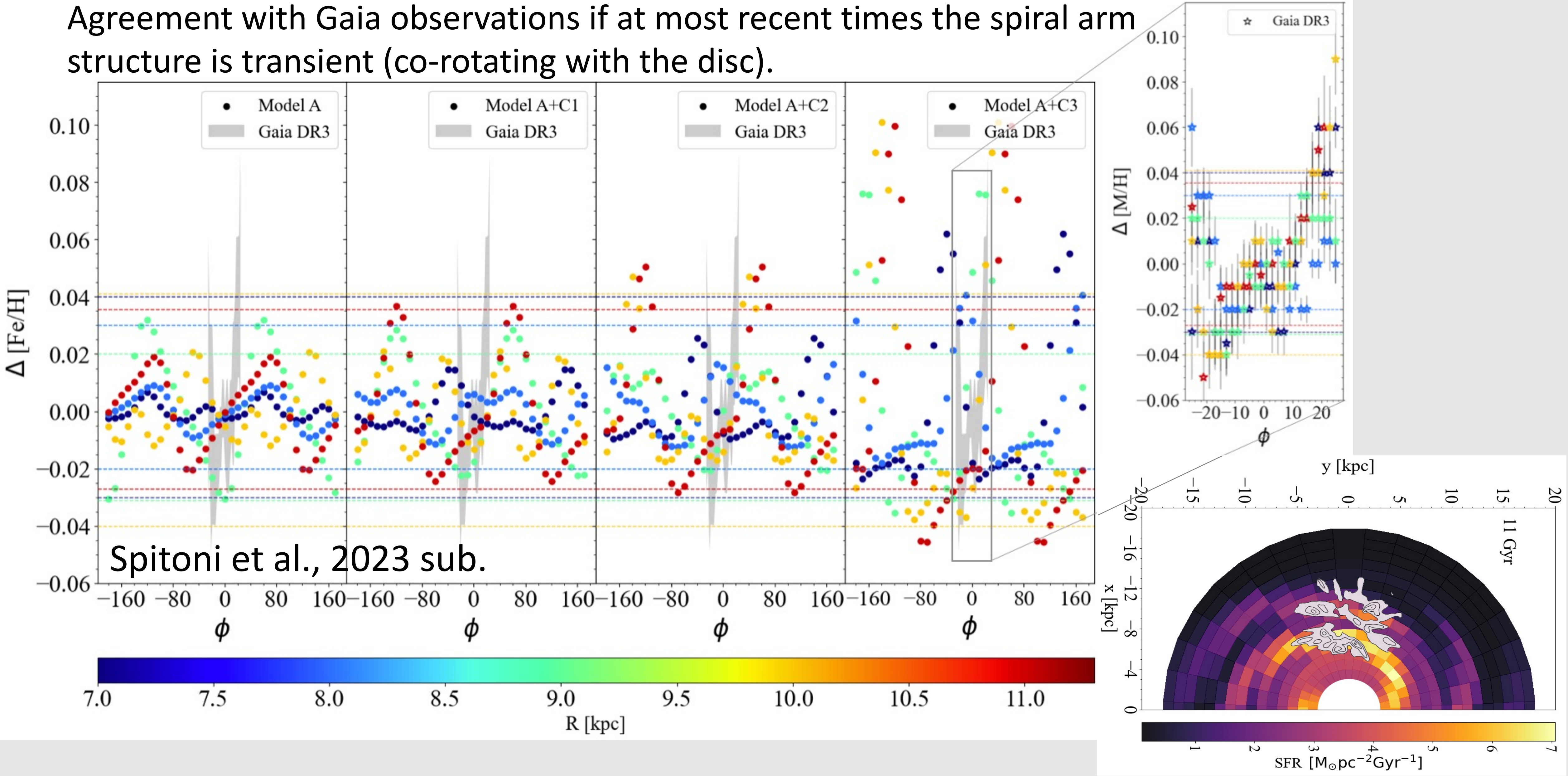

Galactic disc: Open clusters

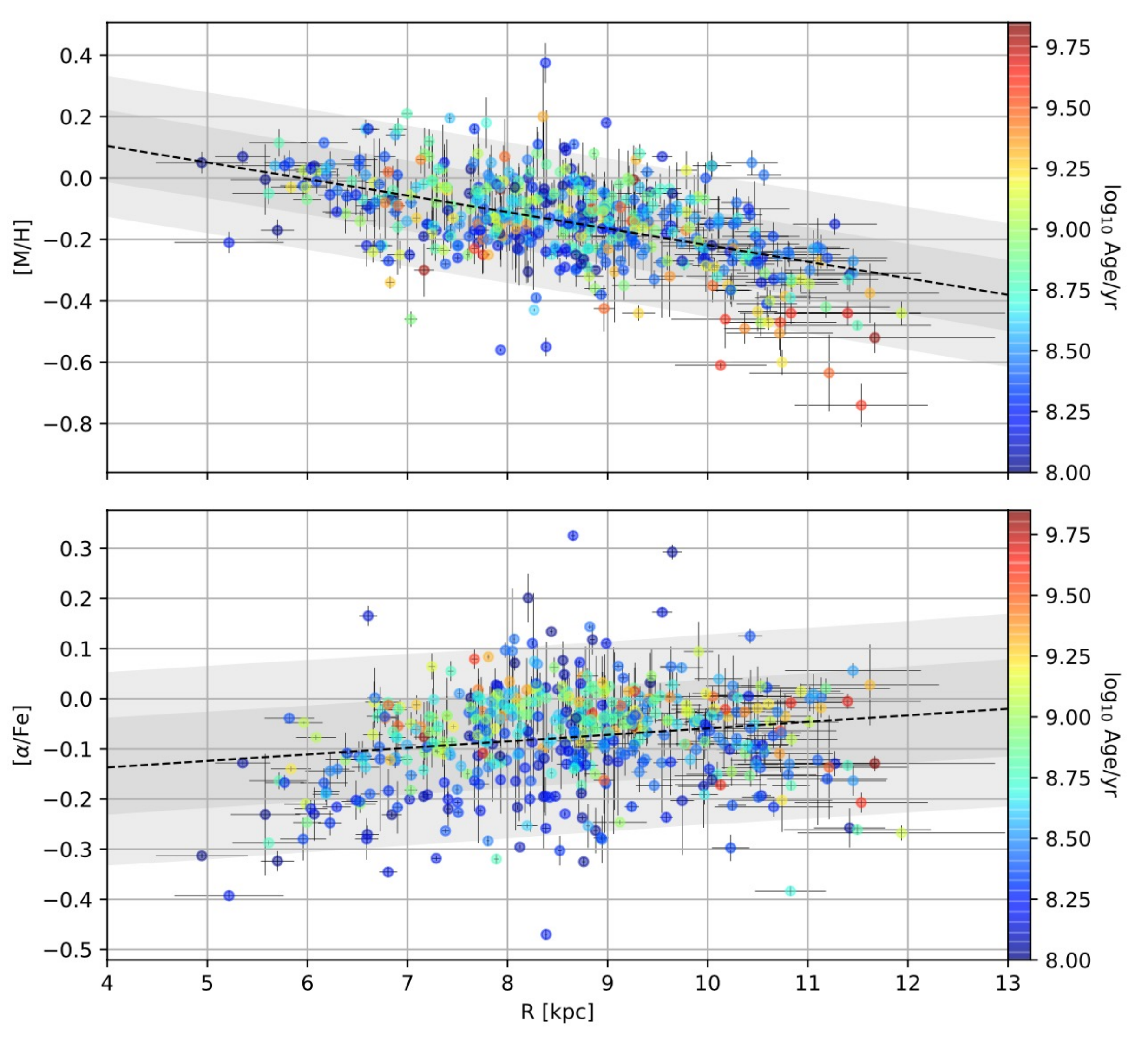

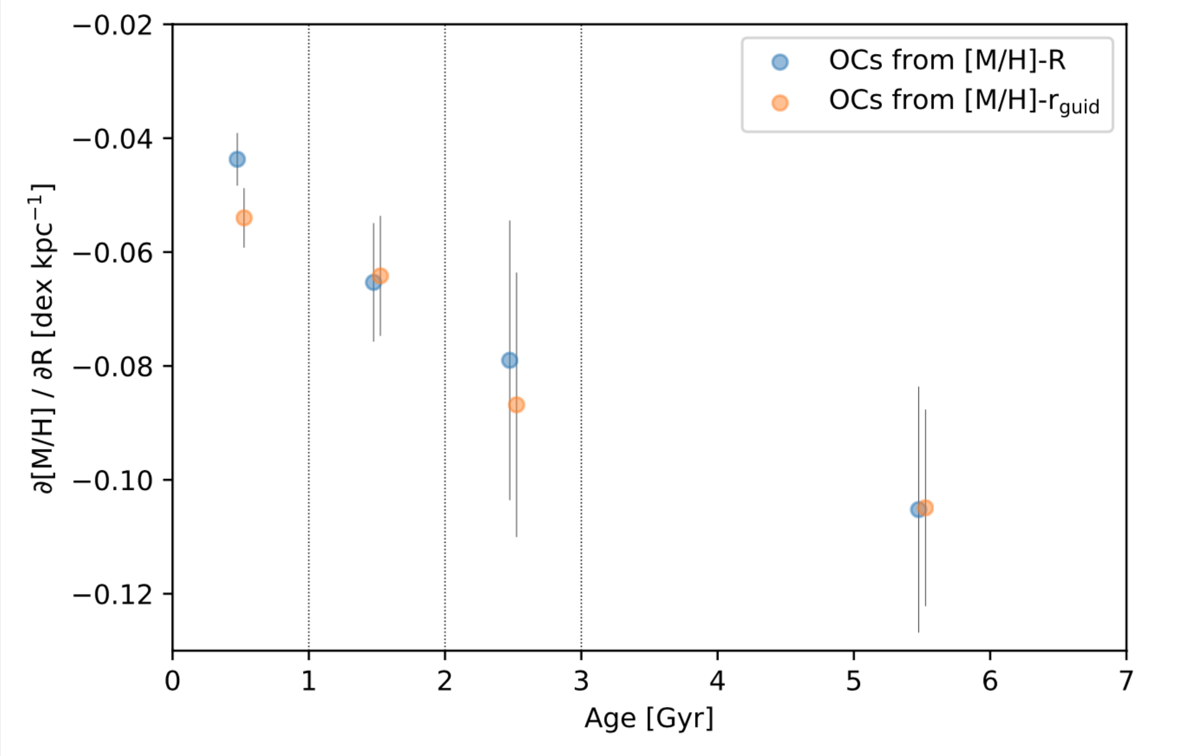

687 open clusters in the Gaia DR3 chemical database

Gaia Collaboration, Recio-Blanco et al. (2022)

Galactic disc: Open clusters

Prantzos et al. chemical evolution model

Multi-zone semi-analytical models + radial migration

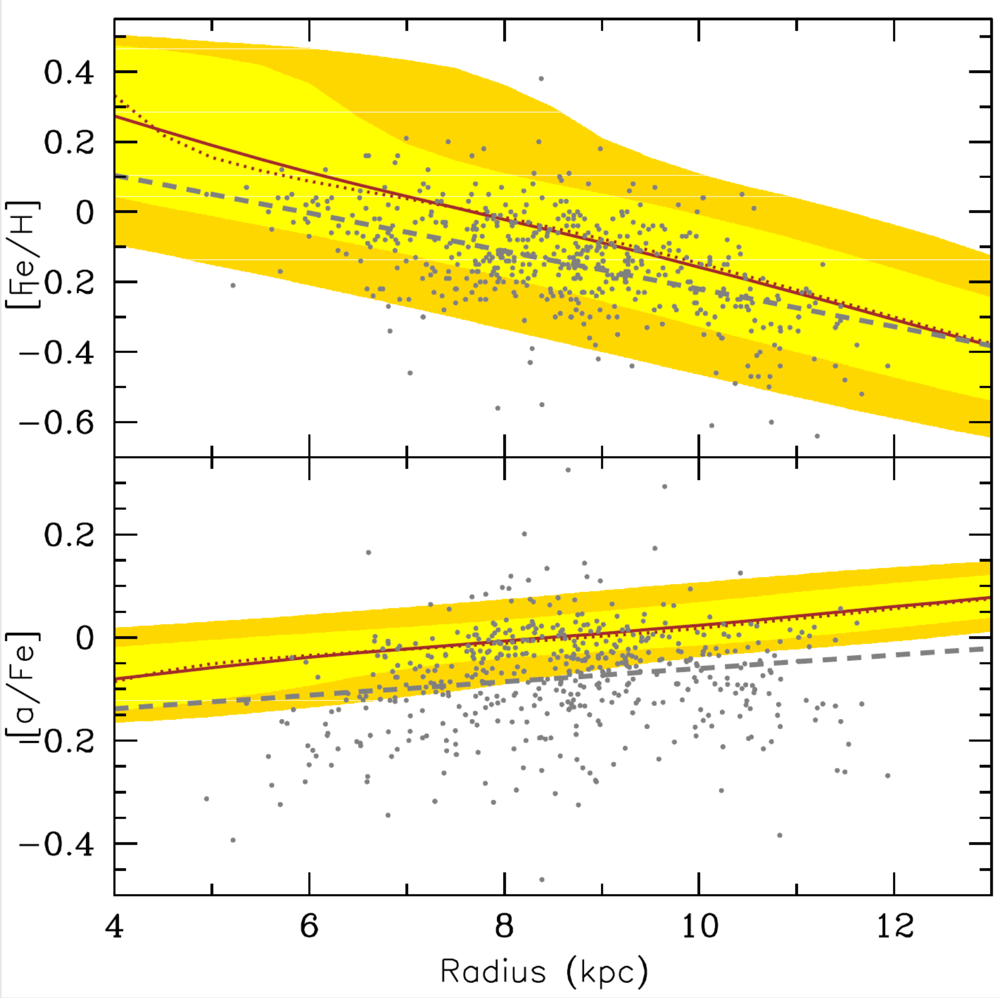

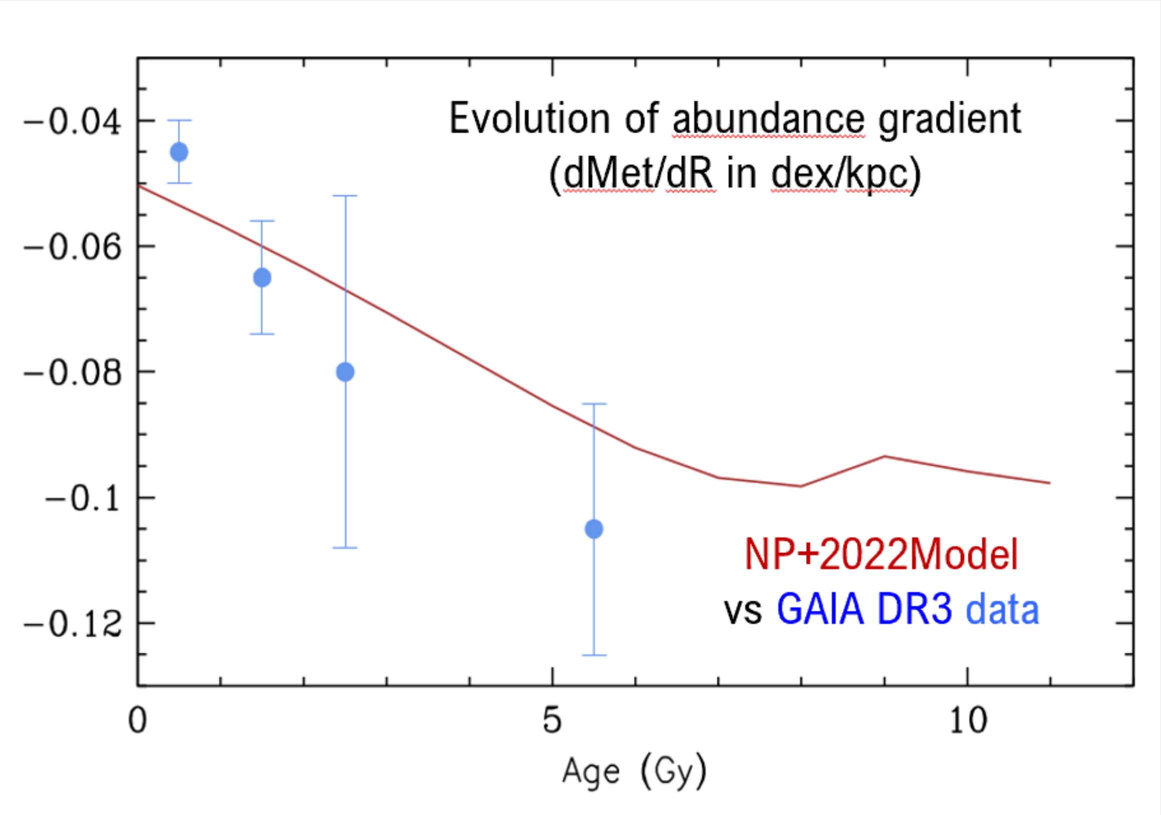

Prantzos et al. 2023

THE [X/Fe] vs. [Fe/H] DIAGRAMME : chemical tracers of stellar populations

- A common diagnostic of precise abundances is the capability to chemically separate thin/thick disc populations in the [alpha/Fe] vs. [Fe/H]

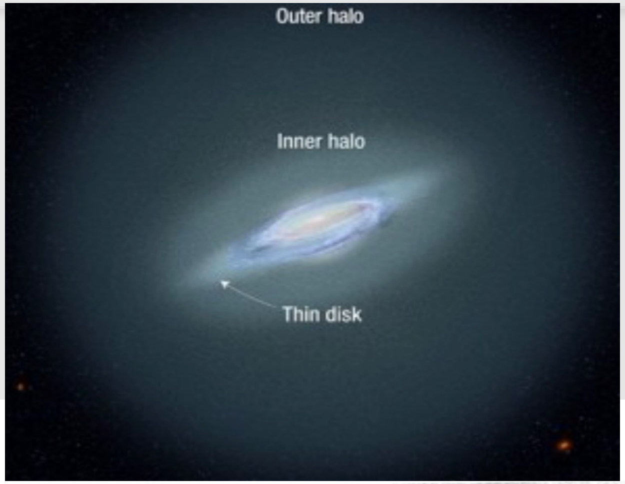

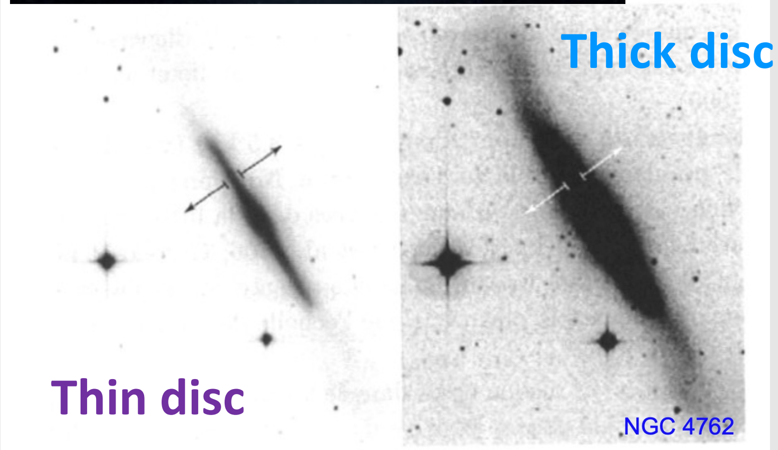

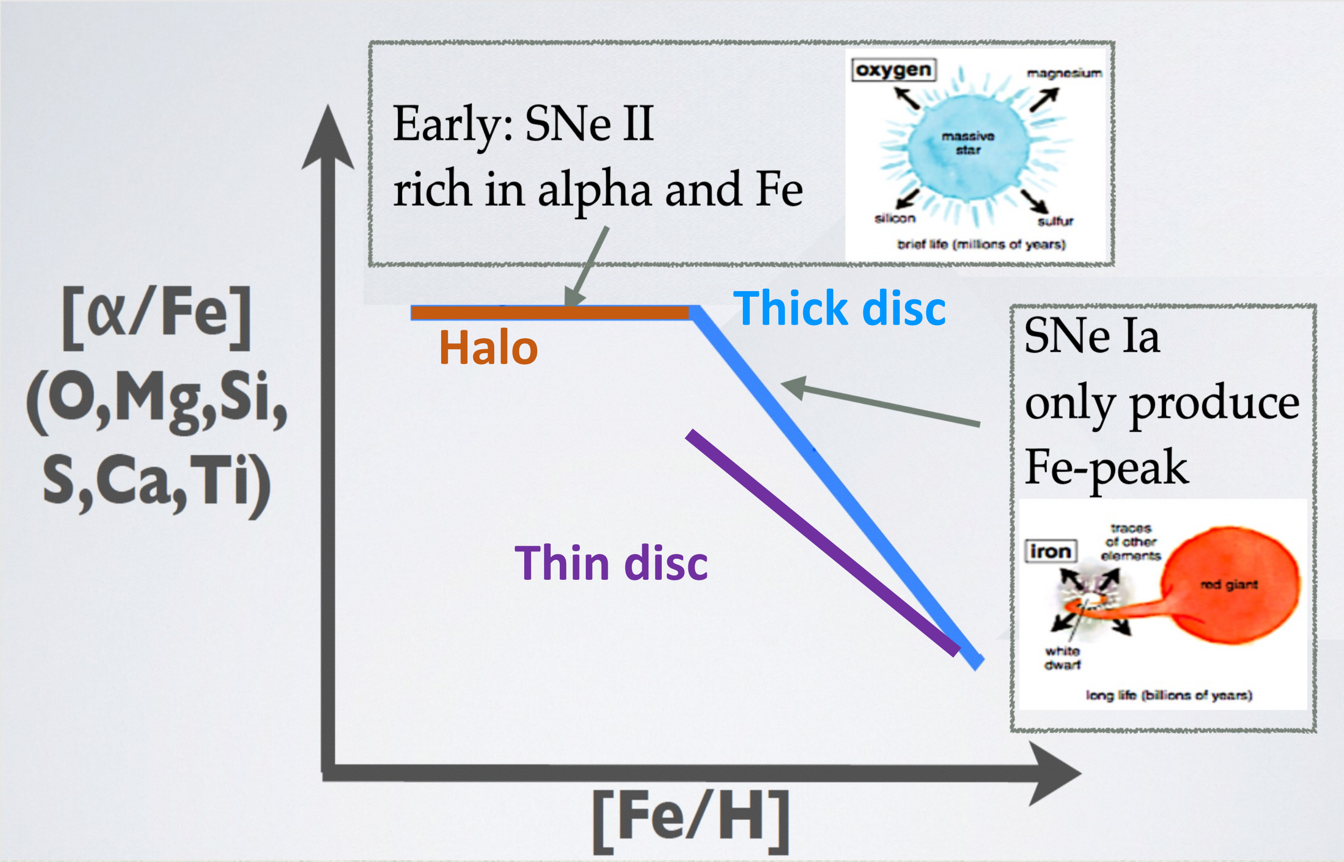

THE [X/Fe] vs. [Fe/H] DIAGRAMME : stellar populations chemical tracers

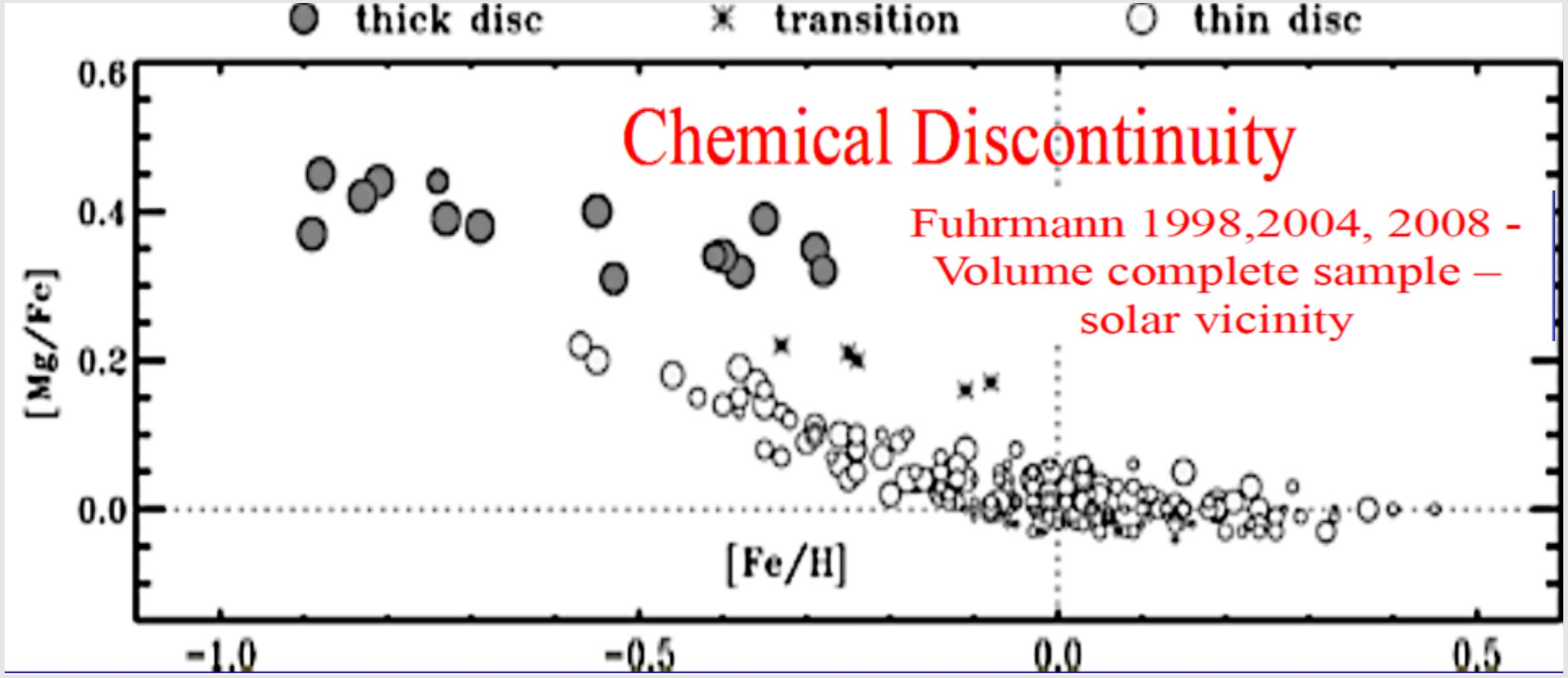

The bimodality is seem if:

1. Uncertainties are low enough.

2. The considered alpha-element is mostly produced by short lived sources

See for instance 1) **chemical evolution models :** Prantzos et al. (2023), Spitoni et al. (2023) 2) **GES data** (Mikolaitis et al. 2014), **APOGEE data** (Abdurro'uf et al. 2022), **etc...**

THE [X/Fe] vs. [Fe/H] DIAGRAMME : stellar populations chemical tracers

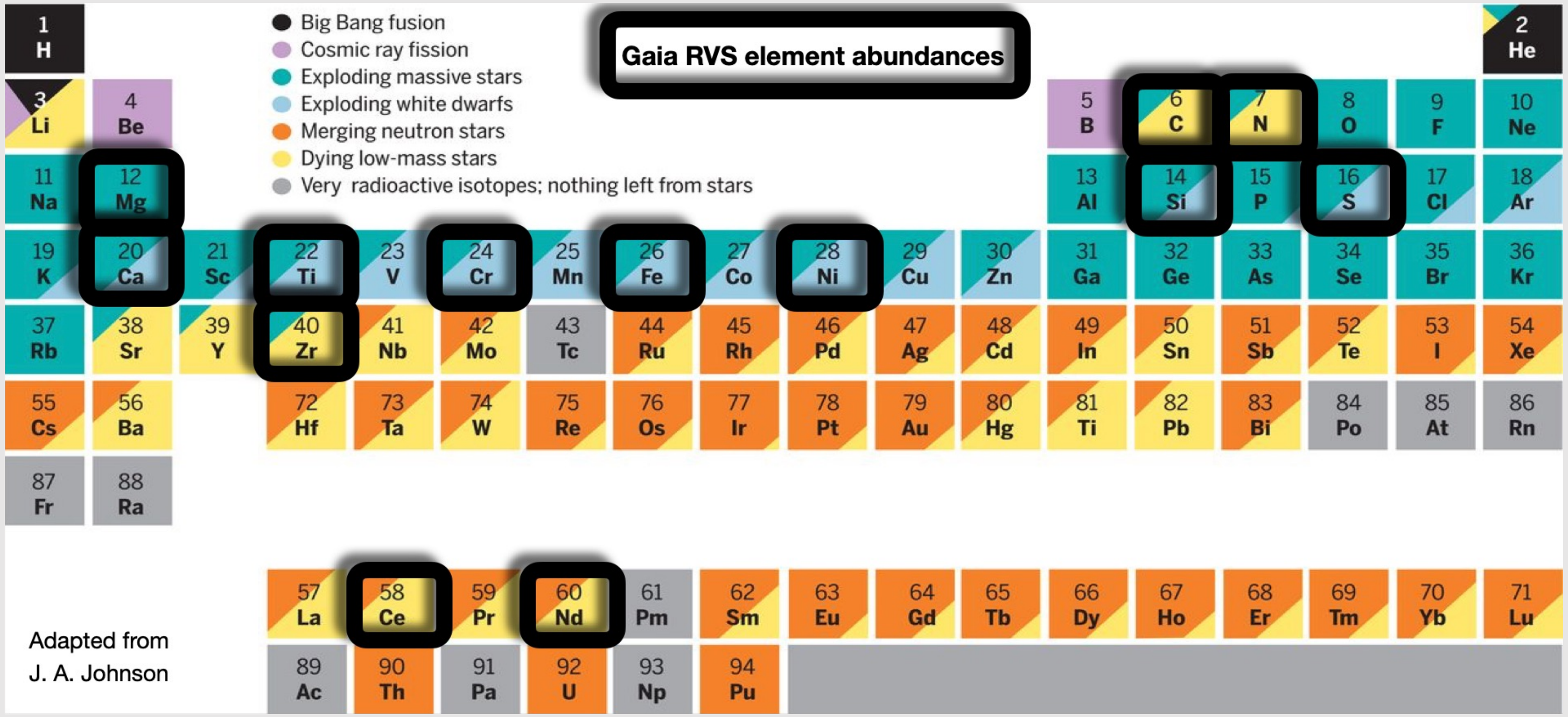

credits C. Chiappini

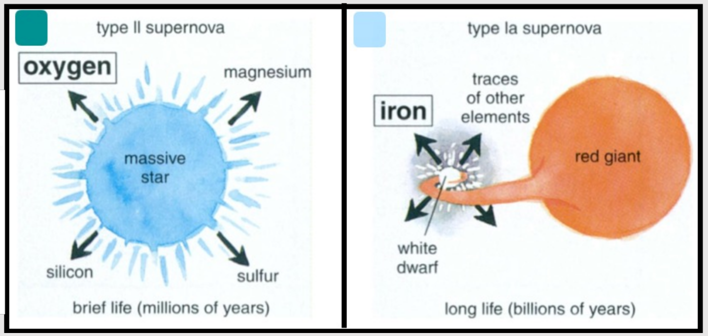

Short lived **Long lived** **Short lived** **Long lived**

For high precision abundances

<u>Large</u> separation if:

Mostly Short lived producers

e.g. Mg

[X/Fe]

Mostly long lived

THE [X/Fe] vs. [Fe/H] DIAGRAMME : stellar populations chemical tracers

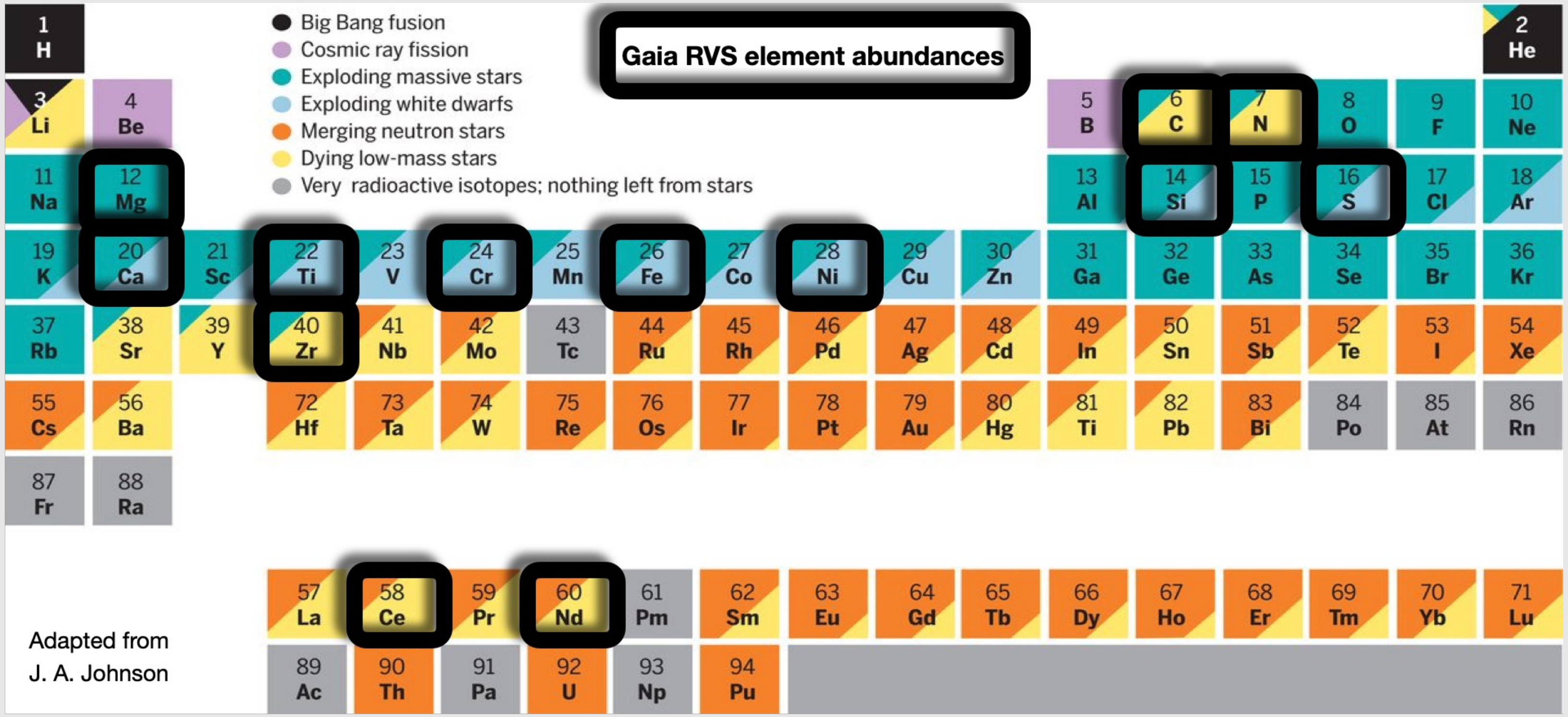

For high precision abundances

<u>Small</u> separation if:

Low long lived contribution

e.g Ca or Ti

[X/Fe]

Mostly long lived

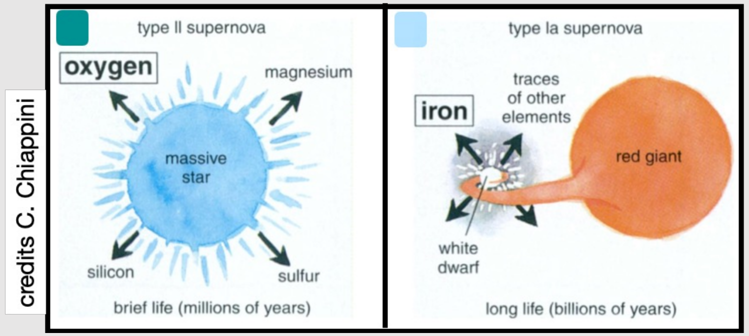

Short lived **Long lived** **Short lived** **Long lived**

Thin/thick disc chemical bimodality

The Gaia GSPspec global α diagnostic is dominated by the CaT lines:

GSPspec $[\alpha/Fe] \simeq$ [Ca/Fe]

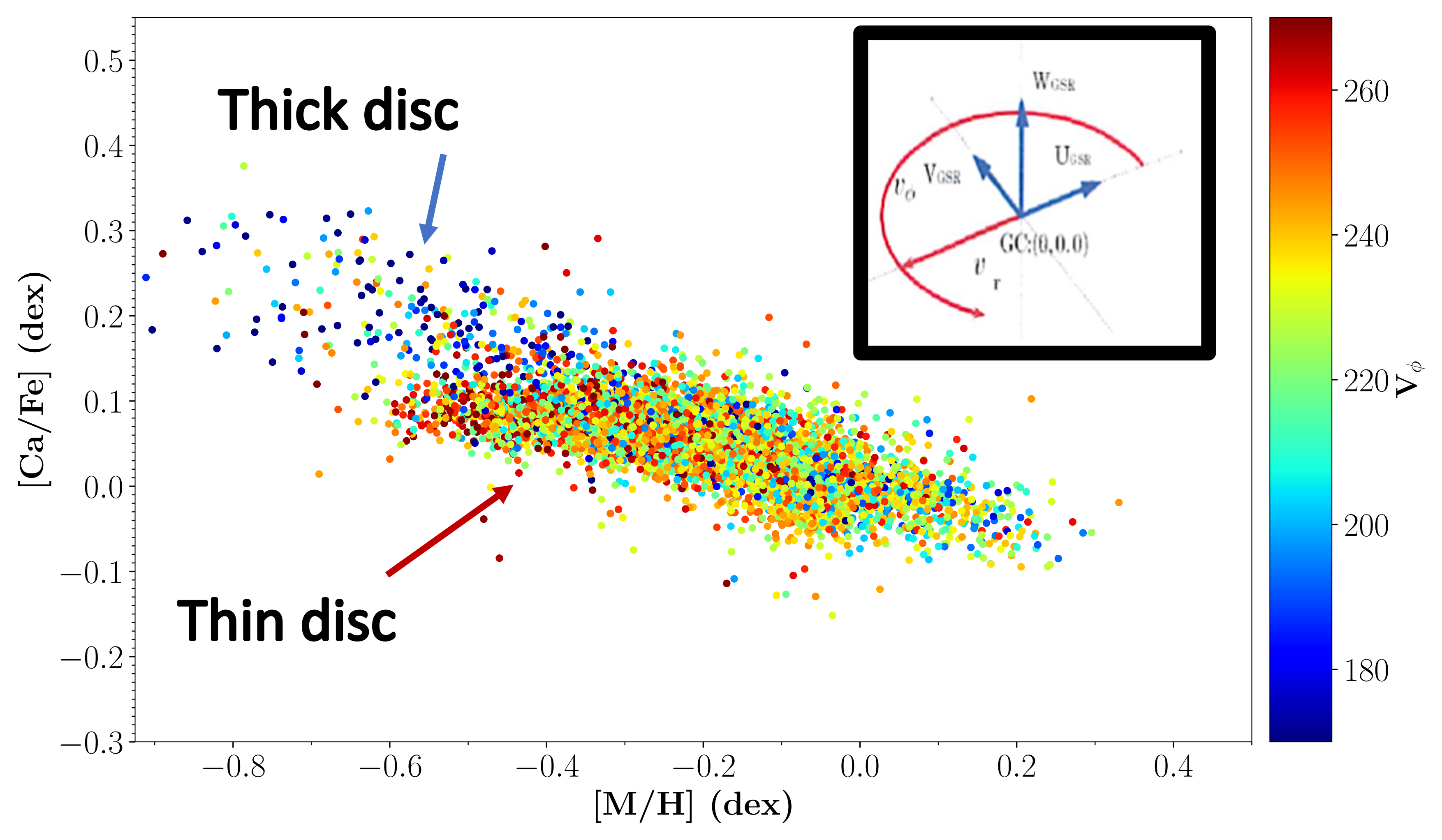

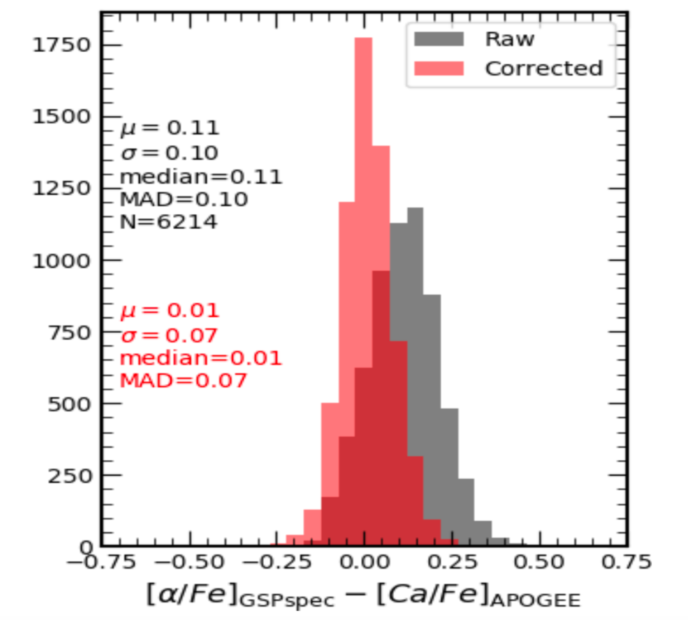

Small thin/thick disc sequences separation even with low uncertainties

Thin/thick disc chemical bimodality

The Gaia GSPspec global α diagnostic is dominated by the CaT lines:

GSPspec $[\alpha/Fe] \simeq [Ca/Fe]$

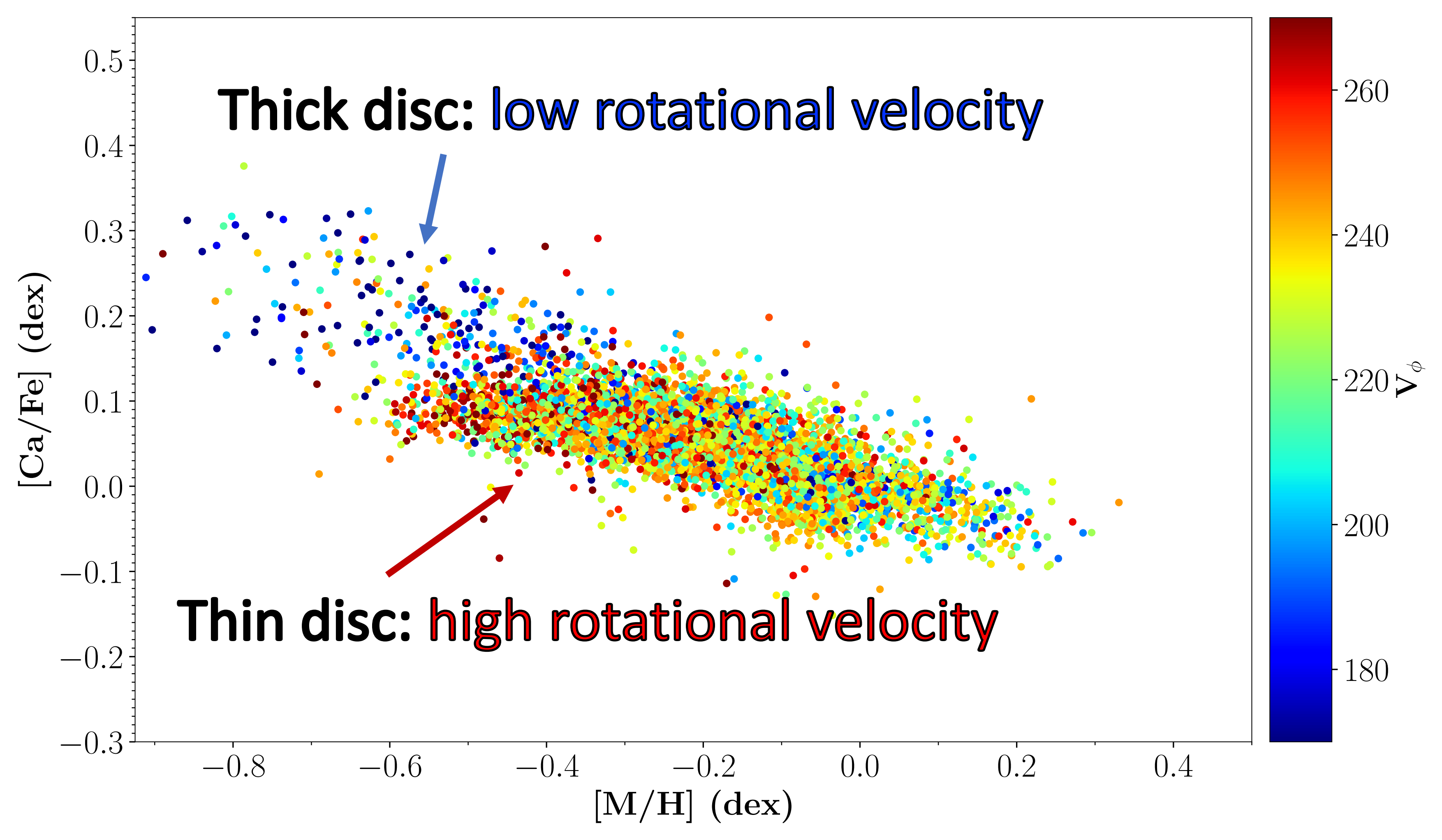

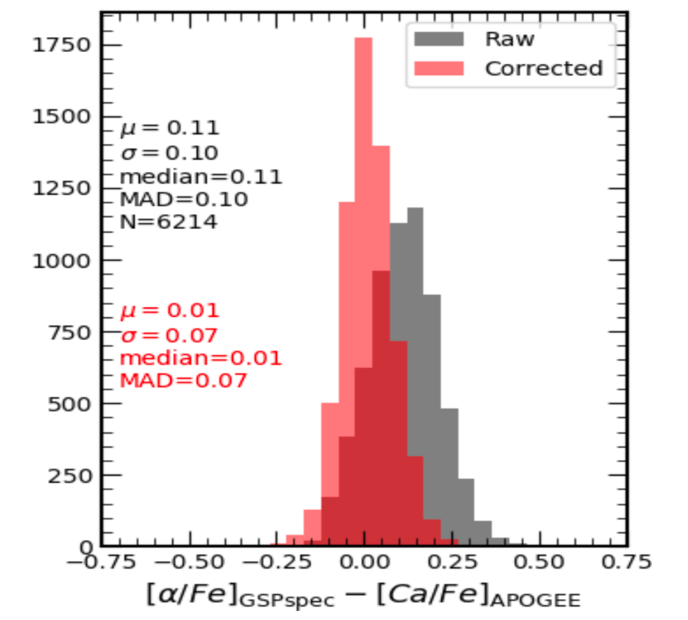

Small thin/thick disc sequences separation even with low uncertainties

Thin/thick disc chemical bimodality

But choosing **[Mg/Fe] abundances with low uncertainties**

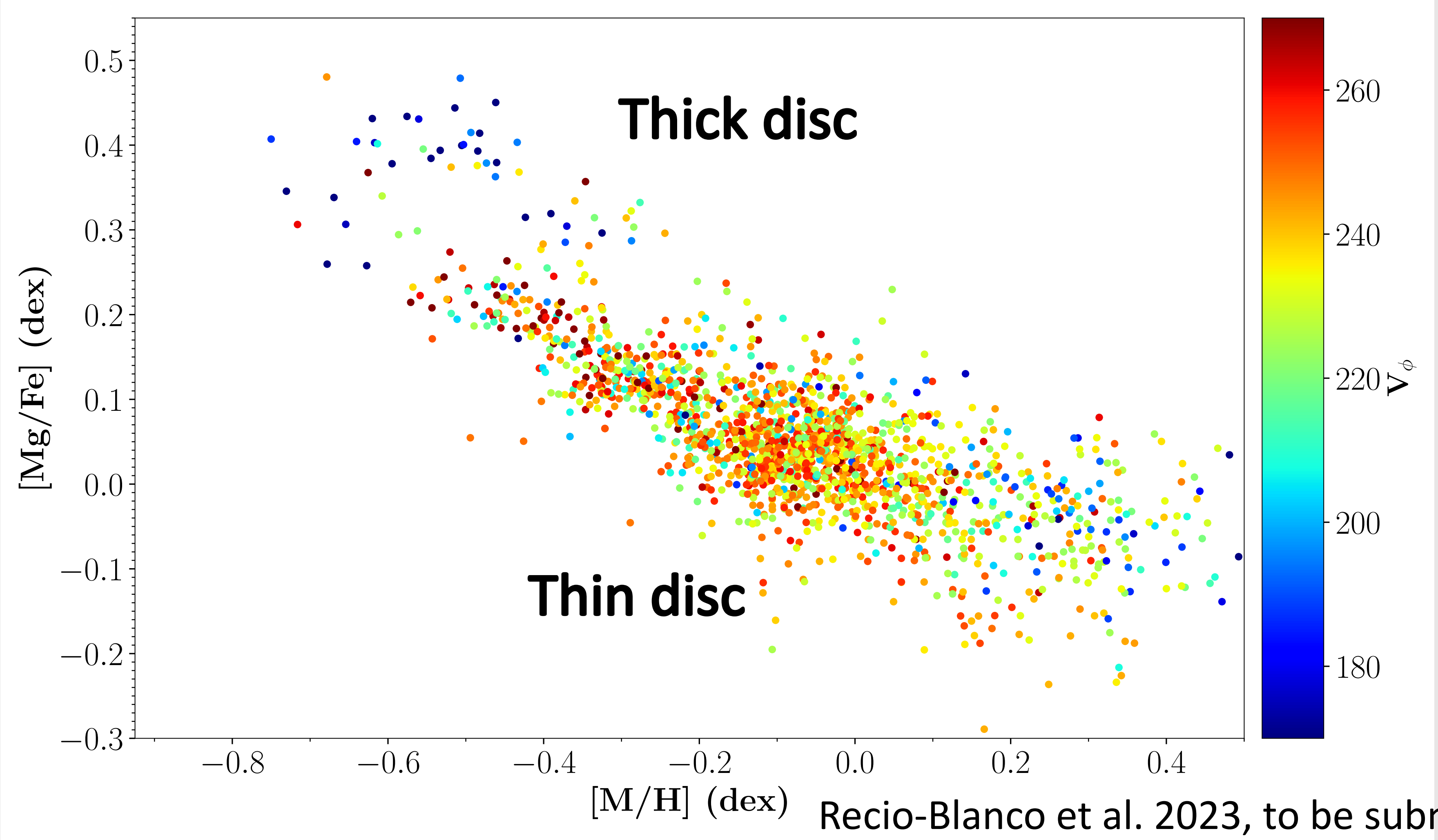

Recio-Blanco et al. 2023, to be submited

Large thin/thick disc sequences separation, as expected...

and with only
R=11 500
at 846 - 870 nm !!

Bimodal disc RBG and RC from high precision parameters

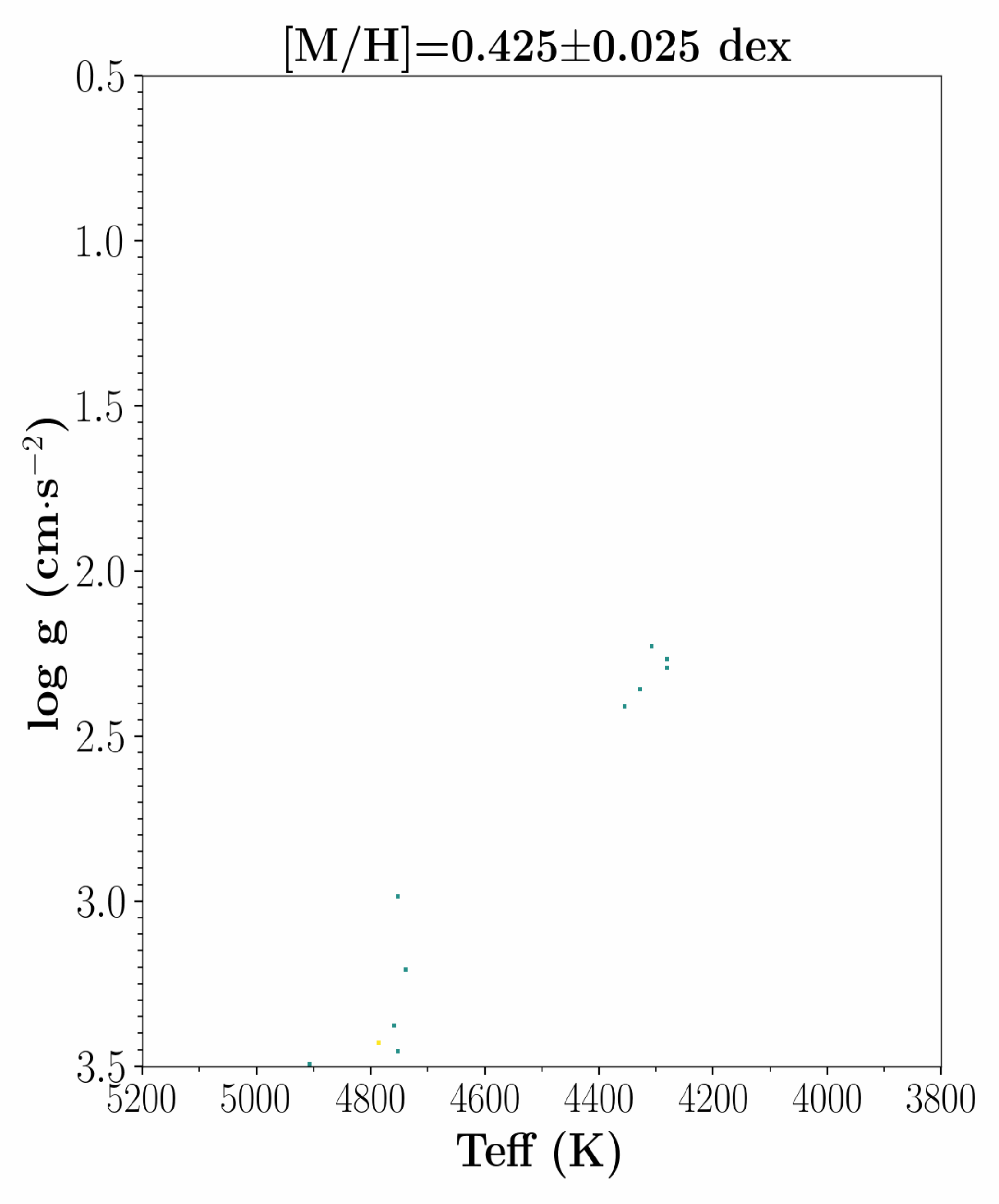

Gaia GSPspec : mono-abundance disc populations

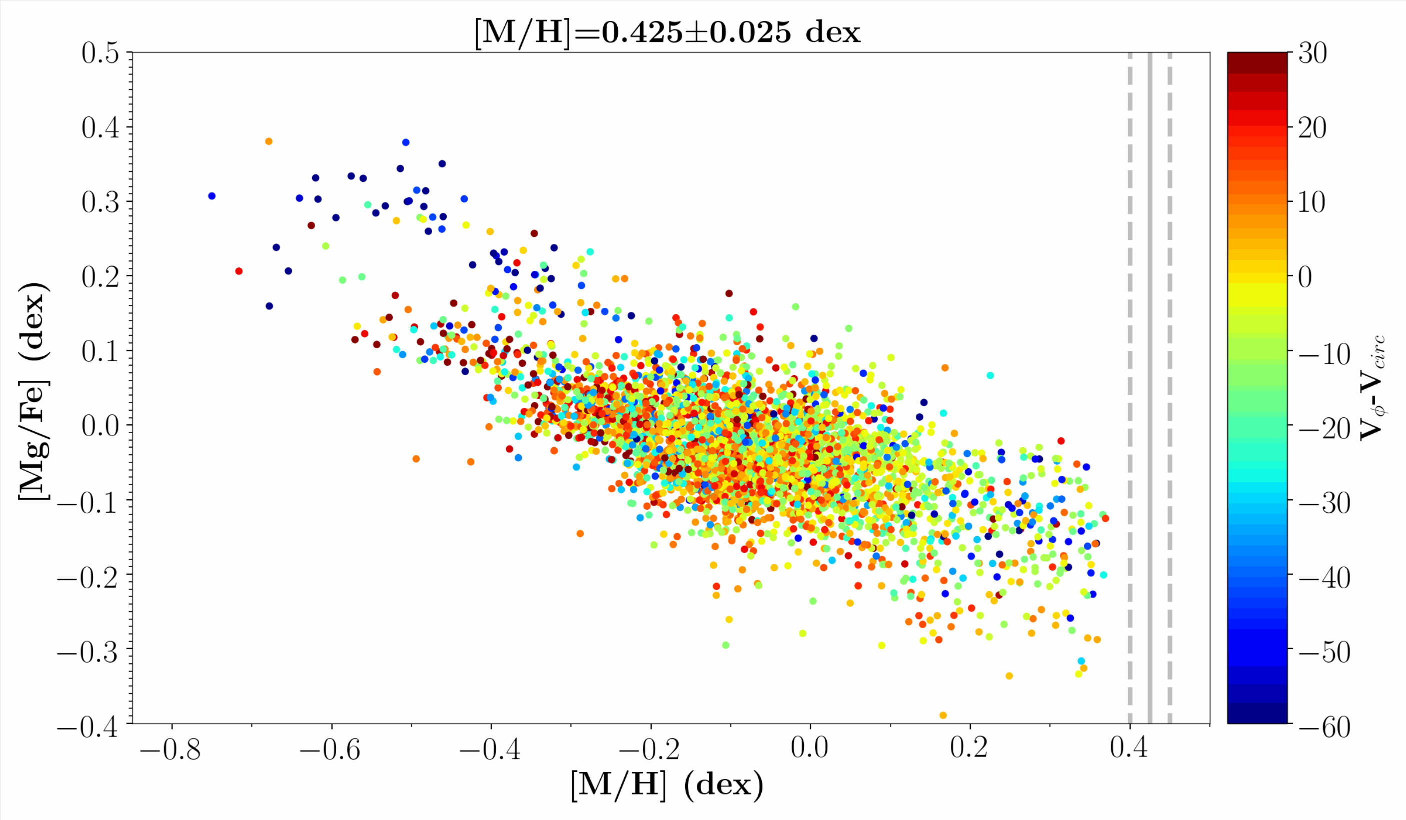

Recio-Blanco et al. 2023, to be submited

Galactic disc: structure and chemical gradients

Vertical and radial cartography of [alpha/Fe] vs. [M/H] colour coded with Galactic azimuthal velocity

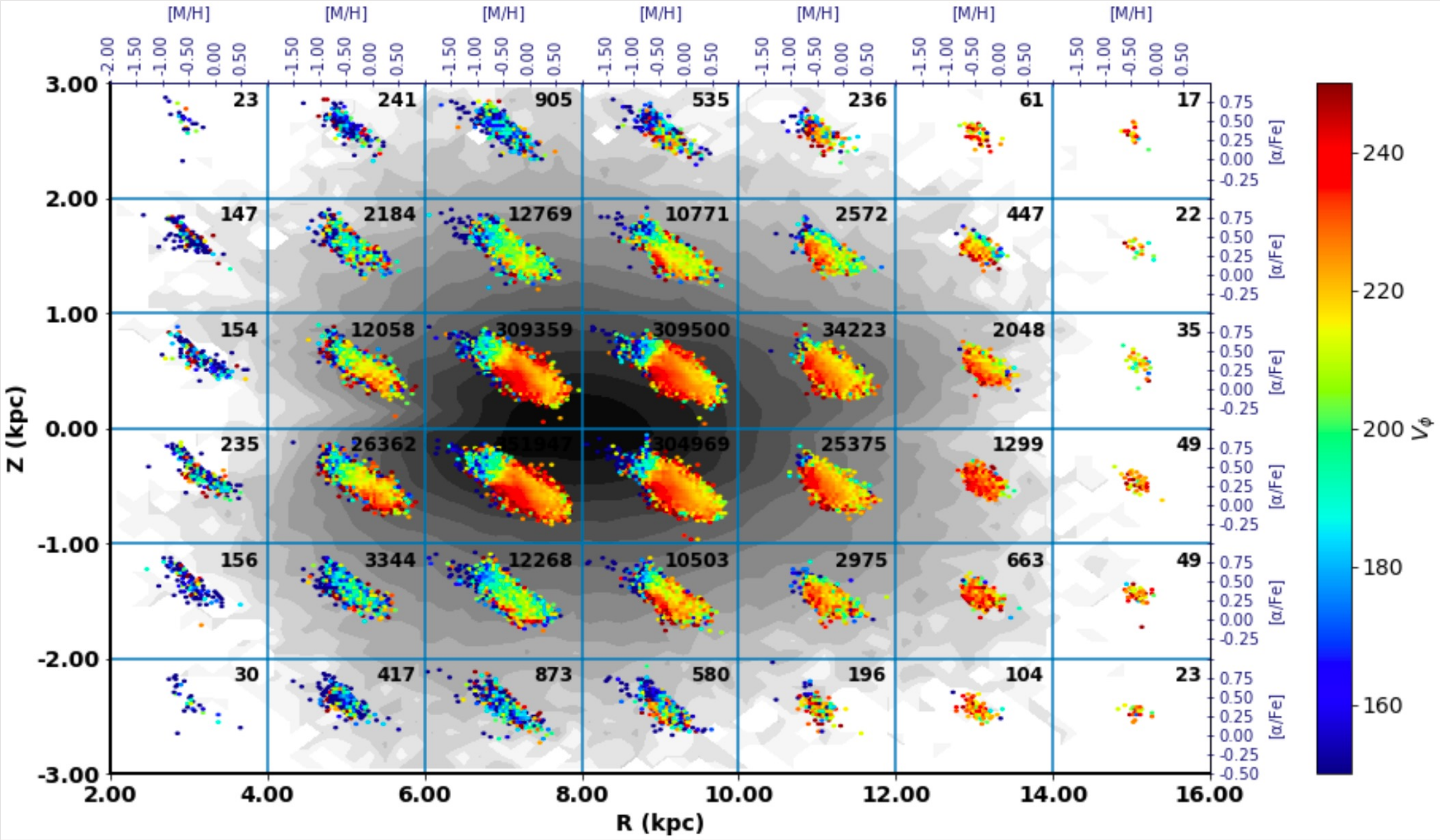

Thin disc stars are found at 3 kpc from the plane in the outer regions !

Galactic disc: structure and chemical gradients

[Ca/Fe]

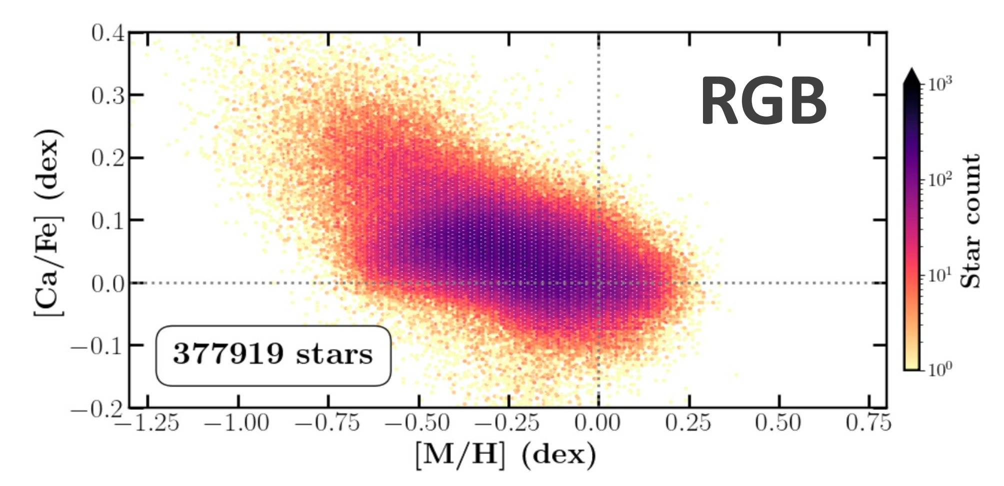

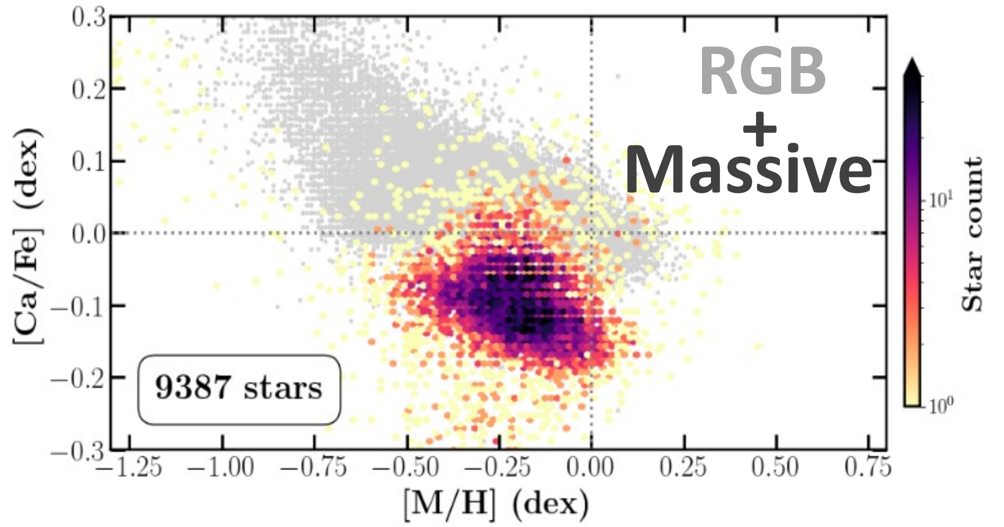

[α/Fe]

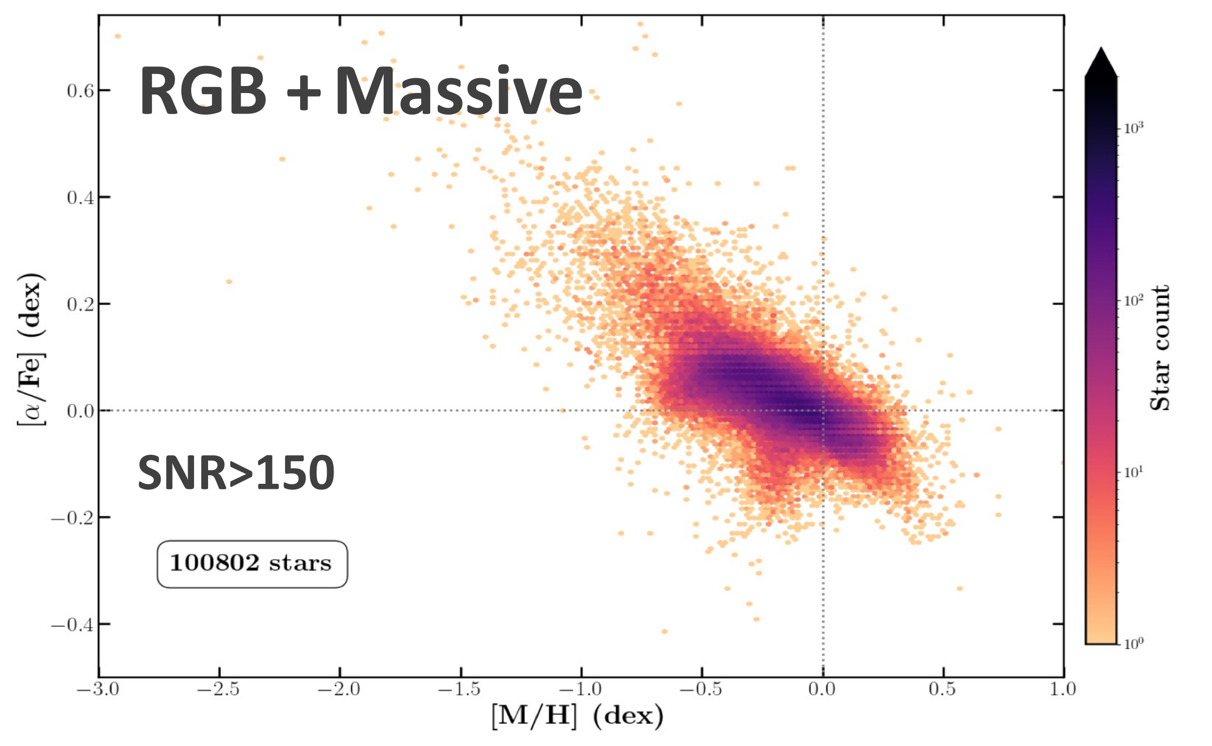

Galactic disc: a young chemically impoverished population?

Young stellar populations in the spiral arms

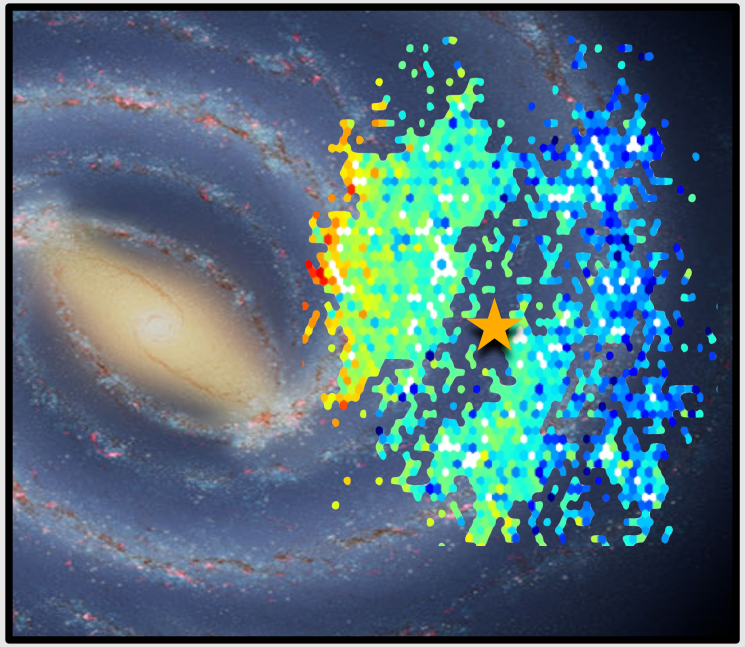

Chemical impoverishment ?

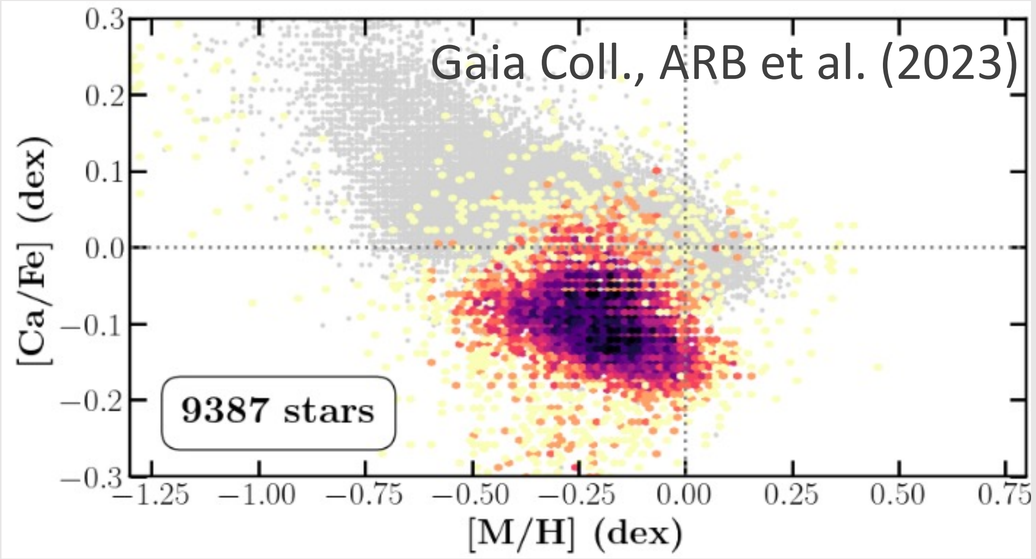

Depletion consistent with other HR surveys (APOGEE)

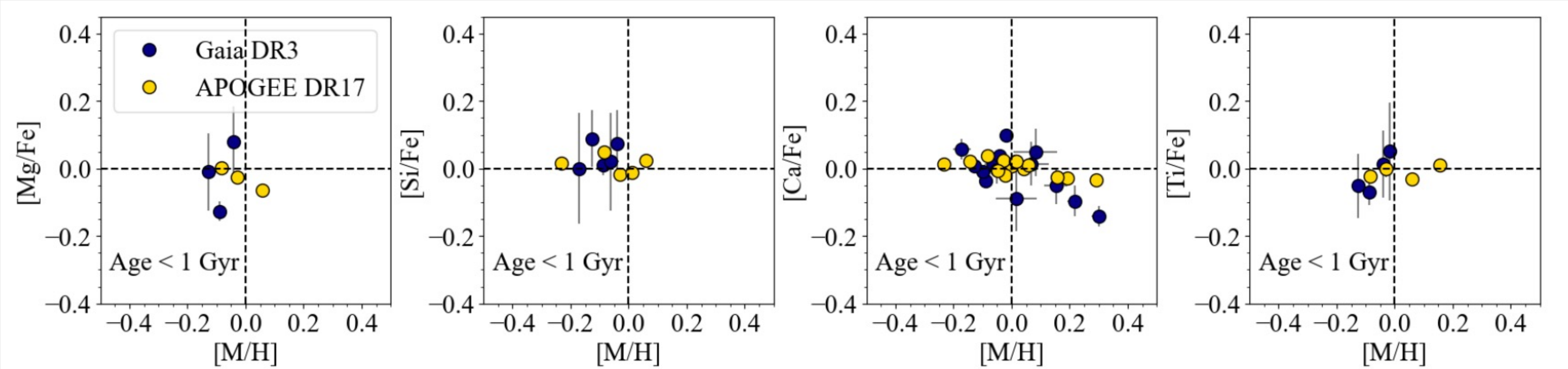

Spitoni et al. (2023)

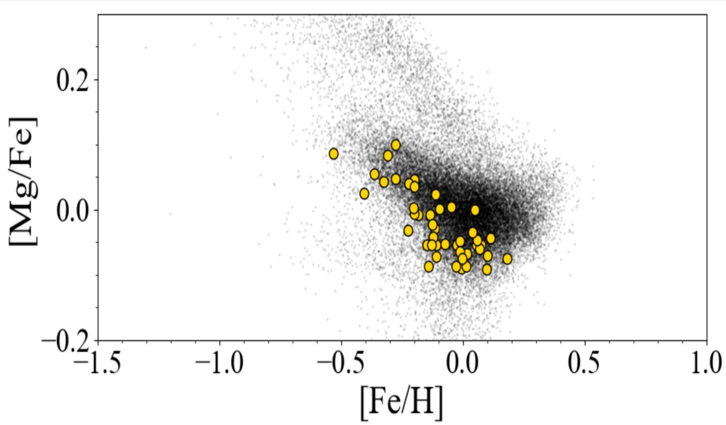

NOTE: These are only the "massive stars" in the Solar Neighbourhood, with [Mg/Fe] and in common with APOGEE

Galactic disc: a young chemically impoverished population?

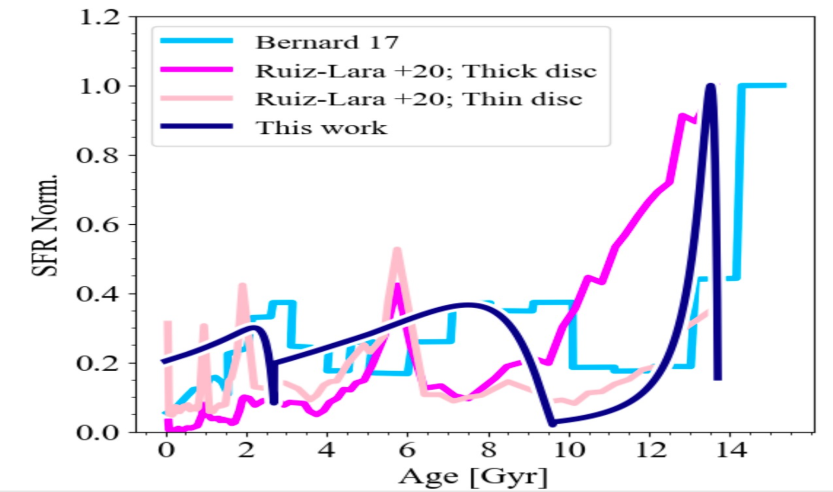

Spitoni et al. models

Galaxy formed by separated accretion episodes, **modelled by decaying exponential infalls of gas.**

Recent infall of gas related to thin disc star formation history and **chemically depleted young populations**

Spitoni et al. (2023)

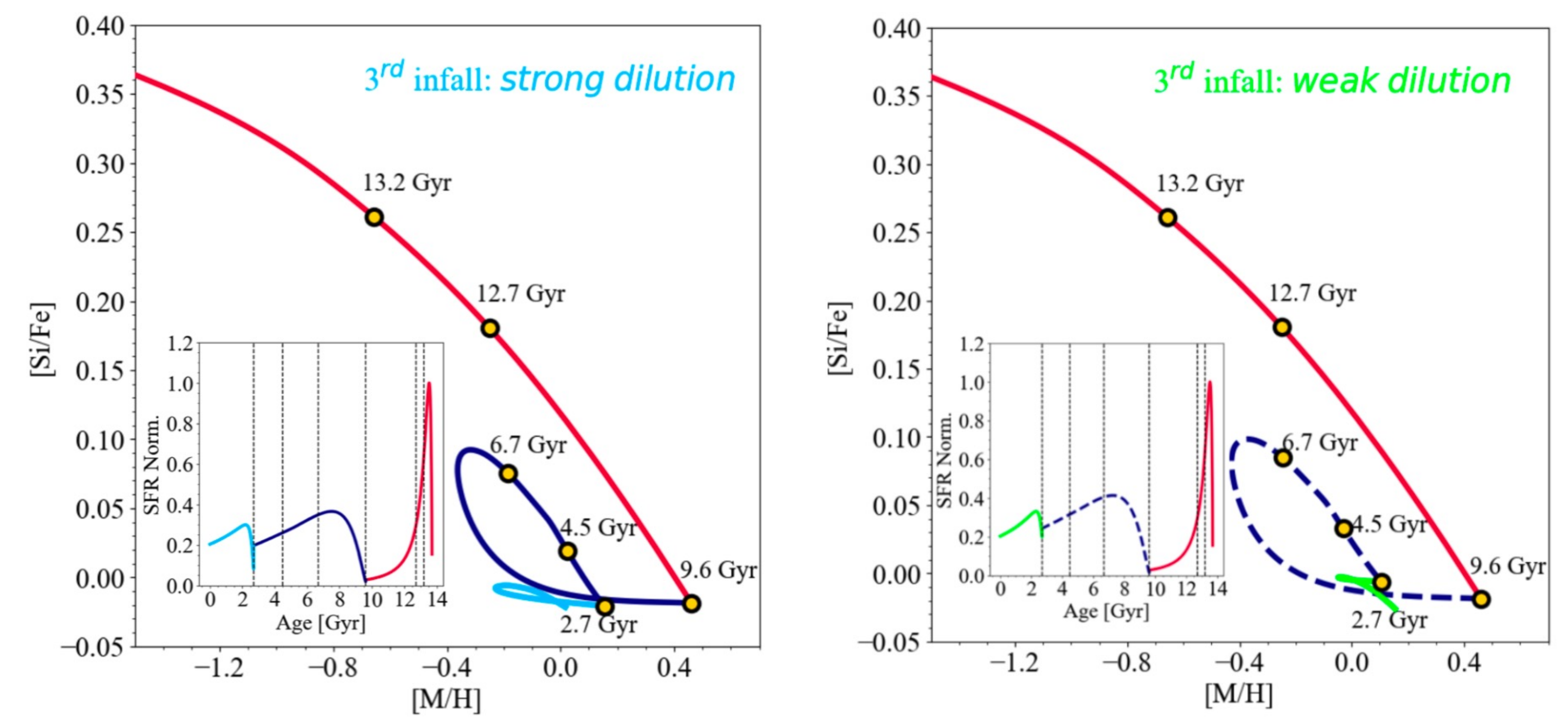

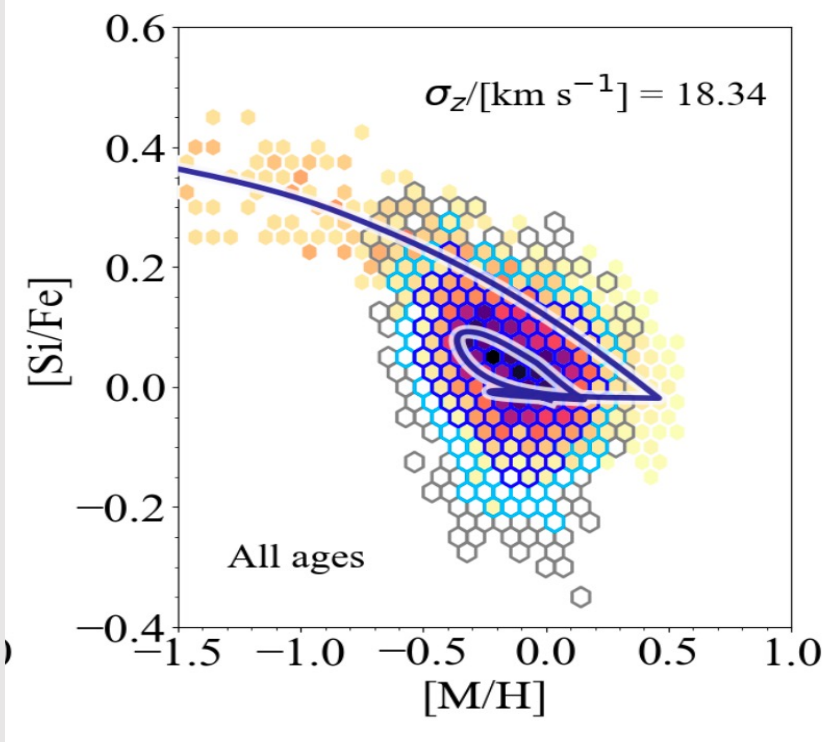

Chemo-dynamics with individual element abundances

Gaia collaboration, ARB et al. (2023)

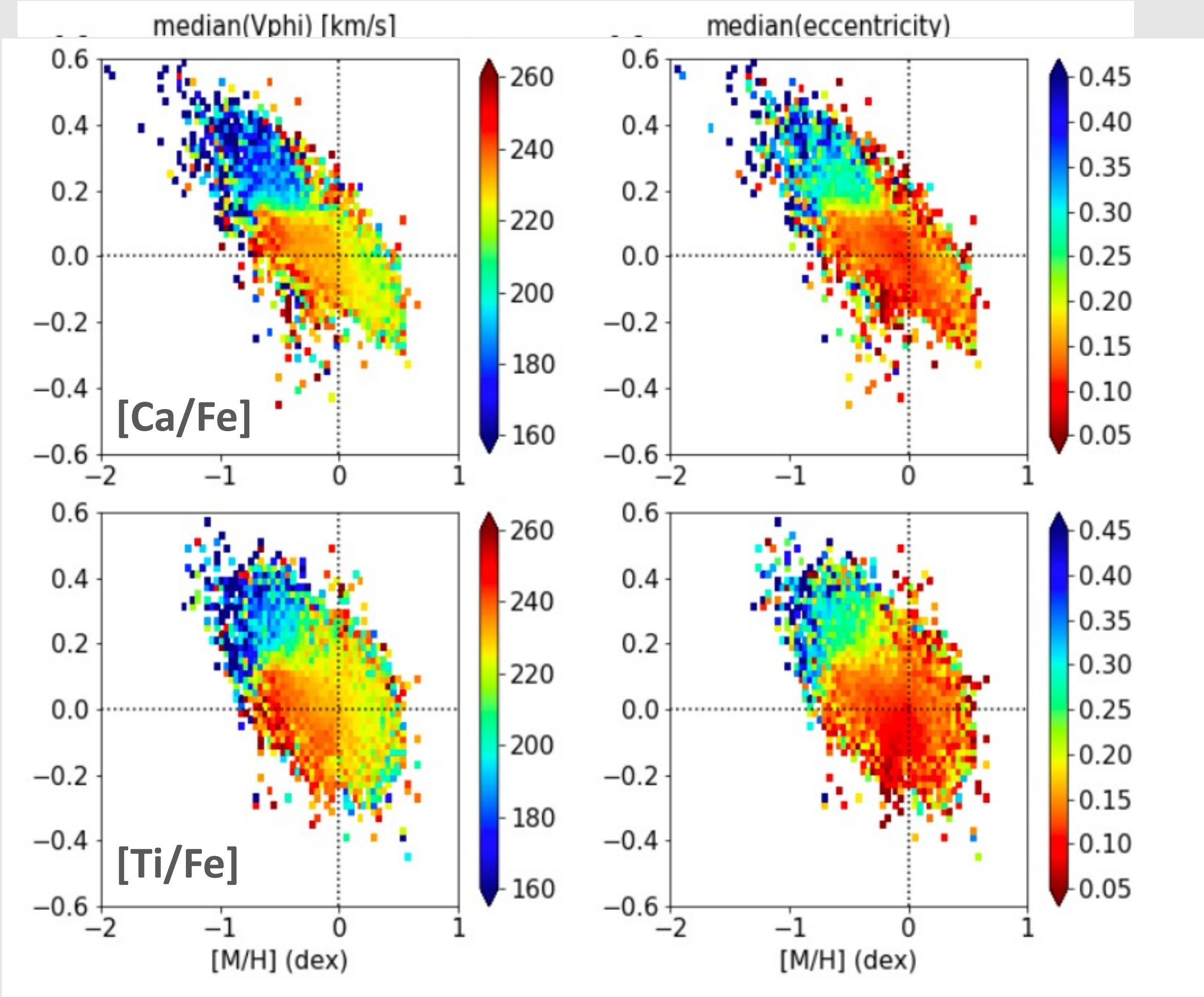

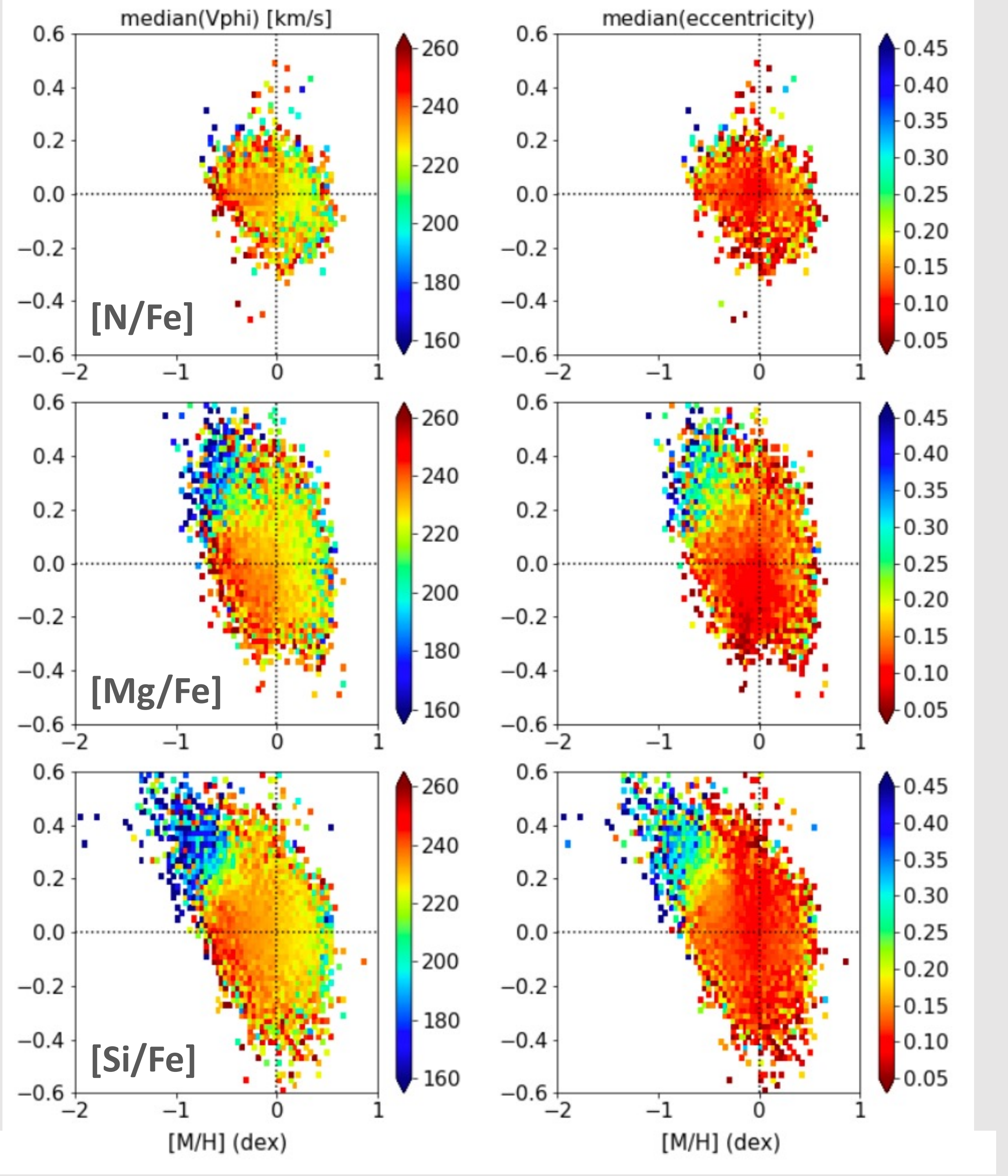

Galactic disc: structure and chemical gradients

Contursi et al. (2022)

Heavy elements: Cerium

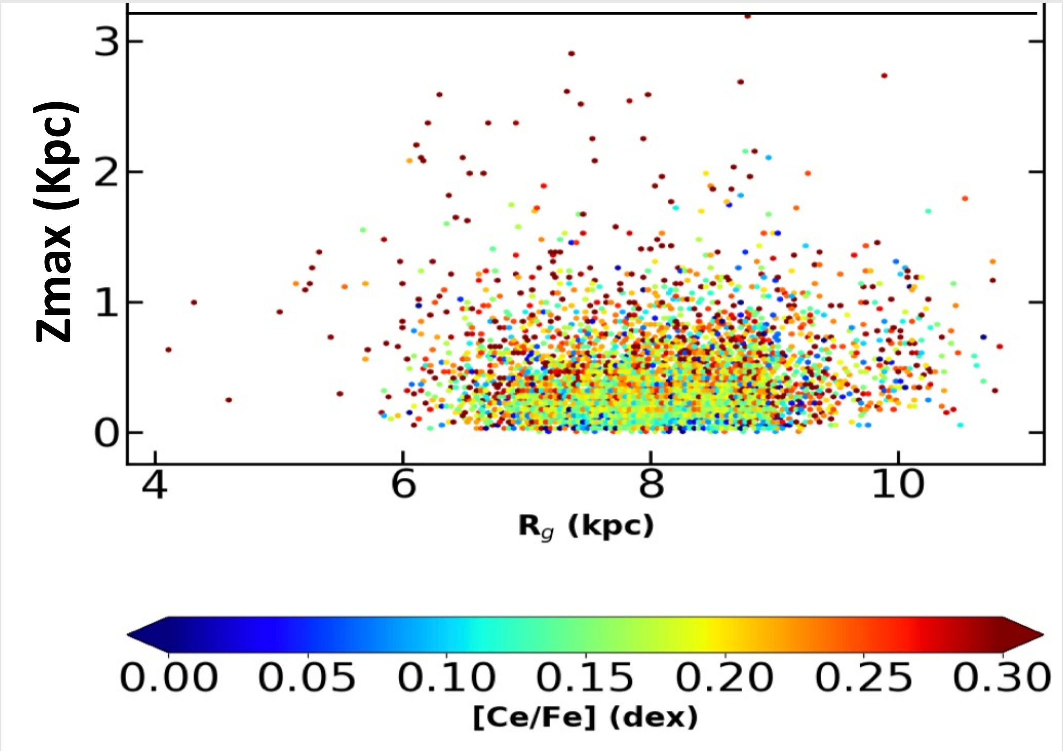

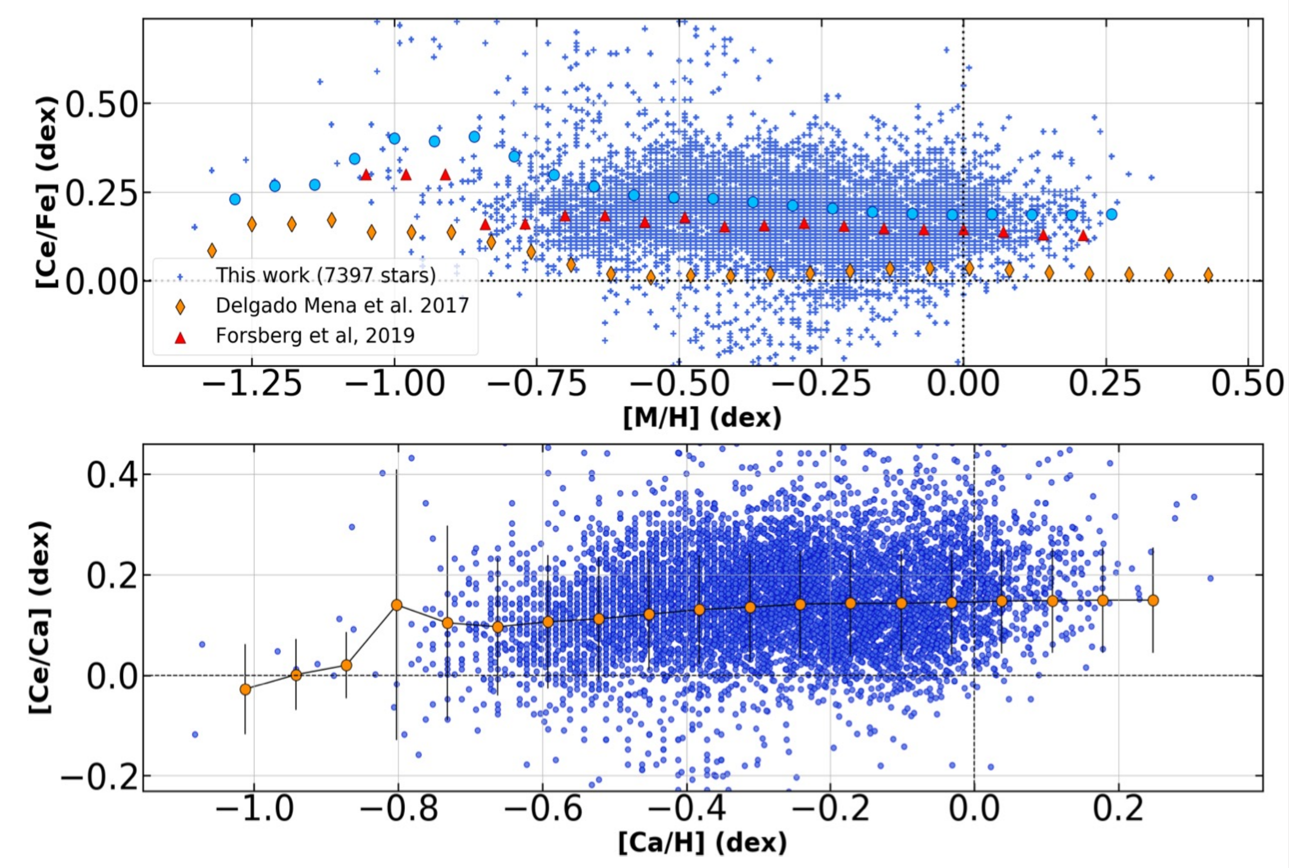

Flat [Ce/Fe] radial gradient and positive vertical gradient
Slightly possitive [Ce/Ca] trend vs. [Ca/H] -> AGB stars are the main responsibles for Cerium abundances in the disc.

Heavy element abundances: Neodymium

Contursi et al. (2023)

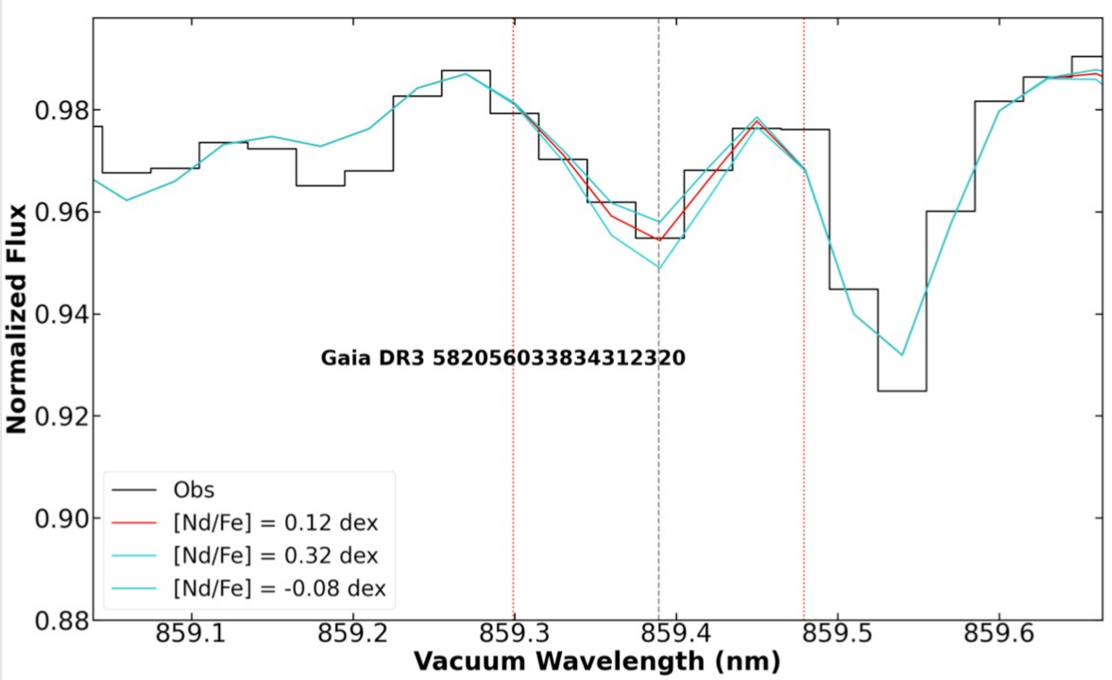

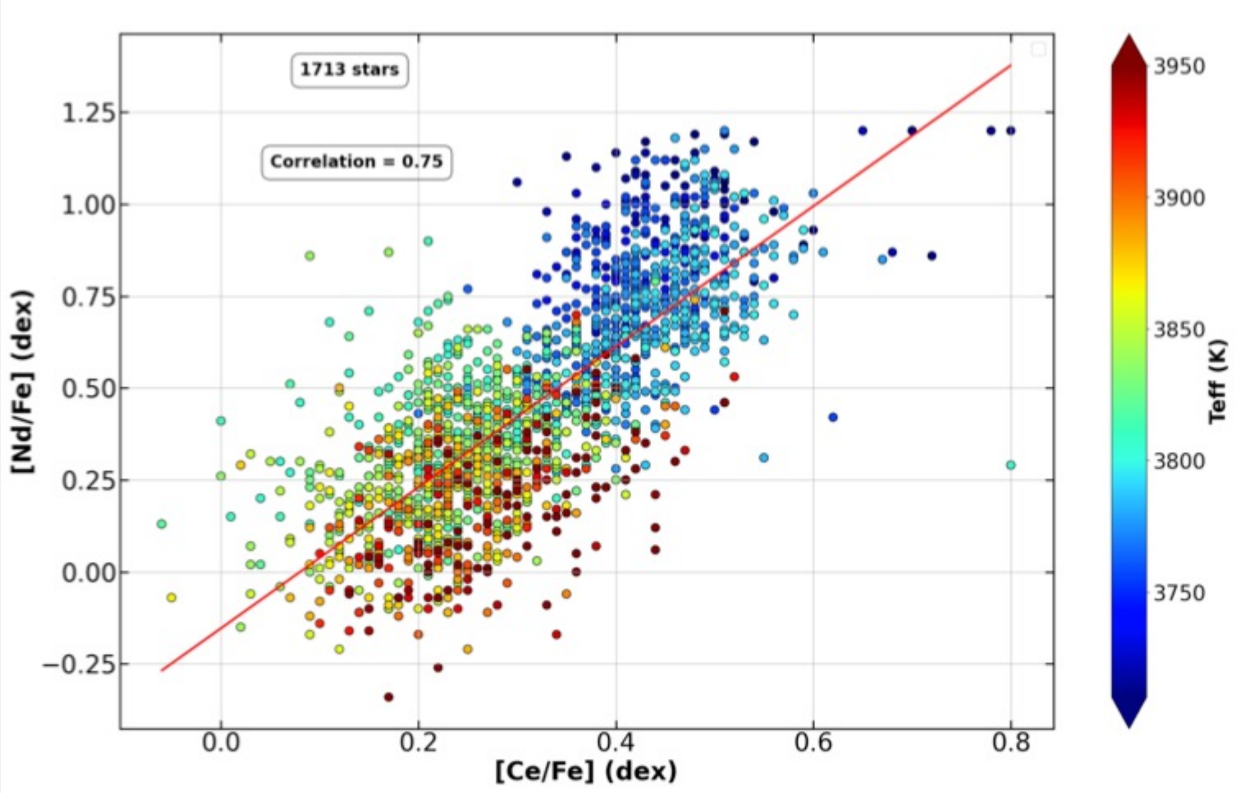

AGB production of s-process elements:

Higher Ce and Nd abundances for more evolved AGB stars of similar metallicity.

THE PHASE SPACE : stellar populations in motion

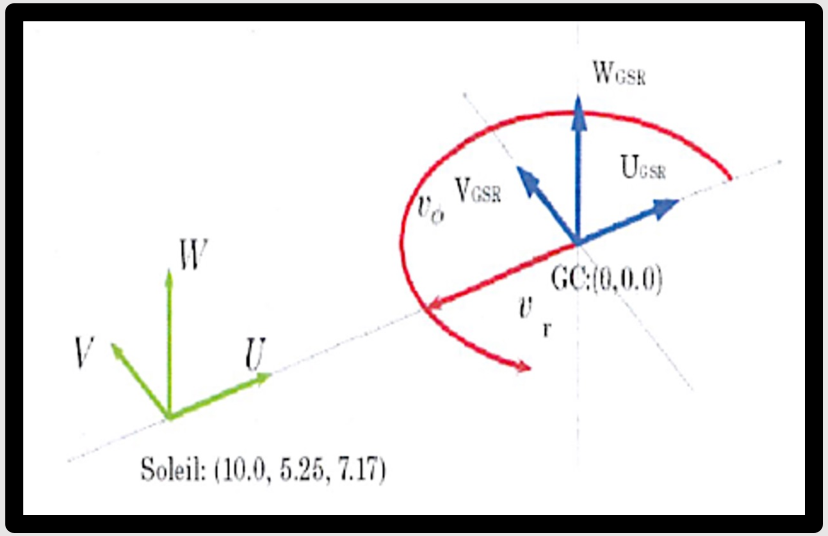

MOVING GROUPS & RIDGES

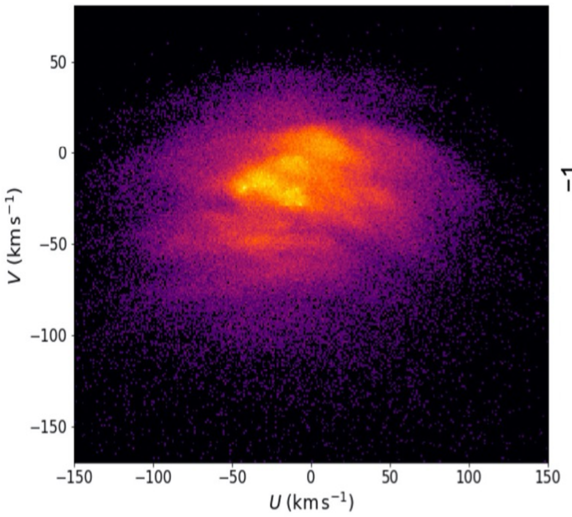

Gaia Collaboration, Katz et al. 2018

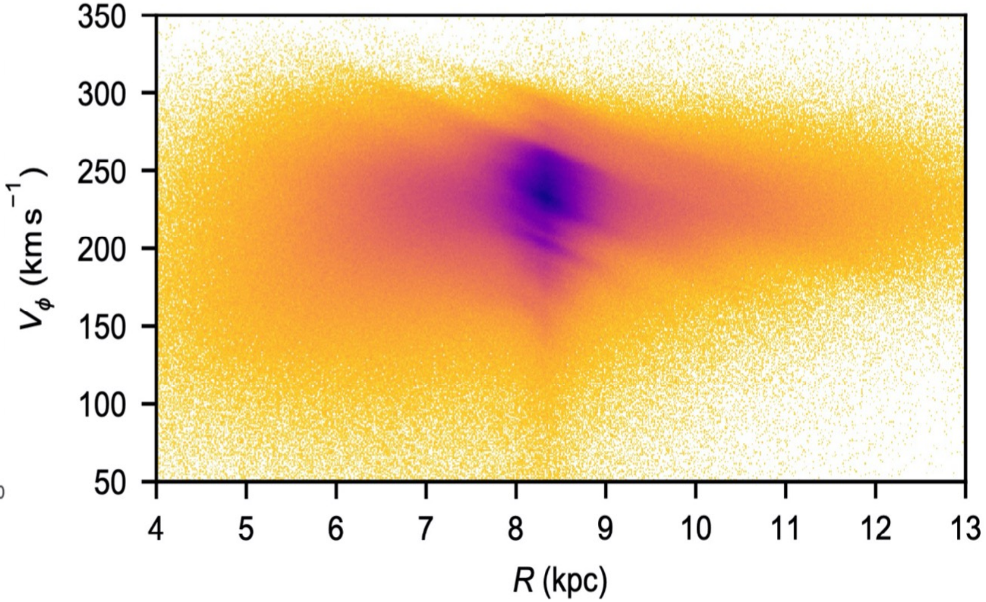

Antoja et al. 2018

PHASE SPIRAL

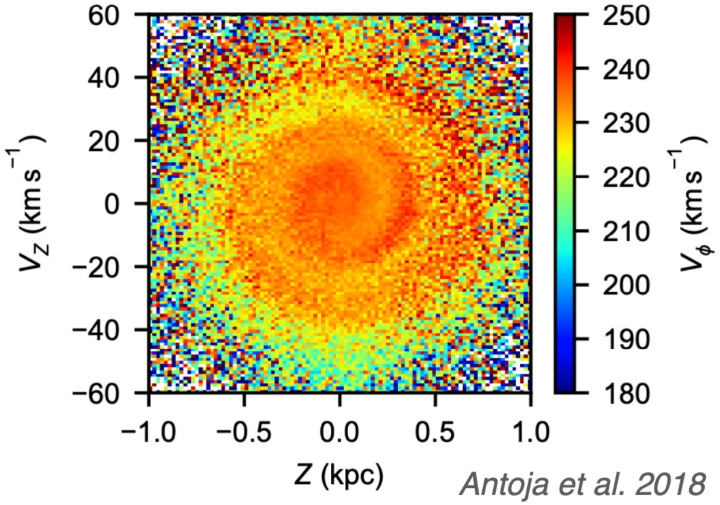

Antoja et al. 2018

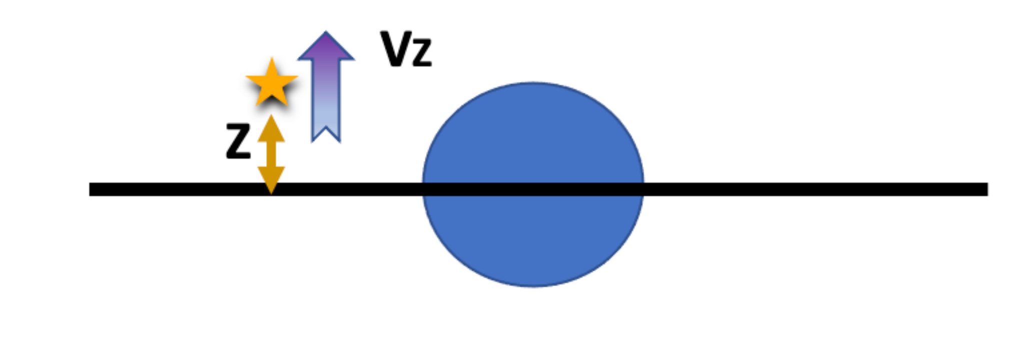

Chemical markers of disc perturbations:

Ridges in chemo-kinematical space

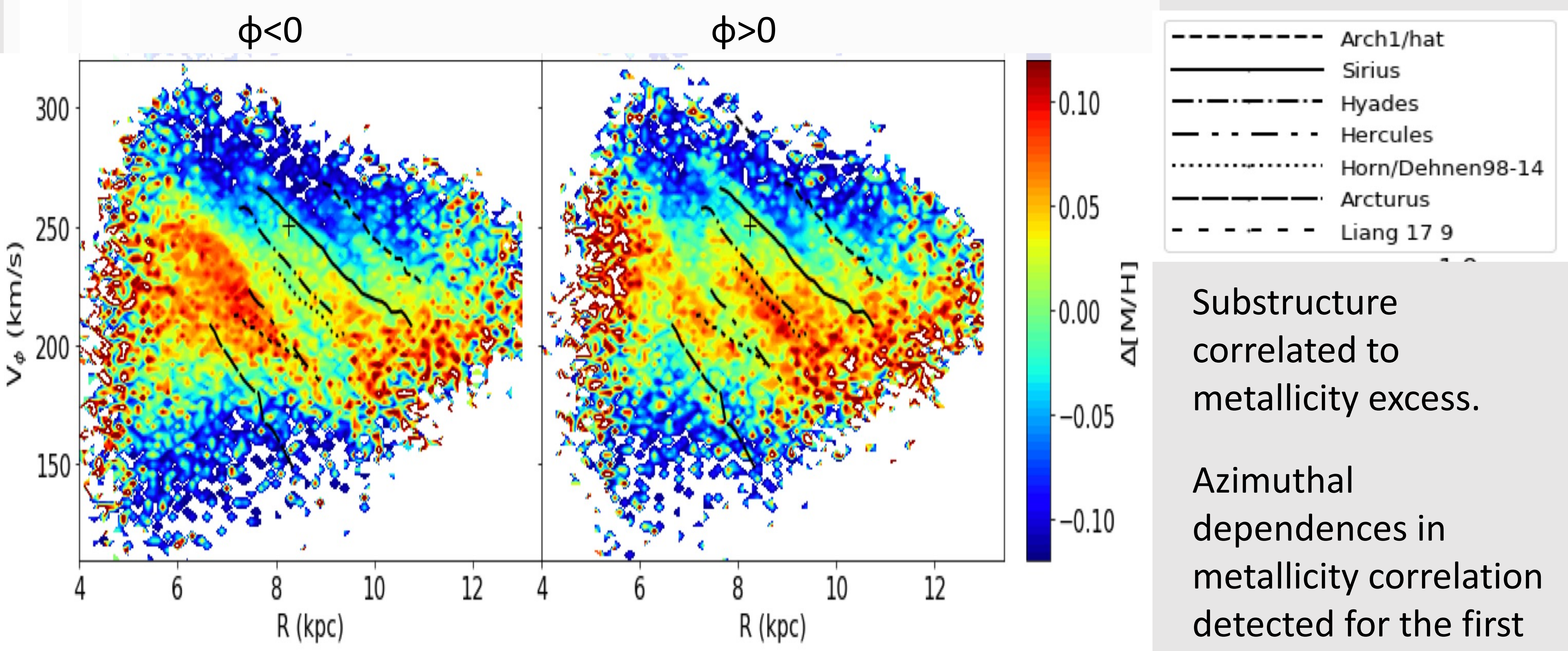

Substructure correlated to metallicity excess.

Azimuthal dependences in metallicity correlation detected for the first time

Crédits: Gaia Collaboration, Recio-Blanco et al. (2022)

Chemical markers of disc perturbations:
kinematics and phase spiral as a function of R

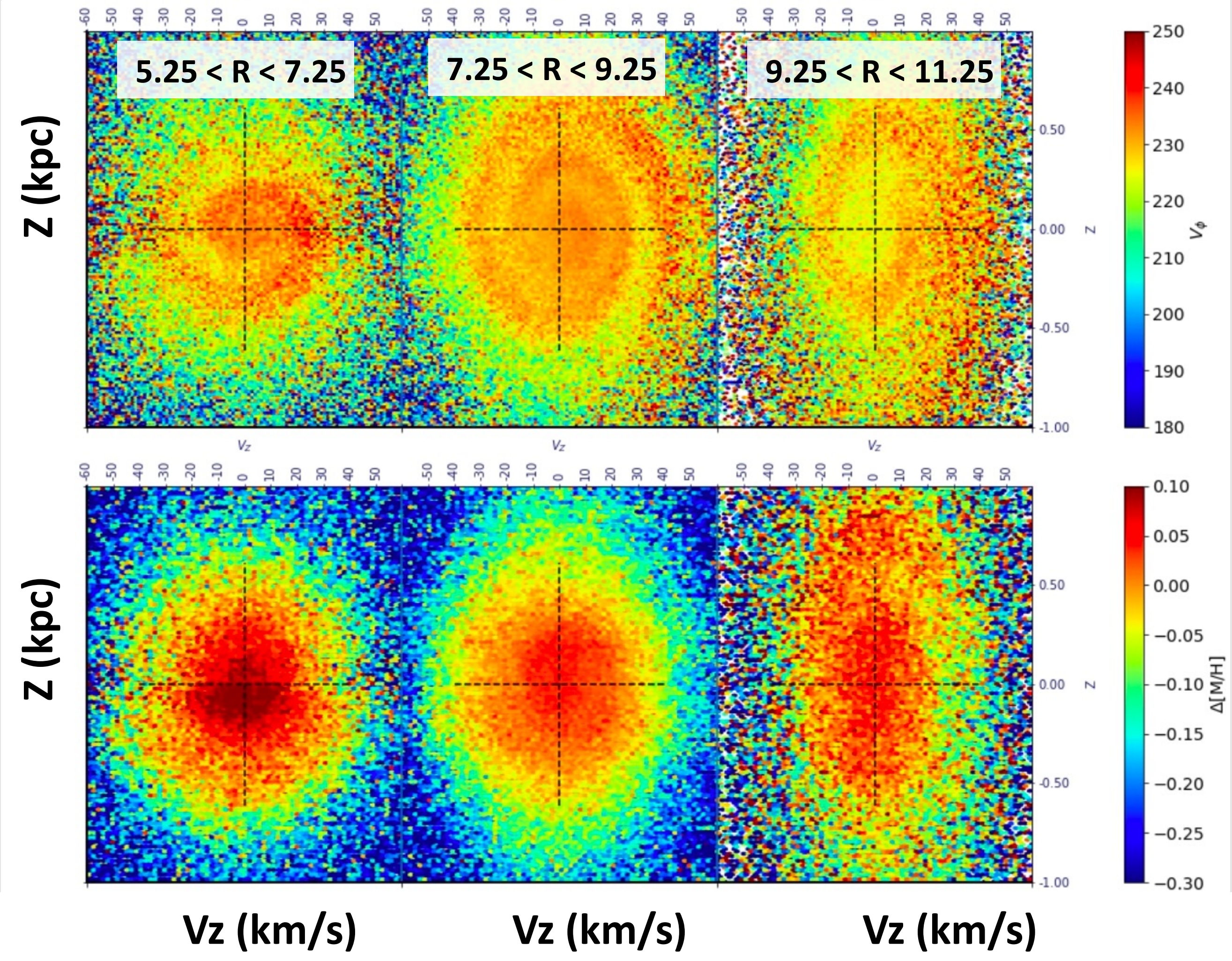

Crédits: Gaia Collaboration, Recio-Blanco et al. (2022)

Wave-like perturbation (Antoja et al. 2018):
- disc-crossing satellite (Binney & Schoenrich 2018, Bland-Hawthorn et al. 2019)
- bar's buckling (Koperskov et al. 2019)

Correlation of thin disc phase spiral **with metallicity excess** detected for the first time

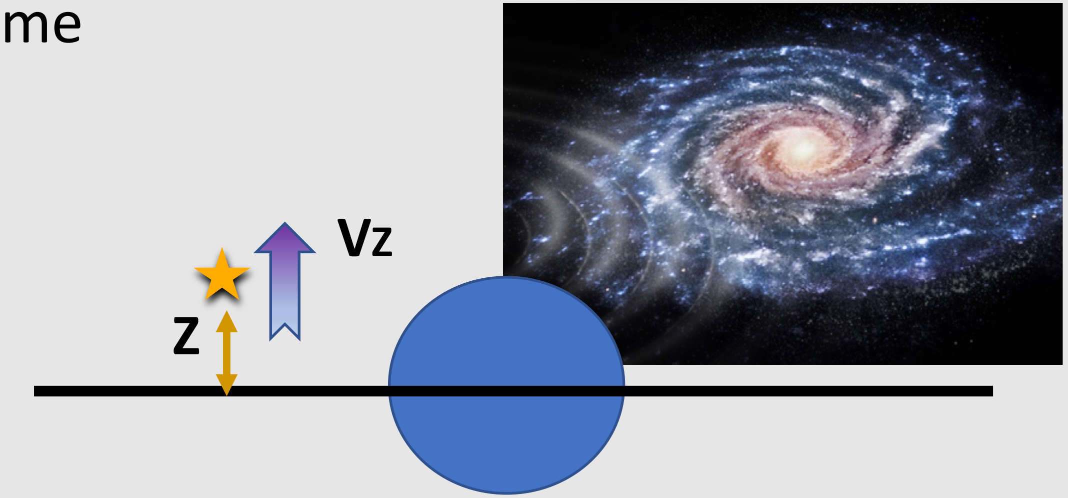

Chemical markers of disc perturbations:

The outer disc

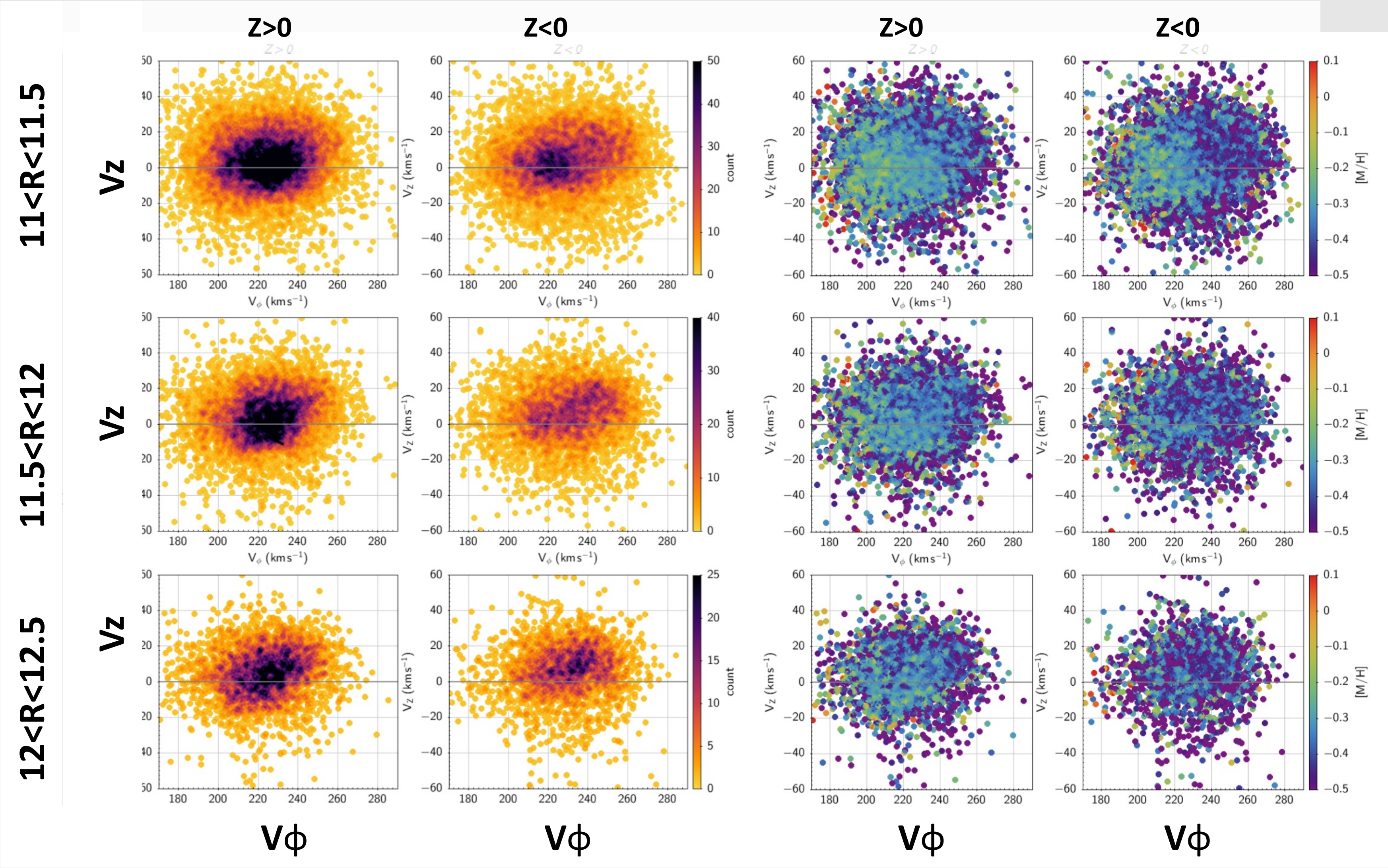

Kinematical bimodality (Gaia Collaboration, Antoja et al. 2021) linked to metallicity bimodality:

The population with lower *V*ϕ is more metal-rich than the second group of stars with higher *V*ϕ and positive *VZ*.

Crédits: Gaia Collaboration, Recio-Blanco et al. (2022)

Chemical markers of disc perturbations:
orbital space

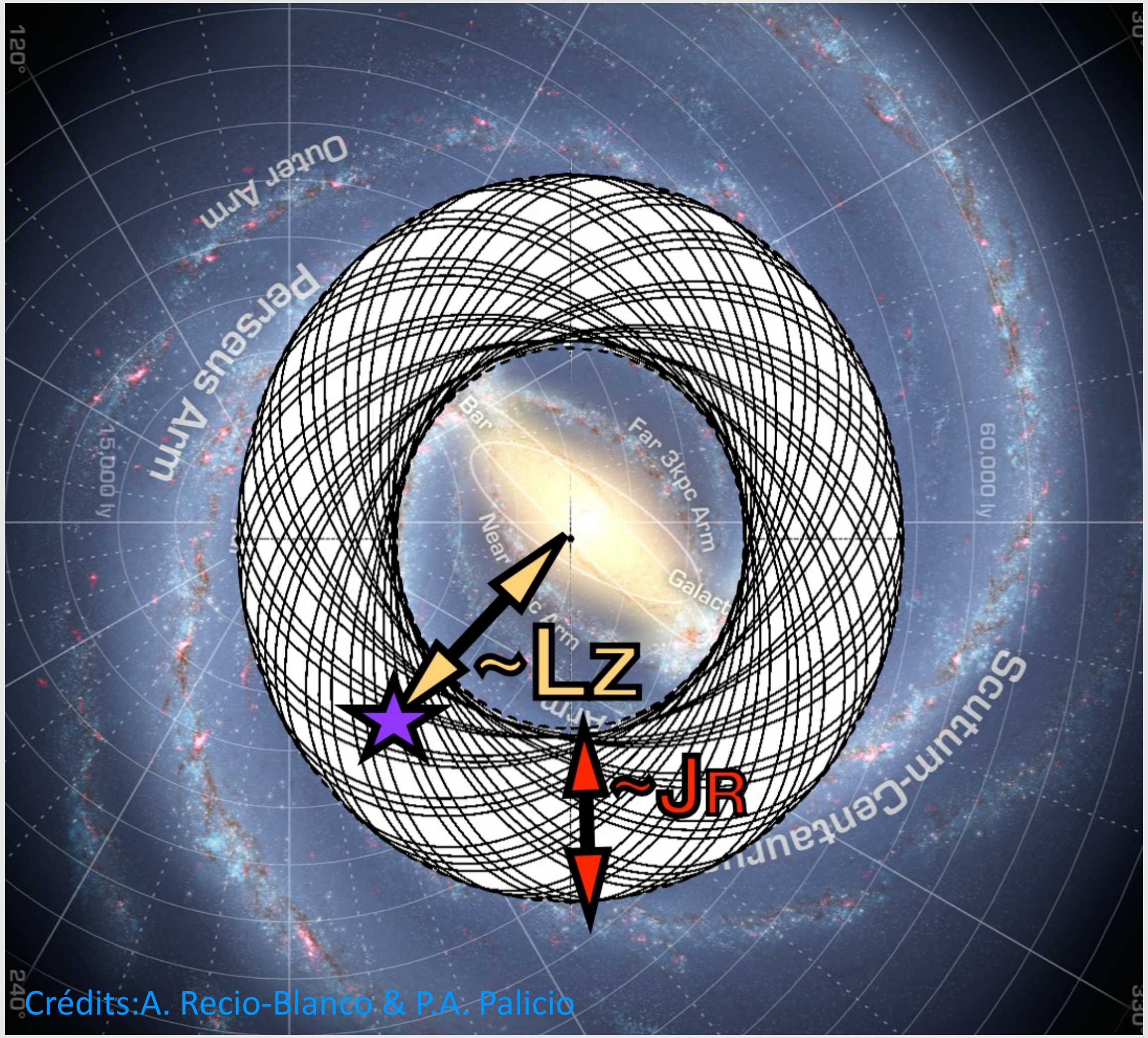

The actions (J_R, J_Z, L_Z) in static potentials are integrals of motion that characterise the orbit of the stars.

- $\boldsymbol{J_R}$ characterises the **radial amplitude** of the epicyclic orbits

- the **angular momentum** $\boldsymbol{L_Z}$ sets the **guiding raidus** a more robust estimate of the typical Galactic distance of the star than the present-day Galactocentric radius R.

Chemical markers of disc perturbations:
orbital space

Ridges of higher stellar density:
- orbits closer to the plane
- metallicities higher than surrounding median values.

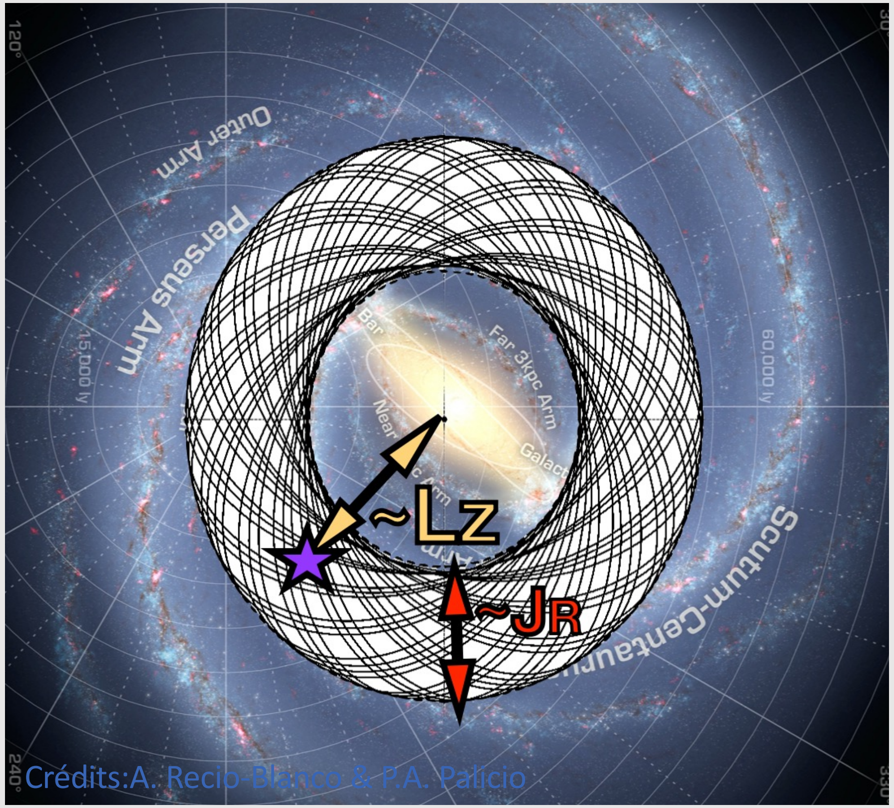

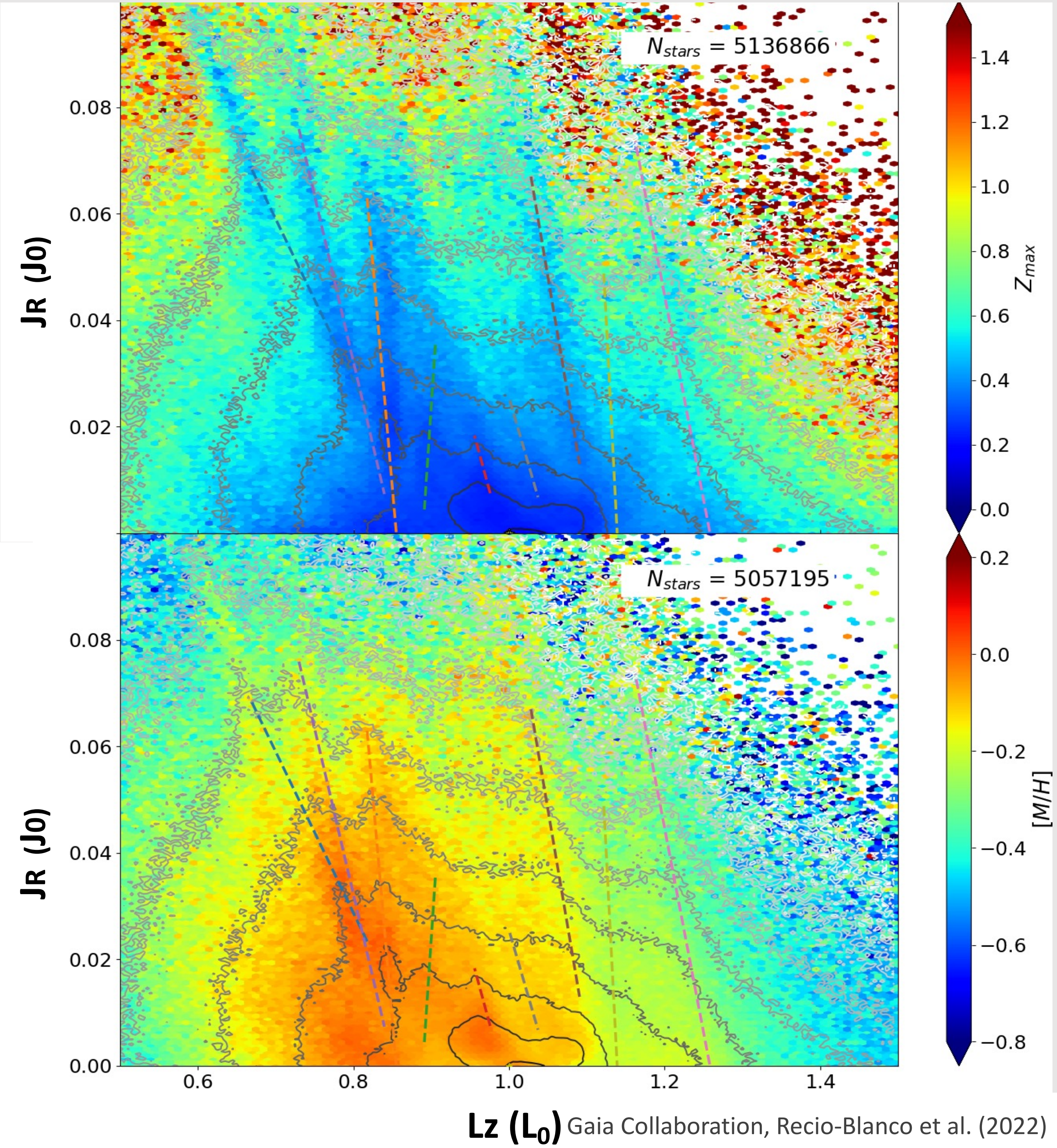

Gaia Collaboration, Recio-Blanco et al. (2022)

Spiral arms : signatures in density, metallicity and orbits

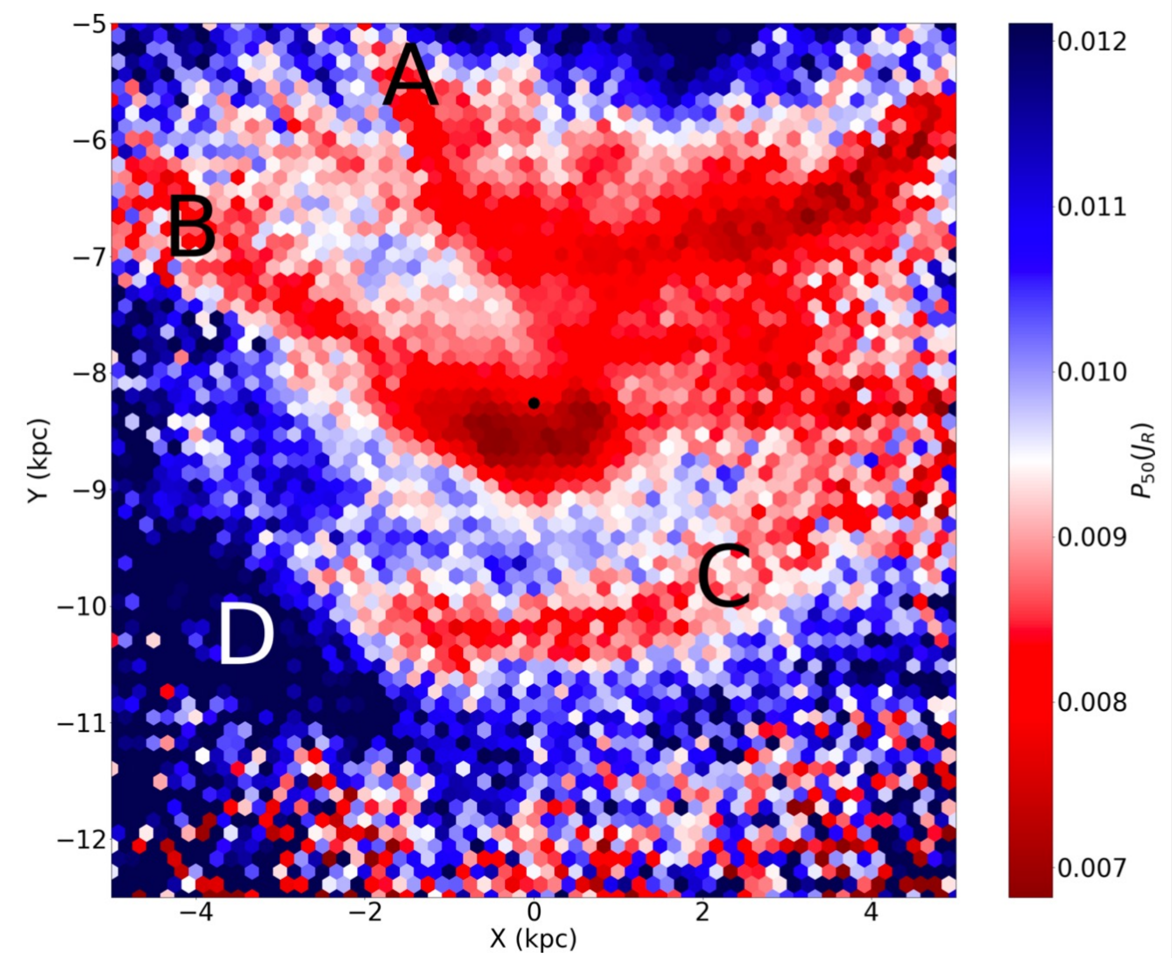

Radial action J_R ~ orbit's excentricity

Lower J_R (red) means more circular

Spiral-like structures in J_R for (old) giant stars

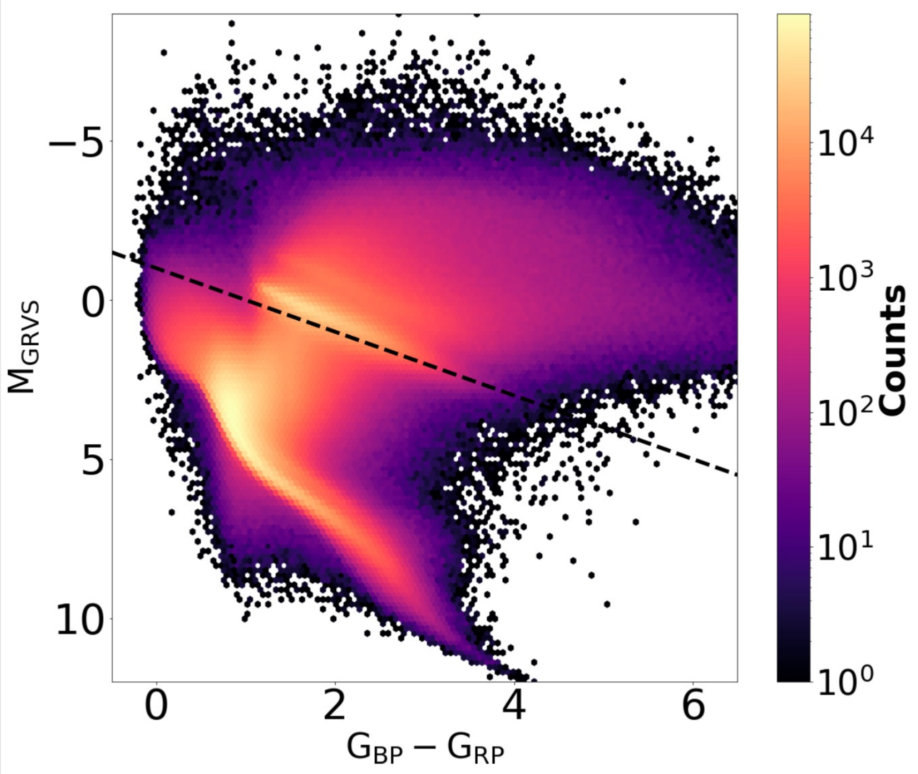

Palicio, ARB et al. (2022)

Spiral arms : signatures in density, metallicity and orbits

Correlation of the JR pattern **with different spiral arms tracers** (in stellar density).

Spiral arms detected in the giant stars density distribution

Old	Young		
Giant stars	Masers	Cepheids	Upper Main Sequence

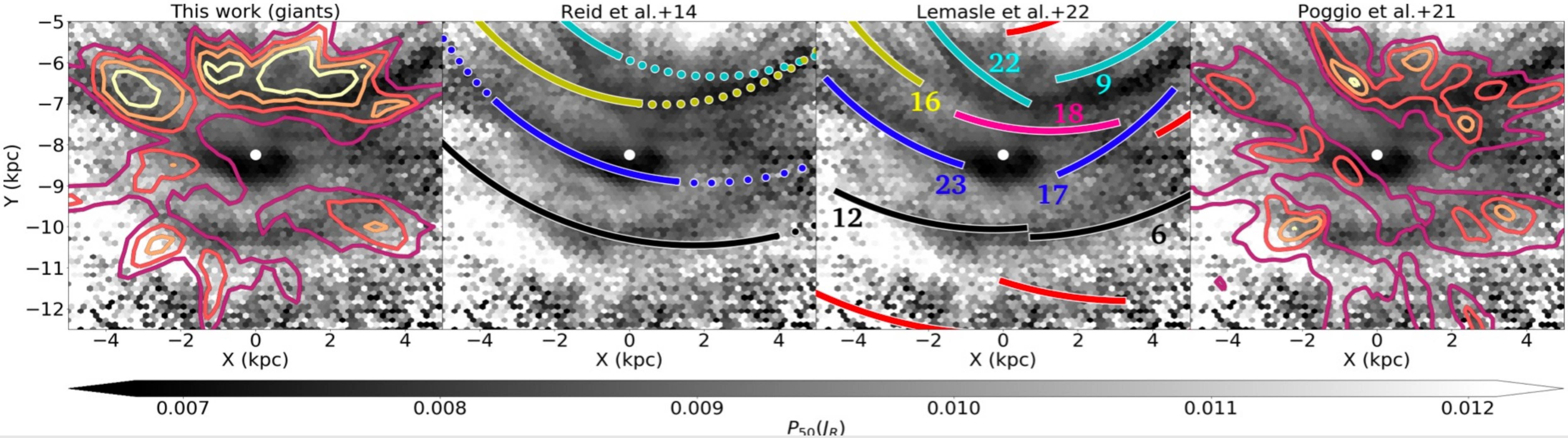

Palicio, ARB et al. (2022)

Chemical markers of satellite accretion

Accreted substructures identified in orbital space and in the chemical one

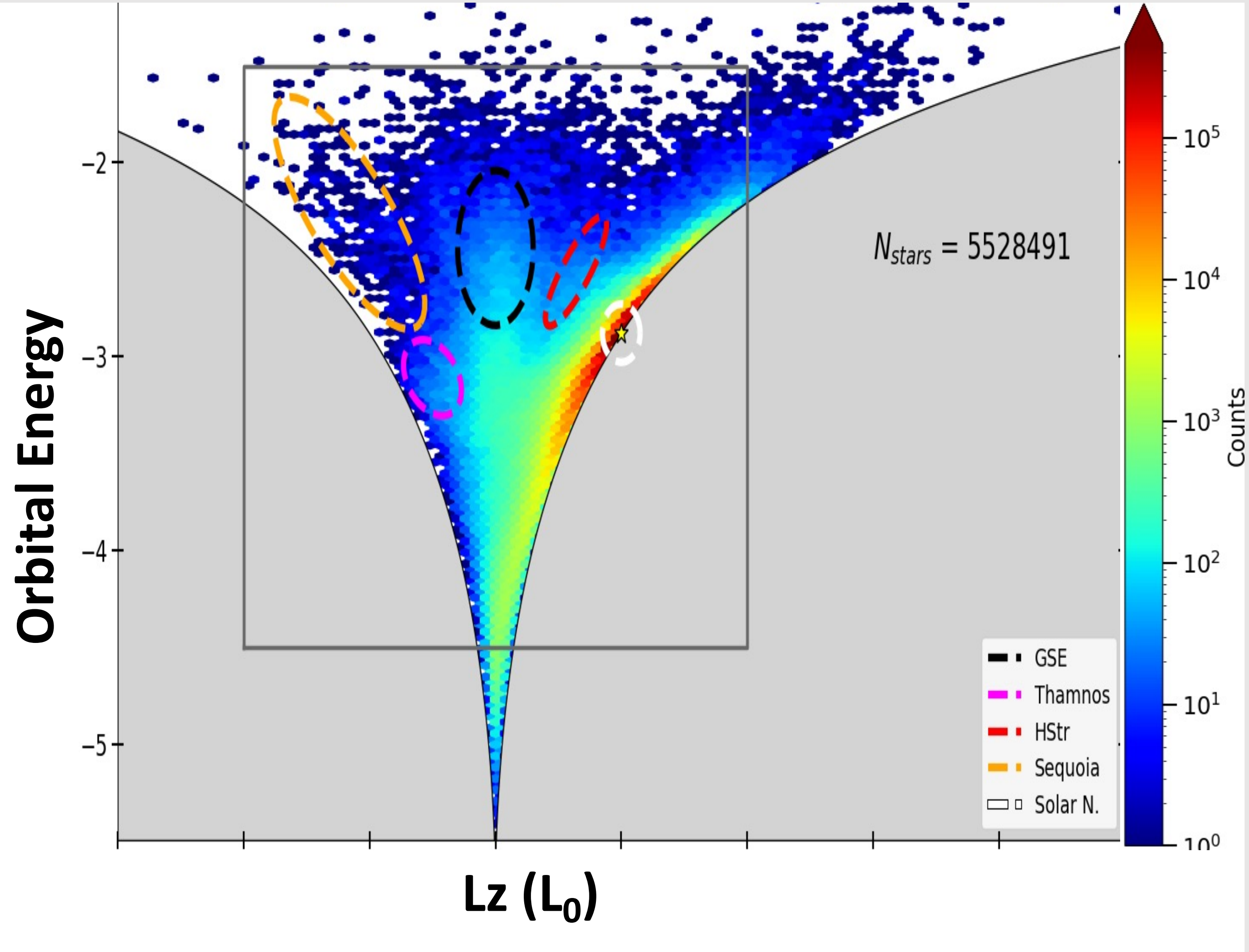

Gaia-Enceladus :

last major merger 8-11 Gyr ago

(e.g. Helmi et al. 2018, Belokurov et al. 2018)

Crédits: ESA/Gaia/DPAC, Jordan, Sagristà, ARB , Palicio, de Laverny, McMillan

Gaia Collaboration, Recio-Blanco et al. (2022)

Chemical markers of satellite accretion

Accreted substructures identified in orbital space and in the chemical one

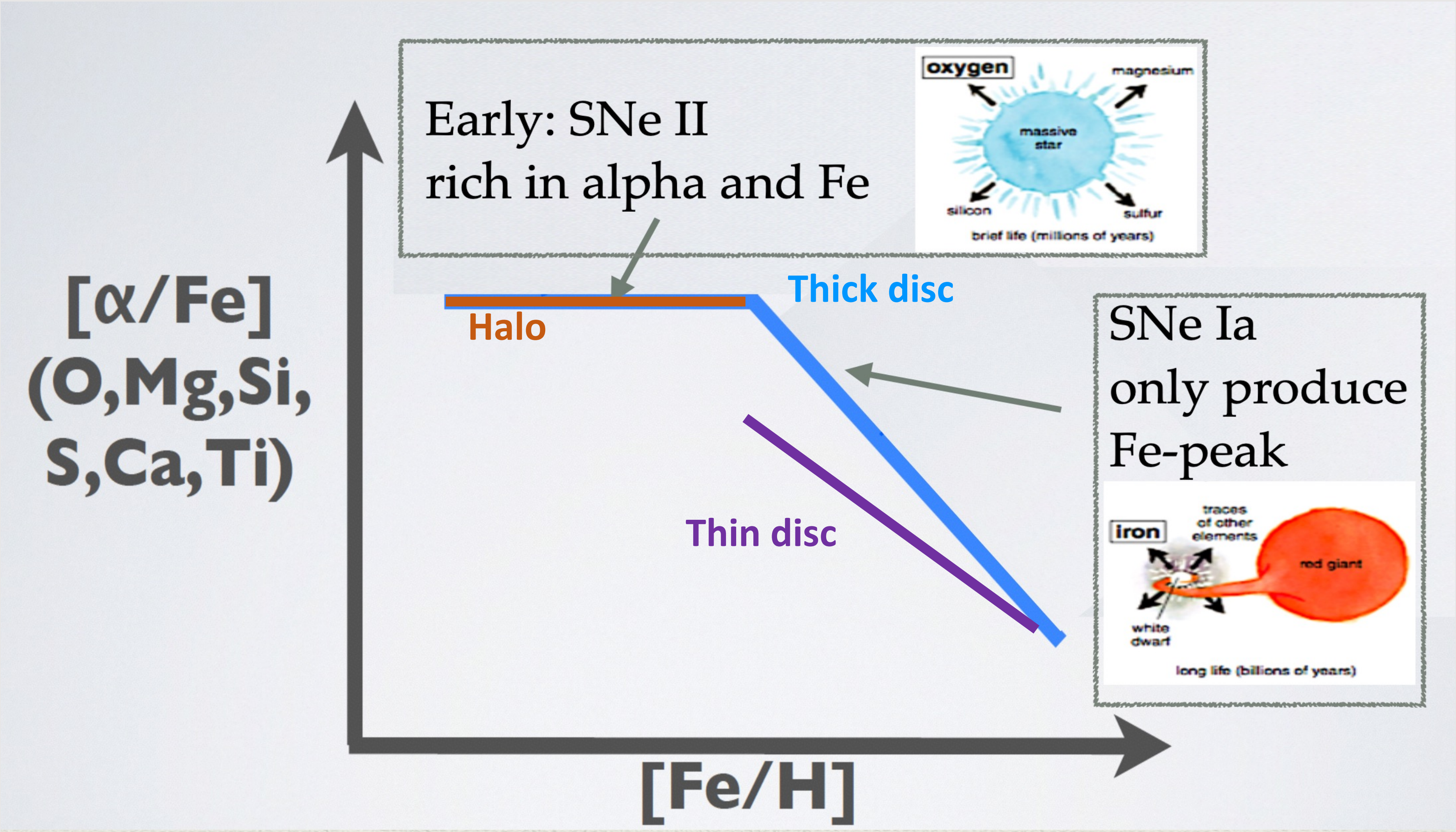

Chemical markers of satellite accretion

Accreted substructures identified in orbital space and in the chemical one

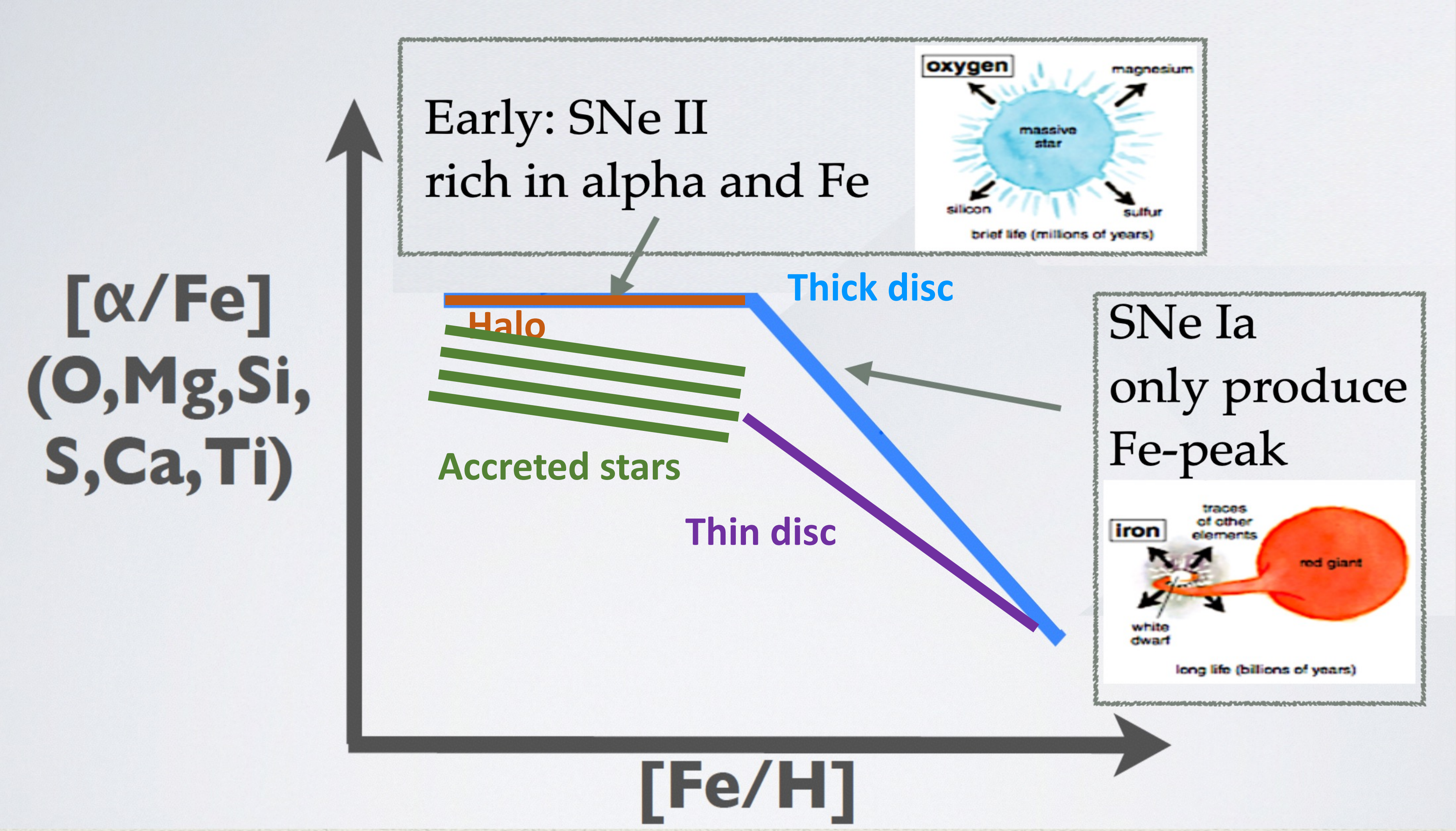

Chemical markers of satellite accretion

Accreted substructures identified in orbital space and in the chemical one

Gaia Collaboration, ARB et al. (2022)

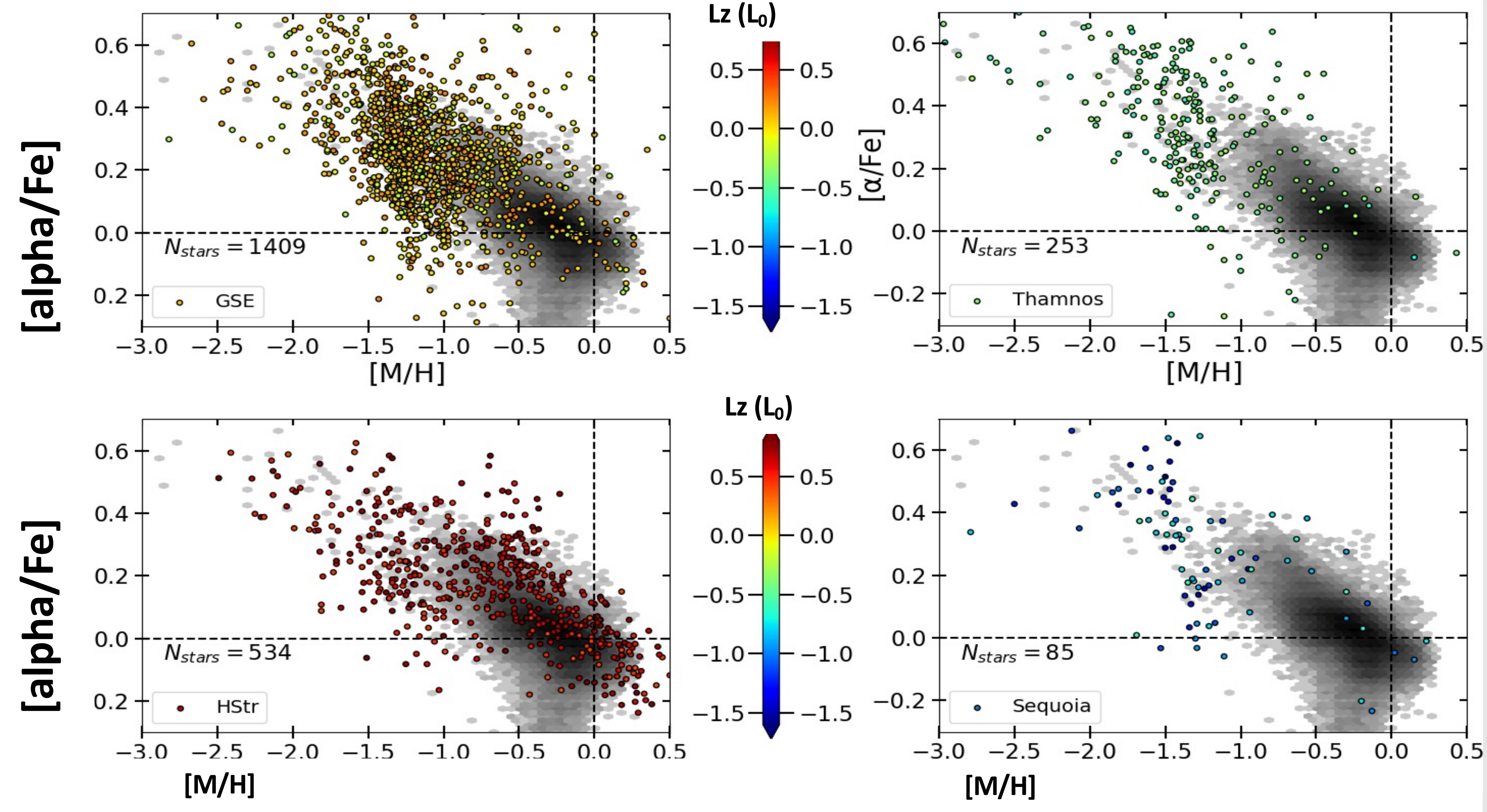

Chemical markers of satellite accretion

Accreted substructures identified in orbital space and in the chemical one

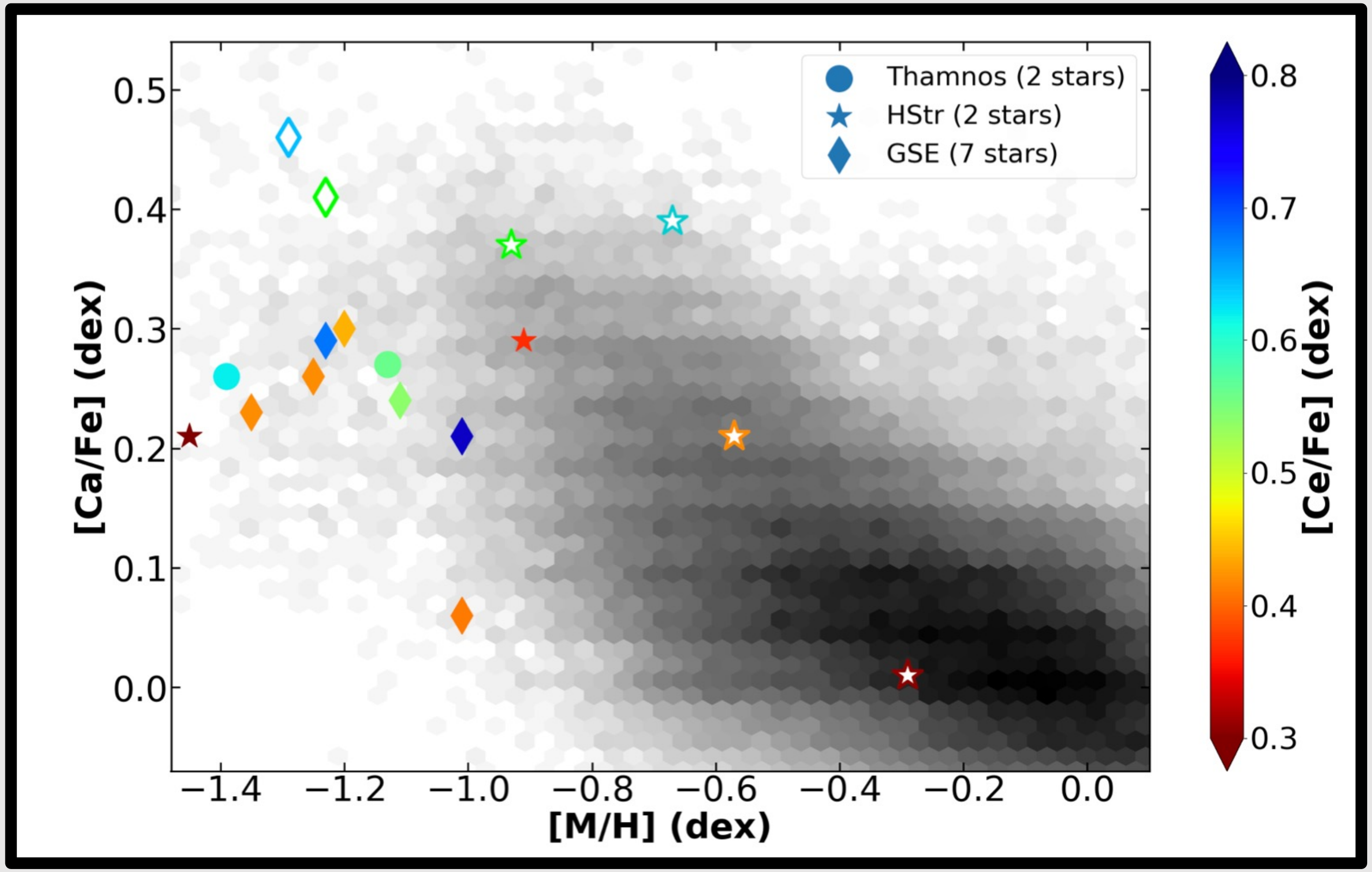

Cerium abundances:

Helmi Stream could be slightly underabundant in [Ce/Fe] with respect to Gaia-Enceladus and Thamnos

Contursi et al. (2022)

Globular clusters

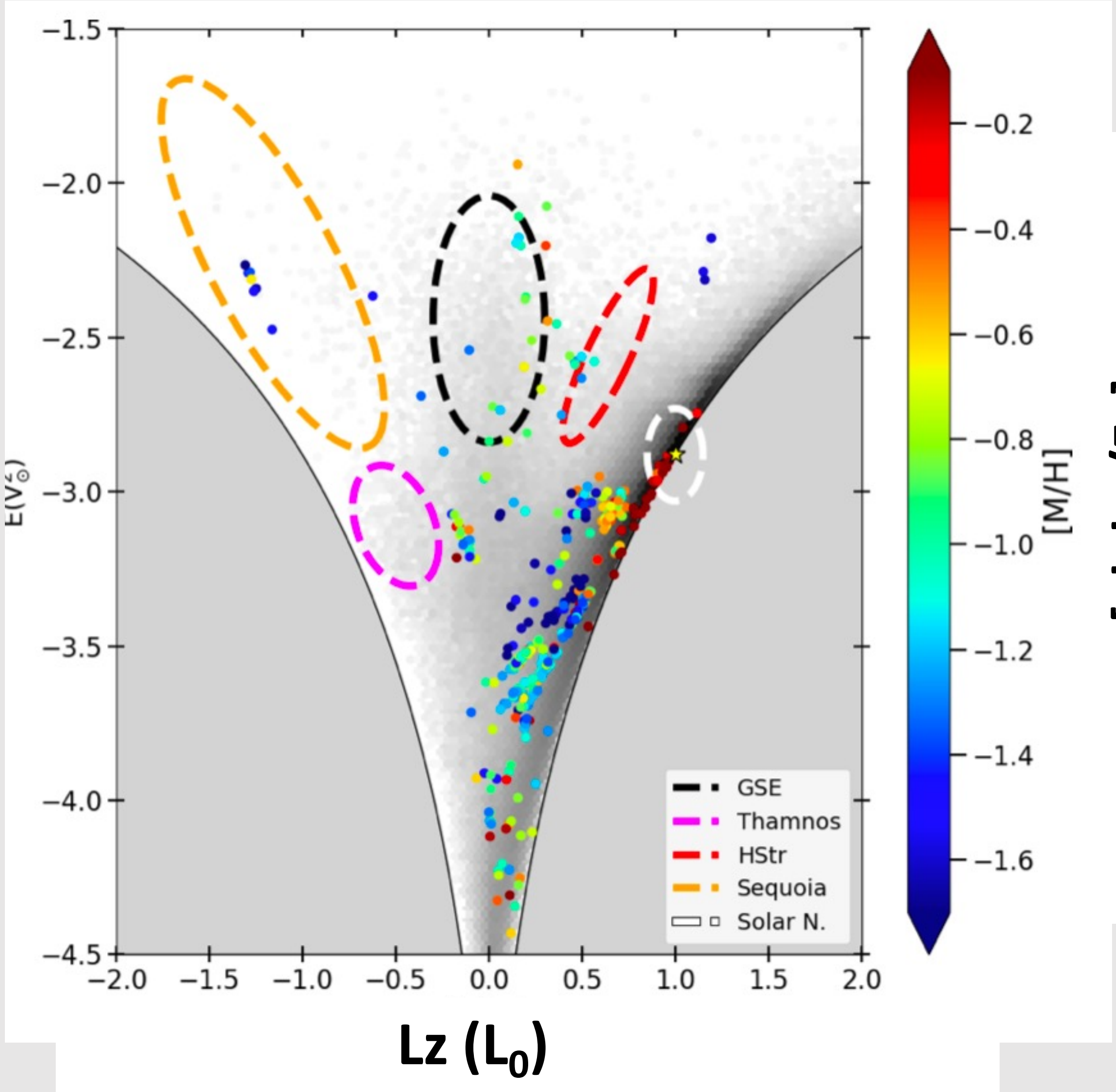

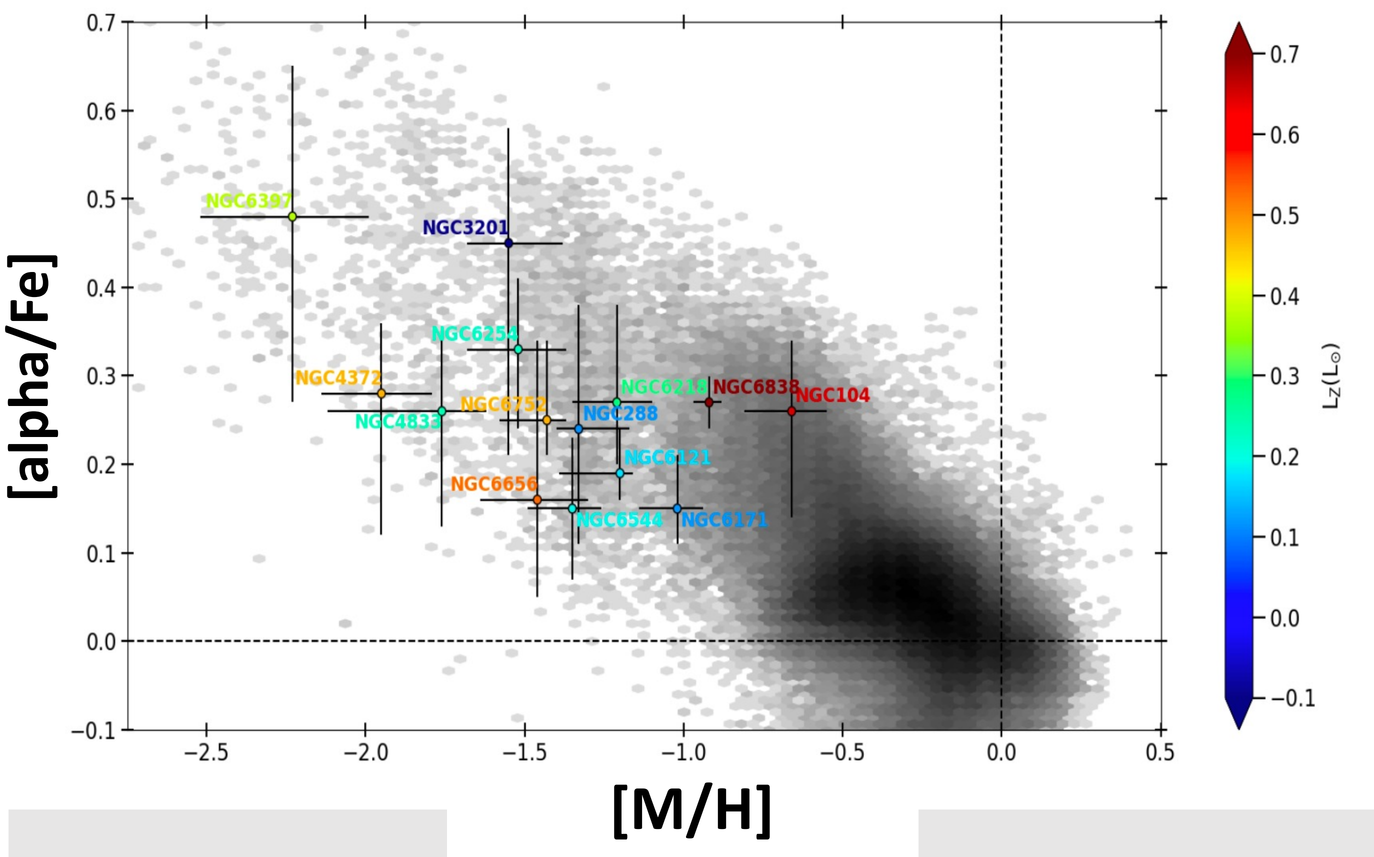

Gaia Collaboration, Recio-Blanco et al. (2022)

Galactic fossils from primordial epochs

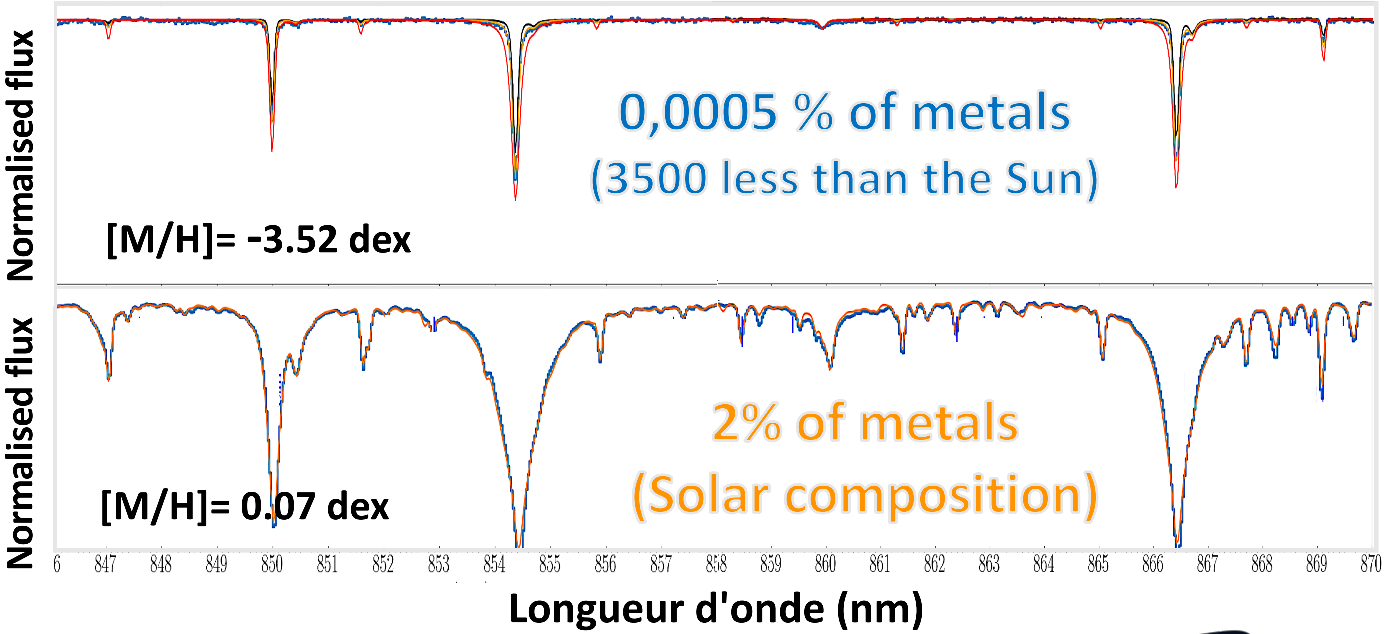

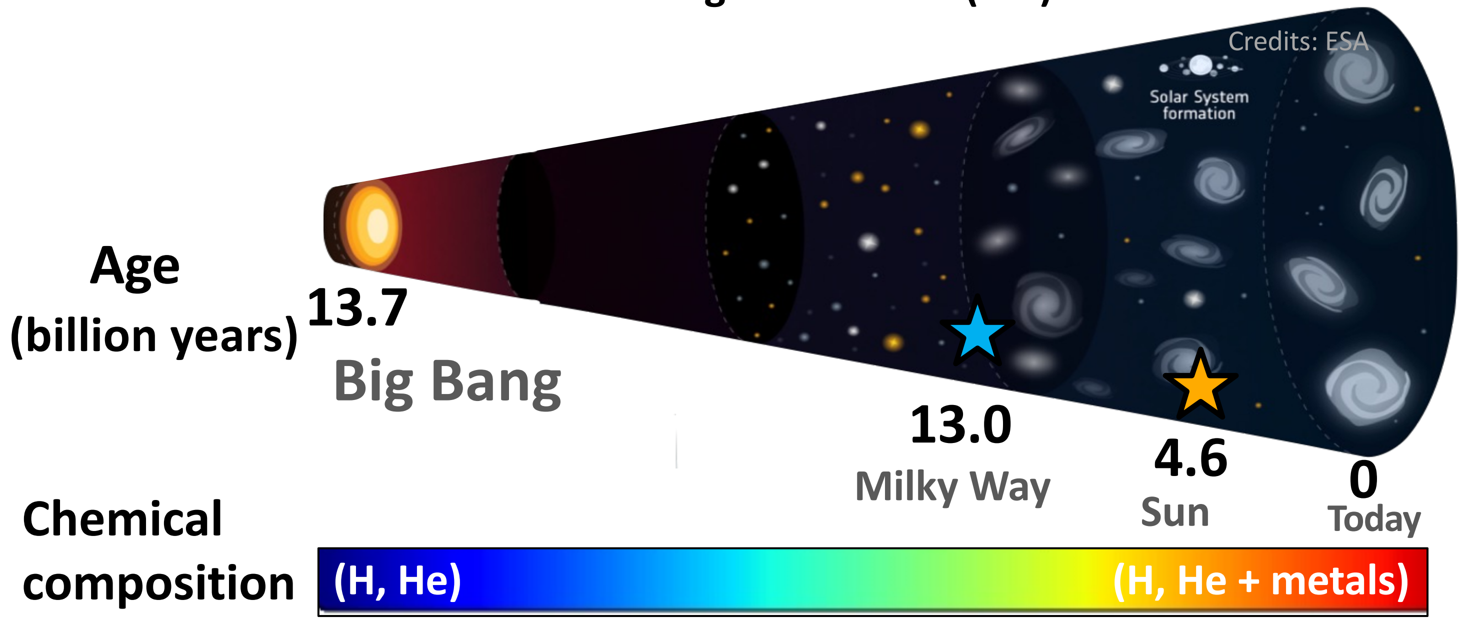

- Extremely metal-poor stars can be selected in the Gaia DR3 GSPspec table

Recio-Blanco et al. (2022)

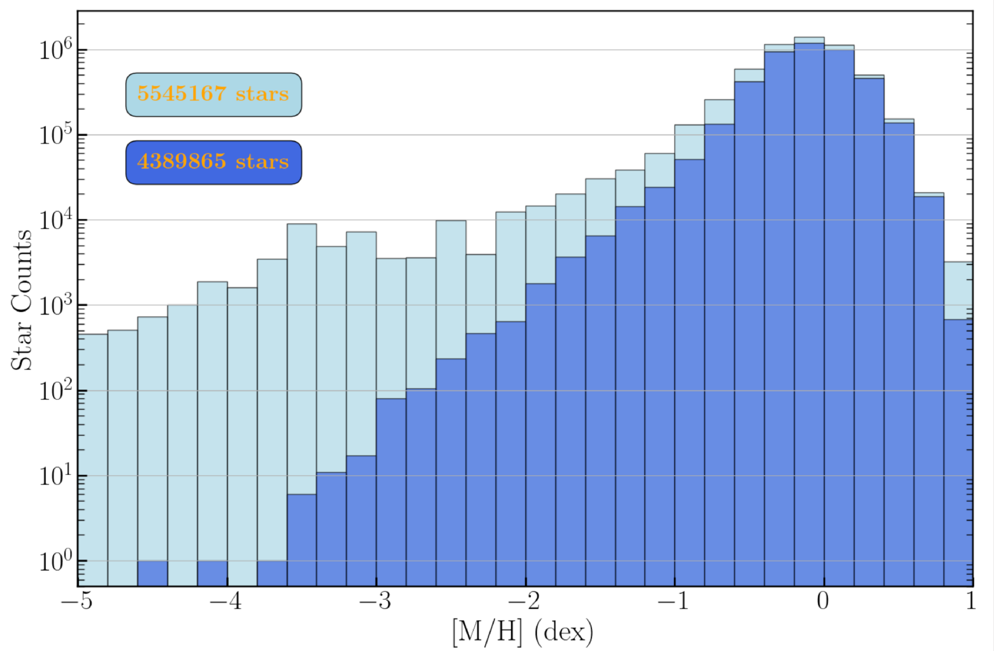

Conclusions

- The Gaia future is bright:
  - only ¼ of the data analysed in DR3!
  - end of cold gas (operational phase) Jan-March 2025
  - RVS data SNR increasing
- Much larger chemo-dynamical catalogues to come:
  - 5.6 million stars with chemo-physical parameters in DR3 (2022)
  - ~ 30 million stars in DR4 (end 2025)
  - ~100 million stars in DR5 (2030)
- Complementary ground based HR spectroscopy (WEAVE+4MOST) 5-10 million

Conclusions

- Time-series chemo-physical parameters for cepheids and RRLyrae from DR4
- Standard candles will increase the precision of Gaia distances towards the bulge, the outer disc, the halo and the surrounding satellites.
- In 2030 Gaia will have recorded 10 years of the Milky Way history!
- Important to keep synergy with models and simulations, including in a cosmological context

Back up slides

Galactic disc: an analytical chemical model including Type Ia SN

Chemical evolution model integrated by extending the instantaneous recycling approximation with the contribution of Type Ia SNe

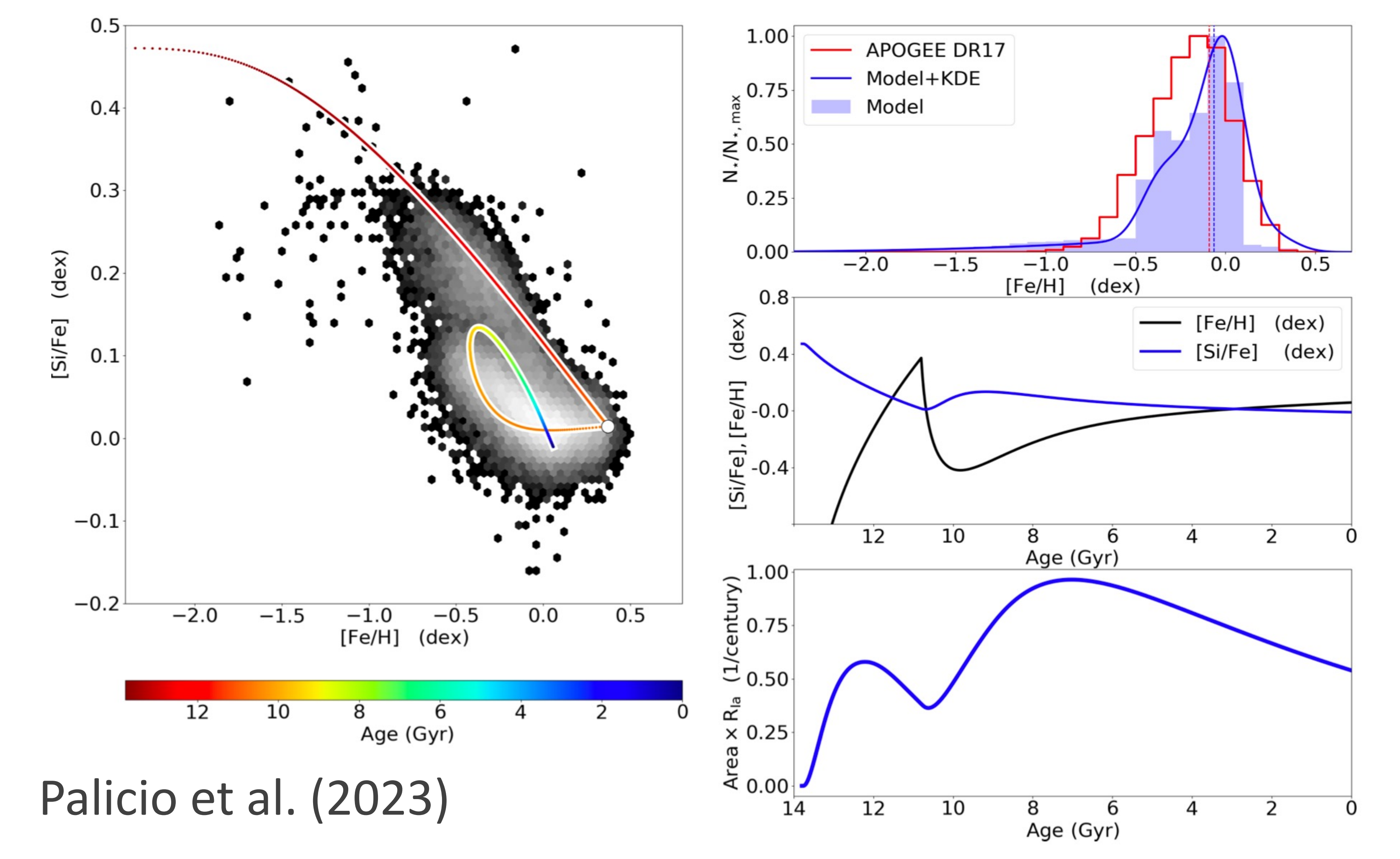

Palicio et al. (2023)

Extra term in the modelling depending
on the Delay Time Distribution (DTD).

Four different DTDs are considered, either analyticaly or as a superposition of Gaussian, exponential and 1/*t* functions using a restricted least-squares fit.

Galactic disc: an analytical chemical model including Type Ia SN

Used to model the chemical evolution of the GALACTICA Milky Way-like simulated galaxy (Park et al. 2021) from its star formation history.

Extracted from a zoom-in hydrodynamical simulation in a cosmological context (S. Peirani) spatial resolution and sub-grid models as in NewHorizon simulation as in Dubois et al. 2021.

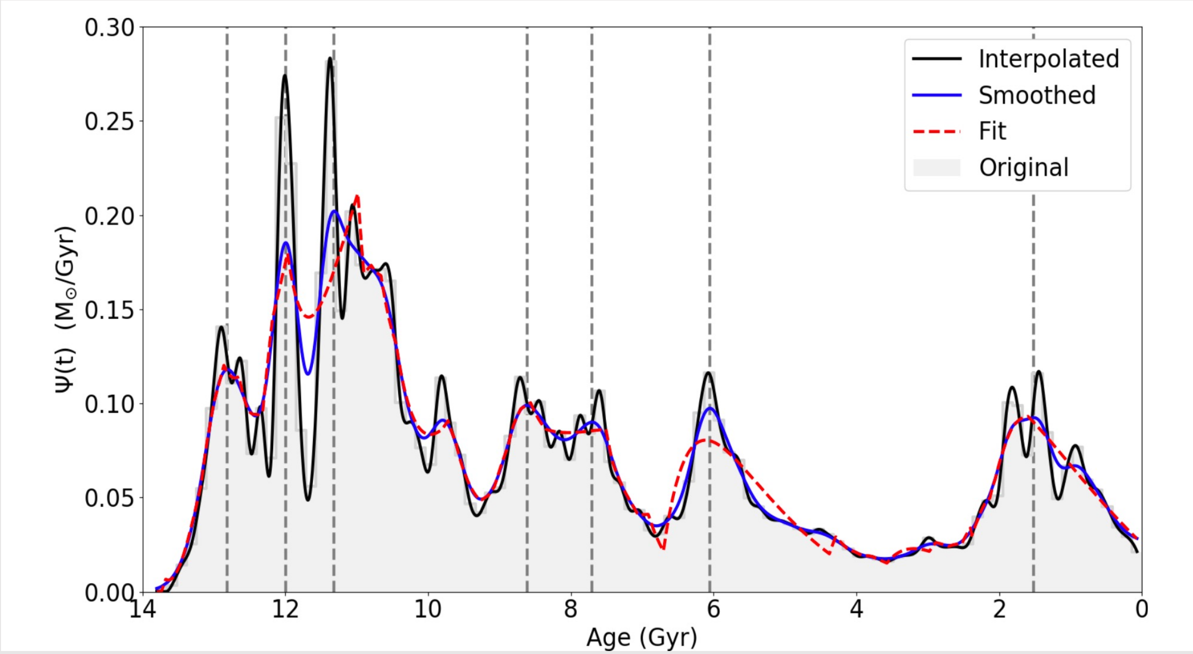

Palicio et al. to be submitted

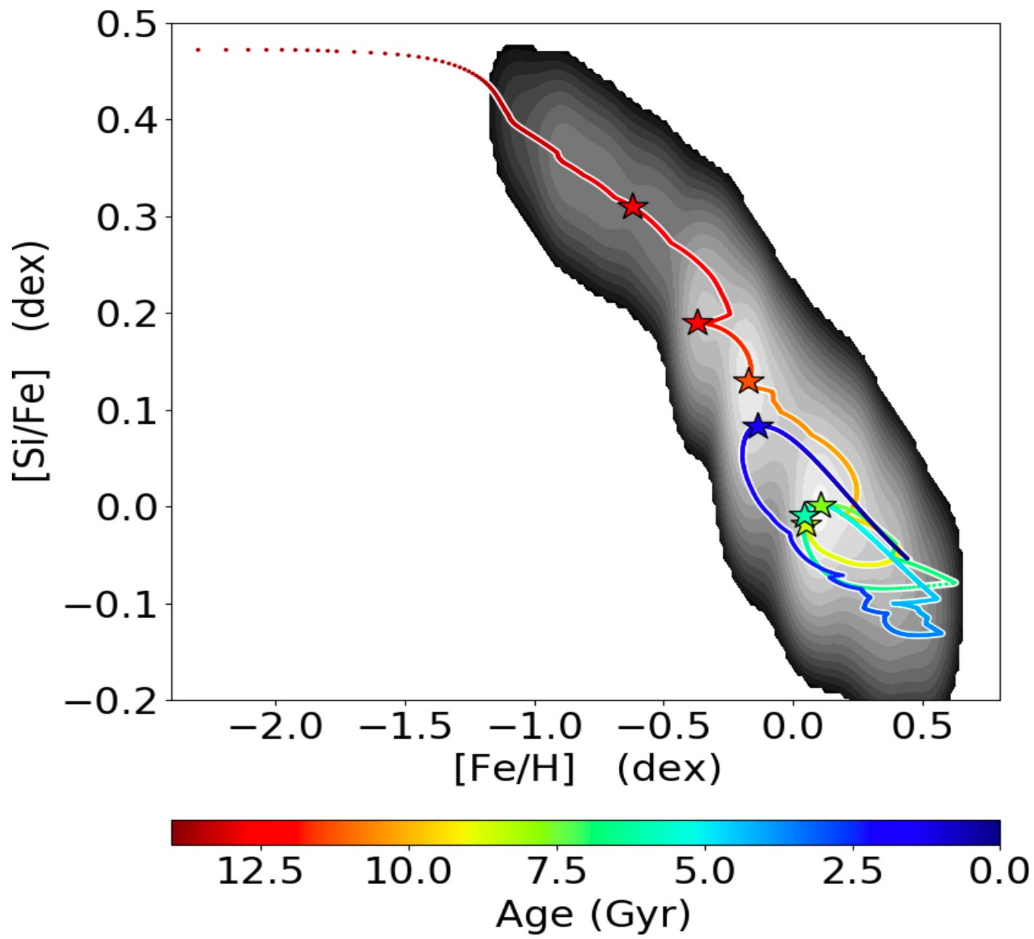

Gaia/RVS: high precision Kiel diagrams

SNR>150
High quality parameter flags

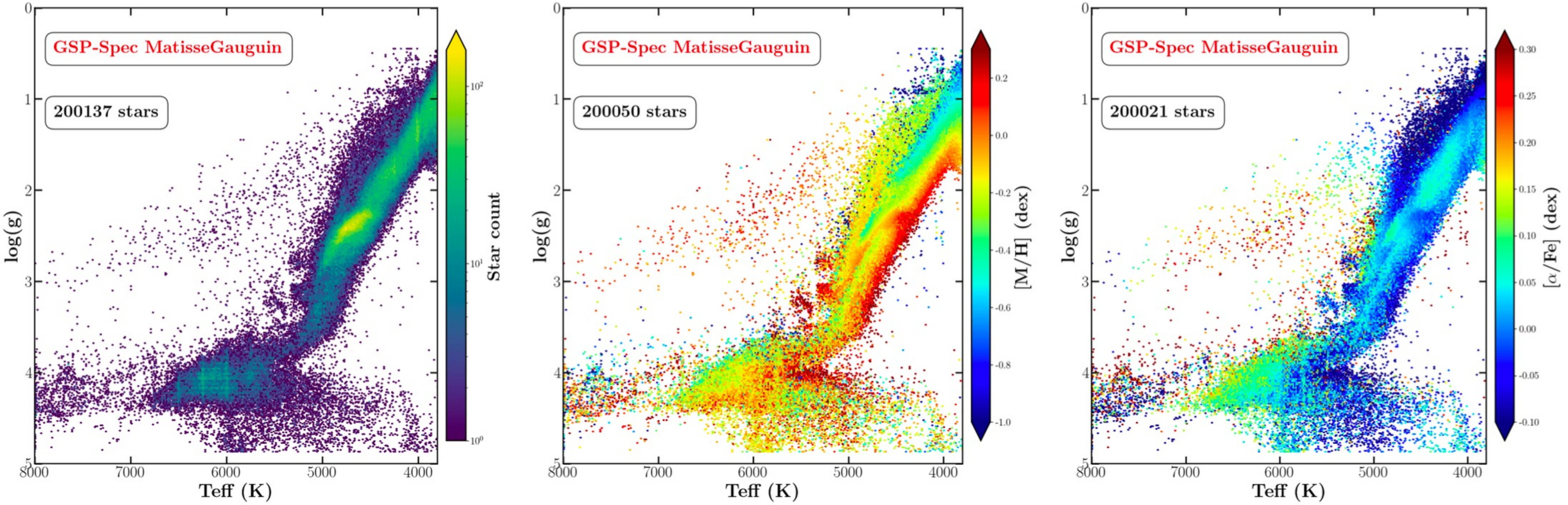

Recio-Blanco et al. (2022)

Gaia/RVS: a space spectroscopic survey

High quality spectra: **continuous observations for 3 years, no atmosphere,**
control of systematics, ... Gaia is not a ground-based survey!

Absorption from interstellar dust molecules (DIB) on an individual spectrum basis

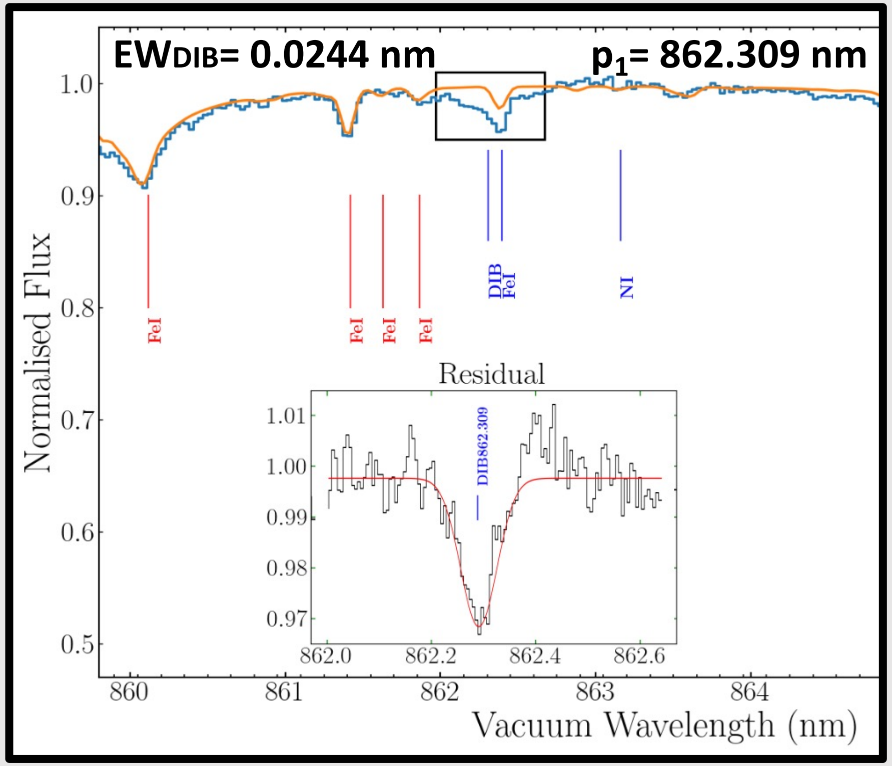

Recio-Blanco et al. (2022)

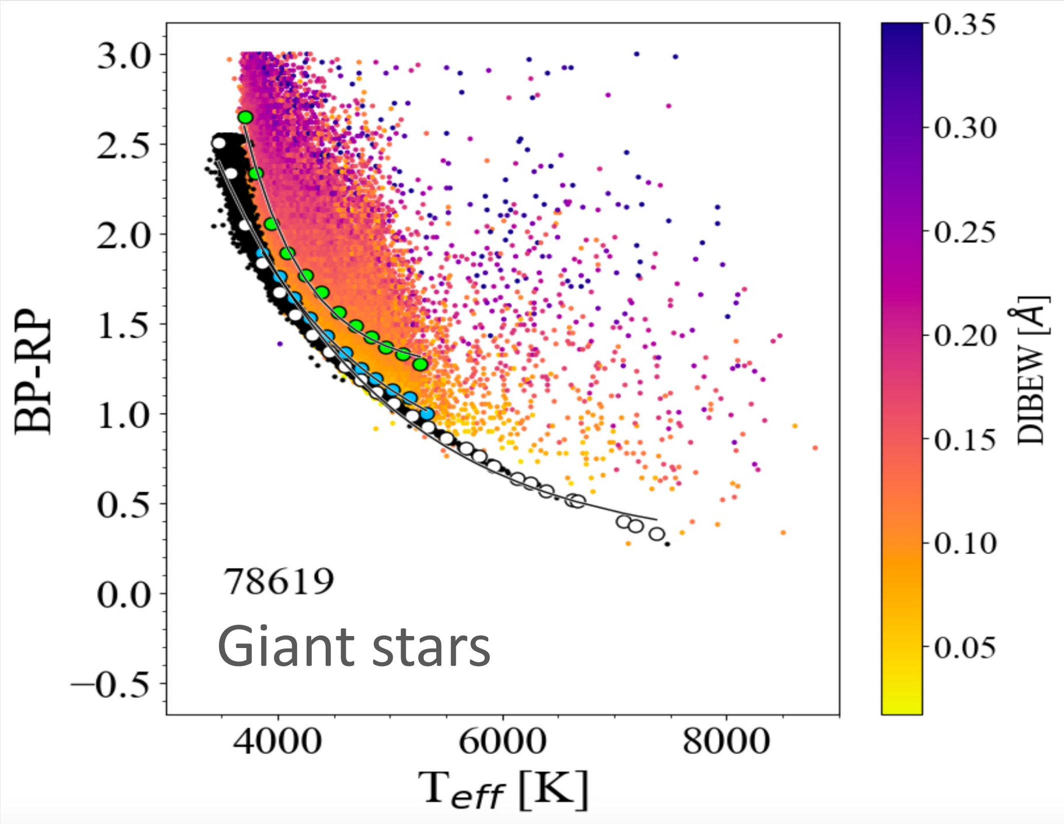

No Teff-absorption denegeneracy

	T_{eff}	log(g)	[M/H]	$log(g)_{calibrated}$	$[M/H]_{calibrated}$	RVS S/N
RAVE-DR6	(-12; 93)	(-0.28; 0.19)	(-0.05; 0.11)	(-0.003; 0.18)	(-0.05; 0.09)	(94; 64)
GALAH-DR3	(20;87)	(-0.26; 0.21)	(0.01; 0.10)	(0.003; 0.18)	(-0.001; 0.10)	(68; 53)
APOGEE-DR17	(-32; 86)	(-0.32; 0.17)	(0.04; 0.12)	(-0.005; 0.15)	(0.06; 0.12)	(65; 80)

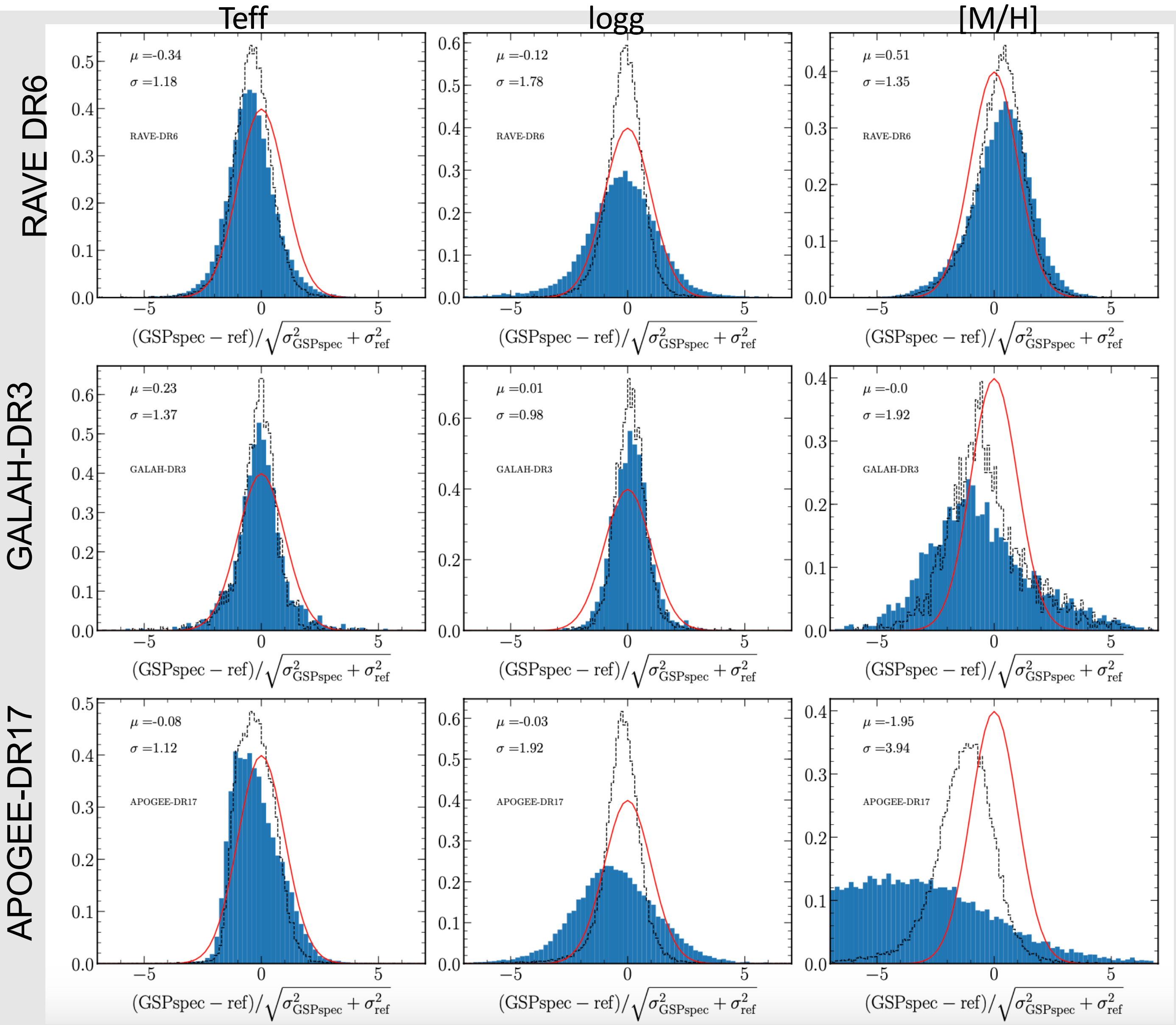

- General very good agreement*
- The extreme homogeneity of Gaia RVS/GSPspec highlights literature inhomogeneity (in methods, models, reference data, uncertainty definitions, selection functions...)

*GSP-Spec values are calibrated.
Dotted line: inflated errors by a factor of 4